DEVELOPMENT OF OPTIMAL BREEDING ZONES FOR WHITE SPRUCE IN ONTARIO UNDER CURRENT, PAST, AND ANTICIPATED FUTURE CLIMATE CHANGE

Ashley Marie Thomson

A Graduate Thesis
Submitted in partial fulfillment of the requirements
For the degree of
Master of Science in Forestry

Faculty of Forestry and the Forest Environment
Lakehead University

July, 2008

Your file Votre référence
ISBN: 978-0-494-43408-6
Our file Notre référence
ISBN: 978-0-494-43408-6

MAJOR ADVISOR'S COMMENTS

ABSTRACT

Thomson, A.M. 2008. Development of optimal breeding zones for white spruce in Ontario under current climate and anticipated future climate change. Master of Science in Forestry, Lakehead University. Advisor, Dr. W.H. Parker.

Key words: forest productivity, white spruce, breeding zones, climate change, adaptive variation, genecology, tree improvement, reforestation, maximal covering problem, focal point seed zones.

Tree breeding zones are delimited areas where trees are selected and bred, and their progeny are planted. Within these zones, the level of adaptation between seedlings and planting sites is controlled to ensure adequate survival and growth. Delineation of adaptively-based zones requires detailed knowledge of patterns of genetic variation within species.

Five-year height, root-collar diameter, current increment and survival were measured at each of six Ontario white spruce provenance trials containing 127 sources from across Ontario and western Quebec. Survival generally did not demonstrate significant variation amongst provenances, except at the Englehart test site, while the remaining three traits were significant at most sites. Intraclass correlation coefficients for significant traits ranged from 0.7% for elongation at the Englehart site to 19.2% for survival at the Englehart site. Growth data from 2007 were combined with 2002-2004 growth and phenological data. Principal components analysis was used to summarize the main components of variation, explaining a total of 53.8% of the total variation with the first three axes. The first principal component represented mainly growth potential, while the second and third represented field trial phenology and greenhouse timing, respectively. Multiple linear regressions revealed significant correlations to both temperature and precipitation variables, explaining 28%, 53%, and 27% of the total variation in the first three principal components axes. Regression equations were used to map predicted performance of white spruce across the study area of Ontario.

The focal point seed zone procedure (FPSZ) was used to determine areas of adaptive similarity for each of 618 gridpoints across Ontario based on current climate. These areas were used to represent candidate breeding zones constructed at levels of +/- 1.0 and +/- 0.5 least significance difference values. A maximal-covering model was then used to determine the optimal combination of a specified number of zones that could be used to maximize the area covered by breeding zones. Thirteen breeding zones were required to cover the entire range of white spruce in Ontario at the 1.0 LSD level of adaptive similarity, while more than 40 zones were required at the 0.5 LSD level. The northwest and northeast forest management regions could be covered with 6 breeding zones at the 1.0 LSD level and the southern region with just 5 zones.

The analysis was repeated using simulated past climate data from the CGCM2, HADCM3, and CSIRO climate models as input to the procedure. The HADCM3 model produced optimal breeding zones that were most similar to those developed for the current climate and is probably most reliable for predicting climate in Ontario. Future climate data for the same 3 models based on the A1 and B2 emissions scenarios was used to predict the location of future breeding zones for each of the six future climate scenarios. The HADCM3 model predicted the location of future zones to be relatively similar to those based on current climate, while CSIRO predicted wide shifts in the location of future zone boundaries and CGCM2 predicted moderate shifts.

TABLE OF CONTENTS

TABLES

FIGURES

ACKNOWLEDGEMENTS

This study was funded by a National Sciences and Engineering Research Council (NSERC) Industrial Postgraduate Scholarship in partnership with the Superior-Woods Tree Improvement Association. Original funding for test establishment and data collection was provided by an Ontario Living Legacy Trust Grant, as well as in-kind support from Kimberly-Clark, Weyerhauser, Tembec, the Petawawa Research Forest, the Ontario Tree Seed Plant, Bowater and Greenmantle Forest Inc. Additional funding was provided through a NSERC Discovery Grant awarded to Dr. William Parker.

I would like to thank Janet Lane of Domtar, Dryden for acting as my industrial supervisor, as well as well as Kate Wood and Craig Beckman of Pacific Regeneration Technologies Inc. (PRT). Special thanks to Dan McKenney and Pia Papadopol of the Great Lakes-St. Lawrence Forestry Centre for providing climate data. Thanks to Joan Lee of the Lakehead University Greenhouse, Megan Thompson of Bowater, Al Foley of the Ontario Tree Seed Plant, and Steve D'eon of the Canadian Forest Service. Thank you to Danielle Letang for her help with data collection during the summer of 2007 and to Phil Stankowski for his help with mapping, as well as to Tomislav Sapic for providing so much help with ArcGIS.

Special thanks to Mark Lesser, whose Masters research provided critical data for this study and whose achievement has inspired me to continue with my graduate studies. As a graduate teaching assistant, he helped me through Dr. Parker's undergraduate Forest Genetics course. He was also a great leader during the two summers I spent working with him as a research assistant for Dr. Parker.

I would like to offer my sincerest thanks to my committee members. Dr. Kevin Crowe has provided critical help with my modeling efforts and very insightful feedback. Mr. Paul Charrette has provided a very thorough and helpful review of my manuscript, as well as a great deal of encouragement. Thank you to my external examiner Dr. Greg O'Neill for such a thoughtful review of my manuscript and for providing direction for publication.

My deepest thanks to my advisor Dr. William Parker. Your advice, support and encouragement have motivated me, your outstanding work has inspired me, and your guidance has provided me with opportunity that I would never have thought possible.

Finally, I would like to thank my family and friends for their ongoing support and encouragement. Thanks for listening, for tolerating, and for helping me get through it.

CHAPTER I: INTRODUCTION AND LITERATURE REVIEW

INTRODUCTION

The genetic structure of forest tree species is shaped primarily by patterns of environmental variation (Campbell 1979, 1986; Morgenstern 1996); most notably the gradients in temperature that occur across a species' range (Matyas 1997; Matyas and Yeatman 1992, Morgenstern 1996; Rehfeldt *et al.* 1999). For over 200 years, provenance tests have been used to study differences in growth and adaptation between seed sources originating from varying environments (Matyas 1997). By analyzing the performance of multiple sources planted in a common environment, it is possible to construct models that predict the performance of transferred seed based on the climate of the planting location (Campbell 1979, 1986). Such models have been used extensively since the early 1900's to guide seed transfer of many species throughout North America and Europe.

In forest management, seed zones and breeding zones are used to limit the transfer of tree seed to ensure that populations are only planted into environments in which they are expected to be adequately adapted (Campbell 1979, 1986; Rehfeldt 1983a, 1991). As previously noted, the delineation of adaptively-based seed zones requires extensive provenance testing to determine patterns of genetic variation among species and subsequent modeling to determine the relationship between source performance and the climate at seed origin (Parker 1992). However, when such information is unavailable, the general approach has been to delineate seed zones on the basis of climatic similarity and to modify boundaries as better information about

species' patterns of adaptive variation becomes available (Rehfeldt 1990). The rationale in this approach is based on the assumption that climatically-similar areas will also reflect similar areas of adaptation. However, numerous studies have shown that while seed source performance often roughly corresponds to climate, patterns are not exact (O'Neill and Aitken 2004; Rehfeldt 1991).

The original seed zones for Ontario were constructed using the climate-based approach; seed zone boundaries reflect the boundaries of Hills (1959) site classification and Ontario Ministry of Natural Resources (OMNR) administrative boundaries (Parker and van Niejenhuis 1996a). However, recent genecology studies of black spruce (Parker and van Niejenhuis 1996b), and jack pine (Parker and van Niejenhuis 1996a) have led to modifications of seed zone boundaries which are expected to result in significant gains in volume (Parker and Crowe 2005).

The challenge in delineating adaptively-based breeding zones for any species is to balance zone size such that zones are not so large that maladaption results and not so small that seedlings could achieve similar gains in adjacent zones (Parker 2000; Crowe and Parker 2005). The total number of breeding zones should be considered also, as costs of tree improvement increase substantially for each additional breeding zone (Crowe and Parker 2005). While the earliest seed transfer zones were generally developed using genetic maps based on multiple regression equations (Campbell 1979, 1986; Rehfeldt 1983a, 1991), recent approaches are more advanced and often include optimization procedures (Crowe and Parker 2005; O'Neill and Aitken 2004; Roberds and Namkoong 1989). O'Neill and Aitken (2004) used a clustering algorithm to partition management areas into a set number of breeding zones such that the regional

maladaptation is minimized. More recently, Crowe and Parker (2005) used a maximal-covering model to maximize the area covered by a fixed number of breeding zones, subject to a constraint on adaptive similarity. These methods have provided both an efficient and objective method of delineating adaptively-based seed zones.

Over the next century, increases in global mean temperature due to anthropogenic activity are expected to lead to significant declines in the health and productivity of many forest tree species (Carter 1996; Cherry and Parker 2003; Matyas 1997; Rehfeldt *et al.* 1999). Such declines are predicted because the rate of warming is expected to be so great, at approximately 2.4-6.4°C over the next century (IPCC 2007b), that neither adaptation nor migration will be sufficient to keep pace (Davis and Shaw 2001; Etterson and Shaw 2001). As such, some manner of assisted migration is required in ensuring the adequate growth and adaptation of forest trees to new environments under climate change (Matyas 1997; Rehfeldt *et al.* 1999).

Seed transfer models provide an effective means of predicting the response of forest trees species to climate change and can be used to guide the redistribution of genotypes to preserve adaptation (Matyas 1994, 1997; Rehfeldt 1991; Rehfeldt *et al.* 1999). When adequate knowledge of future climate is available, it can be used to delineate future seed and breeding zones. However, precise information regarding the exact magnitude of future climate change is not readily available due to uncertainty in future emissions and climate models (Crowe and Parker 2008, Lempert *et al.* 2004, Rivington *et al.* 2008). However, by simulating past or current climate using various climate models and comparing the output to observed climate data, one can evaluate the

accuracy of alternative general circulation models (GCMs) (IPCC 2007b, Rivington *et al.* 2008).

White spruce is a widely-distributed North American conifer and is of considerable economic importance to the Canadian forest sector (Cherry and Parker 2003; Lesser and Parker 2004; Nienstadt and Zasada 1990; Rweyongeza *et al.* 2007). Despite this importance, tree improvement research for white spruce in Ontario has fallen behind that of other economically important boreal conifers including black spruce and jack pine (Lesser 2005). While a recent study was aimed at developing adaptively-based, continuous seed zones for white spruce (Lesser 2005), the delineation of adaptively based breeding zones has yet to be undertaken. Expected gains from tree improvement can only be realized within the limits of adaptation; improved seedlings transferred to climates very different to those in which they have evolved can be expected to demonstrate significant reductions in growth due to maladaptation (Crowe and Parker 2005; O'Neill and Aitken 2004). As such, future climate warming is expected to cause declines in productivity of many white spruce populations (Andalo *et al.* 2005; Carter 1996; Cherry and Parker 2003; Rweyongeza *et al.* 2007). Therefore, modifications to breeding zones to reflect anticipated future warming will be necessary to ensure that anticipated gains from forest tree improvement are ultimately realized (Parker and Crowe 2005).

The primary objective of this study is to optimally delineate current breeding zones for white spruce in Ontario based on demonstrated patterns of adaptive variation. The results will provide the information necessary to refine current climate-based zones and increase overall adaptation of planted sources. Secondary objectives are to delineate

future breeding zones to maintain adaptation and productivity under climate change, and finally, to evaluate the accuracy of three separate climate models in Ontario by comparing simulated past breeding zones to current breeding zones developed herein.

LITERATURE REVIEW

GENETICS OF WHITE SPRUCE

White spruce demonstrates high levels of genetic variation at the population, family, and individual levels (Nienstadt and Teich 1972; Li *et al.* 1993). Analysis of allozyme data and expressed sequence tag polymorphisms (ESTP) has revealed that white spruce demonstrates a high percentage of polymorphic loci, large numbers of alleles per locus, and high observed and expected heterozygosity (Furnier *et al.* 1991; Jaramillo-Correa *et al.* 2001).

White spruce reproduces almost exclusively through out-crossing, and while there is no direct evidence to suggest discrimination against self-pollination, it appears that the majority of self-pollinated embryos abort due to a recessive lethal trait (Nienstadt and Teich 1972). Also, significant inbreeding depression promotes high levels of outcrossing in this species (Park *et al.* 1984).

Jaramillo-Correa *et al.* (2001) found that 13 of 14 allozyme loci were polymorphic, with an average of 3.4 alleles per locus and 83.6% polymorphic loci. In comparison, ESTPs were polymorphic for each of 11 loci, and the average number of alleles per locus was 2.8. The percent polymorphic loci based on ESTPs ranged from 72.7 to 90.1%. Observed and expected heterozygosity at allozyme loci is generally quite consistent across studies, ranging from 0.306-0.348 and from 0.290-0.41 (Furnier *et al.* 1991; Jaramillo-Correa *et al.* 2001).

Extensive natural hybridization occurs between white spruce and Sitka spruce (*Picea sitchensis* (Bong.) Carrière) in a zone of introgression of approximately 200 km in the Nass and Skeena drainage basins of the coastal mountains, BC (Bennuah *et al.* 2004). This area represents an area of transition from the milder maritime climate of the coast to the cooler, drier regions of the interior. Analysis of Sequence Tag Sites (STS) markers revealed that the Sitka spruce contribution to the hybrid genome decreases with increasing distance from the coast where sitka spruce dominates. Significant within-site variation in hybrid index was also shown, and hybrid index values suggest that multiple generations of introgression have occurred. The variation in hybrid index among sampling locations was best explained by physical drainage distances along river valleys, explaining 78% of the variation. It appears that hybrids are superior to pure forms of either species, due to the high cold and drought tolerance of white spruce combined with the fast growth rate of sitka spruce.

In regions where white spruce and Engelmann spruce (*Picea englemanii* Parry ex Engelm.) natural distributions overlap within Alberta and British Columbia, these species form a hybrid swarm where even apparently-pure forms are affected by introgression (Daubenmire 1974). Predominantly white spruce genotypes are generally confined to lower elevations while Engelmann spruce genotypes occupy higher altitudes. However, gene flow is apparently asymmetrical, with greater flow of Engelmann spruce downslope than of white spruce upslope. Historically, the pure and hybrid forms could usually be distinguished only on the basis of cone and needle characteristics (Daubenmire 1974; Taylor 1959), while more recently, allozyme loci have been used (Rajora and Dancik 2000). Generally, pure white spruce has a needle length of up to 25

mm, glabrous twigs, and ovuliferous cone phyllotaxy of 3-5. In contrast, pure Engelmann spruce generally has needle length of up to 50 mm, pubescent twigs, and phyllotaxy of 5-8 (Daubenmire 1974). Taylor (1959) found white spruce and Engelmann spruce so similar as to classify them as subspecies of a single species based on morphology, while analysis of allozyme loci tends to support this classification (Rajora and Dancik 2000). Based on genetic distances, it appears that the pure forms of white spruce and Engelmann spruce diverged relatively recently at approximately 180,000 years BP (Rajora and Dancik 2000). However, studies of oligocene vegetation in Montana reveal the presence of definitive Engelmann spruce, as well as several other *Picea* spp., suggesting that the divergence between white and Engelmann spruce occurred more than 23 million years ago within the cretaceous (Becker 1961). Limited incidences of natural hybridization between white and black spruce (*Picea mariana* (Mill.) B.S.P) have also been reported (Nienstadt and Teich 1972).

VARIATION AMONG POPULATIONS

Inter-population variation in growth traits has been extensively demonstrated for white spruce, with population effects explaining up to 28 and 29% of variation in height and diameter, respectively (Khalil 1985). Significant variation was found for height, diameter, and branch number of 31 provenances tested in Newfoundland; however, crown width and branch angle were not significant. Similarly, Nienstadt and Riemenschneider (1985) reported significant variation among geographic origins for 9- and 15-year height growth, and Cherry and Parker (2003) reported intraclass correlation coefficients (ICCs) of 14 and 15 % for height and diameter, respectively. A more recent

study found that all seedling growth variables measured over two years demonstrated significant differences between provenances planted in 5 field trials and a greenhouse trial across Ontario (Lesser and Parker 2004). Population differences accounted for 16.5% of the variation in first year greenhouse height growth and 6.2 to 16.7% of 2nd year field-trial heights. Diameter differences were somewhat less pronounced, with populations explaining 5.9 to 11.4% of the total variation.

Phenological characteristics, namely the dates of spring budburst and fall budset and their influence on frost-susceptibility, also show significant components of variation among provenances (Lesser and Parker 2004; Li *et al.* 1993; Li *et al.* 1997. However, despite strong differences in growth and phenological traits, among-population differentiation in survival is generally very weak or cannot be detected (Cherry and Parker 2003; Lesser and Parker 2004; Morgenstern and Copis 1999). A study of 15 white spruce provenance trials across Ontario revealed that survival differences among provenances accounted for only 2.8% of the total variation (Cherry and Parker 2003), while Lesser and Parker (2004) reported survival differences among populations as low as 1.97% and 0.0% for first and second-year survival, respectively.

There is also sufficient evidence to suggest that populations differ with respect to wood properties (Corriveau *et al.* 1987; Yu *et al.* 2003). Differences in average ring width, as well as juvenile and mature wood density have been shown for provenances of white spruce grown in Quebec, with populations accounting for 19 and 28% of the variation in juvenile and mature wood, respectively (Corriveau *et al.* 1987). Variation in germination temperatures, insect damage, and secondary compounds such as

monoterpenes has also been demonstrated (Nienstadt and Teich 1972; Wilkinson *et al.* 1971).

Studies of molecular variation in white spruce have revealed significant differences among populations in both allozymes and expressed sequence tag polymorphisms (ESTPs) (Furnier *et al.* 1991; Jaramillo-Correa *et al.* 2001). However, molecular variation is generally quite low in comparison to variation in growth and phenological traits, with populations explaining only 3.8% of the total variation in allozyme data (Furnier *et al.* 1991). Also, molecular traits do not appear to demonstrate any clear trends with respect to geography or climate of seed origin (Furnier *et al.* 1991; Jaramillo-Correa *et al.* 2001).

In contrast, patterns of morphological and phenological variation among white spruce provenances are generally clinal (Nienstadt and Teich 1972). Khalil (1985) found that variation in white spruce provenances from eastern Canada follows primarily an east-west gradient. However, Li *et al.* (1997) found that genetic variation of provenances from Quebec and Ontario follows a stronger latitudinal gradient and a somewhat weaker east-west gradient. In Ontario, Lesser and Parker (2004) found a southeast to northwest cline, with provenances from the southeast demonstrating the highest growth potential, and northern provenances flushing earlier in the spring and setting bud earlier in the fall. This finding was in keeping with a large body of previous research indicating sources from southeastern Ontario, specifically the Ottawa Valley, demonstrate superior height growth across a wide range of test environments (Khalil 1985; Li *et al.* 1997; Nienstadt and Riemenschneider 1985; Nienstadt and Teich 1972; Morgenstern and Copis 1999).

Nienstadt and Reimenschneider (1985) found that 31 provenances from the Ottawa Valley were among the fastest growing at a test site in Wisconsin. Similarly, Morgenstern and Copis (1999) noted that southeastern provenances demonstrated superior performance across many sites in Ontario. Nienstadt and Teich (1972) note that sources from Angus and Douglas, Ontario have been shown to outgrow the relatively faster-growing Norway spruce when planted in a common environment. Moreover, the superior growth of these provenances has been shown to persist well into maturity, with minimal changes in rank. Provenances from southeastern Ontario have also been shown to demonstrate good survival when planted across a wide range of environments, even with northward transfers of several degrees (Lesser and Parker 2004; Li *et al.* 1997; Nienstadt and Teich 1972). When planted in common garden across eastern Canada, the Lake States, and parts of New England, provenances from the Great-Lakes-St Lawrence region demonstrate 15% greater growth than unspecified local sources but have similar survival.

VARIATION WITHIN POPULATIONS

Within-population variation in white spruce has been shown to be quite high, with family variability often approaching or exceeding provenance variability (Nienstadt and Teich 1972; Li *et al.* 1997). Li *et al.* (1993) found for 57 provenances in Quebec that source effects averaged 3.1% of the total variation in seedling growth and phenological traits while family effects accounted for an average of 2.9%. Within a single stand, budburst has been shown to vary up to 21 days, resulting in significant increases in height growth and frost resistance for later-flushing trees (Nienstadt and

Teich 1972). Similarly, Nienstadt (1985) demonstrated significant differences in dates of spring budburst among progenies, with an associated heritability value of 0.70. However, in that study the degree of late spring frost damage was most severe for the fastest-growing trees, possibly because the late-flushing sources had not yet begun to lignify. Pollard and Ying (1979) found that, despite a lack of variation among populations, families within populations varied considerably in their dates of bud flush.

A study of growth of 31 provenances in Newfoundland found extremely large intra-population variation in growth traits including: height, diameter, branch number, branch angle, crown width, and form quotient (Khalil 1985). Nienstadt (1985) demonstrated significant differences in leader extension for progenies of the Lake States and Ottawa Valley. Measures of fecundity also differed, with heritability values for cone length, cone width, number of cone scales, and number of cones per tree of 0.21, 0.32, 0.22, and 0.19 respectively.

Significant within-population variation has been shown for numerous traits related to wood quality of white spruce. Corriveau *et al.* (1987) found that intra-population differences accounted for much larger components of variation than populations, explaining 81 and 72% of the total variation in juvenile and mature wood density, respectively. Yu *et al.* (2003) reported significant variation among 35 white spruce families in Quebec for wood density and resistance to white and brown rot. Heritability estimates ranged from 0.21 for brown rot resistance to 0.35 for wood density. However, the residual variation was much higher than the family variance, indicating that variation among individuals accounted for a significant portion of the overall variation in decay resistance and wood density. Wood density was negatively

genetically correlated to resistance to brown rot, but positively correlated to white rot resistance, suggesting that breeding for resistance to either of these diseases would lead to an increase in susceptibility to the other.

In a follow-up study, Zhang *et al.* (2004) studied differences in veneer quality among the previous 35 families of white spruce and found significant differences for veneer density and wood density. A lesser, non-significant component of variation was demonstrated for ring width and veneer modus of elasticity and veneer roughness. Narrow-sense heritabilities ranged from 0.13 for veneer modus of elasticity to 0.62 to veneer density.

Several studies have demonstrated increases in heritability values with increasing age of white spruce trees (Mohn *et al.* 1976; Nienstadt and Reimenschneider 1985). At age 9, heritabilities ranged from 0.43 to 0.62 across four sites in Ontario and the Lake States, and from 0.63 to 0.98 at age 15 (Nienstadt and Riemenschneider 1985). Similarly, Mohn *et al.* (1976) reported an increase in heritability from 0.27 to 0.35 between 9 and 12-year height measurements. There are also reports of higher heritability values obtained for test sites of cooler or less-productive environments (Nienstadt and Riemenschneider 1985).

A number of studies have demonstrated the reliability of making selections based on early trial measurements, as provenance or family rank changes are generally limited as the trees age. Li *et al.* (1993) found that seedling heights based on family means were strongly correlated to 8-year heights, while Nienstadt and Riemenschneider (1985) found that the correlation between height at age 9 and age 15 was 0.725, while at another site the correlation was even higher with a value of 0.930.

Due to the very large within- and among-population genetic variation and strong heritability, the potential for gains due to tree improvement in white spruce is very large (Nienstadt and Teich). Li *et al.* (1993) reported expected gains in height of 8% if the top 20% of families were selected, while the gains predicted by Mohn *et al.* (1976) were considerably larger, at 15-20% if the top 10% of individuals were selected. Gains reported by Nienstadt and Teich (1972) were intermediate at 10% based on selection of the top 10% of progenies.

DEVELOPMENT OF SEED TRANSFER GUIDELINES

Rehfeldt (1983a) defines seed zones as the geographic area within which seed source differentiation cannot be detected, while Campbell and Sorenson (1978) define them as areas in which genotype x environment interaction is minimized. Seed zones serve as both the collection and deployment areas for seed used in reforestation (van Bujitenen 1992). However, within a given seed zone the area from which seed is collected may differ from the areas in which it is used in regeneration. Thus, the term seed procurement zone is used to define the area in which suitable seed for reforestation is obtained and the term seed deployment zone defines the area in which seed is used (planted). Tree breeding zones are largely analogous to seed deployment zones, but the term is used particularly to refer to a species-specific area of deployment for improved seed cultivated within seed orchards (Crowe and Parker 2005).

Campbell (1979) was among the first to develop predictive models describing patterns of genetic variation in relation to provenance origin. To test the hypothesis that genetic variation of Douglas-fir follows environmental gradients, 115 sources were

collected and established at a common-garden location in Oregon. Sources were measured for early morphological and phenological characteristics including: seed weight, bud burst, bud set, height, and diameter. Principal components analysis was used to reduce the 16 measured variables into 6 main components of variation describing 90% of the total variation in measured traits. Multiple regression analysis was then used to relate principal components factor scores and original trait measurements to the geographic origin of seed sources. Provenance origin was described using variables derived from source elevation and north and east position. Regression equations were then solved for each point in a regular grid across the study area. Contours were used to connect points of the same value and demonstrated strong geographic trends; however, the patterns varied somewhat among each of the variables. Campbell (1986) concluded that the demonstrated clines reflected strong selection by environmental factors during the seedling stage.

Campbell and Sorensen (1978) recognized the need to evaluate the response of populations across a variety of environments when developing clinal models of population structure. Working on the premise that the relationship between provenance performance and climate is variable depending on the environment in which it is tested, they established a common garden trial of Douglas-fir with varying levels of soil and air temperature, as well fertilizer treatment. Populations were measured for 16 growth and phenological traits, and subsequent analysis of variance revealed that all traits differed significantly among provenances. However, the magnitude of the differences was dependent upon the environmental treatment to which the observations belonged.

Subsequent multiple linear regression analysis revealed that the relationship between source performance and geographic location, as predicted by first and second-order polynomial functions of latitude, elevation and distance from the ocean, differed between environmental treatments and the trait examined (Campbell and Sorensen 1978). For example, latitude and distance from the ocean were found to be good predictors of bud set in the cool air treatment, while in the warm air treatment no correlation between budset and latitude could be demonstrated. The complexity of the adaptive clines was such that they could not reasonably be used to devise seed transfer guidelines. The authors suggest that the complex patterning of genetic variation in Douglas-fir is the result of different selection pressures acting in each of the source environments.

Rehfeldt (1982) modeled population differentiation of western larch (*Larix occidentalis* Nutt.) based on measured traits of growth potential, phenology, and cold-hardiness from 2-year seedling trials. Simple regression was used to relate seed source performance variables to each of 28 variables describing geographic location and ecological characteristics of the climate at seed origin. Results consistently demonstrated elevation as the strongest predictor of seed source performance. Model residuals were calculated and related to geographic variables using stepwise multiple regressions. The resultant equations were used to plot predicted values for each of the individual performance variables across the study area and contours were constructed to illustrate geographic differentiation of seed sources. Results illustrated that geographic patterns of variation generally followed gradients of elevation, ecology, and climate and approximately 3 seed zones could be used to guide seed transfer in the region.

Rehfeldt (1982, 1983a 1983b, 1983c, 1991) used least significant difference (LSD) values to quantify the minimum phenotypic differences required to distinguish among populations. He then applied LSDs to trait-source location relationships to infer acceptable transfer distances. A significance level of 20% was used to lower the occurrence of type II errors, indicating no difference between populations when differences actually exist. Contours in maps of genetic variation for various adaptive traits of western larch (Rehfeldt 1982) and ponderosa pine (Rehfeldt 1991) were delineated so that the distance between two adjacent contours represented half of the least significant difference (LSD) value used to detect significant differences among provenances at the 20% significance level. Thus, populations separated by two contour intervals were expected to differ with a confidence level of 80%.

Rehfeldt (1983a) used multiple regression models to relate growth and freezing injury of lodgepole pine (*Pinus contorta* Dougl.) sources to elevation and habitat type. Seed transfer models indicated that source performance could be adequately predicted by elevation and habitat type. Plots of individual growth variables revealed that the relationship between individual growth and freezing tolerance variables was non-linear, so quadratic models were developed. The resulting functions indicated a strong negative correlation between growth potential and frost hardiness; sources transferred from 1500 to 1000 m elevation demonstrated a 30% decrease in growth potential with a concomitant increase in cold-hardiness of 28%. The author notes that the results indicate severe limits to elevational transfer; however, a balance between cold-hardiness and growth potential might be used to define the acceptable limit of safe transfer.

Building on his earlier work, Campbell (1986) developed a method of assessing the relative risk of seed transfer based on the degree of mismatch between genotypes of a planting site and source location. Frequency distributions of genotypes at a source and transfer location were constructed and used to determine the area of "noncongruence" between curves. Relative risk was therefore defined at the proportion of the source and planting site curves which are non-overlapping and represents the probability that the source will be maladapted at the planting location.

To construct genetic maps of Douglas-fir, Campbell (1986) followed similar methodology to his previous work; however, principal components analysis was conducted based on the partitioning of provenance variation into a genetic covariance matrix, rather than on original measured variables. Multiple linear regression was used to develop models describing the relationship between PC factor scores and geographic location and equations were solved for each point in a grid of the study area to determine principal components factor scores. The relative risk value was then used to determine the distance in PC factor scores between contours of the genetic map. The resulting maps showed that seed transfer risks were greatest along steep environmental gradients, such as in the southern and western areas of the region where temperature and precipitation are most variable.

Campbell (1986) outlines 8 critical assumptions that must be met when developing seed transfer guidelines: (1) sampling of a region is conducted at a great enough intensity to capture true patterns of variation; (2) a portion of the variation in adaptive traits can be attributed to the geographic origin of the source and can be separated from other genetic and environmental effects ; (3) provenance variation can be

accurately characterized by phenotypic traits measured in common garden trials; (4) provenance variation can be related to geographic location variables and can be mapped as such; (5) a map of adaptive variation of provenances reflects the environmental factors which shape the process of natural selection; (6) the local population is better-adapted to its source environment than is any other population (7) the relative risks determined using seedling measurements also apply to mature trees; and (8) seed transfer imposes equal relative risk whether movement is to milder or harsher climates.

Following the methods of Campbell (1986), Li *et al.* (1997) developed models of genetic variation of white spruce in Quebec and used them to delineate provisional breeding zones. Growth and phenological traits were measured for a seedling provenance trial composed of 63 Quebec provenances. The matrix of genetic covariance among traits was used as input to principal components analysis, and multiple regression was used to develop models relating seed source performance to latitude, longitude, and elevation terms. The resulting models indicated weak to moderate associations of measured traits with provenance location. A relative risk value of 0.3 was used to determine the distance between adjacent contours in map of predicted principal components scores and the resulting maps indicated that genetically-similar provenances were located across broad areas of approximate 2° latitude. Two breeding zones roughly corresponding to the northern and southern halves of the study area were delineated.

The use of continuous, rather than discrete, seed zones was first suggested by Rehfeldt (1983b, 1983c, 1990). Seed zones were developed for Douglas fir in central Idaho and western Montana by relating adaptive trait differences to ecological and geographic variables (Rehfeldt 1983b, 1983c). In western Montana, Douglas-fir

demonstrated steeper clines in cold-hardiness in the west than in the east, and thus, two separate transfer functions were needed (Rehfeldt 1983c). In the west, differences between populations could be detected at distances of 800 feet elevation, while in the east no differences could be detected at distances below 1600 feet elevation. Rehfeldt (1983c) suggested that the use of either discrete or continuous zones would be appropriate to managing seed transfer of Douglas-fir, as seed from any area in the west could be transferred within 800 feet of elevation with little risk of maladaptation. This is in contrast to previous studies (Campbell 1979, 1986; Rehfeldt 1983a) which used fixed zone boundaries to limit seed transfer; seed could only be moved within a given zone, regardless of whether the source occurred in the center or along the edge of a zone.

Rehfeldt (1991) combined data from two separate provenance trials of ponderosa pine to develop models of genetic variation based on 201 populations in the northwestern United States. Growth and phenological variables obtained from greenhouse and phenological trials in the two studies were scaled based on the performance of a single common population. Principal components analysis was used to reduce the number of variables and multiple linear regression was used to relate seed source performance to latitude, longitude and elevation. The resulting models were used to predict the values of individual performance variables and principal components factor scores across a grid of the study area. Contour lines constructed at an interval of 0.5 LSD 0.2 were plotted to determine geographic patterns of genetic variation.

Maps of genetic differentiation of ponderosa pine generally indicated that growth potential decreased sharply with increasing elevation and that sources located at similar elevations in different drainages tended to be genetically distinct (Rehfeldt

1991). However, similar genotypes could be found in different drainages at varying elevations. Thus, similar genotypes tended to recur across the landscape. The author demonstrated that by determining the areas within ± 0.5 LSD intervals of a specified point, it was possible to determine either the location of similar genotypes that could serve as seed sources for regeneration or the location of sites where seed from that point could be planted without a decrease in adaptation.

In perhaps the first clear demonstration of the benefit of using continuous seed zones, Rehfeldt (1991) demonstrated that 30 breeding zones would be required to manage ponderosa pine across the area of the Inland Northwest if discrete zones were used. In contrast, recognizing the recurrence of similar genotypes allowed the use of the adaptive model to determine seed zones based on genetic similarity, and thereby reduced the total number of zones to 17.

Parker (1992) applied the genecology theory and methods developed by Campbell (1986) and Rehfeldt (1983a, 1983b, 1983c) to delineate site-specific seed zones for jack pine using a geographic information system (GIS). His approach was based on the idea that, rather than using fixed seed zone boundaries, it is more logical to consider each site separately to locate the best adapted seed for reforestation. Using this method, a site for reforestation, referred to as the focal point, is identified and a seed zone of similar adaptation is determined specifically for the point. A unique seed procurement area is identified for each reforestation location.

Similar to the methods of previous studies, short-term field trials were used to provide growth and phenological variables to determine variation in adaptive traits with provenance location (Parker 1992). These phenotypic variables were then reduced to a

few main components of variation using principal components analysis. Rather than using multiple regression to model the relationship between performance and seed source location, the principal components factor scores were plotted for each provenance location and a triangulated irregular network (TIN) was used to determine predicted factor scores for the remaining areas. For each main principal components axis, factor scores were grouped into intervals of ± 1.0 standard deviation of the focal point and intersected to produce an area of adaptive similarity.

Parker (1992) identifies five principal steps used in the construction of focal point seed zones: (1) determine the area of interest and intensively sample provenances from across the range; (2) establish each of the sampled provenances in short-term common garden tests to assess growth and phenological characteristics; (3) use principal components analysis (PCA) to summarize growth and phenological data through several variable-composites; (4) use GIS to generate trend surfaces of principal components factor scores (5) establish contours at intervals of 1.0 standard deviation value from the focal point for each of the trend surfaces and intersect them to produce polygons representing adaptive similarity to the focal point. This GIS-based approach offers several advantages in comparison to previous methodologies (Parker 1992). When scores within a given seed zone are ranked, they can be used to identify a well-adapted source with high growth for regeneration at the focal point. It can also be used to delineate new or refine existing seed zone boundaries and to determine the most suitable deployment areas for seed orchards.

Although the intention of focal point seed zones is to provide the best-matched seed to a particular point, the authors note its utility in refining existing static seed zone

boundaries (Parker 1992). Because true patterns of variation are elucidated, it is possible to construct or refine existing seed zone boundaries such that genotype x environment interaction is minimized. It is also noted that the underlying methodology can be used to investigate species' response to climate change; the adaptive models can be used in conjunction with estimates of future climate to determine best-adapted sources for the future.

Parker and van Niejenhuis (1996a) used a modified form of the focal point seed zone methodology (Parker 1992) to delineate seed zones for jack pine in the northwest of Ontario. Principal components analysis was used to summarize provenance growth and phenological traits. Factor scores for each of the 102 jack pine seed sources were regressed against climate variables obtained from Ontario weather stations including: annual and monthly means for growing season temperatures, precipitation, growing degree days, and dates of spring and fall frost. The resulting regression models were then used to generate maps of principal components factor scores across the study area based on the interpolated climate data. Seed zones for any specified focal point could then be determined by establishing contours at intervals of 0.5 standard deviations from the focal point for each of the PC trend surfaces and intersecting them to produce polygons, each containing trees that are adaptively similar within a polygon. Thus, the approach of Parker and van Niejenhuis (1996a) followed the approach of Rehfeldt (1983a, 1983b, 1983c, 1991) in that only adaptive variation associated with climate was considered.

In a similar study, Parker and van Niejenhuis (1996b) used growth and phenological data obtained from common garden, greenhouse, and freezing trials of 75

black spruce seed sources to determine regression-based focal point seed zones. The results demonstrated that clines of adaptive variation were steepest in areas such as the south where the climate changed most rapidly, and were relatively gradual across other areas where climatic gradients were much gentler.

The use of canonical correlation analysis as an alternative to regression-based focal point seed zones was presented by Lesser and Parker (2006). White spruce seed zones developed using the regression-based focal point seed zone methodology of Parker and van Niejenhuis (1996a, 1996b) were compared to those developed using canonical correlation analysis and were found to produce similar results. However, the authors note that canonical correlation produced smaller zones in areas of rapid climate change, such as the north shore of Lake Superior and in the south (Parker and van Niejenhuis 1996b). Lesser and Parker (2006) proposed that the higher-resolution of canonical zones in these areas is related to the statistical efficiency of the procedure.

Parker (2000) presented a unique method of delineating fixed breeding zone boundaries according to rates of change in adaptive variation for black spruce. The focal point seed zone methodology was used to plot grids of predicted factor scores and a differential systematic coefficient (DSC) was used to determine rates of change in clinal variation across the study area. Values were plotted using a GIS to identify areas of rapid change that can be used to delineate breeding zone boundaries. Although the results corresponded to those of previous studies for black spruce, the authors note that the DSC approach is only useful in areas where abrupt changes in adaptation occur; in areas where adaptive variation changes are gradual, then differences will not be revealed.

Hamann *et al.* (2000) used ordinary kriging to predict performance of red alder based on provenance means at four test sites across British Columbia. Trend surfaces were generated to predict performance at each of the four test sites and principal components analysis was used to reduce the data to two dimensions. The factor scores were then graphed and seed zones could be determined by identifying families from neighboring localities with similar PC factor scores. Variance surfaces obtained from the ordinary kriging process were then used in combination with predicted performance surfaces to generate a new set of seed zone maps, based on the probability of a seed source performing above or below a specified value.

The importance of validating models of species adaptive variation has been suggested by numerous authors throughout the last several decades (Rehfeldt 1991; Li *et al.* 1997). Rehfeldt (1991) was among the first to validate seed transfer models for North American conifer species using independent data. In his 1991 study of Ponderosa pine, Rehfeldt correlated predicted values of performance variables based on regression models to observed performance variables obtained from an independent field test of 54 provenances in northern Idaho. The results indicated that provenance mean heights at the Idaho test were significantly correlated to predicted 3-year height and the first principal component. Several additional significant correlations were also obtained, supporting the validity of the regression models.

Li *et al.* (1997) also used independent data from older white spruce field trials to validate their regression models. Height and survival data from seven field trials in Quebec were correlated to predicted factor scores generated from the previous regression models, as well as to the estimated relative risk of seed transfer. The

correlations between relative risk and survival variables from independent field trials were expected to be negative, because a higher probability of maladaptation of the source to the transfer location should manifest as reduced survival over time. Correlations with survival variables were weak but negative for all but the two northernmost sites, indicating that regression models were not suitable for extrapolation to those areas.

Beaulieu *et al.* (2004) used a similar method to validate models of seed transfer risk for black spruce in Quebec. Principal components analysis was conducted using the genetic covariance matrix calculated from growth and phenology data from 30 provenances of juvenile field tests. Following, PC factor scores were regressed against geoclimatic variables. The resulting models were used to predict scores of the first two PC axes for local and transferred sources at four independent mature provenance trials. The relative risk of seed transfer was then calculated as the degree of mismatch between the local and transferred populations. Correlations between relative risk and phenotypic deviation from the local source indicated that the regression models were appropriate only for application to the two southernmost test sites, and should not be extrapolated north of 48° latitude.

Parker (2000) defines the problem of delineating breeding zones as balancing the size of breeding zones to control maladaptation while ensuring that breeding efforts are not duplicated between adjacent zones; zones must be small enough to minimize maladaptation by controlling the genotype x environment interaction and large enough to ensure that seedlings would not achieve similar gains in adjacent zones (Parker 2000, Crowe and Parker 2005). Recently, several authors have chosen to address the problem

of balancing adaptation with administrative and economic constraints by structuring it as a mathematical operations research problem.

O'Neill and Aitken (2004) presented an optimal method of delineating breeding zone boundaries. They used a method similar to that of the focal point seed zone methodology to determine patterns of adaptive variation in relation to climate and to map predicted factor scores for interior spruce in British Columbia. Areas were assigned to one of a set-number of breeding zones using a disjoint clustering algorithm designed to minimize the average maladaptation across the region. The results demonstrated that overall maladaptation was markedly reduced in comparison to previous methods of delineating breeding zones (Hamann *et al.* 2000) and was particularly suited for use in areas of extreme environmental heterogeneity such as the mountainous areas of BC.

Crowe and Parker (2005) developed an optimal method of delineating breeding zones based on demonstrated patterns of species' adaptive variation. By likening the problem of delineating breeding zones to that of a conventional maximal-covering problem in operations research, the authors devised a model capable of maximizing the total number of geographic points in an area covered by a limited number of breeding zones, while placing limits on the adaptive dissimilarity within zones. In contrast to the work of Rehfeldt (1982, 1983a, 1983b, 1983c, 1991), Crowe and Parker (2005) used a probability of 0.05 to calculate LSD values in constructing jack pine breeding zones, and found that increasing the probability to 0.2 reduced the size of delineated zones by 40-45%.

The approach of Campbell (1979 and 1986), Rehfeldt (1982, 1983a, 1983b, 1983c, 1991) and subsequently Parker (1992, 1996a, 1996b) was to minimize the risk of maladaptation due to seed transfer given the assumption of local adaptation (Lindgren and Ying 2000). However, recent methods have presented seed transfer models aimed at maximizing productivity and do not require the assumption of the local optima (Lindgren and Ying 2000; Raymond and Lindgren 1990; Roberds and Namkoong 1989).

Raymond and Lindgren (1990) developed a mathematical model that could be used to predict the performance of a seed source across a range of environmental conditions. White ash and scots pine seed source performance values were plotted against environmental variables, such as latitude and precipitation, and the plots suggested that quadratic polynomial functions may be appropriate to describe seed source response across an environmental gradient. However, the authors chose to adopt a new function that would be more biologically meaningful and easier to interpret. This response curve, named the Cauchy function, was shown to produce a slightly better fit than quadratic response functions. The width of this curve could be used to determine the relative breadth of environments across which a seed source could be planted in order to achieve a specified percentage of its maximum growth, while the value at which the curve peaked (maximum growth) could be used to determine the optimum planting environment for the source.

Roberds and Namkoong (1989) used Cauchy response functions to determine the combination of 2, 3, and 4 populations that could be used to maximize value of a single trait across a known distribution of environments. Their method was based on the philosophy that by restricting the number of breeding populations, the cost of producing

improved seedlings could be reduced. Response functions were used to determine the environmental distribution of populations, and from these response functions the combination of sources which was best able to maximize value for the entire range of planting locations was selected. With fewer numbers of selected populations, the range across which each source must be planted increased, causing performance to decline in peripheral environments. Thus, the expected value was shown to increase with the number of selected populations.

CLIMATE CHANGE: MODELS, UNCERTAINTY, AND EVALUATION

The Intergovernmental Panel on Climate Change (IPCC) states that "warming of the climate system is unequivocal" (IPCC 2007a). Over the last century, increases in anthropogenic greenhouse gas emissions have caused widespread warming of the earth surface and more frequent occurrence of drought. Temperatures between 1995 and 2006 were among the highest on record and the rate of warming for the last 50 years has been nearly twice that of the last 100 years. Over the next two decades, the climate is predicted to continue warming at a rate of 0.2°C per decade (IPCC 2007a).

While the IPCC (2007b) notes that there is considerable confidence in model projections at the continental scale, projections at smaller or more regional scales are considerably less accurate. Thus, many regions have developed their own smaller-scale models or developed methods of downsizing global models to obtain more accurate regional predictions. Three GCMs are currently available at high-resolution for Canada (McKenney *et al.* 2006) and include: the Commonwealth Scientific and Industrial Research Organization (CSIRO) model (Gordon and O'Farrell 1997), the 2nd coupled

global climate model (CGCM2) model (Flato and Boer 2001), and. The Hadley Centre for Climate Prediction and Research (HADCM3) model (Pope *et al.* 2000).

The CSIRO model is described by Gordon and O'Farrell (1997). In contrast to HADCM3, the CSIRO model uses flux adjustments. Flux adjustments are used to control what is known as climatic drift, or the difference between simulated and observed climate using models. Thus, flux adjustments are used to approximate observed data to improve model accuracy. A simulation of global warming based on 1% increase in CO2 compounding each year predicted a 2°C increase in mean annual temperature. However, warming was greater in the northern hemisphere than in the south, producing a pattern referred to as "asymmetrical warming" that is typical of many models.

The first GCM developed by the Canadian Centre for Climate Modeling and Analysis was referred to as CGCM1 (Flato and Boer 2001). CGCM1 produced what is known as asymmetrical warming, with future climate simulations predicting higher temperatures in the extreme northern latitudes than in the southern. This simulated pattern was the result of greater uptake of heat into the Southern Ocean than in the north; however, the asymmetric warming pattern was in disagreement with observed trends for the 20th century. The CCMA revised the ocean-mixing parameter to reduce the pattern of deep-convective mixing in the Southern Ocean to provide more realistic estimates, and named the enhanced model CGCM2. The newer model did, in fact, reduce the amount of heat sequestered by the southern ocean, resulting in a more symmetrical warming. Both CGCM1 and CGCM2 were used to simulated average observed temperatures from 1990-1995 and it was found that CGCM2 simulations made great

improvements in predictions across the far southern hemisphere in comparison with CGCM1, but were slightly less accurate across the north (~55-45°N). However, despite the change in ocean mixing parameterizations, no change in the global mean annual temperature was observed between CGCM1 and CGCM2.

The Hadley Centre coupled climate model (HADCM3) was first presented by Gordon *et al.* (2000). The HADCM3 model is an improved version of an earlier model (HADCM2) with improved atmospheric and oceanic modeling. The model no longer requires flux-adjustments to control climate drifts. The ocean resolution is improved in comparison with the previous model, leading to better simulation of heat transfer processes.

There are two main sources of uncertainty in modeling future climate; these are scenario uncertainty and modeling uncertainty (Rivington *et al.* 2008). Scenario uncertainty originates from the fact that exact estimates of future warming are not possible because it is not certain what the actual rate of greenhouse gas emissions will be. Modeling uncertainty, however, is related to the fact that models produce varying estimates of future warming even when based on the same emissions scenario. These differences arise because models use various methods of accounting for the key physical processes which affect climate.

To account for scenario uncertainty, the IPCC developed a series of 40 emissions scenarios belonging to 4 overarching scenario families (Nakicenovic and Swart 2000). These scenarios describe a range of possible future greenhouse gas emissions rates resulting from different social and economic environments and are referred to as A1, B1, A2, and B2. The A1 scenario is relatively moderate, describing a

more advanced society with rapid economic growth, more efficient technology, and low population growth, and carbon dioxide emissions ranging from relatively low to high. In contrast the A2 scenario is the most pessimistic, predicting very high population growth, slow economic development and technological change, and high greenhouse gas emissions. The B1 scenario is probably the most optimistic of the four scenarios, predicting low population growth, high economic growth and technological change emphasizing clean technologies. Greenhouse gas emissions are the lowest of the four scenarios. Finally, the B2 scenario is the most neutral of the four scenarios, predicting intermediate values of population growth, economic growth, technological change, and greenhouse gas emissions. Best estimates of future temperature increases based on the four separate families of emission scenarios vary widely; from 1.8°C based on the B1 scenario, to 4.0°C based on the A1 scenario (IPCC 2007a).

Modeling uncertainty is best accounted for by model evaluation; simulations of current or past climates can be compared to observed data to evaluate model accuracy (IPCC 2007b). Models that are better able to predict present or past climate are expected to be more accurate in predicting future climate, because they account for important physical processes. A recent project comparing 15 coupled atmosphere/ocean general circulation models (AOGCMs) revealed that these models vary widely in their ability to simulate current climate (Lambert and Boer 2001). Some models were better able to predict temperature, while others were better at predicting precipitation. Thus, the authors concluded that no one model is "best" in predicting future climate under global warming. Rather, the mean obtained when averaging over all models was better able to simulated observed climate data.

EFFECT OF CLIMATE CHANGE ON FOREST TREES

Aitken *et al.* (2008) note three possible responses of forest trees under rapid climate change; these are adaptation, migration, or extirpation. However, given the rapid rate of climate warming, both adaptation and migration will likely be unable to keep pace and populations will suffer reduced fitness and increased mortality in the absence of human intervention. Etterson and Shaw (2001) found that antagonistic relationships between genetically correlated traits would retard the rate of adaptation to climate change. A population of *Chamaecrista fasciculata* (Michx.) transferred southward from Minnesota to Kansas and Oklahoma was found to demonstrate much slower adaptation towards increased rate of reproduction and leaf thickness than predicted by evolutionary response values for each trait. Also, the Minnesota population demonstrated much lower fecundity in comparison to its native environment. This delayed adaptation was shown to be the result of a negative genetic correlation between leaf number and reproductive stage and a positive correlation between leaf number and leaf thickness. Thus, selection towards lower leaf number results in a higher rate of reproduction but lower leaf thickness. The authors estimate that it would take the Minnesota population 21, 42, and 79 years based on reproductive stage, leaf number, and leaf thickness, respectively, to adapt to the climate of Kansas. This same climate is expected to occur in Minnesota in 25-35 years; thus, the time required to reach adaptation far exceeds the rate of climatic change.

Iverson *et al.* (2008) studied the response of 134 tree species of the eastern United States to climate change and found that 66 of the species would experience more than 10% increase in suitable habitat and 54 would incur a loss of over 10%. Analysis

of the location of the mean centers of species habitat revealed that, under both low and high emissions scenarios, the majority of species habitats shift northeast. However, the magnitude of the shift was generally much greater under the highest emission scenario, with habitat shifts of up to 800 km for the most extreme warming scenario. Maps showing the resulting forest species compositions for each scenario revealed that northern forest types were most greatly affected; the spruce-fir forest was present only in the most moderate warming scenario while the white, red, and jack pine forests were eliminated under all scenarios.

A similar study was conducted using climate envelope models for 130 North American tree species to predict the change in habitat availability under 6 scenarios of future warming; CGCM A2&B2, HADCM3 A2&B2, CSIRO A2&B2 (McKenney *et al.* 2007). Assuming full-dispersal, the average species habitat was predicted to decrease 12% and shift northward by 700 km, with 72 species showing a decrease in habitat and the remaining 58 showing an increase. Those species which demonstrated the greatest increases in future habitat were generally found in the eastern United States and the west coast. Under a scenario precluding species dispersal, the average decrease in habitat was 58% accompanied by a northward shift of the mean centre by 330 km.

Northward range shifts of species during periods of warming, such as after the last period of glaciation, are well-documented (Davis and Shaw 2001). Rates and direction of migration can be expected to differ among species; under warming ranging anywhere from several degrees over a few decades to 1 degree per millennium, migration rates generally ranged between 20-40 km per century. In contrast, the current rate of warming is predicted to be 2.4-6.4°C over the next century (IPCC 2007b),

requiring northward shifts of several hundreds of kilometers (Iverson *et al.* 2008; McKenney *et al.* 2007). Additionally, human-caused barriers to migration due to land-use change and establishment into already occupied habitats will impede natural migration rates (Etterson and Shaw 2001). Thus, we can expect that species will be unable to track the current rate of warming.

For populations condemned to persist in current habitats under global warming, the response is largely predicted to be negative (Cherry and Parker 2003; Matyas 1997; Matyas and Yeatman 1992; Rehfeldt *et al.* 1999; Schmidtling 1994). However, the response to climate differs between populations within a species, and thus, the response to climate change can be expected to vary depending on the population examined (Matyas 1997). In this respect, provenance trials may be used to obtain information about species' climatic adaptation that can be used to predict the effects of environmental change. By analyzing differences in seed source performance and relating these differences to the climate conditions at provenance origin, researchers are able to interpret species or population response across an environmental gradient. These response patterns can be modeled and used to predict the effects of environmental or climatic change on the future performance of a species or population.

A provenance study conducted for 20-year-old loblolly pine (*Pinus taeda* L.) and Norway spruce (*Picea abies* L. Karst) showed that average yearly temperature increases of 4°C would result in a 5 to 10% loss of height growth for both species when compared with growth of a genetically-adapted (local) source (Schmidtling 1994). Average annual minimum temperatures were found to be the strongest predictor of height growth, explaining between 30 and 75% of the variation between seed sources.

In addition, latitude, mean temperature, and frost-free days were found to be significantly correlated to seed source performance. Precipitation was not significant in explaining variation between seed sources, presumably because precipitation is relatively constant through the eastern part of the range of loblolly pine.

A study of within-species variation of ponderosa pine in California examined the relationship between climate and height at 12 years of age (Matyas 1997). Temperature and elevation were found to correlate most strongly with seed source height. When quadratic regressions were plotted for height against ecodistance, the response surface demonstrated similarity to results previously shown for jack pine (Matyas 1994). Mild decreases in temperature were generally not shown to have a negative effect on height growth. In fact, populations transferred north from warmer environments performed better than the local seed source while populations transferred south demonstrated "a consistent and marked height loss" at mid-elevations. Matyas (1997) hypothesized that other consequences of maladaptation would arise as temperatures increase including susceptibility to snow break and loss of resistance to pests and disease. The author further concluded that increases in temperature would lead the reduction and extinction of ponderosa pine at low elevations as it loses competitive advantage to other species while increases in temperature would improve productivity at upper-elevations.

Beuker and Koski (1997) conducted a study of provenance trials of 60 year-old Norway spruce and 24 year-old scots pine (*Pinus sylvestris* L.) and found that stem wood production of northern seed sources was considerably larger when such sources were moved to southern test sites. Present climate warming scenarios predict

temperature increases that would result in an increase of wood production of almost 300% for Norway spruce presently located within northern Finland but a drastic decrease for sources originating from southern Finland. Increases of approximately 40% were predicted for northern scots pine sources while small decreases were predicted for southern sources.

Over a 5-year observation period, northern seed sources were shown to be more sensitive to climate warming as spring bud flush was observed to occur up to two weeks earlier than for southern sources during mild springs (Beuker and Koski 1997). In comparison, both northern and southern seed sources flushed simultaneously during average springs. Onset of winter frost-hardiness was also observed, and it was shown that development of frost-hardiness commences earlier in the fall for northern seed sources of Norway spruce in comparison with southern sources. Frost-hardiness varied throughout the winter with changes in ambient temperature but neither northern nor southern sources demonstrated premature dehardening. No variation in hardiness was shown for scots pine during the winter, and hardiness remained even in temperatures below –40°C.

Matyas (1994) used range-wide jack pine provenance trial data to predict the effect of climate warming on the performance of jack pine seed sources. Response functions were used to estimate the growth of seed sources when transferred southward to imitate an increase in summer temperatures of 4°C. When northern sources were moved southward to the Petawawa, Ontario test site height increases of up to 20% were realized. However, when the local source from Petawawa was transferred south to Turkey Point, the increase in summer temperatures resulted in a 20% loss of height

growth. Similarly, Thomson and Parker (2008) found that southern and central jack pine provenances were currently growing at or above optimal temperatures, and could be expected to suffer reduced productivity under climate change. However, northern sources were growing below optimal temperatures and would benefit from increased temperatures in the future.

A similar study conducted for black spruce used range-wide black spruce provenance data to develop population response functions and to predict the location of optimal seed source height growth under present and future climate conditions (Riddell 2004). Mean monthly temperatures, specifically winter and spring-summer temperatures, were found to be the most effective predictors of seed source performance, whereas precipitation was a poor predictor. Response functions indicated that northern sources would currently benefit from a southward transfer and will likely demonstrate increased growth under global warming, provided that other conditions do not become limiting. Central and southern sources were generally growing at or near their optimum and thus would suffer from increases in temperature in the future.

Lenihan and Neilson (1995) predicted that the area occupied by white spruce under a doubling of CO2 scenario will decline by 20-30% and that the range will shift considerably northward. Cherry and Parker (2003) used quadratic models to determine locations of optimal growth sites of white spruce provenances, as well as to predict future locations under climate change. Growth and survival data were regressed against temperature and precipitation variables to determine values at which the growth of individual provenances could be maximized. Mean January maximum temperature and May precipitation were found to be among the strongest predictors of provenance

performance and were used to map the location of current and future optimal growth from Ontario climate coverages. Under present conditions, northern populations performed better when moved south and southern sources generally performed better when transferred north. Optimal growth locations were predicted to shift north by about 2° latitude due to climate warming, indicating that the majority of central and southern white spruce populations would suffer reduced growth under climate change.

A study of 45 provenances of white spruce in Quebec revealed that populations were expected to suffer decreases in growth under temperature increases of 1-4°C (Andalo *et al.* 2005). Univariate and bivariate quadratic transfer models were developed to describe the relationship between provenance height and diameter to each of 7 climate variables. Regressions revealed maximum daily temperature to be among the best predictors of height and diameter, accounting for 14% and 13% of the total variation, respectively. Models including total summer precipitation were much better predictors of white spruce performance, accounting for 34% and 21% of the respective variation. Transfer functions revealed optimal growth of local populations based on temperature, but sub-optimal growth based on precipitation; transfer to drier environments yielded increased growth for all populations.

Carter (1996) used the concept of transfer distance, defined as the difference in annual minimum temperature between a source and transfer location, to construct quadratic transfer functions for 10 north temperature species. These functions revealed that an increase in annual minimum temperature of 4°C was predicted to reduce growth by 1.6-6.9% for 8 of the 10 species. Of these, white spruce was predicted to suffer a 3.7% reduction in height growth.

CHAPTER II: GENECOLOGY AND PATTERNS OF ADAPTIVE VARIATION IN WHITE SPRUCE

INTRODUCTION

The development of adaptively-based seed transfer guidelines depends on sufficient knowledge of patterns of adaptive variation within species (Parker 2000). Provenance tests provide data describing species response across an environmental gradient, which can then be used to develop models to relate performance to any number of geographic or climatic variables to develop seed or breeding zones (Campbell 1979, 1986).

The focal point seed zone methodology (FPSZ) presented by Parker (1992, 1996a, 1996b) provides a means of delineating continuous seed zones for any specified point within a geographic area. The approach uses principal components analysis of measured growth and phenological variables, followed by multiple linear regression against climatic variables to map patterns of genetic variation within a species. This data can be used in combination with GIS to determine unique seed zones for any specified site for reforestation. One challenge in developing these zones, however, is that the use of principal components analysis requires full replication of each provenance at each test site (Lesser 2005). However, few mature provenance trials contain seed sources duplicated across the range of tests because each site tends to have a greater representation of local sources. To facilitate focal point seed zones analysis for white spruce, a series of six provenance tests was established across Ontario in 2002. Each test site provided full replication of 127 provenances from across Ontario and western Quebec. Subsequent measurements of seedling growth and phenological variables in

2003 and 2004 were used to develop focal point seed zones for Ontario (Lesser 2005).

This chapter presents additional measurements for the same series of provenance trials taken in the summer of 2007. The goal of this chapter is to examine patterns of adaptive variation in growth traits measured in 2007, which will be combined with previous data to update the focal point seed zone model for white spruce in Ontario. The updated seed zone model will be used in the following chapter to develop candidate breeding zones for white spruce across Ontario.

METHODS

TEST ESTABLISHMENT AND DATA COLLECTION

Beginning in 2001, seed of 5 open-pollinated families from each of 127 white spruce provenances from across Ontario and western Quebec were collected with the help of several cooperating organizations including: the Canadian Forest Service (CFS), the Ontario Ministry of Natural Resources (OMNR), Kimberly Clark, Weyerhauser, and Lakehead University (Lesser 2005; Lesser and Parker 2004).

Seeds were sown between January and March 2002 in Jiffy pots in the Lakehead University greenhouse. Germinated seedlings were organized into a completely randomized design for each of 6 trials; each with 3 blocks and 10 single-plot repetitions of each of the 127 provenances located randomly within each block. Two rows of border trees were also placed around the periphery of each block to minimize edge effects.

Trees were hardened-off and outplanted to each of five field trials located in Dryden, Kakabeka, Longlac, Englehart, and Petawawa in the summer of 2002, while the remaining trial was retained within the Lakehead University greenhouse (Lesser and Parker 2006). In the fall of 2003, the greenhouse trial was outplanted to a field site at Angus, Ontario. A map illustrating provenance and test locations is presented in Figure 1 and geographic coordinates of provenances and test locations are presented in Table 1 and Table 2 respectively.

Seedling measurements of height and survival were taken at each trial in 2002, but were not indicative of site differences as the trees were hardened off before planting

(Lesser and Parker 2006). Thus, height measurements from each test were pooled to create a single variable, as were survival values. A series of growth and phenological variables were measured in the following summers of 2003 and 2004. Variables included: seedling height, root collar diameter, and survival at all tests in both years, greenhouse elongation in 2003, and dates of spring budflush and fall budset at each of the field trials in 2003. Each variable at each test site for each year was considered separately, totalling 94 biological variables collected from 2002 through 2004. These data are presented in previous studies (Lesser 2005; Lesser and Parker 2004; Lesser and Parker 2006) and will not be presented in great detail within the current study.

In the summer of 2007, all trials were remeasured for height (cm), current increment (cm), root-collar diameter (mm), and survival (%). These variable measurements were obtained specifically for the purpose of this study to augment previous data and will be presented in more detail in the results to follow. Following sections will present results of analyses based on both current and previous measurements combined.

CLIMATE DATA

Thirty-year climatic averages for the period 1961 to 1990 were provided by Dr. D. McKenney of the Landscape Analysis and Application Section (LAAS), Great Lakes Forestry Centre (GLFC), Sault Ste. Marie, Ontario (McKenney *et al.* 2007). Point data for each of the 127 provenance and 6 test locations, as well as grid coverages (10 km resolution) for the Ontario study area, were provided for each of 36 climate variables including: mean monthly minimum and maximum temperatures, as well as monthly

precipitation. For the purposes of this study, the 1961-1990 climate averages are used to represent current climate in Ontario and are herein referred to as current climate, observed climate, or 1961-1990 normals.

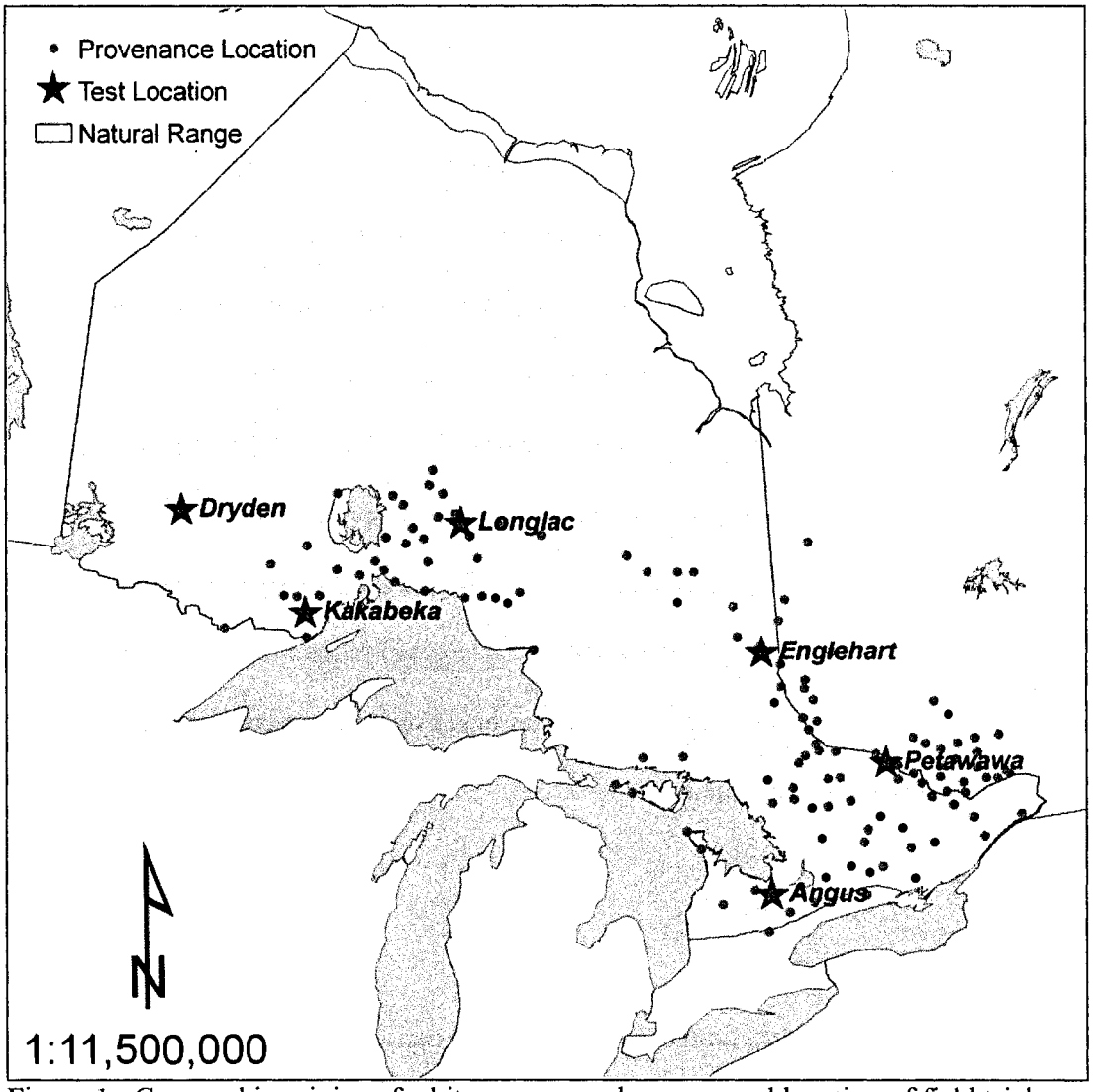

Figure 1. Geographic origins of white spruce seed sources and location of field trials.

Table 1. Geographic coordinates of 127 white spruce provenances

Prov. No.	Lat. (dd)	Long. (dd)	Elev. (m)	Location	Prov. No.	Lat. (dd)	Long. (dd)	Elev. (m)	Location
1	45.07	74.83	80	Cornwall	44	47.70	78.40	305	Canton Sebille
2	45.67	74.97	155	St-Andre Avellin	45	45.87	78.45	442	Lister
3	45.73	75.05	152	St-Andre Avellin	46	46.25	78.50	183	Canton Cameron
4	46.25	75.08	259	Camp 27	47	45.87	78.70	442	Osler
5	45.62	75.23	100	Thurso	48	49.35	78.70	289	Lac Wawagosis
6	45.65	75.45	15	Poupee	49	46.72	78.83	335	Lac Smith
7	46.03	75.57	213	Lac Iroquois	50	46.28	78.85	229	Rutherglen
8	46.25	75.58	304	Ruisseau Murphy	51	47.03	78.87	335	Baie Kelly
9	45.82	75.60	168	Val-Des-Bois	52	46.38	78.90	305	Mattawan Tp
10	44.83	75.63	100	Augusta	53	44.47	78.92	280	Eldon
11	45.12	75.80	90	Marlborough Tp	54	45.03	78.93	335	Hindon Tp
12	45.47	75.92	107	Breckenridge	55	47.33	79.00	305	Canton Gaboury
13	45.62	75.93	244	Wakefield	56	46.60	79.02	306	Jocko Tp
14	46.20	75.95	183	Bouchette	57	47.20	79.03	305	Lac Guay
15	45.97	76.03	152	Aylwin	58	45.47	79.08	370	Sinclair Tp
16	46.63	76.07	244	Grand-Remous	59	46.78	79.12	305	Canton Mercier
17	45.32	76.18	121	Antrim	60	46.23	79.13	245	Bonfield Tp
18	45.52	76.30	91	Wyman	61	44.12	79.18	290	Scott
19	46.15	76.33	274	Lac Cayamant	62	46.13	79.27	275	Chisholm
20	46.85	76.35	305	Lac Du Faucard	63	48.53	79.30	224	Lac Hebecourt
21	45.75	76.40	213	Ladysmith	64	45.78	79.42	381	Strong
22	46.25	76.63	274	Lac Usborne	65	45.62	79.42	300	Armour Tp
23	45.47	76.63	121	Renfrew	66	48.22	79.48	289	Lac Labyrinthe
24	44.82	76.68	180	Silver Lk	67	47.58	79.50	213	N.Dame des Quinze
25	45.68	76.80	137	Beachburg	68	47.25	79.52	240	Lorrain Tp
26	45.90	76.27	244	Grove Creek	69	45.48	78.75	460	Peck Tp
27	46.35	76.87	274	Riviere-Coulonge	70	47.03	79.68	306	Cobalt
28	45.83	76.95	122	Lac Cranson	71	45.58	79.87	275	McKellar
29	44.33	77.13	107	Tyendinaga	72	47.87	79.92	215	Englehart
30	44.78	77.15	274	Barrie	73	45.92	79.93	245	East Mills
31	45.97	77.25	152	Sheenboro	74	43.75	80.12	427	Erin
32	45.08	77.28	305	Denbigh	75	44.35	80.33	503	Osprey
33	45.77	77.28	150	Alice	76	48.03	80.37	304	Kirkland Lk
34	45.98	77.45	160	PNF	77	48.48	80.42	290	Bowman Tp
35	46.17	77.67	183	Rolphton	78	44.17	81.00	305	Bentinck
36	45.27	77.70	366	Carlow	79	49.02	81.23	289	Clute 2
37	44.55	77.75	229	Marmora	80	49.77	85.42	245	Pagwa
38	45.10	77.97	396	Bancroft	81	49.03	81.58	215	Fraserdale
39	44.48	78.02	236	Dummer	82	48.58	81.62	290	Robb Tp
40	44.92	78.07	365	Anstruther Tp	83	45.25	81.63	206	St. Edmunds
41	44.17	78.12	274	Haldimand	84	46.32	81.65	243	Nairn Tp
42	45.53	78.27	396	Whitney	85	49.05	82.25	215	Gurney Tp
43	44.60	78.38	300	Harvey	86	46.33	82.50	249	Proctor

Table 1. Continued.

Prov. No.	Lat. (dd)	Long. (dd)	Elev. (m)	Location	Prov. No.	Lat. (dd)	Long. (dd)	Elev. (m)	Location
87	49.30	82.70	289	Cargill	108	49.55	87.18	404	Grandpa Rd
88	45.83	82.75	191	Elizabeth Bay	109	49.70	87.42	365	Jellicoe
89	45.95	83.08	183	Meldrum Bay	110	49.47	87.57	460	Parks Lk
90	49.62	84.58	275	Arnott Tp	111	50.03	87.65	305	S Onaman R
91	47.92	84.75	306	Wawa	112	48.91	87.77	195	Mountain Bay
92	48.78	85.05	457	Bouchard	113	50.15	87.88	335	Auden
93	48.62	85.32	305	White R	114	49.55	88.00	365	Beardmore
94	49.77	85.47	236	Highway 11	115	49.07	88.02	245	Limestone
95	48.70	85.58	305	Mobert Tp	116	49.20	88.22	229	Nipigon
96	48.72	85.87	335	Strathearn	117	48.98	88.54	267	Stewart Lake
97	49.28	85.97	305	Manitouwadge	118	49.05	89.05	275	Chief Bay
98	49.60	86.15	305	Caramat	119	50.15	89.12	305	Waweig L
99	48.70	86.25	240	Pic R	120	48.65	89.41	457	LU Woodlot
100	49.92	86.48	305	Kenogami	121	48.02	89.65	306	Pigeon R
101	50.20	86.78	335	Nakina	122	49.37	89.75	425	Twist L
102	49.87	86.87	365	False Crk	123	48.62	89.90	410	Shabaqua
103	50.53	87.02	335	O'Sullivan	124	48.62	90.18	459	Shebandowan
104	49.22	87.07	335	Long Lake	125	49.07	90.52	489	Upsala
105	50.32	87.09	328	Maun/Anaconda Rd	126	48.07	91.42	428	Eva L
106	44.98	81.37	191	Eastnor	130	44.00	79.67	240	King
107	48.78	87.12	200	Terrace B					

Source: Adapted from Lesser and Parker (2004)

Table 2. Geographic coordinates of 6 white spruce test sites.

Test	Lat. (dd)	Long. (dd)	Elev. (m)
Angus	44.30	-80.00	229
Petawawa	46.05	-77.47	160
Englehart	47.79	-79.87	252
Kakabeka	48.41	-89.70	360
Dryden	49.77	-92.59	375
Longlac	49.81	-86.35	355

STATISTICAL ANALYSIS

A preliminary examination of the 2007 height, elongation, and root collar diameter measurements was conducted to identify and correct any errors that may have occurred during data entry. The data were screened for the assumptions of normality, including skewness and kurtosis values, and any variables indicating a significant departure from normality were transformed.

Test means and standard deviations of height, elongation, root-collar diameter, and survival were calculated using the means procedure of SAS software (SAS Institute Inc. 2000). Following, two-way analysis of variance (ANOVA) was performed separately for each growth variable and test site using the SAS GLM procedure to determine if significant differences in provenance growth and survival were demonstrated. All effects were considered random. The linear model used was:

$Y_{ijk} = \mu + A_i + B_j + AB_{ij} + \varepsilon_{ijk}$

where: i = 1 to 127 seed sources

j = 1 to 3 blocks per test site

k = 1 to 10 replicates per seed source per block

Y_{ij} = measured variable value of replication k of seed source i in block j;

μ = the population mean;

A_i = the random effect of seed source i;

Bj = the random effect of block j;

$ABij$ = the random interaction effect of the ith seed source with the jth block; and

ε_{ijk} = the random error effect of replication k of provenance i in block j

One-way ANOVAs for survival were calculated using a similar procedure; however, the linear model was modified to account for the lack of within-block repetitions. The model used was:

$$Y_{ij} = \mu + A_i + \varepsilon_{ij}$$

Where: i = 1 to 127 seed sources

j = 1 to 3 replicates (blocks) per test site

Y_{ij} = measured variable value of replication j of seed source i;

μ = the population mean;

A_i = the random effect of seed source i;

ε_{ij} = the random error effect of replication j or provenance i

Components of variation were estimated using the restricted maximum likelihood method (REML) of the Varcomp procedure of SAS. Intraclass correlation coefficients (ICC), used to describe the percent of total variation attributable to provenance effects, were then calculated for each variable and test site (Lesser and Parker 2004):

$$I.C.C. = \left(\frac{\sigma^2 \ provenance}{\sigma^2 \ provenance + \sigma^2 block + \sigma^2 prov \ x \ block + \sigma^2 \ error} \right) x \, 100\%$$

All measured variables with significant probability values ($P < 0.05$) were retained for further analyses. The regression (REG) procedure of SAS software was used to generate a series of simple linear regressions relating provenance means for each significant biological variable to each of 36 climate variables. The simple linear regressions were used to determine whether the observed variation in phenotypic

variables could be attributed to climatic factors. Thus, the ANOVAs in combination with simple linear regressions were used to identify variables which demonstrate clear geographic or climatic patterns and can therefore be considered adaptive in nature (Lesser and Parker 2006).

Measured data for 2007 growth and survival variables were combined with 2002-2004 growth and phenological data for the same tests presented by Lesser and Parker (2006). These variables include 2002 greenhouse height and elongation, 2003 and 2004 height, root collar diameter, and survival, as well as bud flush and budset timing in 2003. However, only those variables which were demonstrated to be adaptive in nature were retained.

The principal components (PRINCOMP) procedure of SAS software was used to summarize the main components of variation in growth and phenological variables. The variance proportions explained by each axis were plotted and used to determine the inflection point past which additional axes account for relatively small portions of variation. All principal components axes up to and including the inflection point were retained for further analysis.

Least significance difference values for each principal components axis were approximated using a weighted average of LSD values of the original variables (Crowe and Parker 2005). The raw LSD values (α=0.05) of each original variable were determined from the analysis of variance output and were divided by their standard deviation values to express the LSD as a number of standard deviations. Standardized LSD values for each original variable were then multiplied by their respective variable loadings (absolute value), summed, and then divided by the sum of the absolute loadings

to produce a weighted average. These values were multiplied by PCA scores, thus converting standard deviation values to LSD values.

Normalized provenance factor scores for each main axis of variation were used in multiple linear regression against each of the 36 climate variables to determine which linear combinations of climate variables explained the largest proportion of variation in each PCA axis. The R^2 selection method of the SAS regression (REG) procedure was used to select 5 alternate combinations of 1, 2, 3, and 4 climate variables that accounted for the highest proportion of variation in each main PCA axis. From the alternate combinations, regressions with the highest R^2 value and acceptable tolerance values (tolerance >= 0.1) were selected to model the main PCA axes.

The parameter values obtained for each selected regression equation were used to generate contoured grids of predicted factor scores for each main PC axis using geographic information systems (GIS). Specifically, each climate grid was multiplied by its corresponding parameter value and the resulting cell values were added or subtracted from one another according to the specified regression equation. The resulting maps display contours of predicted factor scores for the main PC axis based on the modeled regressions. The grid algebra necessary to this procedure was performed using the grid subpackage of ArcGIS software (ESRI 2006).

The focal point seed zone method was then used to generate unique seed zones for each of 618 focal points located across Ontario, based on a 40 km x 40 km grid coverage (Crowe and Parker 2005; Parker and van Niejenhuis 1996a; Parker and van Niejenhuis 1996b). The focal point seed zones program (APPENDIX III), uses Arc Macro Language (AML) programming (ESRI 2006) to manipulate the grids of predicted

principal components factor scores. XY-coordinates for each focal point are specified in an input file. For each focal point, the predicted factor score on each PC grid is retrieved and subtracted from the value of all other cells in the grid to produce 3 adjusted grids of PC factor scores; one for each main axis. The result is three predicted factor score grids, each with a cell value of 0 at the selected point. Areas within a specified adaptive distance of the focal point (+/- 0.5 LSD or +/- 1.0 LSD) are determined for each adjusted grid and are then intersected to produce the unique seed zone for each focal point (Crowe and Parker 2005). Six of the 618 focal point seed zones constructed for Ontario are presented as examples in the results to follow.

RESULTS

LEVELS OF VARIATION

Significant departures from normality were observed for several 2007 variables including: Dryden elongation, Englehart elongation, Longlac height, elongation, diameter, and survival at Angus, Dryden, Kakabeka, and Longlac. Percent survival variables were transformed using the Arcsin transformation as per Lesser (2005), while the remaining variables were normalized using various polynomial functions. However, even after normalization these variables yielded highly non-significant P-values. Therefore, statistical measures for these variables are presented for the original, non-transformed values.

Large variation in test means was observed for each variable; mean height ranged from 38.3 to 68.4 cm for the Dryden and Kakabeka test sites, respectively (Table 3), while mean elongation ranged from 3.0 cm for Dryden to 18.6 cm for Petawawa. Mean diameters ranged from 10.7 mm at the Angus test site to 18.0 mm at Englehart. Mean survival by test was extremely variable, ranging from 65.4% at the Englehart site to 93.5 % at the Kakabeka site. Survival at the Longlac test site was extremely low, with only 255 individuals remaining (6.4% overall survival), due to herbicide damage in the summer of 2004.

Fourteen of the twenty-four biological variables measured in 2007 demonstrated significant variation in provenance means. Significant variation in provenance height and diameter was present at all tests, excluding Longlac, while provenance mean

survival was significant only for the Englehart test site. Mean elongation by provenance was significant at the Angus, Kakabeka, and Petawawa test sites. A measure of significance for survival at the Longlac test site could not be calculated due to the lack of block repetitions.

ICC values for height were generally the highest of the four variables, with provenance effects explaining between 2.6 and 9.3 % of the total variation in height at each test. ICC values for elongation were generally lower than ICCs for height and diameter, ranging from 0.0 % at the Dryden test site to 4.6 % at the Petawawa test site. Diameter values were generally similar to, but slightly lower than those for height, with values ranging from 1.5 to 11.0 % for the Dryden and Longlac test sites, respectively. Survival ICCs were the most variable, explaining 0.0 % of the total variation in survival at the Angus, Dryden, and Petawawa test sites and 19.2 % at the Englehart site. As with the significance value, an ICC value for Longlac survival could not be calculated.

Each of the 14 biological variables that demonstrated significant variation among provenances produced significant regressions against one or more climate variables and were retained for further analysis (Table 4). Mean monthly temperature variables produced the strongest regressions for each of the 14 biological variables, indicating that temperature is generally a more accurate predictor of white spruce performance than is precipitation. Of these, growing season temperature variables (May, June, and August maximum) produced the strongest simple linear regressions for 12 of the 14 growth variables, indicating that temperatures during the growing season play a critical role in determining white spruce growth.

Table 3. Means, significance values, and Intraclass Correlation Coefficients for provenance effects for height, elongation, diameter, and survival at six white spruce provenance field trials.

Test Location	Mean				P > F (prov)				I.C.C. (%)			
	Ht. (cm)	Elong. (cm)	Diam. (mm)	Surv. (%)	Ht.	Elong.	Diam.	Surv.	Ht.	Elong.	Diam.	Surv.
Angus	54.9	10.6	10.7	67.9	<0.0001	0.0004	0.0014	0.9924	4.9	3.6	2.9	0.0
Dryden	38.3	3.0	10.8	89.7	<0.0001	0.7631	0.0069	0.9981	2.6	0.0	1.5	0.0
Englehart	65.1	12.6	18.0	65.4	<0.0001	0.2233	<0.0001	0.0002	7.3	0.7	4.8	19.2
Kakabeka	68.4	18.6	15.5	93.5	<0.0001	<0.0001	<0.0001	0.1119	8.0	4.4	5.6	6.3
Longlac	39.5	6.7	11.3	6.4*	0.1097	0.6208	0.0615	.	9.3	0.6	11.0	.
Petawawa	63.2	15.9	16.2	67.9	<0.0001	<0.0001	<0.0001	1.0000	8.1	4.6	6.5	0.0
								Average	6.7	2.3	5.4	5.1

* Absolute survival value, rather than mean of survival across provenances

Table 4. Significance and R^2 values for the strongest simple linear regression of each significant biological variable against each of 36 climatic predictor variables.

Measured Variable	R^2	Sig.	Strongest Predictor
anght07	0.1127	< 0.0001*	maymaxt
anginc07	0.2794	< 0.0001*	augmaxt
angdiam07	0.0666	0.0034*	maymaxt
dryht07	0.0893	0.0006*	junmaxt
drydiam07	0.0728	0.0022*	maymaxt
enght07	0.2292	< 0.0001*	maymaxt
engdiam07	0.1814	< 0.0001*	octmaxt
engsurv07	0.1175	< 0.0001*	marmint
kakht07	0.1278	< 0.0001*	maymaxt
kakinc07	0.1847	< 0.0001*	maymaxt
kakdiam07	0.0713	0.0024*	maymaxt
petht07	0.2936	< 0.0001*	maymaxt
petinc07	0.1905	< 0.0001*	maymaxt
petdiam07	0.2739	< 0.0001*	maymaxt

PRINCIPAL COMPONENTS ANALYSIS

The proportion of total variation explained by each of the first ten principal components is presented in Figure 2. Principal components axes 1 through 3 cumulatively explained 53.8% of the total variation in biological variables. The remaining 68 axes contributed relatively little to the explained variation, accounting for less than 5.0 % individually and falling past the inflection point at the 3rd axis.

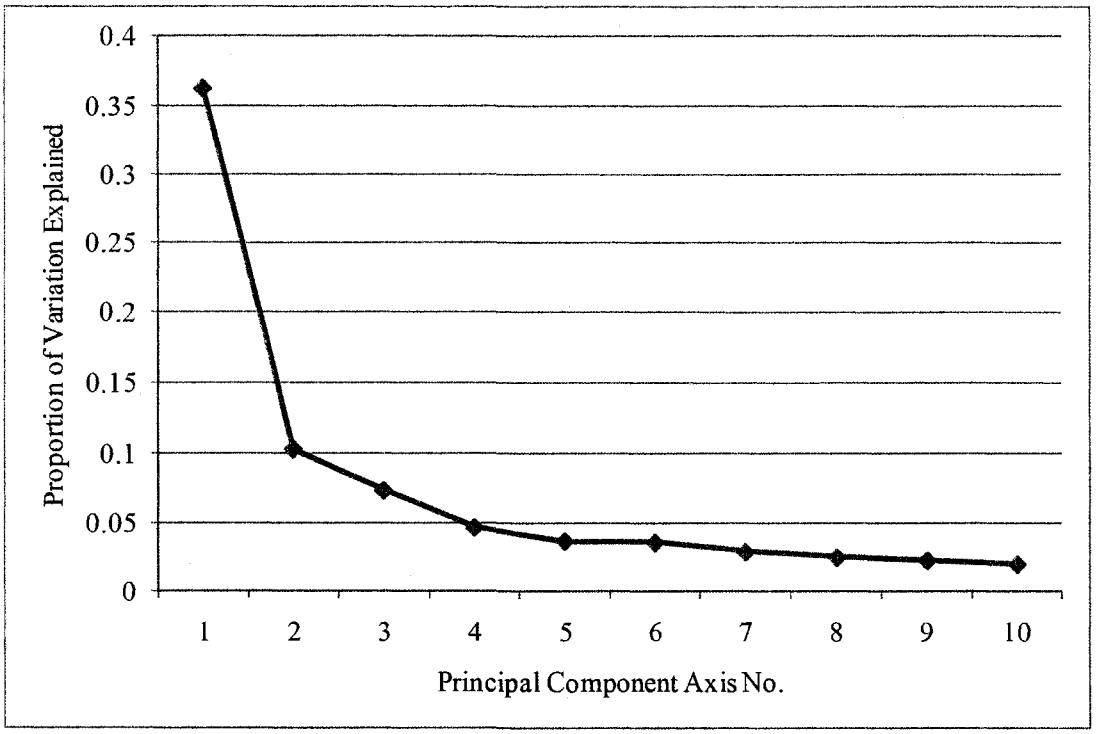

Figure 2. Proportion of total variation in biological variables explained by each of the first ten principal components axes.

The results of the principal components analysis are presented for the first three axes of variation in Table 5. Principal Component 1 (PC1) explained 36.2 % of the total variation, followed by principal components 2 (PC2) and 3 (PC3), explaining 10.3 % and 7.3 %, respectively, for a cumulative total of 53.8 % explained variation. Height, diameter, and elongation variables at all field trials demonstrated the strongest positive eigenvector loadings for PC1, suggesting that this axis represents growth potential. The earliest greenhouse elongation variables were negatively correlated, indicating that sources with low early greenhouse elongation tended to demonstrate high growth potential at field trials. Englehart survival variables and greenhouse budflush dates also showed strong positive correlations to PC1, suggesting that sources with high growth potential tended to flush later in the greenhouse and also demonstrated high survival at

the Englehart test site. Sources with later greenhouse budflush dates also tended to demonstrate later final-stage budflush dates at the Longlac field trial, suggesting that greenhouse budflush dates may be indicative of phenological timing at field trials. In summary, sources with the latest budflush timing dates tended to demonstrate high growth potential at field trial sites, high survival at the Englehart test site, and low early greenhouse elongation followed by relatively high final greenhouse elongation.

Table 5. Proportion of variation explained, variable loadings, and LSD interval calculations for the three main principal component axes.

	PC1	PC2	PC3
Eigenvalue	25.69	7.31	5.21
Proportion Variation	0.362	0.103	0.073
Cumulative Variation	0.362	0.465	0.538

		PC1		PC2		PC3	
	0.05 LSD	Loading	Load x LSD	Loading	Load x LSD	Loading	Load x LSD
Angus height 2007	0.61	0.12	0.07	0.01	0.00	0.08	0.05
Dryden height 2007	0.49	0.12	0.06	-0.02	0.01	-0.05	0.02
Englehart height 2007	0.63	0.15	0.10	0.01	0.00	0.11	0.07
Kakbeka height 2007	0.50	0.16	0.08	-0.06	0.03	0.09	0.04
Petawawa height 2007	0.60	0.15	0.09	0.06	0.04	0.08	0.05
Dryden height 2004	0.49	0.13	0.06	-0.07	0.03	-0.05	0.02
Kakabeka height 2004	0.49	0.17	0.08	-0.08	0.04	0.07	0.03
Longlac height 2004	0.69	0.14	0.10	-0.08	0.05	-0.05	0.03
Englehart height 2004	0.59	0.17	0.10	-0.07	0.04	0.09	0.05
Petawawa height 2004	0.58	0.16	0.09	-0.02	0.01	0.04	0.03
Angus height 2004	0.45	0.15	0.06	-0.09	0.04	0.00	0.00
Dryden height 2003	0.88	0.08	0.07	-0.04	0.04	-0.13	0.11
Kakabeka height 2003	0.49	0.16	0.08	-0.11	0.05	0.06	0.03
Longlac height 2003	0.60	0.15	0.09	-0.11	0.07	0.06	0.03
Englehart height 2003	0.95	0.17	0.16	-0.07	0.07	-0.02	0.02
Petawawa height 2003	0.57	0.16	0.09	-0.04	0.02	0.06	0.03
2002 height	0.18	0.16	0.03	-0.14	0.03	0.01	0.00
Angus elongation 2007	0.61	0.08	0.05	0.11	0.07	0.13	0.08
Kakabeka elongation 2007	0.50	0.15	0.07	-0.03	0.01	0.09	0.04
Petawawa elongation 2007	0.62	0.12	0.08	0.03	0.02	0.08	0.05
Angus diameter 2007	0.63	0.11	0.07	-0.03	0.02	0.05	0.03
Dryden diameter 2007	0.48	0.12	0.06	-0.04	0.02	-0.08	0.04
Englehart diameter 2007	0.64	0.15	0.10	-0.01	0.01	0.09	0.06
Kakabeka diameter 2007	0.51	0.15	0.08	-0.08	0.04	0.08	0.04
Petawawa diameter 2007	0.61	0.15	0.09	0.05	0.03	0.06	0.04
Dryden diameter 2004	0.53	0.14	0.07	-0.06	0.03	-0.08	0.04
Kakabeka diameter 2004	0.49	0.16	0.08	-0.11	0.05	0.05	0.02
Longlac diameter 2004	0.69	0.15	0.10	-0.02	0.02	0.00	0.00
Englehart Diameter 2004	0.58	0.17	0.10	-0.03	0.02	0.12	0.07
Petawawa diameter 2004	0.59	0.15	0.09	-0.01	0.01	0.06	0.03
Angus diameter 2004	0.47	0.16	0.08	-0.05	0.02	0.05	0.02
Dryden diameter 2003	0.88	0.10	0.08	-0.01	0.01	-0.06	0.05
Longlac diameter 2003	0.62	0.15	0.09	0.01	0.00	0.01	0.01
Englehart diameter 2003	0.58	0.17	0.10	-0.06	0.04	0.08	0.05
Petawawa diameter 2003	0.57	0.15	0.09	-0.05	0.03	0.04	0.02
Englehart survival 2007	1.45	0.13	0.19	0.00	0.00	0.11	0.16
Longlac survival 2004	1.47	0.12	0.18	0.00	0.00	0.07	0.11
Englehart survival 2004	1.32	0.01	0.02	-0.13	0.17	-0.05	0.07
Englehart survival 2003	1.39	0.11	0.16	0.00	0.01	0.08	0.11

Table 5. Continued.

	0.05 LSD	PC1 Loading	PC1 Load x LSD	PC2 Loading	PC2 Load x LSD	PC3 Loading	PC3 Load x LSD
Petawawa survival 2002	0.82	0.07	0.06	-0.08	0.07	-0.02	0.02
Dryden budflush stage 2	0.52	0.05	0.03	0.16	0.08	0.01	0.00
Dryden budflush stage 3	0.53	0.06	0.03	0.17	0.09	0.00	0.00
Dryden budflush stage 4	0.56	0.04	0.02	0.20	0.11	-0.06	0.03
Dryden budflush stage 5	0.57	0.04	0.02	0.17	0.10	-0.05	0.03
Dryden budflush stage 6	0.59	0.03	0.02	0.18	0.11	0.02	0.01
Longlac budflush stage 2	0.52	0.08	0.04	0.12	0.06	-0.15	0.08
Longlac budflush stage 3	0.52	0.10	0.05	0.11	0.06	-0.16	0.08
Longlac budflush stage 4	0.54	0.12	0.06	0.09	0.05	-0.17	0.09
Longlac budflush stage 5	0.59	0.10	0.06	0.03	0.02	-0.21	0.12
Longlac budflush stage 6	0.62	0.09	0.05	0.00	0.00	-0.16	0.10
Dryden budset stage 5	0.51	0.06	0.03	0.26	0.13	0.10	0.05
kakabeka budset stage 3	0.58	0.05	0.03	0.24	0.14	0.06	0.03
Kakabeka budset stage4	0.49	0.10	0.05	0.24	0.12	0.10	0.05
Kakabeka budset stage 5	0.52	0.09	0.05	0.21	0.11	0.12	0.06
Longlac budset stage 4	0.61	-0.01	0.01	0.22	0.13	0.11	0.07
Longlac budset stage 5	0.65	0.03	0.02	0.20	0.13	0.16	0.11
Englehart budset stage 3	0.87	0.02	0.02	0.20	0.17	0.13	0.12
Englehart buset stage 4	0.62	0.08	0.05	0.21	0.13	0.12	0.07
Englehart budset stage 5	0.79	0.04	0.03	0.16	0.12	0.11	0.08
Petawawa budset stage 3	0.82	0.01	0.01	0.16	0.13	0.05	0.04
Petawawa budset stage 4	0.60	0.05	0.03	0.24	0.14	0.10	0.06
Greenhouse elongation day 18	0.51	-0.08	0.04	-0.12	0.06	0.26	0.13
Greenhouse elongation day 22	0.49	-0.10	0.05	-0.13	0.07	0.29	0.15
Greenhouse elongation day 26	0.50	-0.08	0.04	-0.19	0.09	0.26	0.13
Greenhouse elongation day 30	0.49	-0.04	0.02	-0.23	0.12	0.21	0.10
Greenhouse elongation day 70	0.46	0.16	0.07	-0.10	0.05	0.06	0.03
Greenhouse budflush stage 2	0.54	0.11	0.06	-0.01	0.01	-0.20	0.11
Greenhouse budflush stage 3	0.49	0.14	0.07	-0.02	0.01	-0.22	0.11
Greenhouse budflush stage 4	0.49	0.14	0.07	-0.02	0.01	-0.20	0.10
Greenhouse budflush stage 5	0.51	0.09	0.04	0.00	0.00	-0.20	0.10
Greenhouse budflush stage 6	0.50	0.07	0.04	0.02	0.01	-0.28	0.14
Sum*		7.74	4.71	6.51	3.83	6.88	4.17
Weighted Average			0.61		0.59		0.61

*sum of variable loadings, and load X LSD values calculated based on absolute values

PC2 mostly represents phenological timing of budflush and budset in the field, as determined by the strong positive correlations of budflush and budset variables across a range of field tests. The strong positive correlations of both budflush and budset variables at field trials with PC2 suggests that sources which flush latest in the spring also tend to set bud latest in the fall. In contrast, greenhouse budflush variables were

not strongly correlated to PC2, suggesting that this axis expresses phenological timing at field trials only. Greenhouse elongation variables, as well as several growth variables (Kakabeka height 2003, Englehart height 2003, 2002 height, and Kakabeka diameter 2004) were strongly negatively correlated to PC2.

Principal component 3 mainly represents the pattern of growth initiation in the greenhouse, as represented by the strong positive correlation of early greenhouse elongation variables and strong negative correlation of greenhouse budflush variables. This relationship indicates that sources which flushed earliest in the greenhouse tended to demonstrate the greatest early elongation. The high negative correlation of Longlac budflush variables to PC3 combined with the low correlation to PC2 suggests that the pattern of budflush timing for the Longlac test site may be essentially uncorrelated to phenological timing at other field trials. Similarly, the low correlation of day 70 greenhouse elongation suggests that the pattern of growth initiation in the greenhouse is uncorrelated to the first two principal components axes representing growth potential and phenology in the field.

MULTIPLE LINEAR REGRESSION ANALYSIS

The multiple linear regression models selected for each of the three main axes of variation are presented in Table 6. Each of the selected models was significant ($P < 0.05$) in explaining the variation in principal components factor scores, while each of the entered variables demonstrated significant t-values (<0.05) and tolerances greater than 0.2.

Multiple linear regressions of principal component axis against climate variables revealed that PC1 is most strongly determined by September maximum temperature, January precipitation, and August precipitation, with a corresponding R^2 of 0.28. PC2 factor scores are best predicted by the combination of July minimum temperature, February precipitation, and October precipitation, which accounts for 53% of the total variation. The combination of April maximum temperature, June maximum temperature, and March precipitation accounts for 27% of the variation in PC3 factor scores.

Table 6. Strongest multiple linear regression models predicted by regression of principal components 1, 2, and 3 against each of 36 climate variables.

Dependent	Independents	Coefficient	P > t	Tolerance	P > F	R^2
PC1	intercept	-8.8417	<0.0001	.	<0.0001	0.2804
	sepmaxt	0.3477	<0.0001	0.7297		
	janprec	-0.0176	0.0074	0.6518		
	augprec	0.0425	0.0001	0.7976		
PC2	intercept	-2.1436	0.0365	.	<0.0001	0.5329
	julmint	0.2706	<0.0001	0.4072		
	febprec	0.0365	0.0003	0.2683		
	octprec	-0.0355	0.0015	0.4613		
PC3	intercept	4.5208	0.0056	.	<0.0001	0.2696
	aprmaxt	0.6913	<0.0001	0.2110		
	junmaxt	-0.3677	0.0005	0.2841		
	marprec	-0.0474	<0.0001	0.4898		

Figure 3 to Figure 5 present grids of predicted factor scores for each of the three main principal components axes, generated by regression of climate grids according to the selected multiple regression equations. The factor scores for each grid are expressed as units of standard deviation (SD). The first principal component grid, representing growth potential, shows a strong latitudinal trend with decreasing factor scores moving northward. This pattern indicates that white spruce growth potential is

greatest in the extreme southeast of the province and decreases northward to a minimum in the area adjacent to Hudson Bay. Interestingly, similar factor scores occurring in the southeast and the northwest along the Ontario-Minnesota border indicate that growth potential is comparably high in these areas.

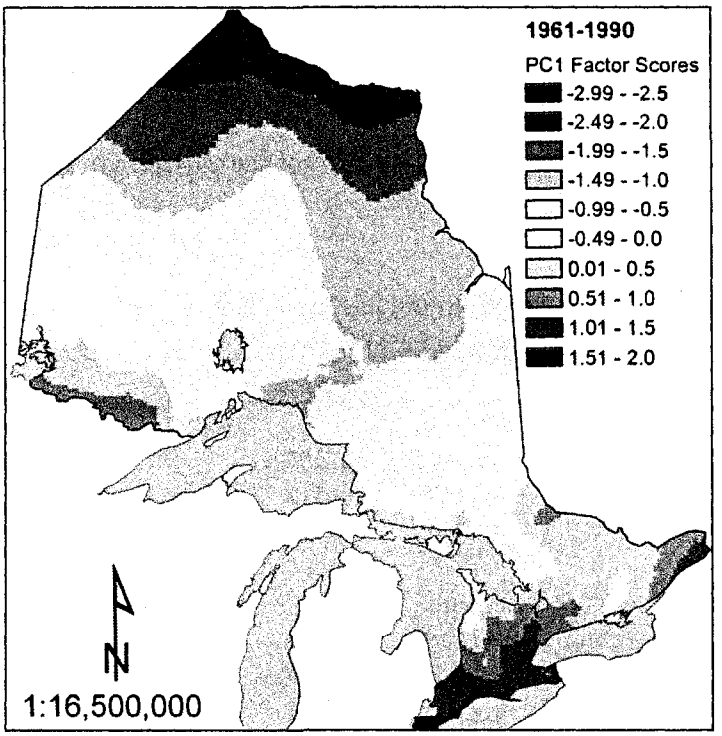

Figure 3. Predicted factor scores for PC1 based on regression of 1961-1990 climate normals.

Factor scores for principal component 2, representing field trial phenology, are strongly influenced by July minimum temperature, and display a similar lack of a clear north-south or east-west trend (APPENDIX I). The darkest green areas, representing the highest predicted factor scores, occur in the extreme southeast of the province and indicate areas where sources are predicted to flush latest in the spring and set bud later in the fall (Figure 4). Scores decrease northwards and westwards where they reach a band of relatively low values. This band stretches northward from the shore of Lake Superior and closely resembles the one demonstrated for July minimum temperature contours.

North of this band scores decrease to a minimum, indicating sources with the earliest predicted dates of budflush and budset. To the west, scores increase and reach a maximum in a small area to the north of Lake of the Woods. Factor Scores in the northwest region adjacent to the Ontario-Manitoba border are quite similar to those of the Ottawa-Valley area, indicating that budflush and budset timing are predicted to be comparable in these areas. Finally, the influence of February and October precipitation variables is evident in several disjunct pockets of relatively low or high factor scores that occur along the shores of Lake Superior and Lake Huron. One such area of relatively low factor scores occurs directly to the north of Lake Superior and surrounds the perimeter of Lake Nipigon to the north, while another area occurs along the eastern shore.

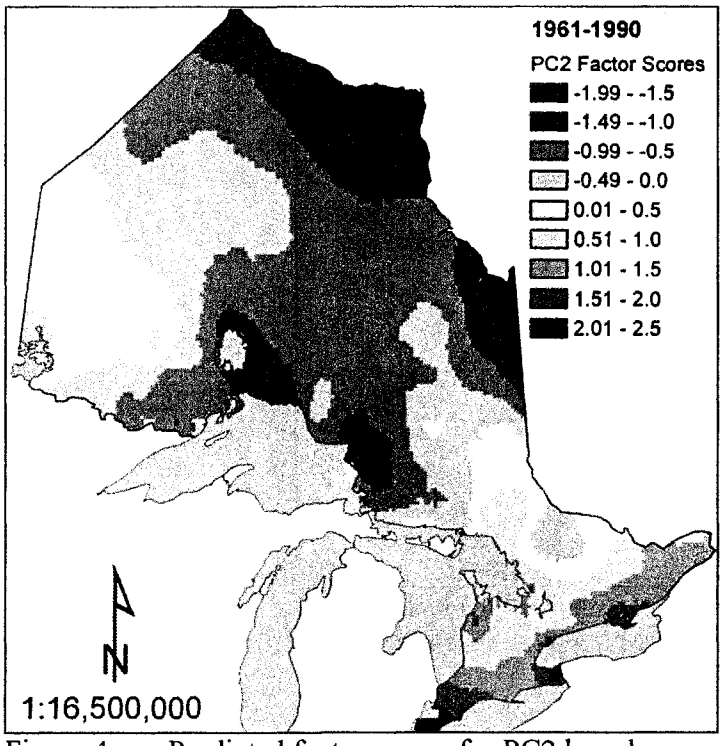

Figure 4. Predicted factor scores for PC2 based on regression of 1961-1990 climate normals.

Predicted factor scores for principal component 3, representing primarily greenhouse elongation, demonstrate a clear latitudinal trend, with values increasing from north to south (Figure 5). This pattern indicates that sources that had low early greenhouse elongation and later greenhouse budflush dates occur in the southeast and northwest regions. Similar to PC2, predicted factor scores for the third principal component are comparable in the Ottawa Valley and northwest regions of the province. A disjunct region surrounding Lake Nipigon is also evident. In contrast to PC2, PC3 factor scores indicate that the Lake Nipigon area is adaptively similar to the south, whereas the PC2 grids indicates that it is similar to the far north.

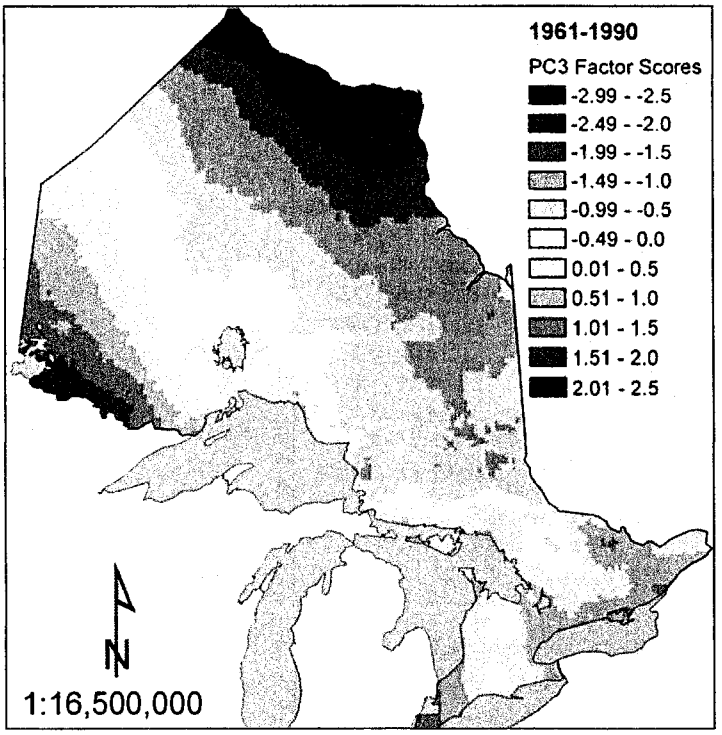

Figure 5. Predicted factor scores for PC3 based on regression of 1961-1990 climate normals.

FOCAL POINT SEED ZONES EXAMPLES

Six examples of the 618 focal point seed zones constructed for Ontario are presented in Figure 6 through Figure 11. These figures depict areas of adaptively similarity and encompass areas within 0.5 and 1.0 LSD values from the selected focal point. The six focal points (planting locations) used for these examples were selected to encompass a wide geographic area, to compare patterns of adaptive variation across the province. The selected points will also provide a reference with which to compare changes in adaptive variation between present, past (Chapter IV), and future (Chapter V) climates.

In Figure 6 to Figure 11, the areas within ± 0.5 LSD of the focal point represent areas of highest adaptive similarity and are presented in the darkest shading. Areas that lie with ±1.0 LSD represent areas of moderate adaptive similarity and are presented in the lighter shading. Areas without shading represent areas that fall outside the ± 0.5 or 1.0 LSD intervals, where adaptive similarity is likely too low to allow for effective seed transfer. Finally, the shaded star in each of the figures represents the selected focal point.

Figure 6 presents the seed zones for focal point 345, located just to the north of Lake Nipigon. The 1.0 LSD seed zones for this point extends across most of the central portion of the province, beginning in the northwest at 53°N and stretching southeast across the north shore of Lake Superior to terminate at 46°N along the north shore of Lake Huron. At 88°W, along the same line of longitude as the focal point, this zone extends all the way from the north shore of Lake Superior to approximately 52°N. Interestingly, this zone fails to encompass a small area running along the north shore of

Lake Superior that extends from just west of Lake Nipigon to the southern border of Pukaskwa National Park. In contrast to the 1.0 LSD zones, areas that lie within 0.5 LSD values of Focal Point 345 are relatively restricted and often occur as small disjunct fragments. The main zone loosely encircles the area north of Lake Nipigon, extending from approximately 90°W to 85°W in a southeastward band spanning approximately 2° latitude.

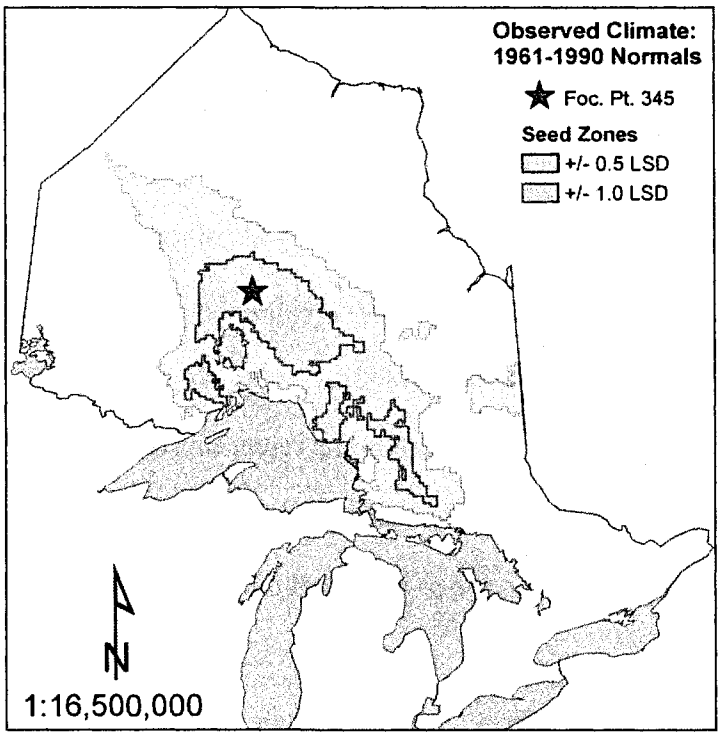

Figure 6. Seed zones for focal point 345, based on 1961-1990 observed climate normals.

Seed zones for focal point 325 are presented in Figure 7. Similar to focal point 345, the 1.0 LSD seed zone for point 325 is strikingly large, encompassing the greater portion of the mid-northern latitudes of western and eastern Ontario. This zone spans approximately 3° latitude and 12° longitude, or approximately 30% of the province's total area. Again, the 0.5 LSD zone is much more restricted and fragmented in

comparison to the 1.0 LSD zone. For focal point 325, the 0.5 LSD zone is composed of two main segments, one located immediately surrounding the focal point in the northeast of the province, and the other located to the far northwest.

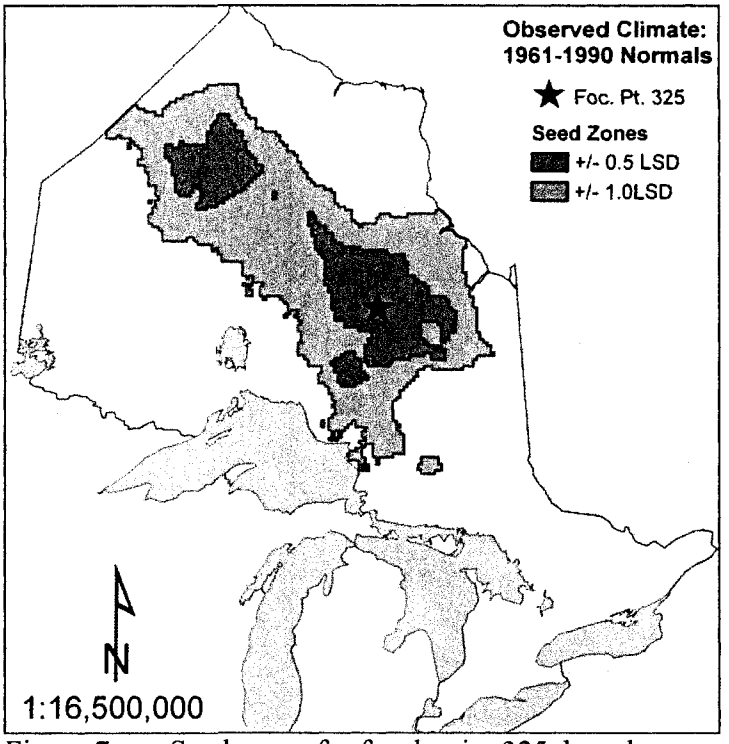

Figure 7. Seed zones for focal point 325, based on 1961-1990 observed climate normals.

Figure 8 illustrates the seed zones for focal point 336, located in the northwest region of the province. The 1.0 LSD seed zone for this point is much smaller in comparison with the previous focal points, and illustrates the adaptive similarity between the northwest region and the Ottawa Valley area. This zone is composed of two main segments, one immediately surrounding the focal point covering a modest portion of the northwest region, and the other extending in a narrow latitudinal band across the north shore of Lake Huron into the Ottawa Valley. The 0.5 LSD zone is quite similar in shape, but covers a relatively small area that does not encompass the area to the northeast of the focal point. This zone contains only tiny, disjunct areas in the

Ottawa Valley area but, interestingly, encompasses the whole of Manitoulin Island to the south.

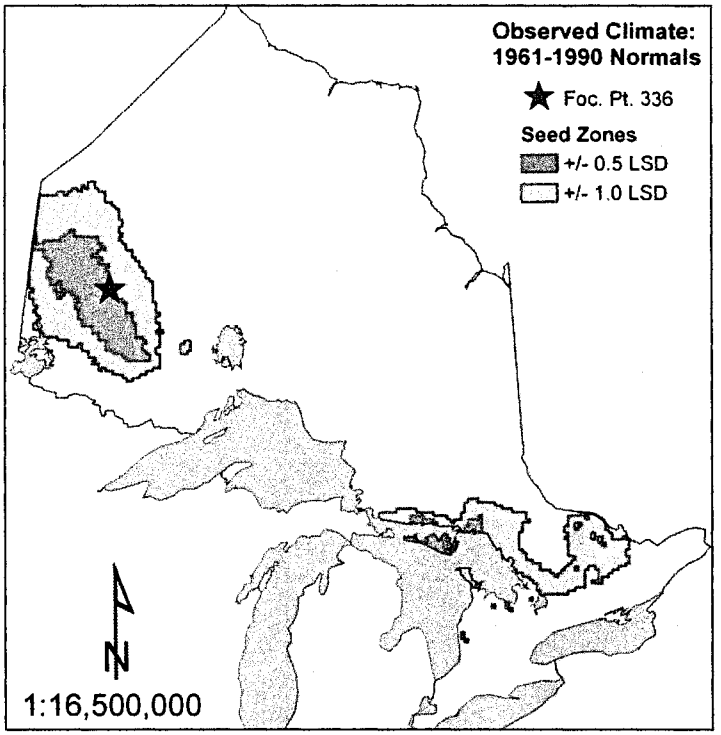

Figure 8. Seed zones for focal point 336, based on 1961-1990 observed climate normals.

In the far north of the province, focal point 584 is encompassed by a single continuous seed zone (Figure 9). The 1.0 LSD zone extends from the Manitoba border east to James Bay, and runs from Hudson Bay southward in a band spanning approximately 3° latitude. The 0.5 LSD zone extends through the center of the 1.0 LSD band, but falls just short of the Manitoba border. In comparison with previous seed zones, the zones for this focal point are unique in that they are composed of a single, contiguous zone and are more limited in extent.

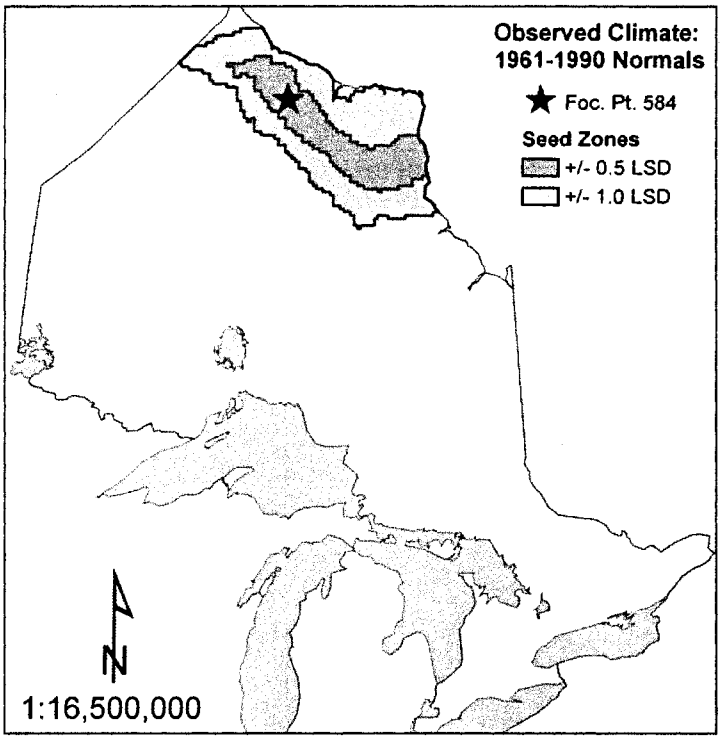

Figure 9. Seed zones for focal point 584, based on 1961-1990 observed climate normals.

Figure 10 displays the seed zones for focal point 146. The 1.0 LSD zone is composed of 2 main areas; the first surrounding the focal point in northeastern Ontario and the second located to the west and north of Lake Nipigon in northwestern Ontario. The first segment stretches from 83°W to approximately 79°30' W along the Quebec border. The southern border of this zone terminates before reaching the north shore of Lake Huron, excluding areas where PC3 factor scores indicate the lake's effect on the surrounding climate (Figure 5). A third, much smaller area that also demonstrates the exclusion of lake effect areas is located southeast of the focal point in the south-central region of Ontario. The second main area of this zone is located in northwestern Ontario, again indicating the adaptive similarity between areas in the northeast and the parts of the northwest region. The 0.5 LSD zone for focal point 146 is composed entirely of small discontinuous areas, located within the region immediately surrounding the focal

point. In contrast to the 1.0 LSD zone, the 0.5 LSD zone does not indicate any areas of adaptive similarity within northwestern Ontario.

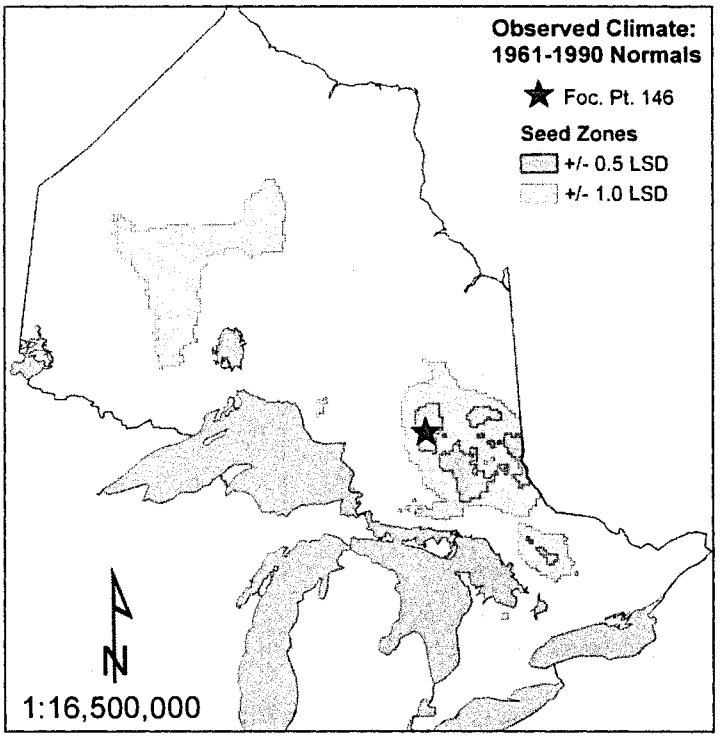

Figure 10. Seed zones for focal point 146, based on 1961-1990 observed climate normals.

The 1.0 LSD seed zone for focal point 35, located in southeastern Ontario, stretches from the Ottawa Valley south to the London area. This zone is mostly restricted to the southeast, indicating that this region may be adaptively distinct from other areas of the province. However, a few discontinuous fragments located to the north of Lake of the Woods may again indicate the similarity in performance between the Ottawa Valley area and the northwest region. The 0.5 LSD zone is composed of several very small, discontinuous fragments that are scattered from the Ottawa Valley south to approximately 42°30' N. The small, fragmented nature of the 0.5 LSD zones is likely an indicator of the relative diversity of climate close the southern edge of the range.

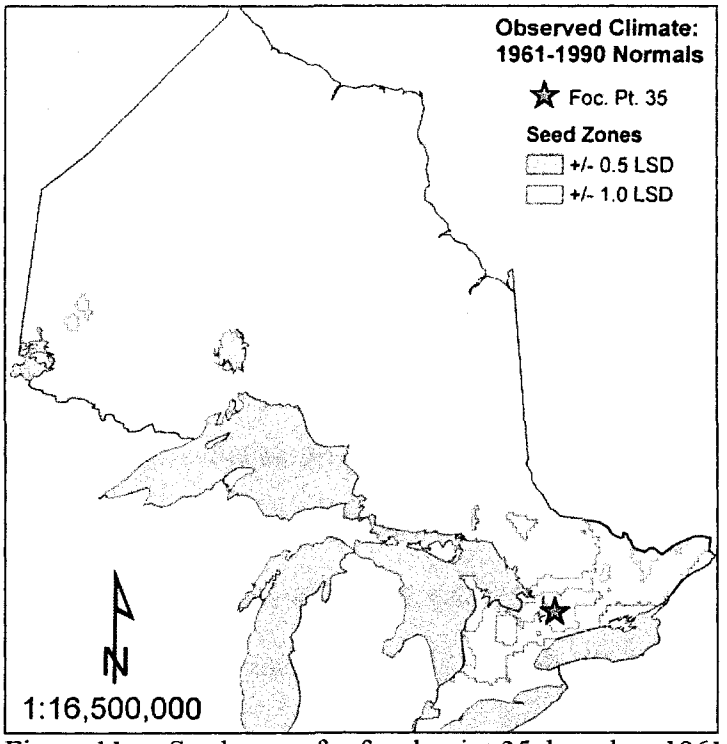

Figure 11. Seed zones for focal point 35, based on 1961-1990 observed climate normals.

DISCUSSION

LEVELS OF VARIATION

As with an earlier study of this series of white spruce provenance trials (Lesser 2005), survival generally did not vary significantly between provenances at each test site. This result may be related to the relatively young age of these tests; factors such as establishment success and herbivory may play a much greater role in determining seedling survival than climate (Wang *et al.* 2006). However, the lack of strong differentiation is consistent with the majority of other studies which indicate similar survival among sources (Cherry and Parker 2003; Lesser and Parker 2004; Nienstadt and Teich 1972; Rweyongeza *et al.* 2007). In contrast, the relatively high proportion of variation among sources at the Englehart test site may be related to frequent incidents of frost heaving in the first years of growth which may have impacted sources differently; fast-growing sources with vigorous root systems would be less susceptible and, thereby, demonstrate greater survival.

The ICC values for population variation for height and diameter ranged from 2.6-9.3% and 1.5-11.0% respectively, and are somewhat lower relative to the values of 6.2-16.68% and 5.9-11.36% obtained for a previous study (Lesser and Parker 2004). This decline in provenance variation is probably the result of increased competition at field trials over recent years. When measurements were obtained in 2007, many of the trials had become overgrown with grasses or other competitive species, and many of the

white spruce seedlings were completely overgrown. In contrast, there was little competition in the first few years of growth due to site treatments and vegetation control. Thus, recent measurements probably do not fully reflect the differences in growth potential between sources, as even the fastest-growing provenances are over-topped at several sites.

In comparison to other studies, inter-provenance variation in growth traits is somewhat low in the current study. Source effects accounted for 8.9-21.1% of the variation in 24-year height at white spruce trials in Alberta, compared to 2.6-9.3% of the variation in 6-year height in the current study (Rweyongeza *et al.* 2007). The proportion of variation due to provenances was also quite high for a series of trials in Ontario, accounting for 14 and 15% of the total variation in height and diameter, respectively (Cherry and Parker 2003). Another test of 22 range-wide provenances found that 46 and 54% of the variation in height at age 9 and 19, respectively, could be attributed to provenance effects (Furnier *et al.* 1991).

The much higher levels of variation due to provenance in these other studies may be attributed to three factors: the possibility of inclusion of hybrid sources, the much broader range of provenance sampling, and test age. Rweyongeza *et al.* (2007) note that the white spruce sources collected from the zone of introgression with Engelmann spruce in Alberta were assumed to be pure white spruce; however, this assumption was not tested (Rajora and Dancik 2000). Given that pure and introgressed hybrid forms of white spruce are virtually indistinguishable, it stands to reason that some hybrid sources may have been included in the tests. Thus, the levels of variation due to provenance would be inflated in comparison to a trial of truly pure white spruce.

The higher levels of variation in the Ontario tests (Cherry and Parker 2003) and Minnesota test (Furnier *et al.* 1991) can be explained by the fact that these studies included provenances collected from throughout the range of white spruce. In comparison, the current study only examines provenances from Ontario and western Quebec. Previous studies have shown that levels of variation due to provenance are much lower when sources originate from a much more localized area (Pollard and Ying 1979). In contrast, data from range-wide white spruce provenance trials demonstrates much greater inter-provenance variation with mean ICC values of 24.6 and 25.5% for height and diameter respectively (Parker 2008, unpublished data). Nienstadt and Reimenschneider (1985) found that heritability increased markedly from age 9 to 15 at tests sites across the Lake States and Ontario. Thus, it is possible that the low ICC values of the current study are due at least in part to the relatively young age of the tests and that the strength of the genetic effects will increase in later years.

Moreover, true levels of variation among provenances are probably somewhat underestimated in the current study because family effects were not accounted for; white spruce demonstrates high levels of family variation that generally account for almost the same proportion of variation as do provenances (Li *et al.* 1993). Thus, accounting for family effects would reduce the level of error and likely increase the estimate of variation due to provenances.

In comparison to studies of a more comparable range, the ICCs obtained for growth variables in this study are equal to or somewhat higher; Li *et al.* (1993) found that variation due to provenance averaged 3.1% of the total variation in growth and phenological traits, while a later study (Li *et al.* 1997) found that 3.83-11.92% of the

total variation was due to provenance effects. Similar values have also been obtained for jack pine in Ontario, with ICCs for seedling heights across 5 sites ranging from 3.87-21.02% (Parker and van Niejenhuis 1996a).

PRINCIPAL COMPONENTS ANALYSIS

In comparison with a previous study of the same series of provenance trials (Lesser 2005), the addition of 13 growth and survival variables did little to change the results of the principal components analysis. The biological interpretation of the main axis of variation remains essentially unchanged, with PC1 representing growth potential in the field, PC2 representing phenological timing in the field, and PC3 representing greenhouse growth initiation. The proportion of total variance explained by each of the 3 main principal components is also quite similar; in the previous study, the three PC axes accounted for 34.0, 46.4, and 54.6 % of the total variation in growth and phenological variables, while in the current study they account for 36.2, 46.5, and 53.8% respectively. Variable loadings on each of the three axes are also quite similar.

Height, diameter, and elongation variables measured throughout time (2002-2007) and at multiple sites were strongly correlated to PC1. This suggests that principal component 1 captures growth potential in early years before crown closure, rather than just the first few years' growth. It also suggests that PC1 describes growth potential across the sampled range of environmental conditions, versus representing growth potential at only a single site. If growth potential at 6 years were essentially uncorrelated to early growth, then the 2007 growth measurements would have loading values that approached zero on the first axis. Therefore, provenance performance

appears relatively stable over time and across sites. This result is in keeping with earlier studies reporting that fast-growing provenances and families tended to perform well across a wide range of sites and maintained superior performance into later stand ages (Khalil 1985; Li *et al.* 1993; Ying and Morgenstern 1979). This observation also lends further support to previous authors' conclusions that early growth traits seem to provide a reliable basis for selection (Khalil 1985; Li *et al.* 1993; Ying and Morgenstern 1979).

REGRESSION MODELS

Each of the selected regression models was highly significant with acceptable tolerance values. R^2 values were extremely comparable to those obtained by Lesser (2005), explaining 28 to 53% of the total variation in factor scores.

Variables included in multiple regression models reflect both growing season temperatures and a variety of precipitation variables. However, temperature is of relatively greater importance in predicting growth potential and phenological timing, as growing season temperature variables were selected as the best single-variable predictors for PC1 and PC2 using the R^2 selection method (APPENDIX II). The addition of 2 precipitation variables increased the explained variation in PC1 by only 7.4% and by 3.0% for PC2.

Climate variables selected to model the pattern of white spruce adaptation are very similar in comparison to those previously constructed for the same provenance trials (Lesser 2005). In the current study, PC1 was best predicted by September maximum temperature, January precipitation, and August precipitation, while in the previous study precipitation of the wettest period, August maximum temperature, and

August precipitation were used. PC2 was modeled solely with June minimum temperature, whereas in the current study July minimum temperature, February and October precipitation were used. Finally, Lesser (2005) used annual precipitation, March maximum temperature, and October precipitation to predict PC3 factor scores, while this study uses April and June maximum temperature, and March precipitation.

The similarity of variables used in the two studies is striking, and supports the previous conclusion that the addition of 2007 growth data did little to change the overall result. However, this similarity strengthens confidence in the modeled relationships, as widely differing regression variables could indicate unstable or inaccurate modeled relationships between performance and climate.

The selection of September maximum temperature to model PC1 in the current study, and of August maximum temperature in the previous study (Lesser 2005), indicates the importance of late-summer and early fall temperatures to growth. The positive coefficients of these variables indicate that sources originating from areas where temperatures remain warmer into late summer and early fall have greater growth potential than sources originating from relatively cool temperatures. Sources from cooler environments have been shown to set bud earlier in the fall, presumably as a strategy to minimize the risk of early fall frost damage (Nienstadt and Teich 1972). In contrast, warmer environments pose a much lesser risk of fall-frost and, thus, sources are able to adapt to the more favorable environment by increasing growth through a delayed onset of winter dormancy.

The importance of July minimum temperature in influencing phenological timing is unclear, but could be explained if this variable is substituted for another highly

correlated temperature variable in multiple regressions. Though the single best predictor of PC2 is June minimum temperature (APPENDIX II), the addition of February and October precipitation results in extreme multicollinearity ($t<0.1$), so the model must be considered unstable (Chatterjee and Price 1977). Thus, the model containing July minimum temperature was selected to avoid over-fitting.

Precipitation variables demonstrate a complex relationship with both growth potential and phenology. No clear trends are evident, as precipitation is indicated to have either a negative or positive effect, depending on the month examined. However, growing season precipitation is selected to model PC1 in both the current and previous study (Lesser 2005), and demonstrates a positive correlation with white spruce growth. Regression models based on the R^2 selection method indicate both June and August precipitation as important predictors of PC1 factor scores. Thus, it appears that warm temperatures combined with adequate precipitation during the growing season and bud formation combine to increase the growth of white spruce.

It is interesting that 5 of the 9 climate variables selected to model white spruce performance are precipitation variables, given that simple linear regression analyses of individual variables overwhelmingly select early growing season temperatures as the single best predictors. However, this finding is in agreement to previous studies indicating a significant influence of precipitation on white spruce adaptation (Andalo *et al.* 2005; Cherry and Parker 2003; Nienstadt and Teich 1972). Andalo *et al.* (2005) found mean maximum daily temperature to be the strongest single predictor white spruce growth in Quebec, explaining 13.7 and 12.8% of the total variation in height and diameter, respectively. However, when bivariate models including precipitation

variables were constructed, they were found to explain an additional 20% and 8% of the variation. Subsequent correlations of predicted values data from an independent field trial demonstrated significant positive correlations, indicating the validity of the selected climate variables in predicting white spruce growth.

Cherry and Parker (2003) modeled height growth of white spruce provenances in relation to winter temperatures and growing season precipitation and found that the resulting models accounted for up to 90% of the observed variation. O'Neill and Aitken (2004) found aridity index, extreme maximum temperature, and mean temperature of the warmest month to be reliable predictors in multiple regression models for interior (hybrid) spruce in BC. Similarly, Nienstadt and Teich (1972) suggest temperature regime and precipitation to be among the most import factors shaping white spruce adaptation following the last period of glaciation.

Climate envelope models constructed to predict the potential habitat distribution of white spruce under climate change use many of the same climate variables as the current study. Thiberville and Parker (2007) used current species distribution maps to predict the occurrence of potential white spruce habitat based on climate. Two methods of modeling were used; for the first method (inflection point), variables selected as the best predictors included September, October, and August minimum temperature, as well as January precipitation. For the second method (saturation point), the previous four variables, as well as February and October precipitation, October maximum temperature, and April minimum temperature were selected.

This and previous studies all suggest that temperature alone is not enough to fully account for patterns of adaptive variation in white spruce. Indeed, prescriptions for seed transfer based on temperature or precipitation variables alone should be avoided because the interaction between summer temperatures and precipitation may have a significant effect on growth (Cherry and Parker 2003; Hofgaard *et al.* 1999; Matyas 1994). However, this observation is in contrast to studies of other boreal conifers indicating a lesser or non-significant effect of precipitation (Maytas and Yeatman 1992; Thomson and Parker 2008). Population response functions constructed for jack pine demonstrated that height growth is not reliably correlated to precipitation, but is instead driven primarily by growing season temperatures. Similarly, Riddell (2004) found that black spruce growth is only moderately correlated to precipitation in comparison with temperature. Thus, it appears that patterns of adaptation for white spruce may be relatively more strongly influenced by precipitation than are those of black spruce and jack pine.

PATTERNS OF VARIATION

Mapped patterns of genetic variation (PC1, PC2, and PC3) indicate a mixture of strong latitudinal and moderate east-west clines. Growth potential generally increases from north to south, and is at a maximum in the southeast stretching from the Michigan border north to the Ottawa Valley. Sources from this area also demonstrate the latest dates of budflush and budset. Phenological timing varies along a north-south and east-west gradient, decreasing northwards and along the shores of Lake Superior and Lake

Huron. These patterns indicate the role of temperature in shaping strong north-south clines and the somewhat lesser role of precipitation in shaping east-west gradients.

Patterns of variation are very similar to those reported for other studies indicating a mixture of strong latitudinal and more moderate east-west clines in variation (Jaramillo-Correa *et al.* 2001; Khalil 1985; Lesser 2005; Li *et al.* 1997). Li *et al.* (1997) also reported a stronger latitudinal cline and a more moderate east-west cline in genetic variation of white spruce. Khalil (1985) reported a predominantly east-west cline in variation of Ontario and Quebec provenances in Newfoundland based on growth traits, while Jaramillo-Correa *et al.* (2001) report significant genetic correlations with both latitude and longitude in Quebec.

Seed zones constructed based on current climate normals bear great similarity to those of Lesser (2005), indicating a strong latitudinal cline, with growth potential and bud phenology timing increasing from north to south. Zones are generally broad across the central latitudes of the province and become increasingly narrow moving toward the southeast. Both studies indicate the differentiation of sources along the north shore of Lake Superior and around Lake Nipigon and areas of relatively high growth potential in the northwest and Ottawa Valley area.

The relatively high growth potential indicated for sources originating from the southeast is in keeping with numerous studies reporting superior performance of sources from the Ottawa Valley area (Khalil 1985; Lesser and Parker 2004; Li *et al.* 1997; Morgenstern and Copis 1999; Nienstadt and Teich 1972). These provenances have been shown to perform well even when transferred relatively great differences. Khalil (1985) reported sources from the southeast of Ontario to be among the most vigorous

provenances at a Newfoundland provenance trial, and found that their performance remained stable over time. When considering the high growth potential and high stability of these provenances, it seems that they are ideal candidates for tree improvement, as greater than 15% increases in merchantable volume can be expected when using these sources in place of the local source (Nienstadt and Teich 1972).

CHAPTER III: DETERMINATION OF CURRENT OPTIMAL BREEDING ZONES FOR WHITE SPRUCE IN ONTARIO

INTRODUCTION

Crowe and Parker (2005) presented a model that could be used to delineate optimal breeding zones based on a modification of the focal point seed zones program (Parker 1992, 1996a, 1996b). The problem of delineating fixed breeding zones for jack pine was likened to that of a traditional maximal-covering type problem in operations research, where the goal is to maximize the area serviced by a set number of facilities (Crowe and Parker 2005). In this way, focal points were used to represent potential seed orchard locations serving discrete breeding zones. First, a grid of potential orchard locations (focal points) was constructed across the study area. The focal point seed zone method was then used to determine a unique seed zone for each of the grid points based on a specified level of adaptive similarity (+/- 0.5 & 1.0 LSD). Each seed zone was used to represent a candidate breeding zone served by the corresponding orchard focal point. A second grid of higher resolution was used to determine the area covered by each individual zone.

The candidate breeding zones were then used as input to the maximal covering model to select combinations of a specified number of zones that could be used to maximize the area covered (Crowe and Parker 2005). Thus, the model could be used to determine the number of breeding zones required to completely cover the area of interest, as well as to determine how many zones are required based on varying levels of adaptive similarity.

This chapter will use the focal point seed zone model developed in the previous chapter, in combination with the maximal covering decision-support model of Crowe and Parker (2005), to develop current optimal breeding zones for white spruce in Ontario. As adaptively-based breeding zones have not yet been developed for white spruce in Ontario, it is the intention that the zones presented herein may guide the establishment of discrete breeding zones to ensure adequate performance of improved white spruce seedlings.

METHODS

The determination of optimal breeding zones requires that a set of candidate breeding zones first be developed for the area of interest. To accomplish this, a grid of focal points representing potential seed orchard locations was established at 40 km x 40 km resolution. A second grid was created at a higher resolution of 20 km x 20 km to represent the geographic points, hereto referred to as cover points, to be covered. The choice of grid resolution was influenced by the work of Parker and Crowe (2005), and by software limitations and computing time requirements; the 40-km and 20-km resolution was intended to provide acceptable coverage while ensuring model feasibility and reasonable computing time. The resulting grids consisted of 2324 cover points distributed evenly across the entire range of white spruce in Ontario, and of 618 focal points across the entire province to ensure adequate coverage along the edges of the range. The location of both focal and cover points corresponds to the centers of principal components factor scores grid cells (CHAPTER II), and is presented in Figure 12.

The focal point seed zone methodology, described in detail in Chapter II, was used determine a set of 618 candidate breeding zones (1-zone per focal point) based on 1.0 LSD of adaptive similarity for each of the three principal components. ArcGIS was used to generate grids of the location of each of the candidate breeding zones and to determine the number and location of geographic points covered by each zone. The

process was repeated to generate a second set of candidate breeding zones based on adaptive similarity of 0.5 LSD.

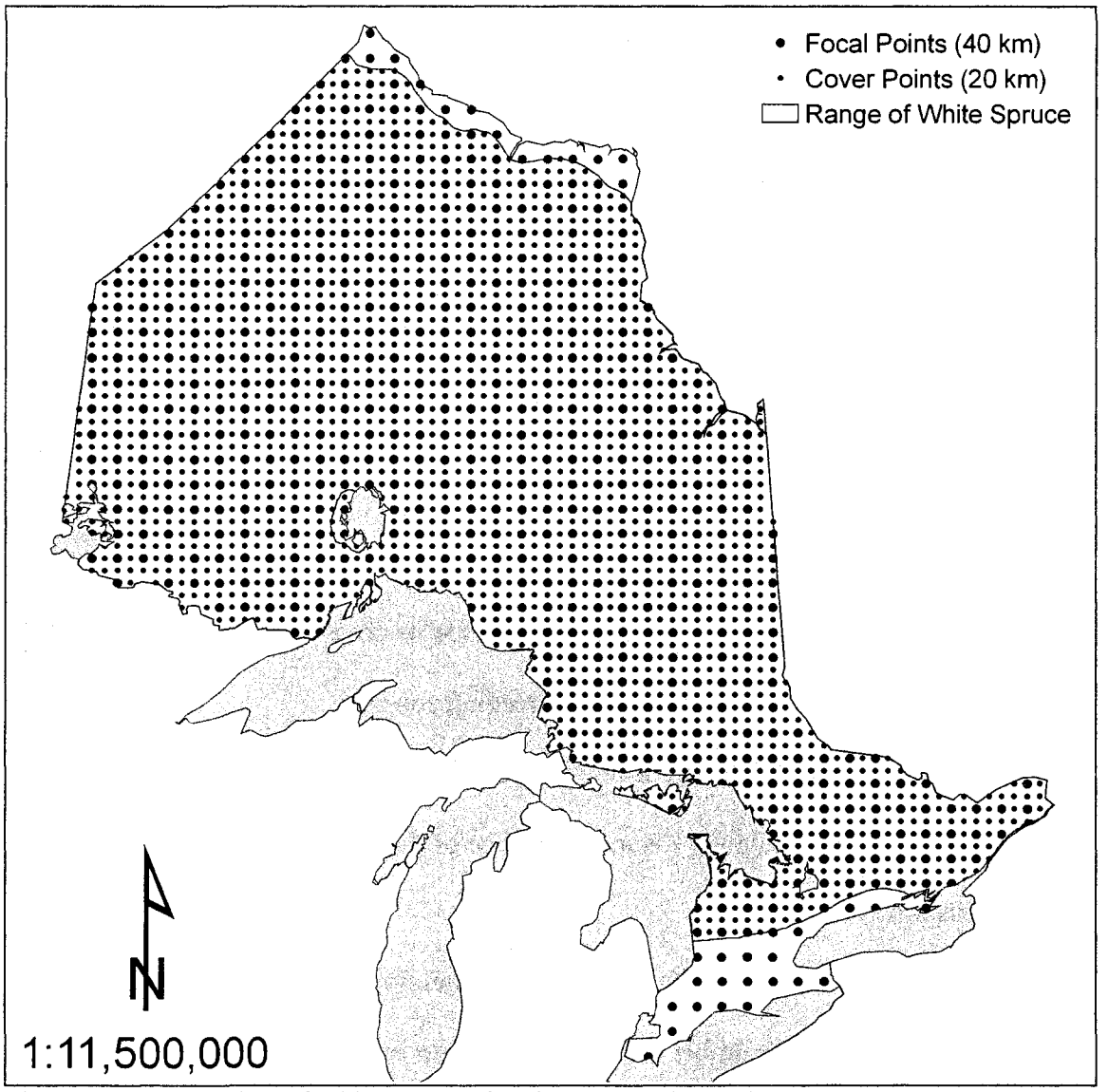

Figure 12. Location of white spruce focal and covering points used to construct candidate breeding zones for Ontario.

The decision-support model could then be used to select a subset of candidate breeding zones in order to maximize the number of points covered by a limited number

of breeding zones. The structure of this model is identical to that of Parker and Crowe (2005) and is of the following form:

$$[1] \quad \max \sum_{i \in I} y_i$$

$$[2] \quad \sum_{j \in N_i} x_j \geq y_i \qquad \forall i \in I$$

$$[3] \quad \sum_{j \in J} x_j \leq k$$

$$[4] \quad x_j \in \{0,1\} \quad \forall j \in J$$

$$[5] \quad 0 \leq y_i \leq 1$$

where:

i, I = the index and set of geographic points to be covered in a region;

j, J = the index and set of candidate breeding zones;

x_j = 1 if candidate breeding zone j is selected and = 0 otherwise;

y_i = 1 if geographic point i is in at least one of the selected breeding zones and = 0 otherwise;

Ni = the set of candidate breeding zones containing geographic point i; and

K = the maximum number of breeding zones to be selected

Equation [1] pertains to the objective function, which is to maximize the sum of geographic points covered by the selected breeding zones. Equation [2] dictates that if

the candidate breeding zone x_j is selected, then x_j and y_i are equal to 1, and equal to 0 otherwise. Equation [3] is the constraint on the number of selected breeding zones, which may not exceed k in number. Equation [4] dictates that the x_j decision variable is binary in form; that is, the value of x_j can only be equal to 0 or 1. Finally, equation [5] dictates that the value of decision variable y_i is between 0 and 1.

Thus, the model is used to determine the subset of breeding zones which maximizes geographic coverage subject to a constraint on the total number of allowable zones (Parker and Crowe 2005). The constraint on the number of zones is enforced to manage costs of the tree improvement program; each breeding zone requires a substantial investment over the duration of the tree improvement program. Successive model runs can be used to determine how many zones are needed to cover the entire set of points in Ontario. Also, the model can also be used to explore how many breeding zones are required for complete coverage when zones are developed at various levels of adaptive similarity (*i.e.* 0.5 or 1.0 LSD).

The model was first solved based on the set of 1.0 LSD candidate breeding zones; 1 zone was selected from the set of 618 candidates to achieve the maximum possible coverage. Subsequent iterations were used to determine the increase in coverage when the number of selected zones was increased by 1, and were continued until all points were covered. The process was repeated, starting from 1-zone and using the 0.5 LSD candidate breeding zones as input to the model, to determine the total number of zones required for full coverage at the 0.5 LSD level of adaptive similarity. All 1.0 LSD solutions were solved to an exact optimal solution using the CPLEX 8.1 MIP solver, as per Crowe and Parker (2005). However, to reduce computation time, all

solutions with greater than 18 zones at the 0.5 LSD level were solved within a high probability of optimality of 0.001.

Operational breeding zones were also developed for three forest management regions in Ontario. Additional sets of candidate breeding zones were developed at the 1.0 LSD level of similarity for the northwest, northeast, and southern forest management regions. The grid of focal points was developed at 40-km resolution to coincide with the Ontario-wide grid, resulting in 124, 125, and 60 candidate breeding zones for the northwest, northeast, and southern regions, respectively. The grid of cover points was developed at 20-km resolution, resulting in 559 points for the northwest, 524 points in the northeast, and 227 cover points in the southern region. The location of the focal and cover points is presented in Figure 13 to Figure 15 for the northwest, northeast, and southern regions, respectively.

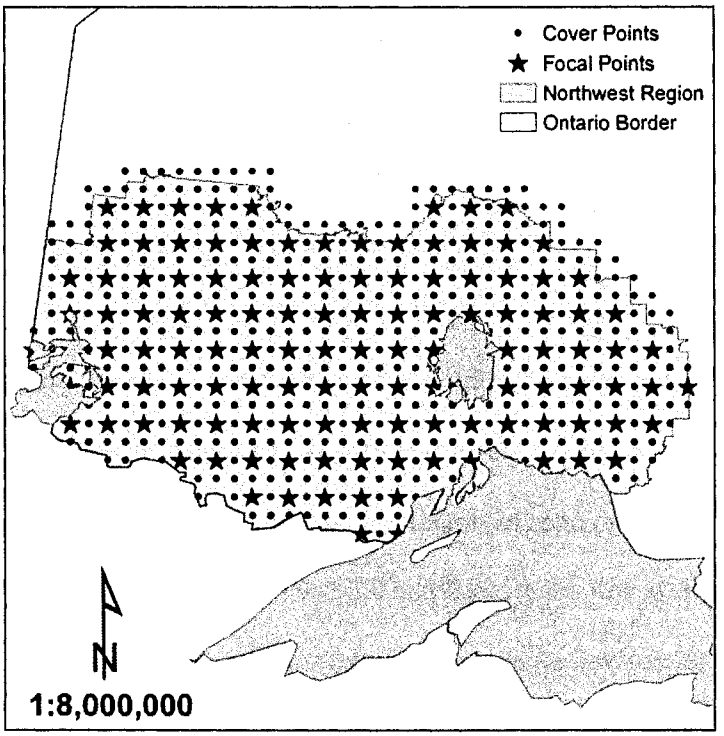

Figure 13. Location of focal and cover points for the northwest management region of Ontario.

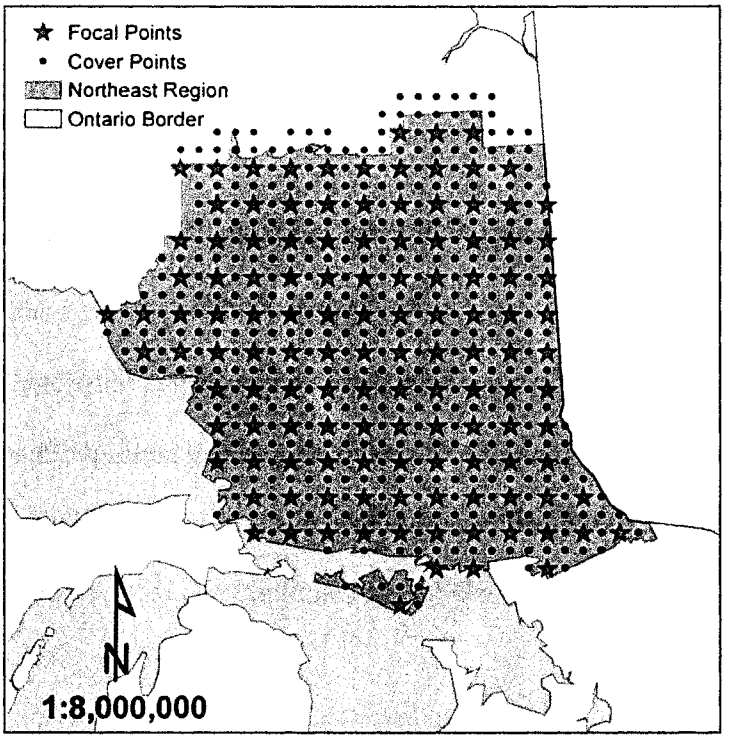

Figure 14. Location of focal and cover points for the northeast management region of Ontario.

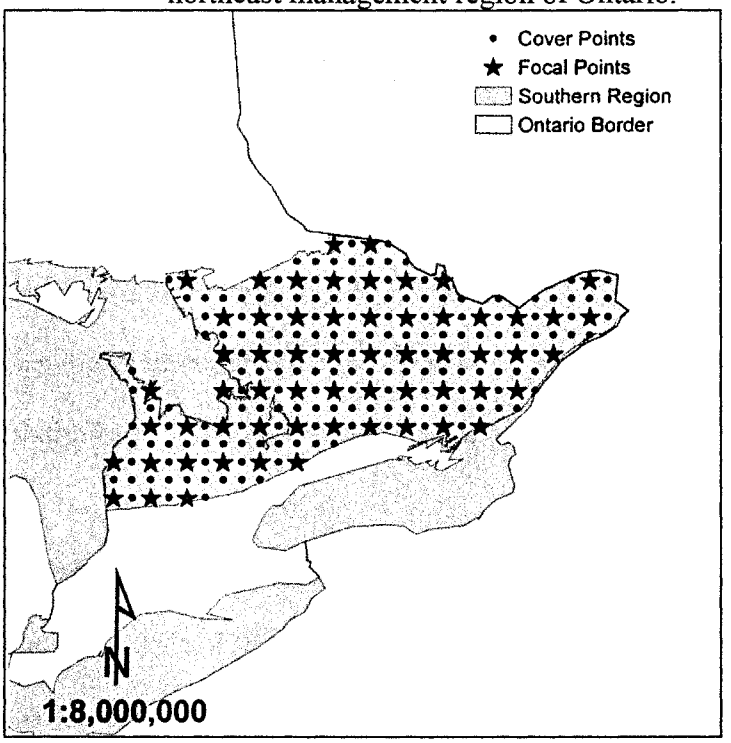

Figure 15. Location of focal and cover points for the southern management region of Ontario.

RESULTS

BREEDING ZONES FOR THE RANGE OF WHITE SPRUCE IN ONTARIO

The relative tradeoff between the level of coverage that is achieved and the number of breeding zones selected by the maximal covering model is illustrated in Figure 16. The solution for the first set of 618 candidate breeding zones produced at the 1.0 LSD level of similarity is presented by the green series line, and the solution for the second set of zones produced at the 0.5 LSD level of similarity is presented by the purple series line.

As the number of selected zones increases, the gain in percent area covered decreases dramatically. The first 3 zones for the 1.0 LSD solution produce the greatest gains, each contributing at least 15% of the total coverage. When four or more zones are chosen for the solution, each additional zone contributes less than 10% to the total coverage. As the number of zones increases past 11, it is evident that the contribution of additional zones is negligible (< 1%). For the 0.5 LSD solution, only the first two zones produce more than 10% additional coverage. The 3 to 19-zone solutions produce 2-6% additional coverage, while the 20-zone solution produces less than 1% additional coverage.

When comparing the 1.0 and 0.5 LSD solutions, it is apparent that there exists a tradeoff between the chosen level of adaptive similarity (i.e. 0.5 or 1.0 LSD) and the number of zones required for complete coverage. The number of zones required for complete coverage based on the 1.0 LSD solution is 14 while the 0.5 LSD solution

requires more than 45 breeding zones (not shown). Also, relative gains produced by each additional breeding zone decrease much more quickly for the 0.5 LSD solution in comparison with 1.0 LSD.

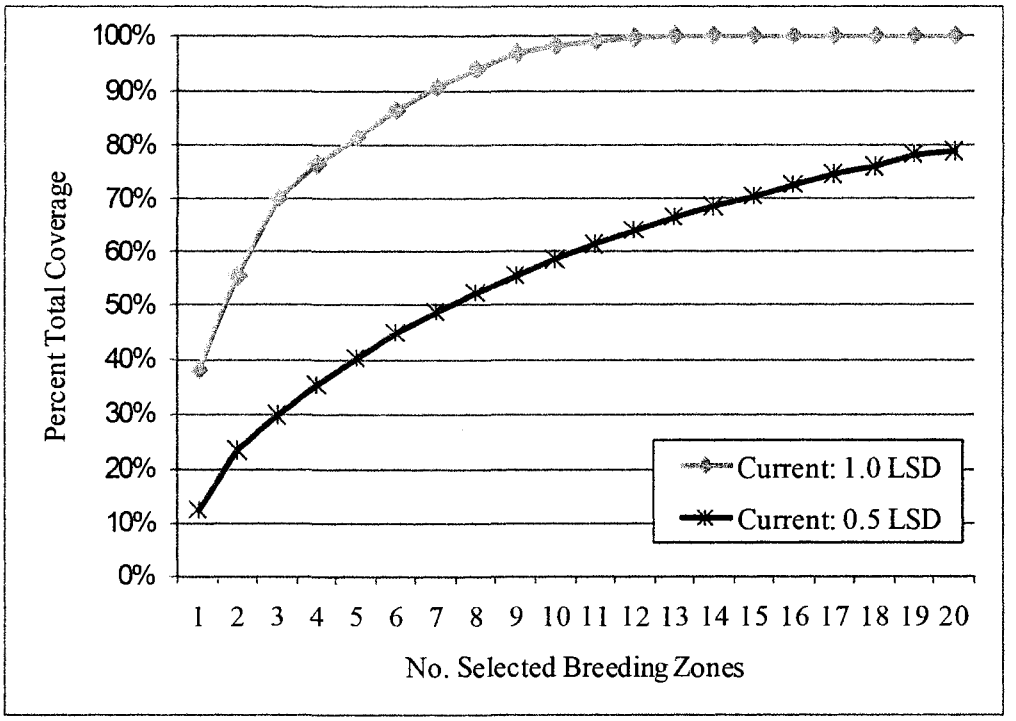

Figure 16. Percent of the white spruce distribution within Ontario covered with increasing number of breeding zones selected by the maximal covering model based on current (1961-1990) climate.

Figure 17 to Figure 29 illustrate current breeding zones selected by the maximal covering model based on the allowance of 1 through 7 zones at the 1.0 LSD level of adaptive similarity. Each zone within a solution set is indicated by a polygon of a different color, while the focal point associated with a given zone is indicated by a star of the same color in darker shading. Areas of overlap between breeding zones are presented in intermediate shading; for example the overlap of a blue and yellow zone would produce green shading in the area of intersection. Due to the difficulty in distinguishing breeding zone boundaries as a result of overlap in solutions based on

four-or-more zones, the most recently added zone for each iteration is presented individually preceding the full solution to more clearly identify its location. Note that the boundaries of previously selected breeding zones may vary somewhat between subsequent solutions, reflecting the dynamic nature of the maximal covering model. These slight changes reflect the fact that the model does not simply select the next largest zone to be added to the solution. Rather, the model considers all possible combinations to arrive at the solution that provides the greatest possible coverage.

Figure 17 presents the solution when only 1 breeding zone is selected from the set of 618 candidate breeding zones at the 1.0 LSD level of adaptive similarity. The breeding zone associated with focal point 215 was the first to be selected and covers a total of 38.0% of the distribution of white spruce in Ontario. This zone is surprisingly large, extending approximately 4° latitude and 11° longitude, across much of the mid to northern latitudes of northwestern and northeastern Ontario.

The addition of a second breeding zone immediately to the north (Figure 18) increases the total area covered to 55.4% and introduces a very small area of overlap between zones (Figure 19). The zone associated with focal point 477 extends northwards from the border of the adjacent zone (373) and terminates before reaching Hudson and James Bay. The central breeding zone (373) is somewhat narrower in latitude than the central zone of the previous solution (215) and indicates the exclusion of an area surrounding Lake Nipigon along the north shore of Lake Superior.

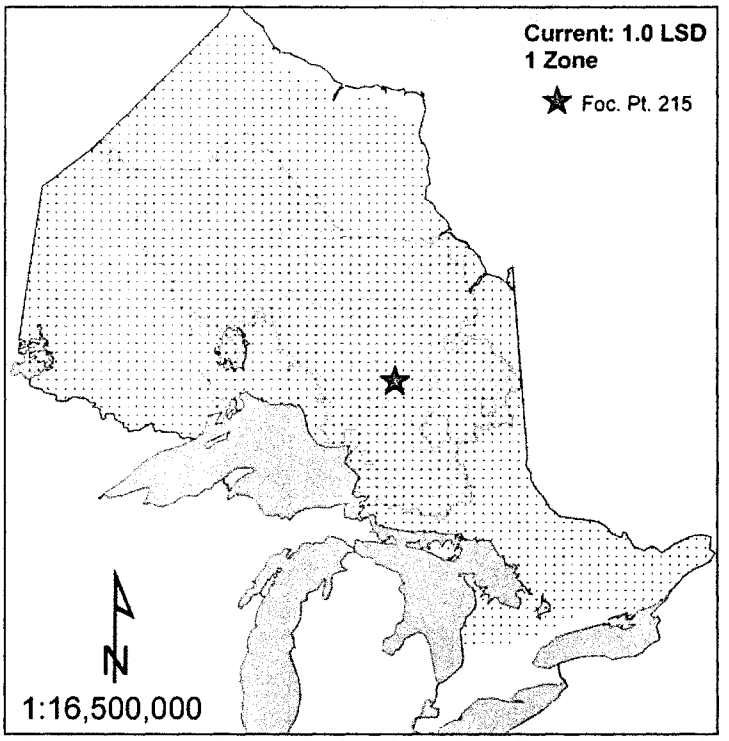

Figure 17. Optimal solution for 1 breeding zone based on the 1.0 LSD level of adaptive similarity.

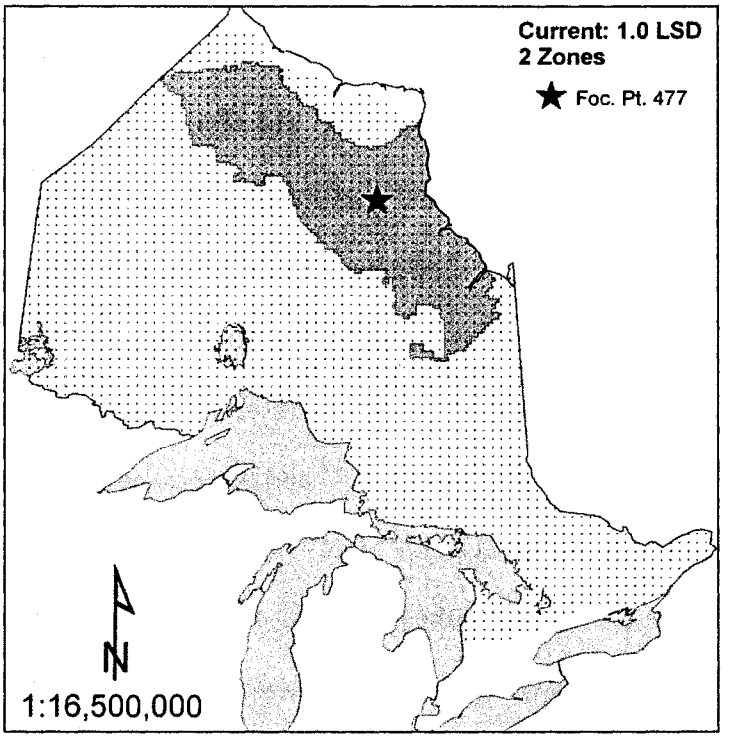

Figure 18. Breeding zone for focal point 477, based on the 1.0 LSD level of adaptive similarity.

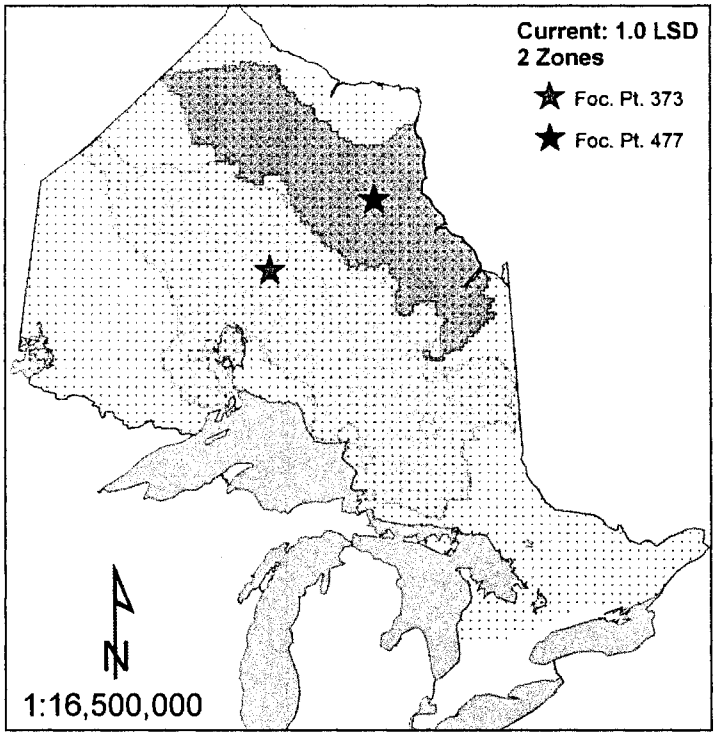

Figure 19. Optimal solution for 2 breeding zones, based on the 1.0 LSD level of adaptive similarity.

The 3-zone solution selects focal points 373, 477, and 75. Focal point 75 consist of two additional areas of coverage (Figure 20). The first of these is located in the southeast surrounding the focal point while the second is located in the northwest adjacent to the Manitoba border. This breeding zone reflects the similarity in adaptation between the northwest and southeast that is indicated by principal components factor scores (Figure 3 to Figure 5) and by seed zone examples (Figure 6 to Figure 11). The three-zone solution results in a total coverage of 70.1% and demonstrates very little overlap between adjacent zones (Figure 21). The large central zone (373) and adjacent mid-northerly zone (477) are the same as in the previous 2-zone solution. The majority of the interior of the province is now covered, and the remaining areas are largely restricted to the periphery of the study area.

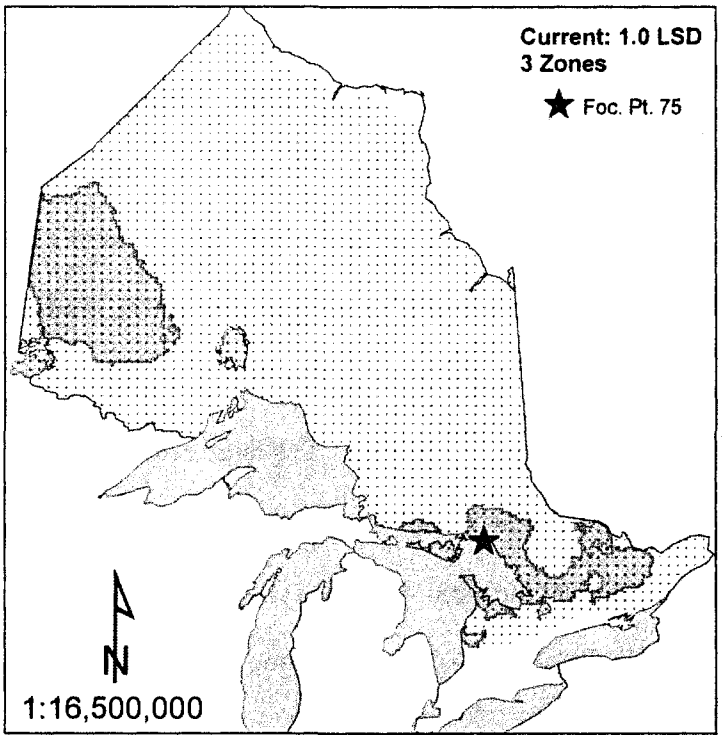

Figure 20. Breeding zone for focal point 75 based on the 1.0 LSD level of adaptive similarity.

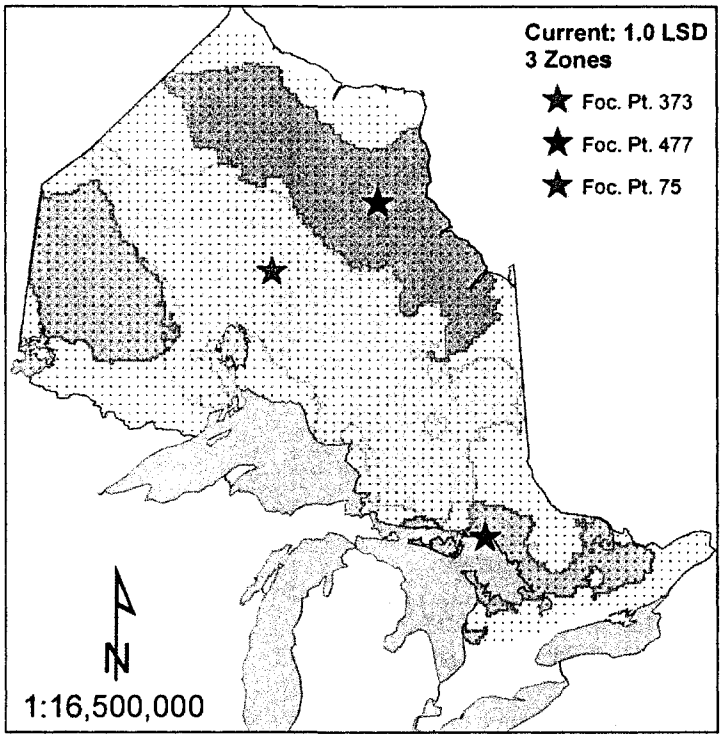

Figure 21. Optimal solution for 3 breeding zones based on the 1.0 LSD level of adaptive similarity.

The optimal 4-zone solution selects focal points 131, 325, 75, and 584. Focal point 584 covers the far north of Ontario, stretching northward to Hudson Bay (Figure 22). A total coverage of 76.4% is achieved with the 4-zone solution (Figure 23). The mid-northerly zone (325) shifts southward in comparison with the previous 3 solutions, creating a large area of overlap between the adjacent central zone (131). The eastern perimeter of the mid-northerly zone also expands northwards and southwards to cover much greater latitude than in the previous 3 solutions. The large central zone (131) is much the same as for the 3-zone solution, though a notable difference is the large southeastward shift of the focal point location. The zone covering the northwest/southeast portions of the province (75) is the same as for the 3-zone solution.

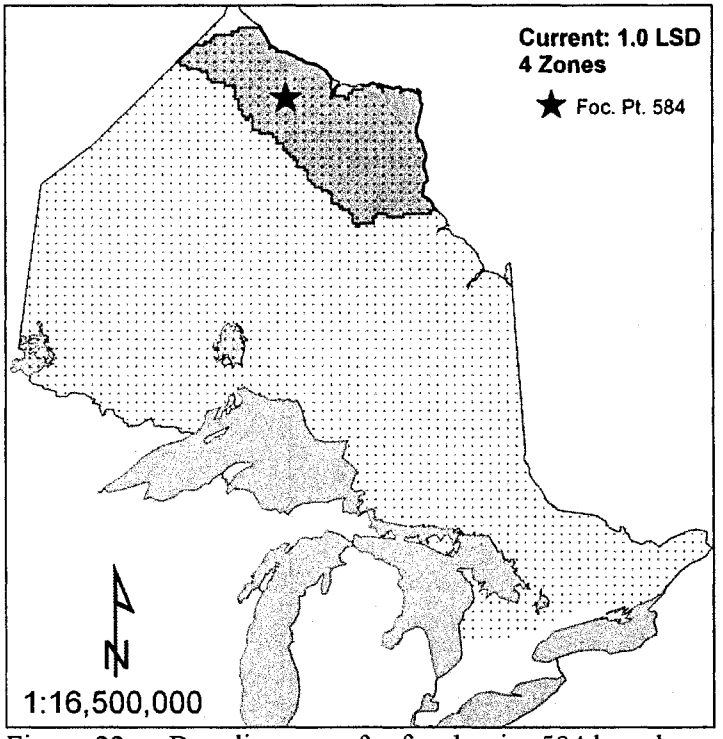

Figure 22. Breeding zone for focal point 584 based on the 1.0 LSD level of adaptive similarity.

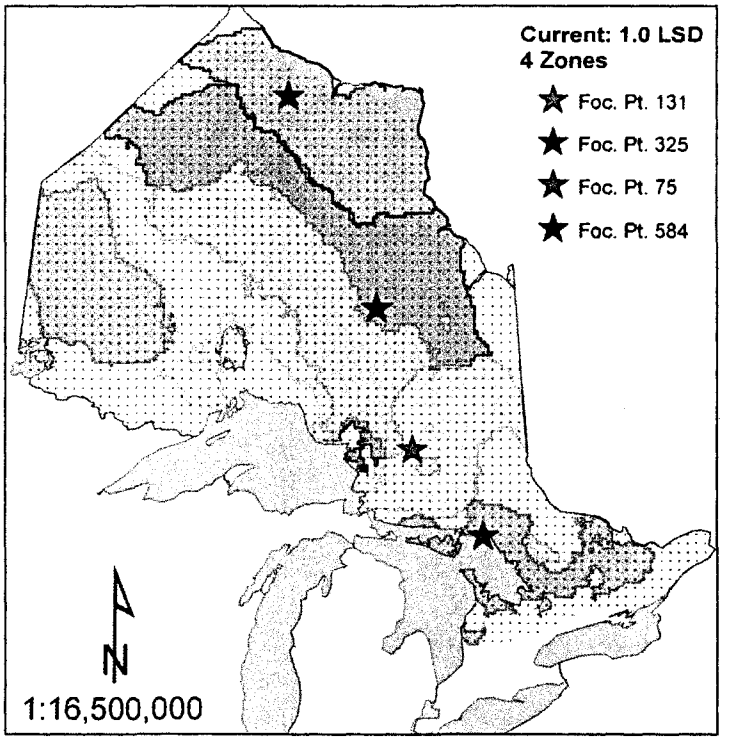

Figure 23. Optimal solution for 4 breeding zones based on the 1.0 LSD level of adaptive similarity.

The optimal 5-zone solution results in the selection of another disjunct zone (146) with coverage in the northeast adjacent to the Quebec border and in the northwest approximately 60 km removed from, but skirting the western and northern perimeter of Lake Nipigon (Figure 24). The optimal 5-zone solution results in total coverage of 81.5%. The addition of focal point 146 results in additional areas of overlap where it intersects with zones 345 and 325 in the northwest and zone 345 in the northeast. The mid-northerly (325) and far northern (584) zones are the same as in the 4-zone solution. The focal point for the northwestern/southeastern zone (336) shifts from the southeast to the northwest, but the boundaries of this zone remains much the same. The focal point for the central zone (345) shifts to the northwest and the zone narrows in the east.

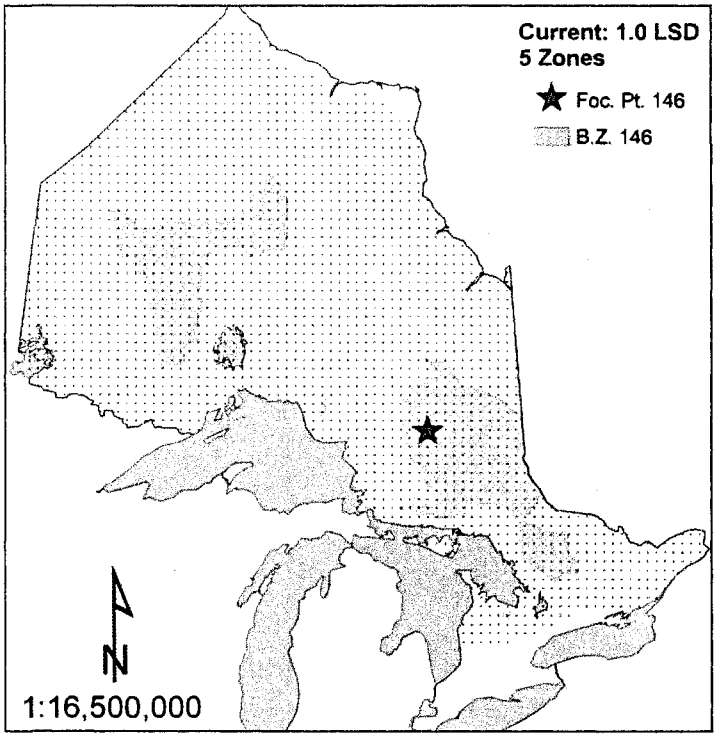

Figure 24. Breeding zone for focal point 146 based on the 1.0 LSD level of adaptive similarity.

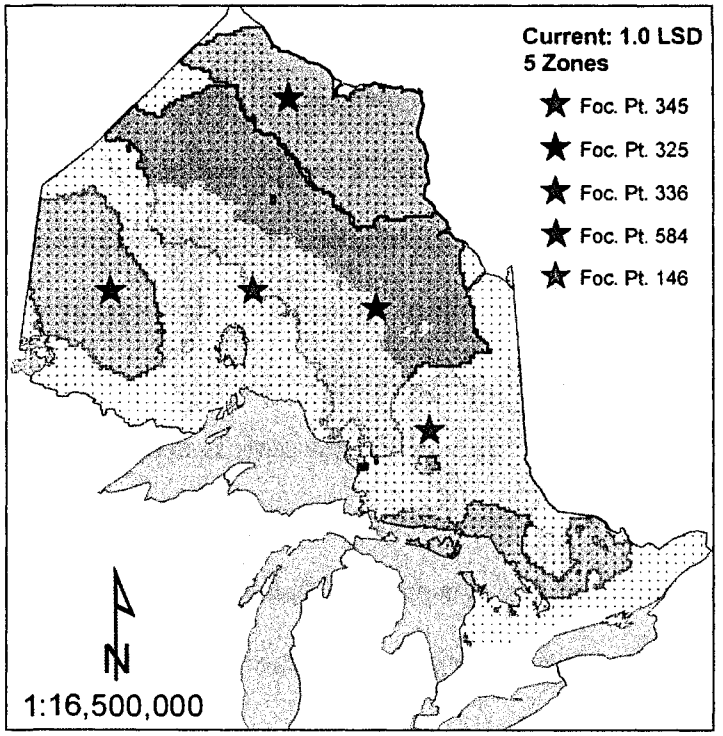

Figure 25. Optimal solution for 5 breeding zones based on the 1.0 LSD level of adaptive similarity.

The addition of focal point 17 creates a breeding zone covering the far southeastern portion of the province, extending from the southern range limit of white spruce northwards to the Ottawa Valley and Quebec border (Figure 26). This breeding zone also covers several small, disjunct patches; one is located in the northeast and two are located in the northwest of Ontario. The optimal solution for 6 zones covers an additional 5%, or a total of 86.5% of the area (Figure 27). The addition of focal point 17 creates very little additional areas of overlap, which occur mostly where the three disjunct segments and zone 387 intersect. The central (345), mid-northerly (325), and far northern (584) zones are the same, while the disjunct northwest/southeast (387) and northwest/northeast (106) zones are similar to the 5-zone solution.

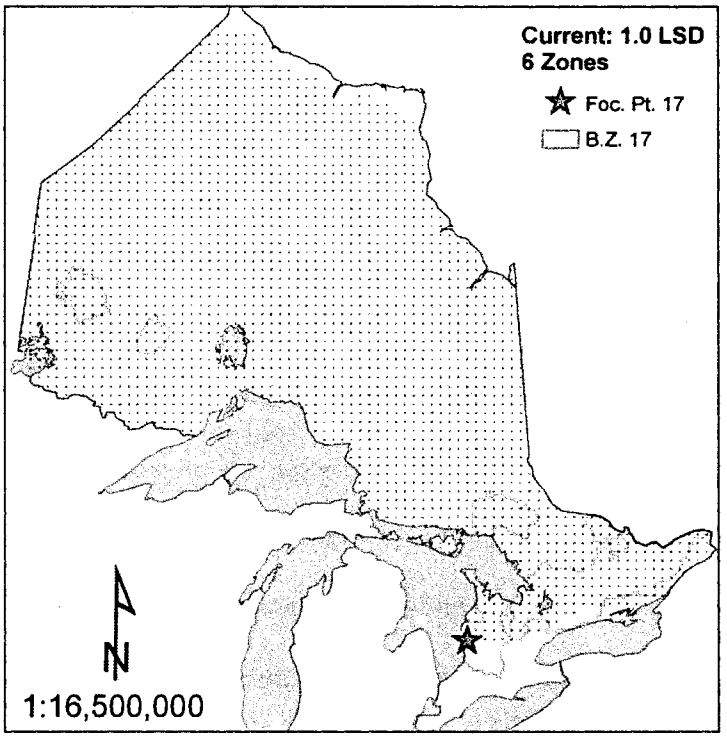

Figure 26. Breeding zone for focal point 17 based on the 1.0 LSD level of adaptive similarity.

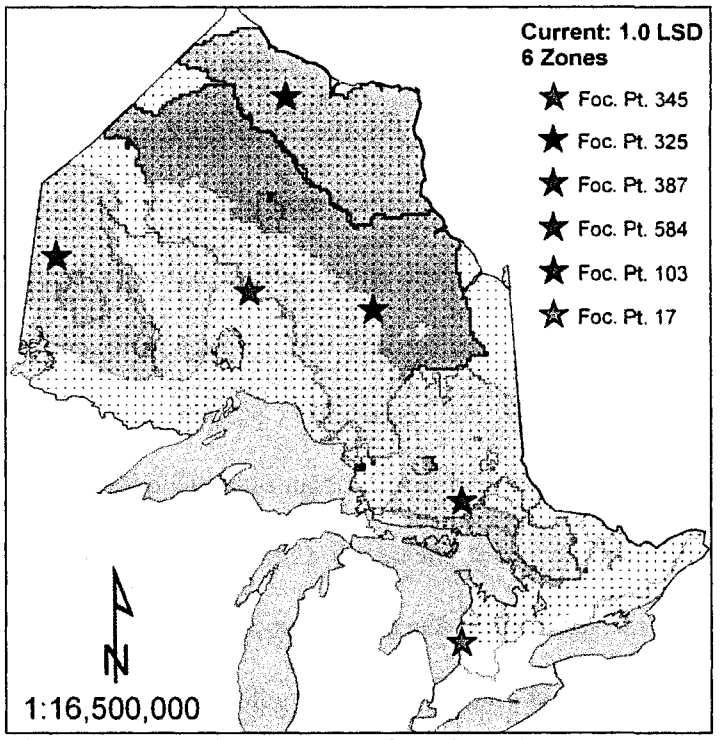

Figure 27. Optimal solution for 6 breeding zones based on the 1.0 LSD level of adaptive similarity.

The addition of focal point 330 results in a breeding zone covering the far northeast adjacent to James Bay (Figure 28). Total coverage for the 7-zone solution is equal 90.8% of the total area (Figure 29). The remaining uncovered area is mostly limited to the far south of the northwest region, extending from the Thunder Bay area westward to the Fort Frances area. The addition of focal point 330 results in a great deal more overlap, most notably with zone 508 in the northwest. Overlap between zones in the central latitudes of the province is now quite extreme, making it difficult to interpret where the boundary of each zone lies. The mid-northern zone (508) is notably changed from that of the 6-zone solution, specifically due to the extreme latitudinal narrowing in the central portion of the zone. In contrast, the central zone (345) remains unchanged and the northwest/southeast (283), northwest/northeast (146), far northern (598), and southeastern (35) zones remain very similar to the 6-zone solution.

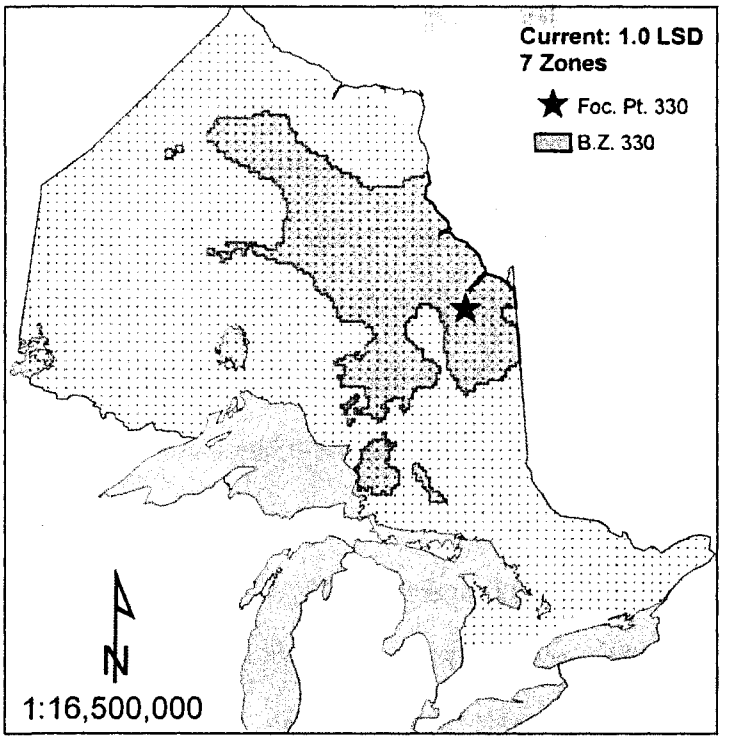

Figure 28. Breeding zone for focal point 330 based on the 1.0 LSD level of adaptive similarity.

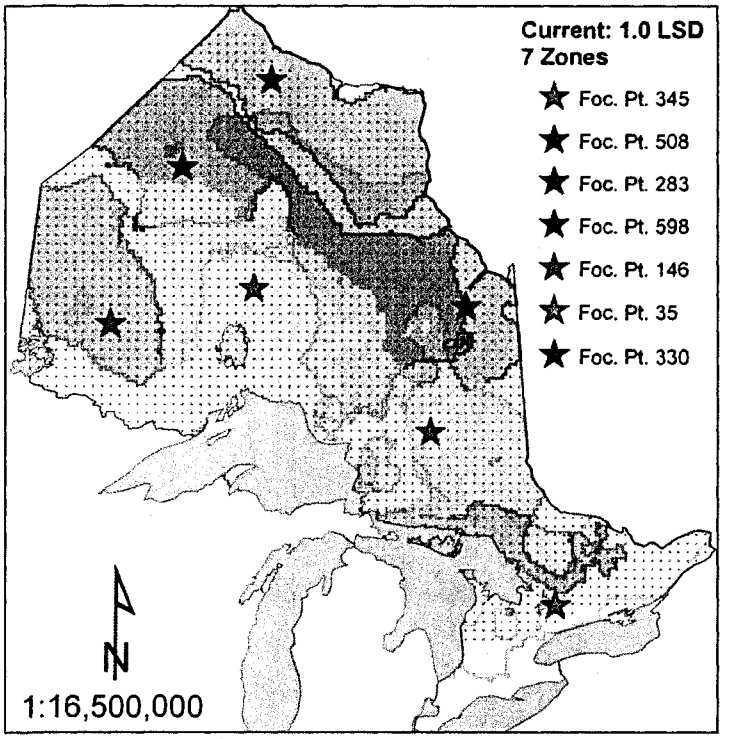

Figure 29. Optimal solution for 7 breeding zones based on the 1.0 LSD level of adaptive similarity.

Figure 30 to Figure 39 illustrate current breeding zones selected by the maximal covering model based on the allowance of 1 through 10 zones at the 0.5 LSD level of adaptive similarity. Similar to figures for the 1.0 LSD solutions, each zone within a solution set is indicated by a polygon of a different color, while the focal point associated with a that zone is indicated by a star of darker shading. Areas of overlap are again indicated by intermediate shading. However, the most recently added zone for each iteration is not presented separately from the main solution due to the very small degree of overlap between zones.

The first solution results in total coverage of 12.5% with the addition of an elongate zone in the center of the province (Figure 30). This zone is very similar to that of the 1-zone solution at the 1.0 LSD level of adaptive similarity, but is much narrower.

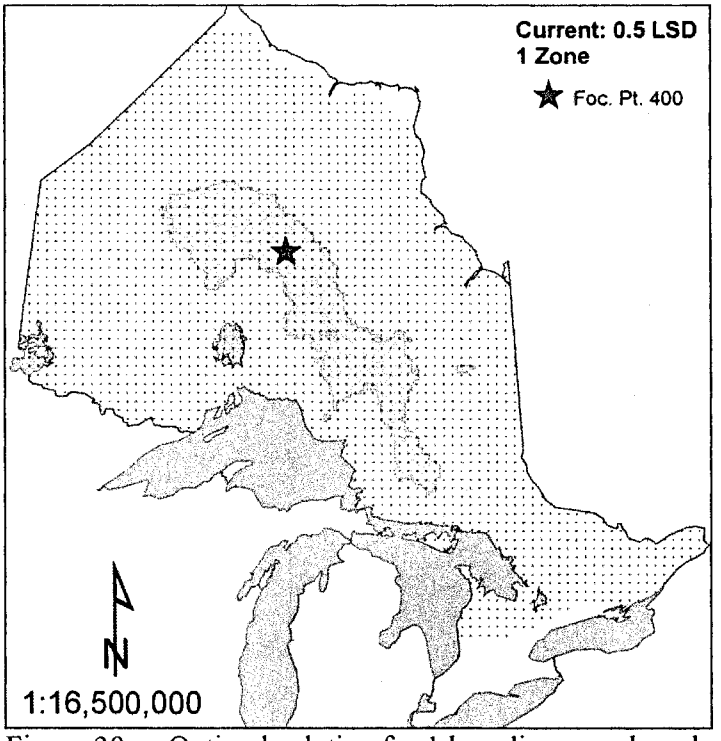

Figure 30. Optimal solution for 1 breeding zone based on the 0.5 LSD level of adaptive similarity.

The addition of zone 381 immediately to the north brings the total coverage to 23.3% for the optimal 2-zone solution (Figure 31). The central zone is extremely similar to that of the previous 1-zone solution. In contrast to the 1.0 LSD solution set, there is notable gap between the borders of the central and mid-northern zones at the 0.5 level. Also, the mid-northern zone is similar to that of the 2-zone solution at the 1.0 LSD level, but is much narrower in the central longitudes of the zone.

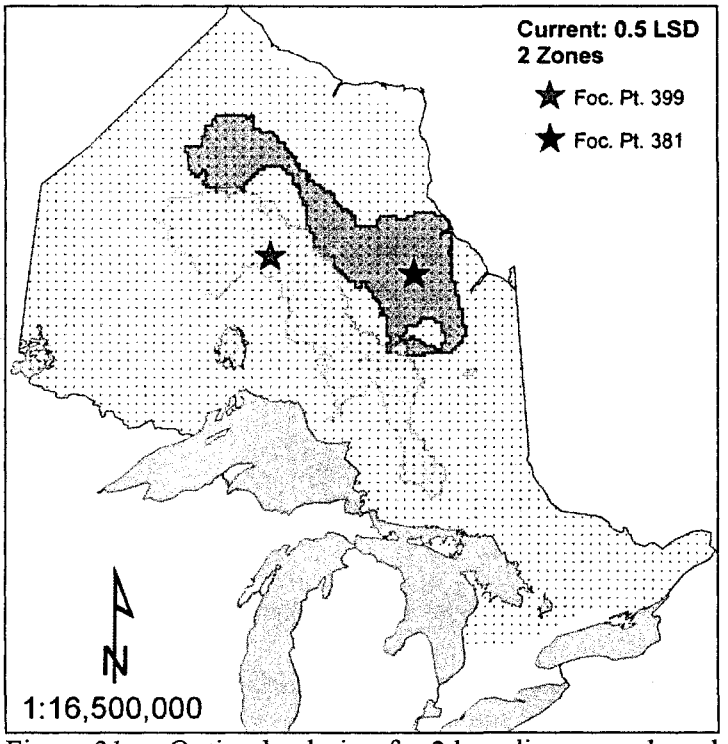

Figure 31. Optimal solution for 2 breeding zones based on the 0.5 LSD level of adaptive similarity.

The addition of breeding zone 345 just to the north of Lake Nipigon brings the total coverage for the optimal 3-zone solution to 29.7% (Figure 32). This main portion of this zone skirts the shores of Lake Nipigon in the west, indicating the exclusion of the lake effect areas. Several small, disjunct areas are also located to the south of the main zone. The central zone is latitudinally broader than that of the 2-zone solution and is truncated along its eastern border. The mid-northern zone is also broader, greatly

increasing coverage along the adjacent borders of the mid-northern and central zones in comparison to the 2-zone solution.

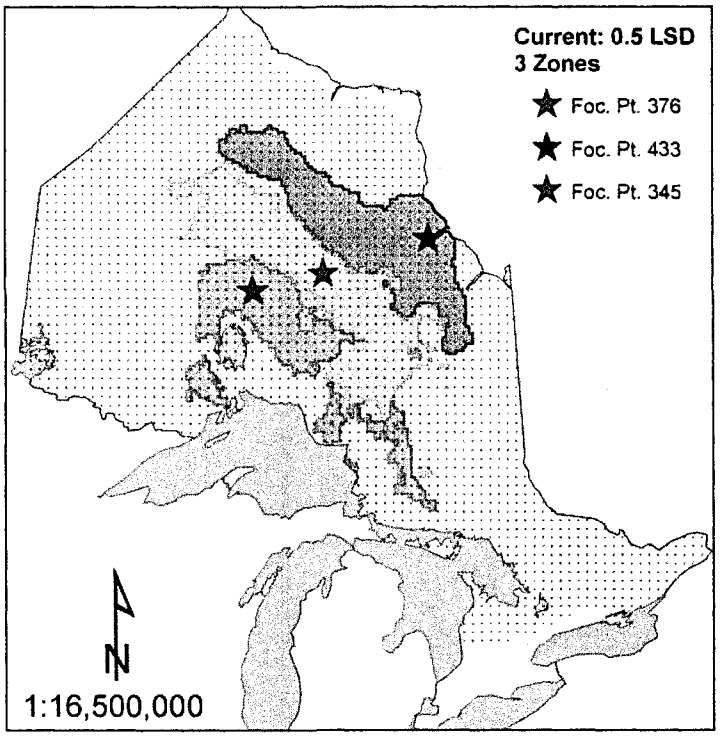

Figure 32. Optimal solution for 3 breeding zones based on the 0.5 LSD level of adaptive similarity.

The four-zone solution covers 35.3% of the total area (Figure 33). The addition of focal point 365 introduces an area of coverage in the northwest and also two tiny areas in the southeast. The central, mid-northern, and northern Lake-Nipigon zones are the same as for the 3-zone solution. Breeding zone 365 appears to coincide with the northern portion of the northwest zone (283) at the 1.0 LSD level of adaptive similarity (Figure 29).

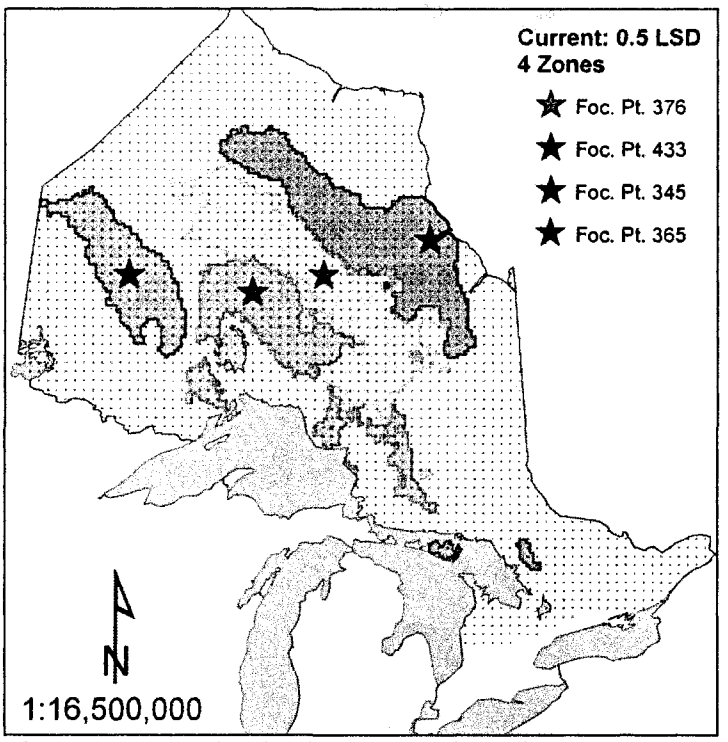

Figure 33. Optimal solution for 4 breeding zones based on the 0.5 LSD level of adaptive similarity.

For the optimal 5-zone solution, the addition of focal point 113 increases the total area covered to 40.1% (Figure 34). This zone is composed of two disjunct segments; the larger of which is located surrounding the focal point in the northeast and the smaller is located in the northwest. The central (376), northern Lake Nipigon (345), and north-northwest (365) zones are the same, while the mid-northern zone (432) is very similar to the 4-zone solution.

The addition of focal point 535 increases the total coverage to 44.8% for the optimal 6-zone solution (Figure 35). Breeding zone 535 is located in the far north adjacent to James Bay. In comparison the optimal 5-zone solution, the mid northern zone (433) is very similar, while the remaining four zones are the same.

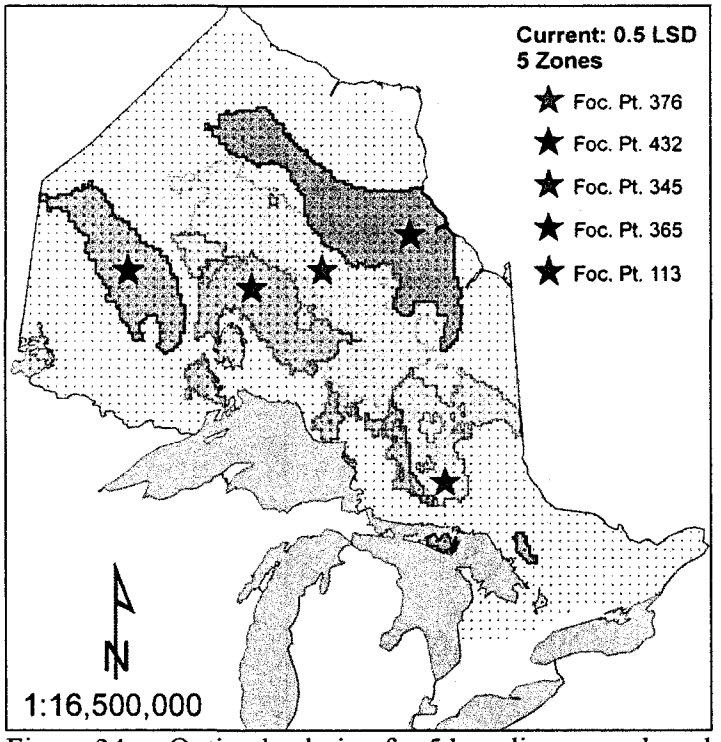

Figure 34. Optimal solution for 5 breeding zones based on the 0.5 LSD level of adaptive similarity.

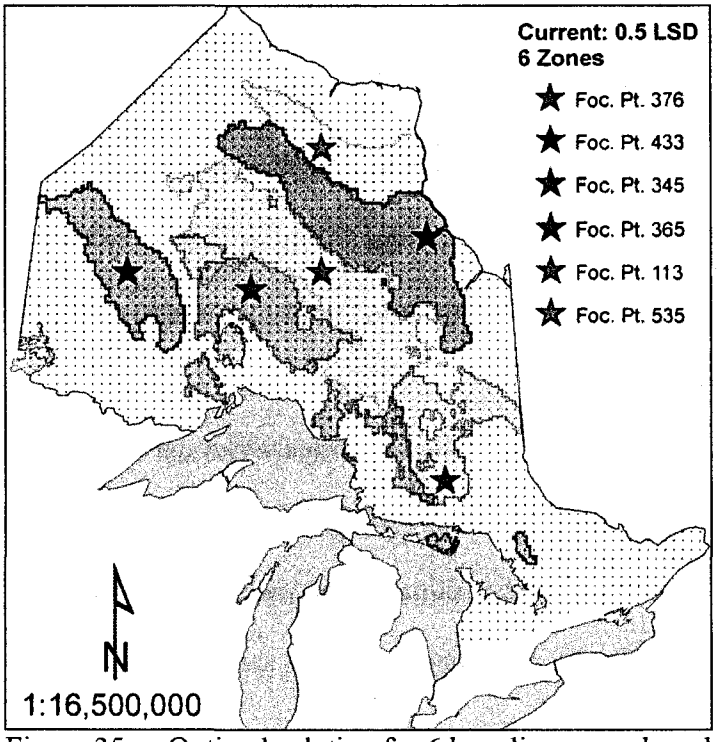

Figure 35. Optimal solution for 6 breeding zones based on the 0.5 LSD level of adaptive similarity.

For the optimal 7-zone solution, the coverage increases only 3.9% to a total of 48.7% (Figure 36). The addition of focal point 361 creates a second breeding zone in the northwest. In comparison to the optimal 6-zone solution, the mid-northern zone (408) is very similar, while the remaining 5 zones (376, 345, 365, 113, and 535) are exactly the same.

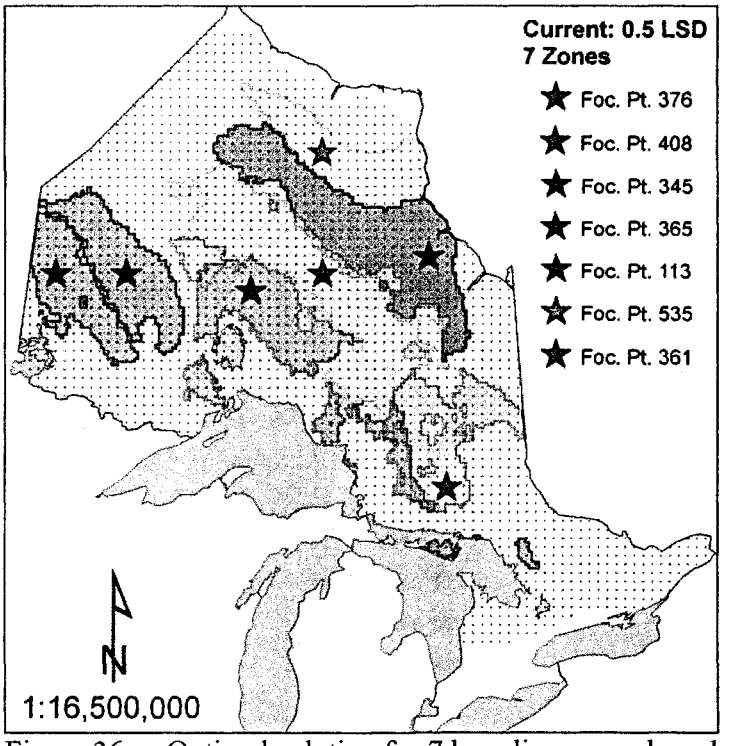

Figure 36. Optimal solution for 7 breeding zones based on the 0.5 LSD level of adaptive similarity.

The addition of focal points 554 (Figure 37), 545 (Figure 38), and 464 (Figure 39) increases the total coverage to 52.4, 55.6, and 58.5% for the optimal 8, 9, and 10-zone solutions, respectively. The majority of the central portion of the province is now covered. However, virtually the entire south-central region and large portions of the northeast region remain uncovered. There are numerous other void areas located throughout the northwest such as in: the far northwest adjacent to Hudson Bay, the south along the Minnesota border, and the area immediately south of Lake Nipigon.

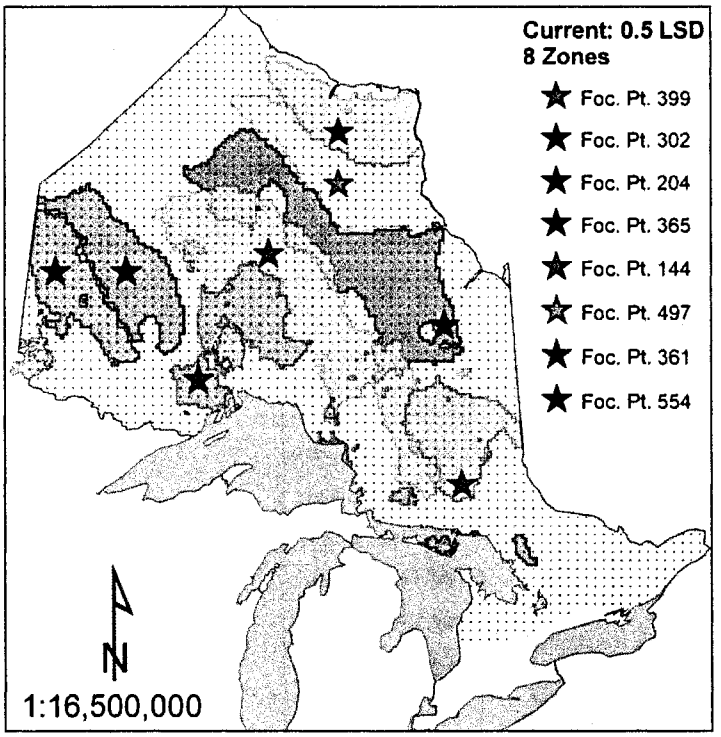

Figure 37. Optimal solution for 8 breeding zones based on the 0.5 LSD level of adaptive similarity.

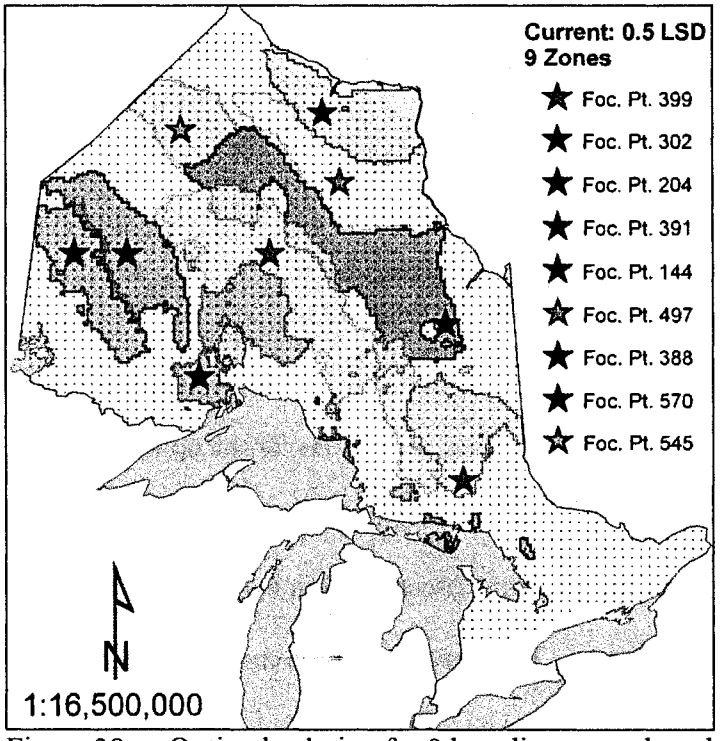

Figure 38. Optimal solution for 9 breeding zones based on the 0.5 LSD level of adaptive similarity.

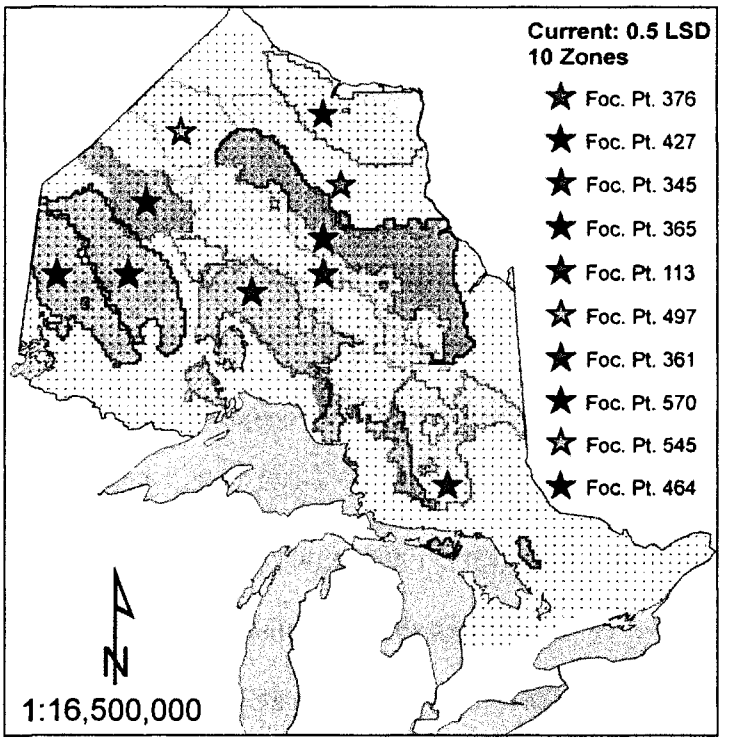

Figure 39. Optimal solution for 10 breeding zones based on the 0.5 LSD level of adaptive similarity.

There are a number of evident trends when comparing optimal breeding zones for the 0.5 LSD level of adaptive similarity (Figure 39) and those constructed at the 1.0 LSD level (Figure 29). The most obvious of these patterns is that the 0.5 LSD zones are more latitudinally restricted. Also, the 0.5 LSD zones are generally composed of a single area surrounding the focal point, in comparison with the 1.0 LSD zones that are often composed of several discontinuous areas. Interestingly, the zones for the 1.0 LSD and 0.5 LSD solutions are similar in shape and location, though smaller in size. That is, a number of zones resembling those of the 1.0 LSD solution can be distinguished from the 0.5 LSD solutions. For example, the combination of the 0.5 LSD zones 365 and 361 resembles the northwest zone (283) in the 1.0 LSD solution. Also, breeding zone 144 resembles the discontinuous northwest/northeast zone (146) demonstrated for the 1.0

LSD solution. For both the 0.5 and 1.0 LSD solution sets, the southern portion of the northwest region and the area south of Lake Nipigon are among the last to be covered.

BREEDING ZONES FOR ONTARIO'S FOREST MANAGEMENT REGIONS

Figure 40 presents the level of coverage that is achieved for each management region, for 1- to 6-zone solutions at the 1.0 LSD level of adaptive similarity. Full coverage of both the northwest and northeast regions is achieved with just 6 breeding zones. Interestingly, the southern management region, which is 43.7% of the size of the northwest forest management region, requires almost as many zones (5) for complete coverage. Both the northeast and southern regions achieve higher percent coverage than the northwest when either 1 or 2 zones are selected. However, at 3 or more zones the northwest is similarly covered and all 3 regions achieve at least 90% total coverage with just 3 breeding zones.

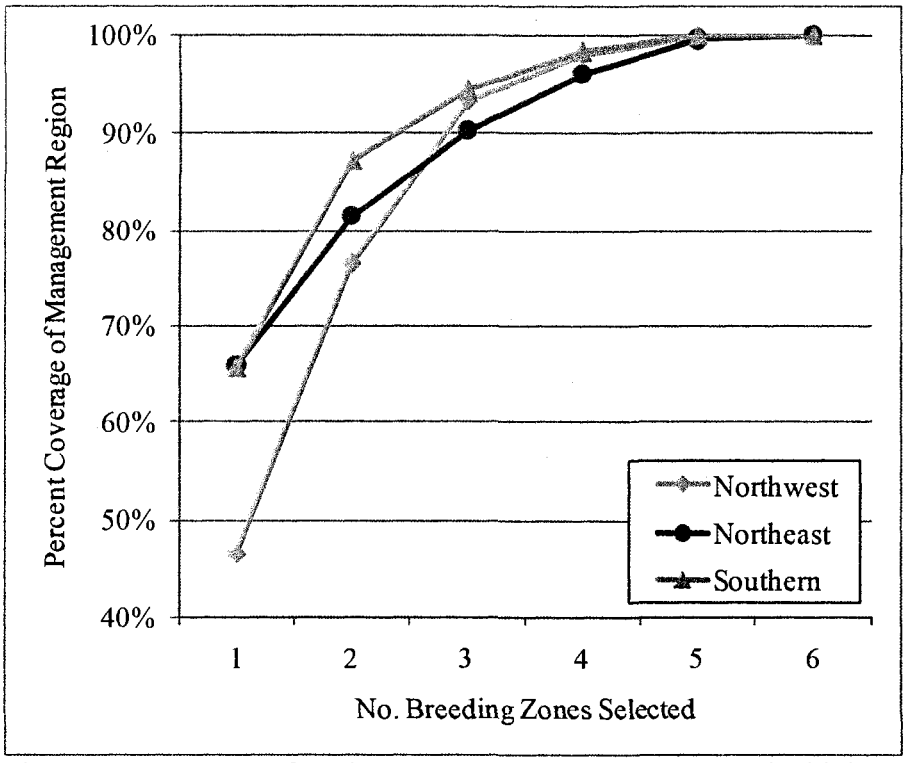

Figure 40. Percent of total management region area covered with increasing number of breeding zones for the northwest, northeast, and southern management regions based on observed 1961-1990 climate normals and 1.0 LSD level of adaptive similarity.

Figure 41 to Figure 45 present the current breeding zones for the northwest region based on the allowance of 1 through 5 zones at the 1.0 LSD level of adaptive similarity. The optimal 1-zone solution for the northwest achieves 46.5% coverage with the selection of focal point 261 to the west of Lake Nipigon (Figure 41). Breeding zone 261 stretches from approximately 110 km west of Lake Nipigon to the eastern edge of the region, excluding an area between the north shore of Lake Superior and the southeastern edge of Lake Nipigon.

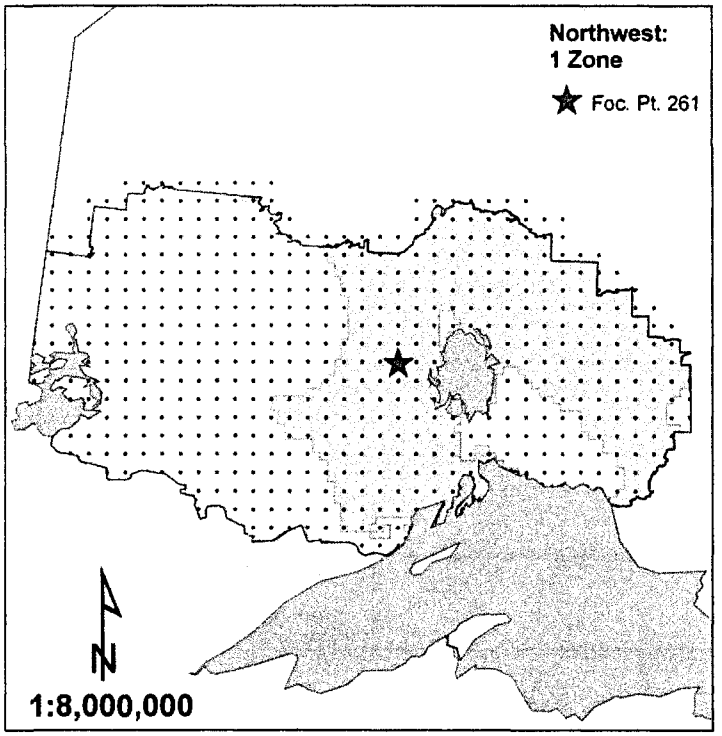

Figure 41. Optimal solution for the northwest region based on 1 breeding zone at the 1.0 LSD level of adaptive similarity.

The selection of focal point 229 brings total coverage for the optimal 2-zone solution to 76.4% (Figure 42). Breeding zone 229 covers most of the western portion of the northwest region, stretching from the adjacent border of the eastern breeding zone westward almost to the Manitoba border. A small area of overlap occurs along the central latitudes of the adjoining boundaries of zone 319 and 229. In comparison with the 1-zone solution, the area between Lake Superior and Lake Nipigon that was previously excluded is now enclosed within the eastern breeding zone (319).

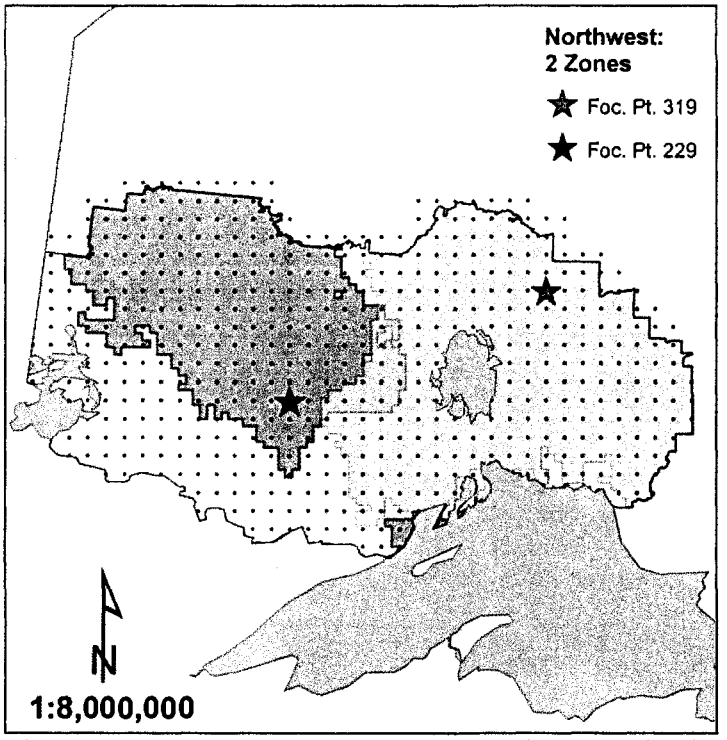

Figure 42. Optimal solution for the northwest region based on 2 breeding zones at the 1.0 LSD level of adaptive similarity.

The selection of focal point 225 in the southwest increases the total coverage to 93.2 % for the optimal 3-zone solution (Figure 43). Breeding zone 225 covers most of the southwest of the region, excluding a small area to the south of Lake of the Woods along the Minnesota border. The selection of breeding zone 225 creates a small area of overlap along the adjoining border of zone 364. In comparison with the 2-zone solution, there is a very clear demarcation between the western and eastern zone at approximately 90° longitude, which virtually eliminates overlap between these zones.

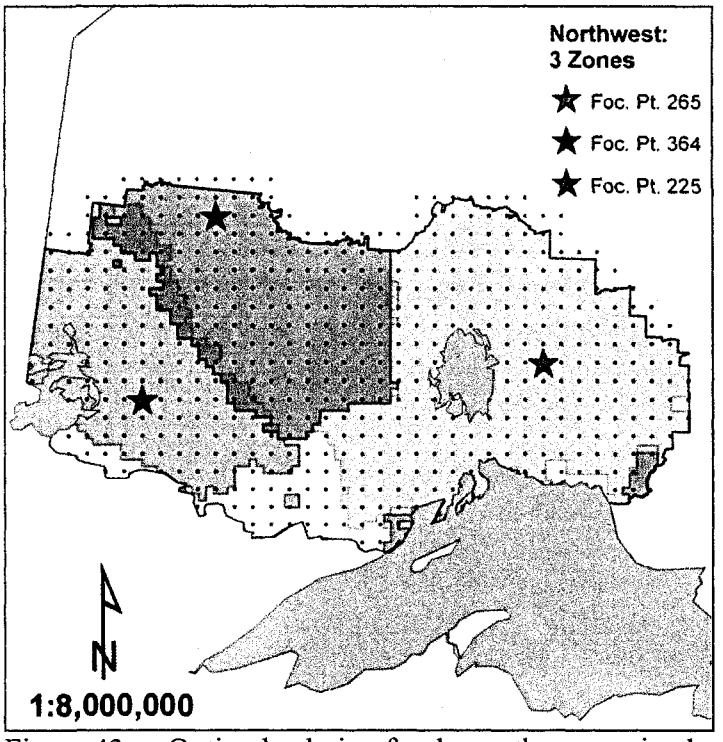

Figure 43. Optimal solution for the northwest region based on 3 breeding zones at the 1.0 LSD level of adaptive similarity.

The selection of focal point 174 covers most of the remaining area along the southern edge of the Thunder Bay and Fort Frances districts, bringing the total coverage to 97.9 % (Figure 44). Overlap between the southwest (224) and western (284) zones is minimal in the 4-zone solution, but the selection of the southern zone creates new areas of overlap in the west. The western (284) and eastern (237) zones are very similar in comparison with the 3-zone solution.

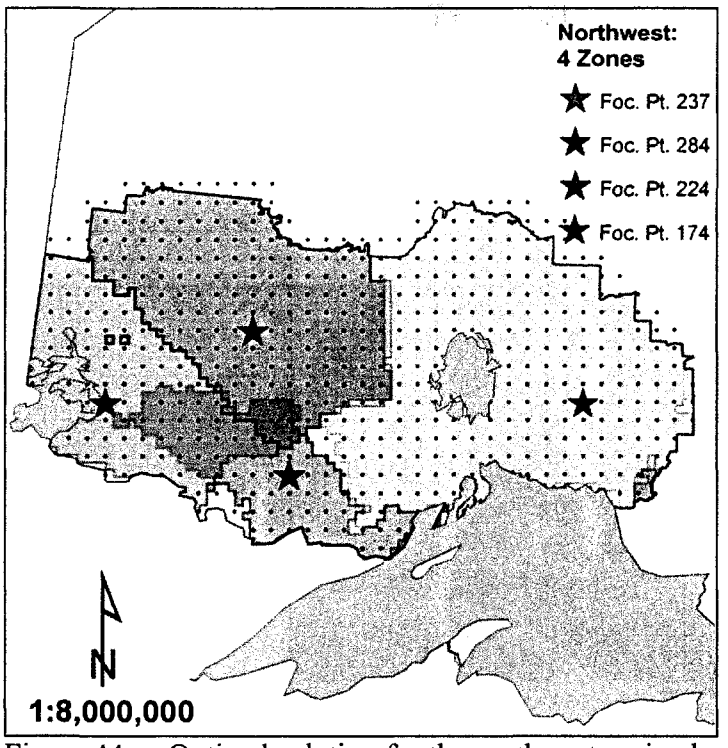

Figure 44. Optimal solution for the northwest region based on 4 breeding zones at the 1.0 LSD level of adaptive similarity.

The selection of focal point 175 increases coverage by only 1.8%, but significantly increases the area of overlap between zones (Figure 45). Total coverage for the optimal 5-zone solution is 99.6%. The selection of breeding zone 175 in the south results in a westward shift of the southern zone (171) and increases overlap between the southern and southwestern (254) zones in comparison with the 4-zone solution.

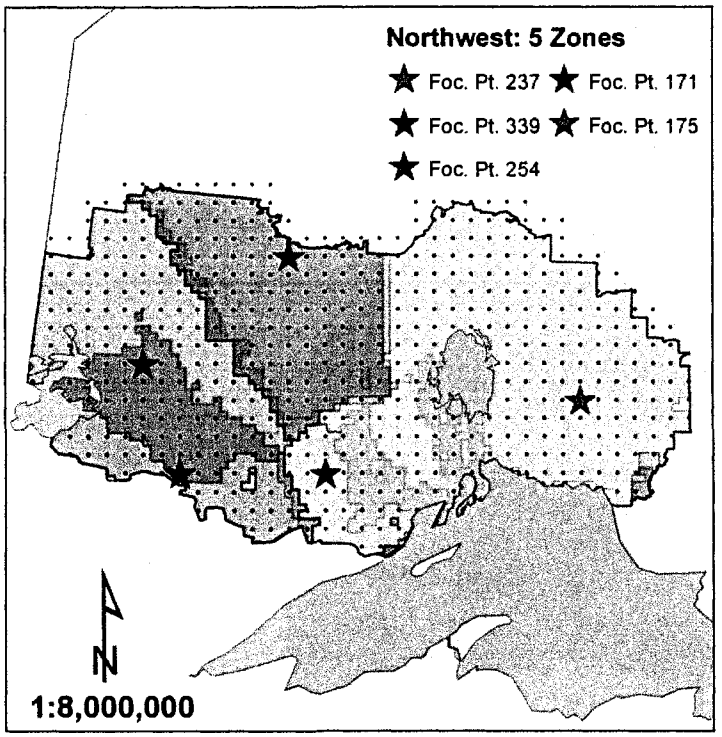

Figure 45. Optimal solution for the northwest region based on 5 breeding zones at the 1.0 LSD level of adaptive similarity.

Figure 46 to Figure 50 present the current breeding zones for the northeast region based on the allowance of 1 through 5 zones at the 1.0 LSD level of adaptive similarity. The optimal 1-zone solution produces 65.8% coverage with the selection of a broad zone (187) that covers the majority of the northern and central latitudes of the region (Figure 46).

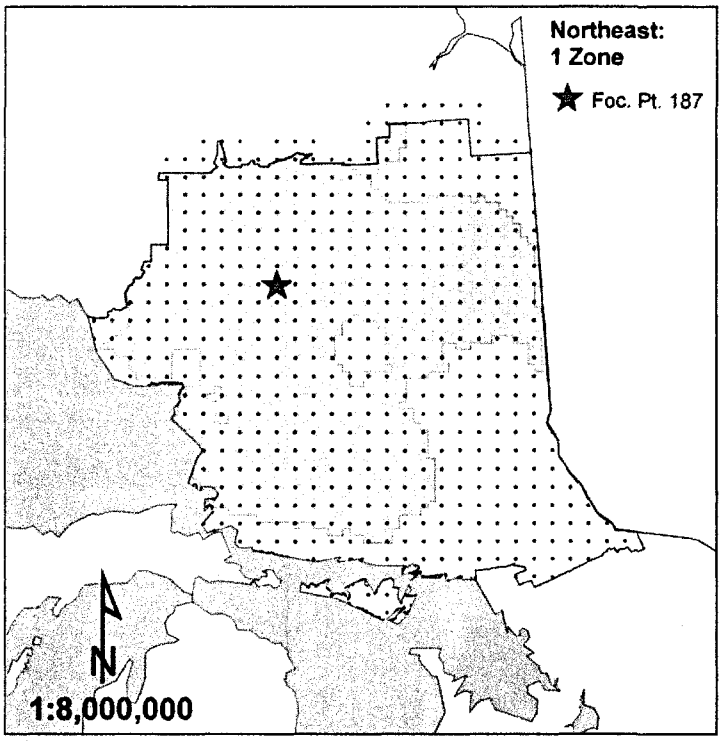

Figure 46. Optimal solution for the northeast region based on 1 breeding zone at the 1.0 LSD level of adaptive similarity.

The selection of focal point 118 increases coverage to 81.5% for the optimal 2-zone solution (Figure 47). Breeding zone 118 is composed of two disjunct areas in the north of the region that overlap moderately with the broad north-central (103) zone. The larger of the two areas is located surrounding the focal point in the west and the other is located along the Quebec border in the east. In comparison with the 1-zone solution, the broad north-central zone shifts southeast, increasing coverage in that area.

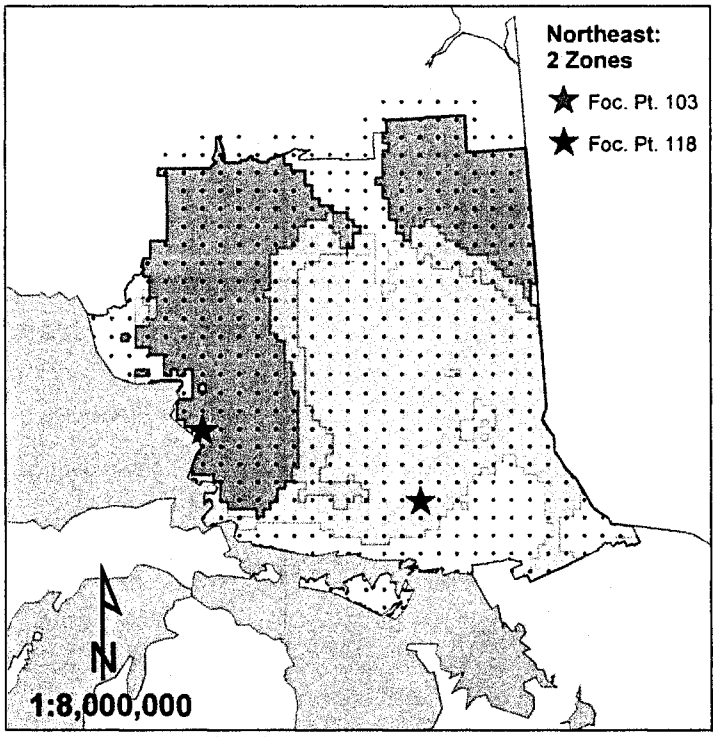

Figure 47. Optimal solution for the northeast region based on 2 breeding zones at the 1.0 LSD level of adaptive similarity.

The selection of focal point 74 results in near-complete coverage of the remaining area in the southwest and increases coverage to 90.3% (Figure 48). The disjunct northern zone is the same as for the 2-zone solution. However, the broader northern zone extends further northward to include most of previously uncovered area along the border with the northwest region. Minimal overlap occurs between zone 74 and the two northern zones.

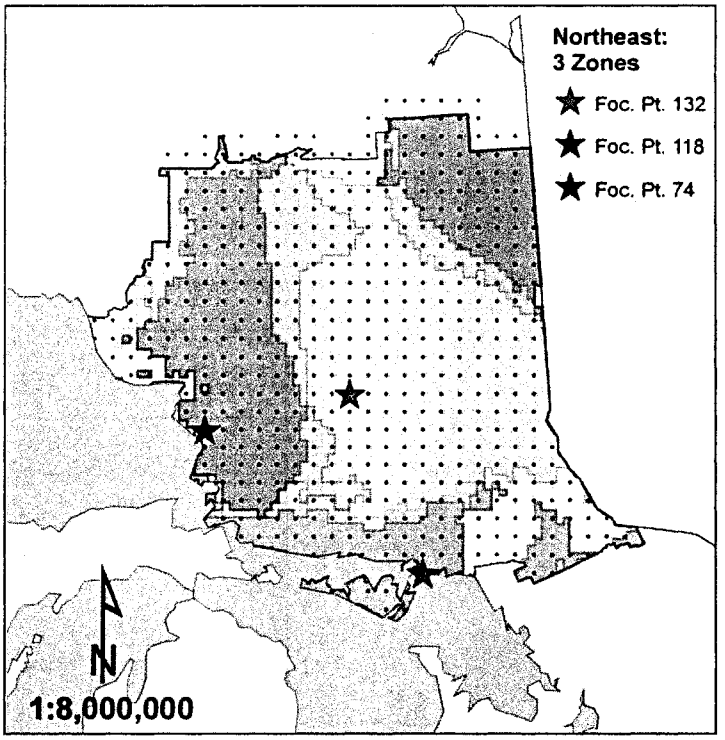

Figure 48. Optimal solution for the northeast region based on 3 breeding zones at the 1.0 LSD level of adaptive similarity.

The selection of focal point 107 in the southeast increases coverage to a total of 96.0% for the optimal 4-zone solution (Figure 49). Uncovered portions are now limited to a small area along the border with the southern region and another small area in the far northwest. In comparison to the 3-zone solution, the broad northern zone shifts north and east, greatly increasing overlap with the adjacent northern zone. In the southeast, breeding zone 74 overlaps moderately with the adjacent southwestern zone and more substantially with the broad northern zone.

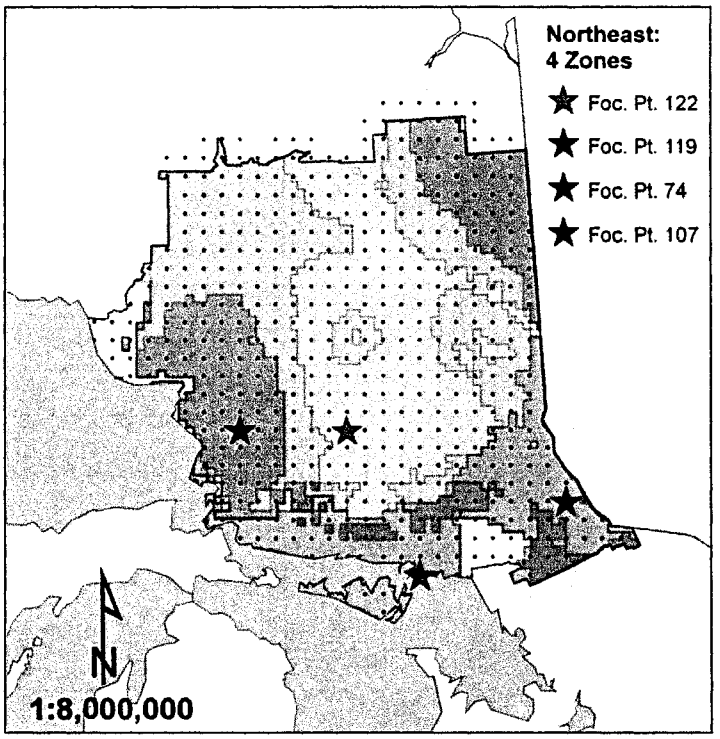

Figure 49. Optimal solution for the northeast region based on 4 breeding zones at the 1.0 LSD level of adaptive similarity.

The optimal 5-zone solution produces near total coverage of 99.4% (Figure 50). The selection of focal point 122 creates another large northern zone that almost entirely overlaps with the other two northern zones. The original northern zone expands westward and eastward, further increasing overlap with the disjunct northern zone, which remains similar to that of the 2-zone solution. The southwestern zone expands eastward to cover the last remaining gap in the south, while the southeastern zone remains unchanged.

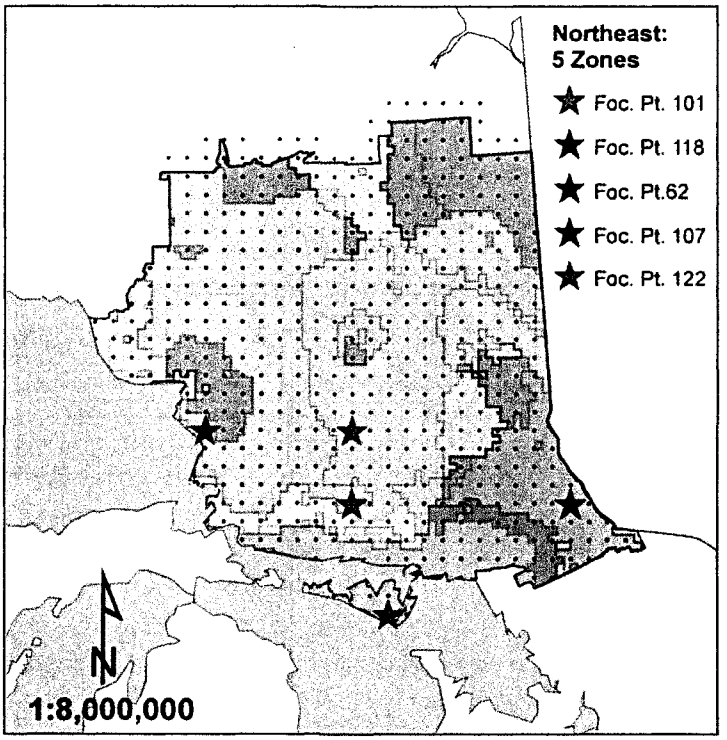

Figure 50. Optimal solution for the northeast region based on 5 breeding zones at the 1.0 LSD level of adaptive similarity.

Figure 51 to Figure 53 present the current breeding zones for the southern region based on the allowance of 5 zones at the 1.0 LSD level of adaptive similarity. The optimal 1-zone solution for the southern region achieves 65.5% coverage with the selection of focal point 35 (Figure 51). Breeding zone 35 covers most of the southern latitudes of the region, stretching from the eastern shore of Lake Huron north through the Ottawa Valley and to the Quebec border. Interestingly, this zone excludes the area of the Bruce Peninsula in the west.

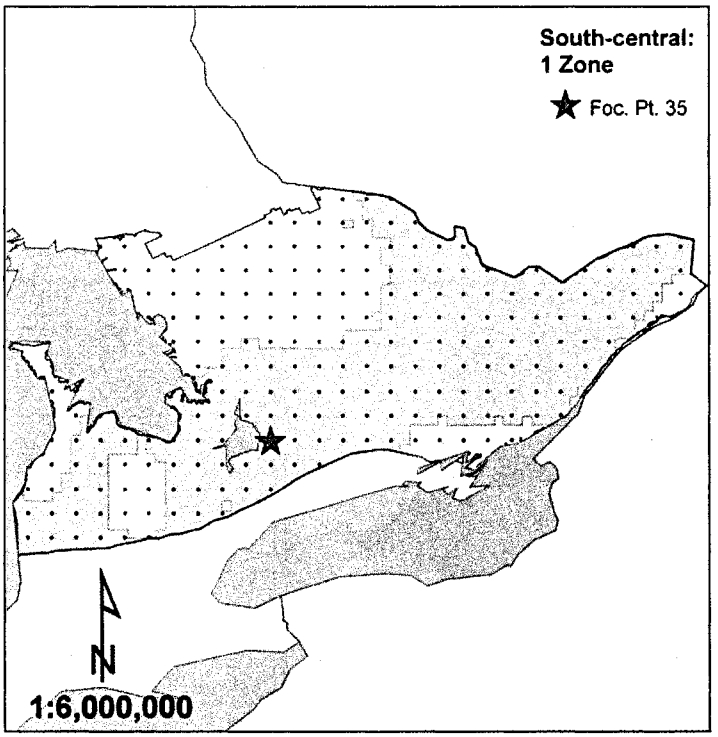

Figure 51. Optimal solution for the southern region based on 1 breeding zone at the 1.0 LSD level of adaptive similarity.

The selection of focal point 55 increases total coverage to 87.2%, but creates a substantial area of overlap with the southern zone (Figure 52). Breeding zone 55 covers most of the remaining area to the north, but is noticeably fragmented. In comparison with the 1-zone solution, the uncovered insular area within the southern breeding zone is now mostly covered by breeding zone 55.

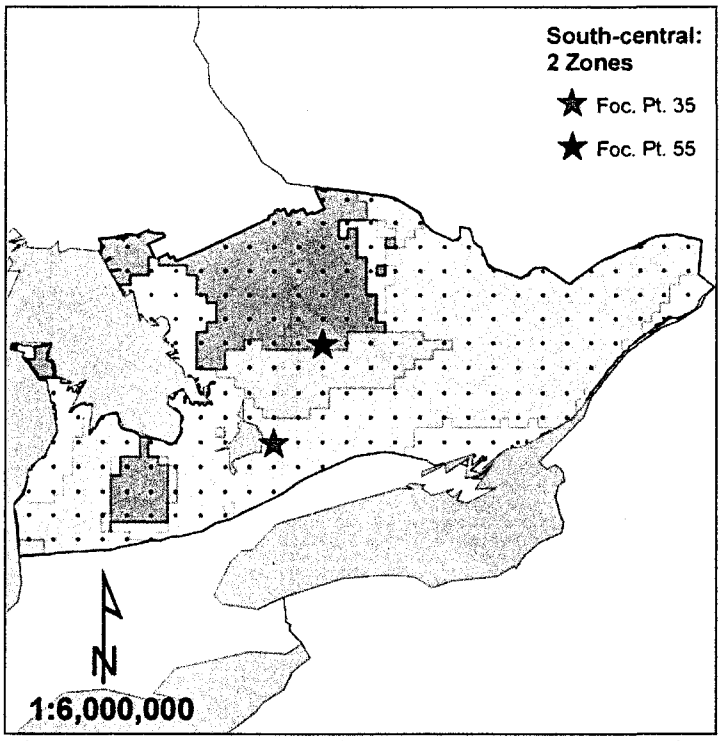

Figure 52. Optimal solution for the southern region based on 2 breeding zones at the 1.0 LSD level of adaptive similarity.

The selection of focal point 53 in the north increases total coverage to 94.3% for the optimal 3-zone solution (Figure 53). Breeding zone 53 overlaps substantially with the two other zones and creates only small, fragmented areas of additional coverage in the north. Several small areas without coverage remain in the south along the edge of the white spruce range.

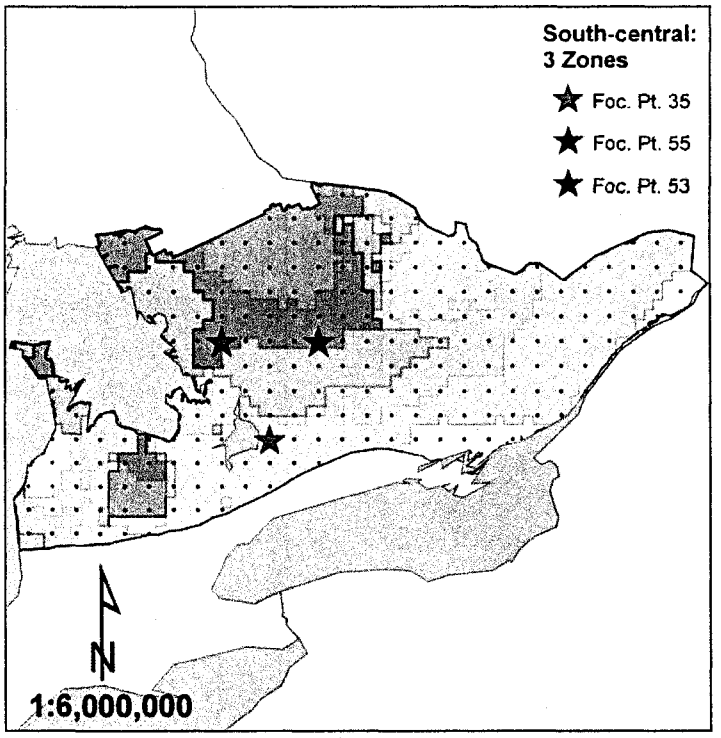

Figure 53. Optimal solution for the southern region based on 3 breeding zones at the 1.0 LSD level of adaptive similarity.

DISCUSSION

It is clear that there exists a tradeoff between the number of breeding zones required to achieve full coverage and a desired level of adaptive similarity; as the level of adaptive similarity increases, so too does the number of zones required to achieve full coverage. Since gains from tree improvement can only be realized within adaptive limits of a species or population (O'Neill and Aitken 2004), it may be desirable to use a more rigorous threshold (e.g. 0.5 LSD) to be certain that maladaptation is minimized. However, as previously noted, selecting a high threshold of similarity increases the number of breeding zones required and thereby increases the costs of tree improvement. In some programs, it may be more desirable to accept a slightly increased risk of maladaptation in favour of reducing the costs of tree improvement; thus, selecting a more liberal threshold of adaptive similarity (e.g. 1.0 LSD) may be appropriate. Thus, the determination of what is an "acceptable" level of adaptive similarity is somewhat subjective and will vary depending on the breeder's objectives; a desire to achieve maximum gain would favour the selection of a higher level of adaptive similarity and greater number of breeding zones, while a desire to manage costs of tree improvement would favour the selection of a lower adaptive similarity threshold and fewer number of breeding zones. Managers should, therefore, clarify the breeding program objectives before deciding on a desired level of adaptive similarity. However, the 0.5 and 1.0 LSD levels presented here provide a reasonable guideline.

It might be imprudent to exceed 1.0 LSD of adaptive similarity when devising candidate breeding zones for white spruce, as the resulting zones might be too wide to be effective. The range of several of the selected zones at 1.0 LSD is greater than 3° latitude. Therefore, increasing the LSD could yield zones that span an incredible range of latitudes and would likely increase the occurrence of widely disjunct zones. The management of such disjunct breeding zones would pose obvious managerial challenges and may not be appropriate to the program objectives, while the problem that arises with wide latitudinal transfer is that it may result in very large differences in photoperiod between the source and planting location. Southern sources, which are indicated to have later dates of budset, could be at increased risk of fall frost damage or mortality if transferred far northward under current climate (Beaulieu *et al.* 2004). However, the R^2 of 0.53 suggests that the regression model adequately accounts for variation in phenological timing among sources. Presumably, July minimum temperature used to predict phenological timing (as indicated by PC2) is highly correlated, and thereby accounts for photoperiodic effects, limiting excessive northward transfer in the maps.

It is important to note that the present models of seed source adaptation do not account for survival effects; all survival variables except Petawawa 2002, Longlac 2004, and those at the Englehart test site were not included within principal components analysis due to a lack of significant variation between provenances. Those survival variables that were included in the PCA were not captured by the first three principal components axes and were therefore not used to model seed source adaptation. Thus, extreme long-distances transfers should be made cautiously, even when models indicate otherwise, to guard against maladaptation in some non-quantified trait. Campbell

(1986) states "aspects of the genotype selected by nature to guard against rare adverse climatic events may be particularly elusive." Similarly, Rehfeldt (1991) notes that the validity of a model of seed transfer in part depends on "recognizing that genetic variation in additional variables might be occurring along clines that are independent of those already detected. This eventuality would mean that the recurrence of similar populations across the landscape is more restricted than implied." In this case, the omission of survival variables may mean that areas of similarity are narrower than implied by the models.

Campbell (1986) indicates that the probability of a source being well-adapted to the environment of a planting location decreases as the planting and source environments become increasingly dissimilar, regardless of whether the transfer is to milder or harsher climates. Thus, the occurrence of widely-separated areas of adaptive similarity should be treated with some caution, and may indicate that the 1.0 LSD level of similarity is biologically too liberal. Although 1.0 LSD breeding zones for the current study indicate similarity between northwestern Ontario and the Ottawa valley, it would be prudent to treat the two areas as separate breeding zones.

The application of adaptive models to areas outside the sampling region is ill-advised (Campbell 1986). Thus, the regression models used here to predict white spruce adaptation should not be applied to areas in the far north, as neither tests nor provenances extended beyond 50.5°N. However, the test sites and seed sources do sample across the range of environments encountered in current forest management areas and are therefore suitable in devising operational breeding zones for the area of undertaking. However, the areas west of Fort Frances and east of Sault Ste. Marie

should be treated with some caution, as the seed source representation is relatively poor in these areas (Lesser 2005). The presentation of breeding zones constructed for the province as a whole is purely for exploratory purposes; only the solutions presented for the northwest, northeast, and southern forest management regions are intended to have managerial application.

There is general agreement that adaptive models used to devise seed or breeding zones require long-term validation using independent data (Beaulieu *et al.* 2004; Campbell 1986; Li *et al.* 1997; Rehfeldt 1991). The general procedure for validation is to correlate predicted variables based on the model to observed values in an entirely different set of populations. The model's validity is supported if correlations are significant. Beaulieu *et al.* (2004) validated models of relative risk of seed transfer using independent long-term provenance field trials of black spruce and found that models were inaccurate for test sites north of 48° latitude. Although no attempt at validation was made for the current study, there are several long-term white spruce provenance trials located across Ontario that could provide the basis of comparison. However in other cases where long-term test data is unavailable and the costs of widespread testing are prohibitive, genetic mapping based on short-term field data provides a reasonable means of devising seed transfer zones (Campbell 1986).

It is clear that the effectiveness of additional breeding zones declines substantially as full-coverage is approached; past a threshold of approximately 80-90% coverage, additional breeding zones cover very little additional area. Indeed, the amount of overlap introduced by these zones is usually such that practical interpretation is greatly reduced or virtually unfeasible. This suggests that it is probably practical in

most situations to select a solution with less than full coverage to avoid creating multiple zones of similar performance (Parker and Crowe 2005). Parker and Crowe (2005) suggest that an approach might be to continue adding zones only so long as the total uncovered area is greater than the area of overlap between zones. An alternate approach might be to stop adding zones when a greater percentage of points in the zone contribute to the area of overlap rather than additional coverage, or to stop adding zones once a predetermined level of coverage (e.g. 90%) is reached.

If the approach is to stop selecting zones once the efficiency of coverage decreases past some point, then there are a number of methods of dealing with the remaining uncovered areas. Parker and Crowe (2005) suggest uncovered areas within the interior of the region may receive improved seed from adjacent breeding zones but, due to adaptive dissimilarity, these areas should not serve as seed collection sites for adjacent zones. However, given that the amount of improved seed that is currently produced in orchards cannot supply the full demand for reforestation (Parker 1992), it may be more prudent to utilize the improved seed or stock only within the areas where it is most highly adapted.

In the case of small uncovered areas in the periphery of a region, it may be acceptable to simply forsake tree improvement in favour of concentrating breeding efforts elsewhere. For example, small peripheral northern areas might be excluded from tree improvement in favour of larger breeding programs in more central latitudes that are likely to yield larger gains. The rationale is that growth potential is much greater for central and southern latitudes and, thus, equal percentage gains should translate into higher absolute volume gains for breeding programs in these areas. Also, central

breeding zones serve a much larger area, increasing the return on investment. If smaller peripheral areas are to be excluded from tree improvement programs, the delineation of optimal breeding zones still presents a useful method of determining the location of well-adapted seed for regeneration. A separate breeding zone optimization could be conducted separately for each peripheral area to determine the location of discrete seed zone boundaries from which to collect wild seed for regeneration (Parker 1992). However, it is probably preferable to use a floating seed transfer model to determine seed sources for regeneration on an as-needed basis.

If complete coverage is necessary, it may be advisable to first conduct a widespread analysis and continue adding breeding zones until such point as the efficiency of coverage begins to decline sharply. A smaller optimization problem can then be constructed to determine optimum zones in each of the remaining areas (Crowe and Parker 2005). For example, the area along the Minnesota border in the northwest is one of the last areas to be covered when the whole province is analyzed simultaneously. As the results show, it is very costly to obtain coverage of remaining areas in the periphery when considered as part of the larger solution. Generally, a large number of zones will be required to cover these relatively small areas and will result in a considerable amount of overlap. However, an approach such as shown here in modeling the northwest region separately allows the user to construct breeding zones at a finer resolution. The resulting zones will inevitably be of higher quality because they allow more rigorous examination of patterns of adaptive similarity within the region. Finally, the solution is much more operable because it limits the excessive overlap that is

generated when attempting to achieve coverage for the last 10% of the area in the larger problem instance.

In contrast to the results of Crowe and Parker (2005), the solutions approaching full coverage for white spruce at the 1.0 LSD level of similarity generate a considerable amount of overlap between zones. This creates a unique question of how best to deal with overlap in the optimal solution. Firstly, it should be stated that although overlap between zones may result in managerial complexity, it also presents a number of opportunities. If some circumstance, such as fire or poor seed yield, limits the availability of improved seed, then the overlapping zone provides an alternate source of improved seed for regeneration. An interesting possibility is that areas of overlap can be regenerated with improved seed from either of the overlapping zones, allowing managers to choose from the fastest-growing sources of both zones and potentially increase return in those areas.

If the management objective precludes the acceptance of overlapping zones, there are a number of ways in which the solution may be treated. Firstly, areas of overlap from adjacent zones that appear as islands within a larger continuous zone should always be appended to the breeding zone in which they are encompassed. In contrast, areas of overlap occurring along adjacent zone boundaries may be appended to any of the overlapping zones or equally partitioned into each overlapping zone. Also, an area of overlap may be appended to the smallest of the overlapping zones to create a larger, more efficient zone. Alternatively, the area can be partitioned into zones based on consideration of management unit boundaries. However, it should be explicitly stated that such modifications result in a solution that is not optimal in the true sense.

It may be most desirable to use the 0.5 LSD level of similarity in determining breeding zones for white spruce, as the optimal zones demonstrate very little overlap and express a higher probability of adaptedness. However, it is probably only economical to use zones with a very high level of similarity over more localized areas where expected returns are relatively great. In the present study, more than 45 breeding zones were required to cover the range of white spruce in Ontario at the 0.5 level. Obviously, the cost of establishing and maintaining such a large number of breeding zones would be great. Across larger areas where gains from tree improvement are expected to be relatively low, the 1.0 LSD level is probably appropriate. Thus, breeding zones for a larger study area can be constructed at several different levels of adaptive similarity if the area is divided into subsections and each is treated separately. The example for Ontario would be to construct breeding zones for the areas outside of the Area of the Undertaking (AOU) at the 1.0 LSD level and at the 0.5 level for active forest management areas.

If the predominant goal is to achieve 100% coverage and the level of adaptive similarity within zones is allowed some flexibility, the approach of O'Neill and Aitken (2004) presents a reasonable solution. They delineated optimal breeding zones using cluster analysis with the objective of minimizing regional maladaptation. The number of desired breeding zones is specified and each cell is assigned to the zone that minimizes the difference between the adaptive value of the cell and the mean adaptive value of the cluster. While this approach is similar to the maximal covering problem in that it also uses a specified limit on the allowable number of zones, it differs in that there is no constraint on the level of adaptive similarity and the entire area must be covered (Crowe

and Parker 2005). Also, the solution is incapable of producing areas of overlap because each cell is assigned only to a single breeding zone.

The results of this study indicate that the most prudent approach to designing breeding zones using the maximal covering model may be to evaluate a number of different solution sets using various levels of adaptive similarity, as the number of zones required for an acceptable solution will inevitably vary between species, data sets, study areas, and management objectives. Crowe and Parker (2005) found that breeding zones constructed for jack pine at the 0.5 LSD level of adaptive similarity were so fragmented that operational implementation would be difficult. In contrast, 0.5 LSD zones determined for white spruce are generally continuous while 1.0 LSD zones are so large that they often include discontinuous areas separated by great distances. By evaluating the optimal solution at different levels of adaptive similarity, managers are able to examine tradeoffs unique to their species or area of interest to arrive at the most desirable solution for a particular management objective.

Optimal breeding zones at the 1.0 LSD level generally indicate very large distances of safe transfer in the central portions of Ontario, with zones ranging approximately 3-4° latitude and 10-12° longitude. An earlier study of the seedling provenance trials examined within the current report also revealed several instances in which white spruce could be transferred large distances with similar predicted adaptation (Lesser 2005). Focal point seed zones constructed for Ontario's forest management regions indicated that seed could be transferred between the Ottawa Valley area and the northwest region with little risk of maladaption. The optimal breeding zones based on 1.0 LSD similarity confirm this result for the present study, as indicated by the selection

of a breeding zone with widely disjunct areas of similarity in the northwest and southeast.

A study of the genetic structure of white spruce populations in Quebec reports large areas of similar adaptation, ranging about 2-3° latitude and several degrees of longitude (Li *et al.* 1997). The authors conclude that populations of white spruce are relatively similar across a large geographic area and that currently only 2 breeding zones are necessary to differentiate between similarly adapted populations in Quebec. They suggest that an explanation for the broad zone size is that populations have not had adequate time to become closely adapted to their source environments since the retreat of the glaciers in eastern Canada (Li *et al.* 1997). While this explanation is logical in theory, it does not explain the high population differentiation in the southern areas of the present study (Parker 2008, unpublished data).

Li *et al.* (1997) also suggest that weak geographic differentiation of white spruce may be the result of relatively weak environmental gradients across the Quebec study area. This conclusion is supported by the results of the current study, which demonstrate relatively weak geographic differentiation of white spruce sources across the central portion of the study area where climate gradients are relatively gradual. In contrast, breeding zones in southern Ontario are comparatively very restricted due to relatively steep climatic gradients. These results tend to corroborate those obtained for numerous other North American conifer species; Campbell (1986) demonstrated for Douglas-fir that areas possessing the greatest risk of seed transfer corresponded to areas of greatest climatic heterogeneity. Similarly, Parker (1996b) found that black spruce

seed zones were quite small in the area along the shores of Lake Superior and Lake Nipigon where the climate changes rapidly.

However, breeding zones of white spruce are still relatively large in comparison to those of other boreal conifers. Crowe and Parker (2005) found that jack pine breeding zones for northwestern Ontario spanned a relatively narrow range of latitudes at the 1.0 LSD level of similarity. Approximately 5 breeding zones were necessary to achieve near-complete coverage of the study area, whereas only 3 zones are necessary to cover the same area for white spruce. Similarly, black spruce focal point seed zones constructed for areas of northwestern Ontario (Parker 1996b) are comparatively much more restricted than those of white spruce.

This result then raises the question: what is the explanation for the relatively broad regions of similarity for white spruce in comparison to other boreal conifers? Given that white spruce demonstrates high levels of genetic variation (Nienstaedt and Teich 1972) and occupies a wide range of environmental conditions, it seems reasonable that it should demonstrate much stronger adaptive differentiation between populations of different regions. Two possible explanations seem feasible; the first is statistical in nature, and the second biological. To calculate the LSD value for each axis, the 0.05 probability LSD value for each variable was first divided by its associated standard deviation to express the LSD value as the number of standard deviations required to detect significant differences amongst provenances. Herein lies the issue: LSD values are not comparable between species or traits because they are expressed in relative, rather than absolute terms. More clearly, a trait with a relatively low standard deviation value and low error variance could result in the same LSD value as a trait with a

relatively high standard deviation and error variance when expressed in relative terms. Therefore, the calculation of the same relative LSD value for two separate species or traits does not necessarily result in a similar absolute interval width.

As the variation amongst provenances is likely to increase across a wider sampling range, so too is the error variance of each trait and the calculated LSD value for each axis. Thus, the value by which populations must differ to be considered statistically significant is also greater. It is possible that the relatively large size of the white spruce breeding zones in comparison to black spruce and jack pine is related to the fact that the present study includes seed sources sampled from across a wider range of environments. In the present study, calculated LSD values were equal to 0.61, 0.59, and 0.61 for PC1, PC2, and PC3 respectively. In comparison, LSD values for jack pine on the first and second axis were 0.55, and 0.58 (Crowe and Parker 2005). Thus, larger areas of similarity are at least in part due to wider LSD intervals.

Rehfeldt (1984) proposes two different models of species adaptation to environment; specialists are species that tend to occupy a wide range of environments and are composed of populations that are physiologically specialized for performance within some relatively small portion of the overall range. In comparison, generalists may also occupy a broad range of environments, but the mechanism by which this is achieved is different. Generalists tend to demonstrate a high level of phenotypic plasticity, allowing a single genotype to produce optimal physiology under varying environmental conditions. They are also characterized as possessing alleles with broad environmental tolerances and high levels of genetic heterozygosity.

Rehfeldt (1984) notes that it is possible for species to demonstrate intermediate strategies, as adaptation to environment always reflects a tradeoff between adaptation over space (specialist) and over time (generalist). Significant adaptive variation was detected among Ponderosa pine (*Pinus ponderosa* Dougl. ex Laws.) populations in central Idaho that were separated by at least 360 m of elevation. While the climate and elevation of seed origin were shown to account for 61% of the differentiation among populations, geographic clines were gentle and only half as many contours were needed to describe geographic clines in comparison to Douglas-fir.

Thus, it is possible that white spruce is relatively more of a generalist species in comparison to black spruce and jack pine, but strong population differentiation in areas of extreme environmental heterogeneity implies that it also demonstrates some level of specialization. If such is the case, then white spruce is perhaps the most ideally suited to withstand the effects of environmental change; its broad distribution suggests that at least some of the environments it currently occupies (i.e. northern areas) will remain within ecological tolerance limits, while its generalist characteristics may allow it to maintain adequate performance even under warmer temperatures in the future.

CHAPTER IV: USE OF PAST CLIMATE SIMULATIONS TO EVALUATE ACCURACY OF CLIMATE MODELS FOR ONTARIO

INTRODUCTION

A great source of uncertainty in modeling future climate change is associated with the accuracy of models used to generate predictions (Rivington *et al.* 2008). Atmospheric-oceanic general circulation models (AOGCMs) produce widely varying estimates of future climate, partly due to differences in how key physical climatic processes are represented within each model. The "best estimate" of future warming based on various climate models is 2.5°C, but models range from 1.5-4.5°C in their predictions (Risbey and Kandlikar 2007). Thus, one must question which of the many available models is the most accurate. One possible way to evaluate model accuracy is to simulate past or current climates and compare the output to observed data (Rivington *et al.* 2008).

The purpose of this chapter is to develop simulated past breeding zones for each of three climate models commonly used in Ontario. The results will be compared to the optimal breeding zones developed for 1961-1990 observed climate normals to determine which of the three models may be most accurate in predicting climate in Ontario. The results will inform future seed transfer decisions and the analysis of future breeding zones presented in the next chapter.

METHODS

Annual models of simulated past climate were obtained for CGCM2 for the years 1900 and 1950, HADCM3 for the year 1950, and CSIRO 1961 from Dr. D. McKenney, Great Lakes-St. Lawrence Forestry Centre (McKenney *et al.* 2006). The choice of annual models was restricted by the availability of past climate simulations; CGCM2 was available for 1900-2100, HADCM3 for 1950-2099, and CSIRO from 1961-2100. Thus, the earliest possible year of each scenario was chosen assuming that this would force greater expression of differences between observed climate (1961-1990) and simulated past climates. The CGCM2 1950 scenario was also used so that it could be compared to CSIRO and HADCM3 for a similar time period. For each past climate simulation, 10-km grids were obtained for each of the 36 climate variables used in previous analyses including: mean monthly minimum and maximum temperature, and mean monthly precipitation.

The analysis used to determine past seed zones and breeding zones is identical to the process used to determine current seed zones and breeding zones as described in the previous chapters. However, values of past climate are used to predict principal components factors across the study area, in comparison to the previous analyses which used 1961-1990 climate normals. Thus, grids of predicted principal components factor scores based on each of the four past climate simulations were generated and used to create focal point seed zones for each of four locations to allow comparison with current seed zones for the same points. For each past climate simulation, the focal point seed

zone procedure was used to create candidate breeding zones for the same 618 focal points used to construct the current zones. The candidate zones for each simulation were then input into the maximal covering model to determine optimal past breeding zones based on 1, 2, 3, and 4 zones for comparison with 1961-1990 breeding zone solutions.

RESULTS

PREDICTED FACTOR SCORES FOR SIMULATED PAST CLIMATES

Factor scores obtained by regression of simulated past climate values for CGCM2 1900, CGCM2 1950, HADCM3 1950, and CSIRO 1961 are presented in Figure 54 to Figure 65.

Figure 54 to Figure 56 present predicted factor scores for principal components 1 through 3 in the year 1900 based on CGCM2. The general pattern of PC1 factor scores for CGCM2 1900 (Figure 54) is fairly similar to the 1961-1990 PC1 scores (Figure 3), with both grids demonstrating a general increase in growth potential from north to south. However, the CGCM2 1900 estimate demonstrates several differences in comparison with the 1961-1990 grids; notably, the dissimilarity between contours in the north. For the 1961-1990 grid, the northern contours are latitudinally-oriented, and for the simulated 1900 grid they shift from a latitudinal-orientation to an east-west orientation adjacent to Hudson Bay. This discrepancy is attributable to variation in January precipitation between the two climate scenarios (APPENDIX I).

Another key difference between the grids is that the CGCM2 estimate demonstrates a much wider variability in growth potential, ranging from -3.6 to 5.7 std. dev in comparison with the 1961-1990 grid which ranges from -2.9 to 2.5 std. dev. Although both grids predict the highest growth potential in the south, the maximum growth potential is much greater for the CGCM2 1900 data. This greater variation in growth potential for the CGCM2 1900 estimate is the result of the increased variability

of September maximum temperature and August precipitation in comparison with 1961-1990 observed normals.

PC2 factor scores contours for CGCM2 1900 (Figure 55) loosely resemble those predicted based on 1961-1990 climate normals (Figure 4). Both figures indicate a general trend of increasing factor scores from north to south, indicating later dates of budflush and budset in the south relative to the north. The CGCM2 1900 contours also indicate areas of adaptive similarity between the northwest and south; however, the area of similarity extends further northward than for the 1961-1990 contours. PC2 factor scores based on CGCM2 1900 are more variable than those predicted for 1961-1990, ranging from -2.99 to 2.5 and from -1.99 to 2.5 respectively. This may be due in part to the wider variability of July minimum temperature for CGCM2 1900 in comparison with the 1961-1990 normal values (APPENDIX I). The CGCM2 1900 factor scores for PC2 indicate a similar area of low predicted factor scores extending northward from the shores of Lake Superior and Lake Huron. However, the area with near-minimum factor scores immediately surrounding Lake Nipigon is not evident in the CGCM2 1900 grid.

Discrepancies between the CGCM2 1900 and 1961-1900 PC2 factor scores can mostly be explained by differences in February and October precipitation patterns (APPENDIX I). February and October precipitation for CCGM2 1900 are much less variable and patterns are broadly divergent from those demonstrated for 1961-1990 normals. In contrast, July minimum temperature patterns are largely similar.

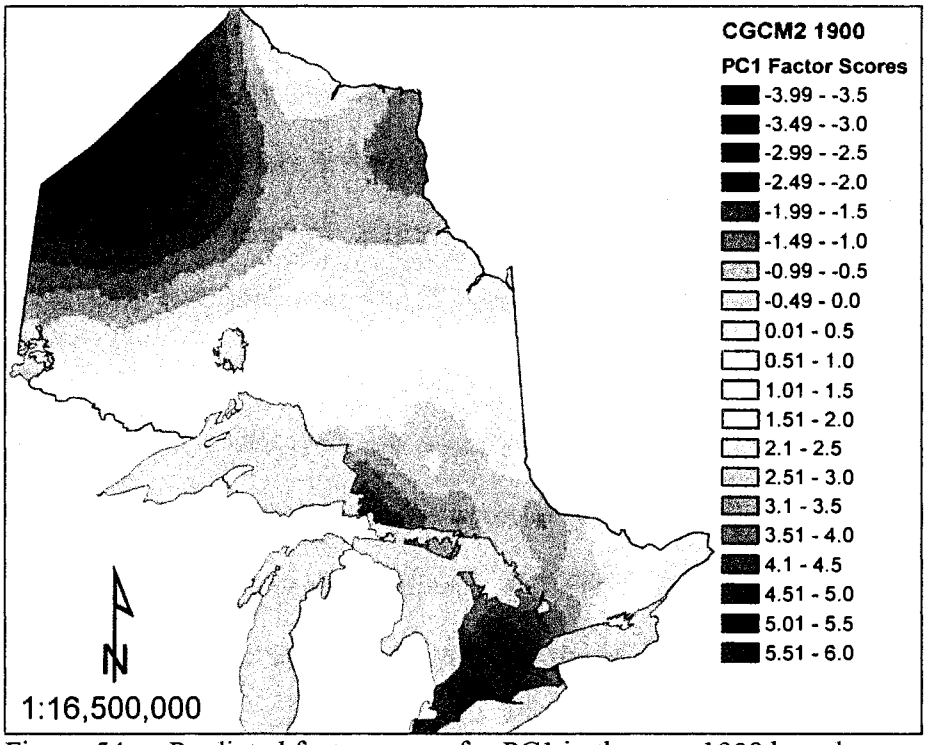

Figure 54. Predicted factor scores for PC1 in the year 1900 based on CGCM2.

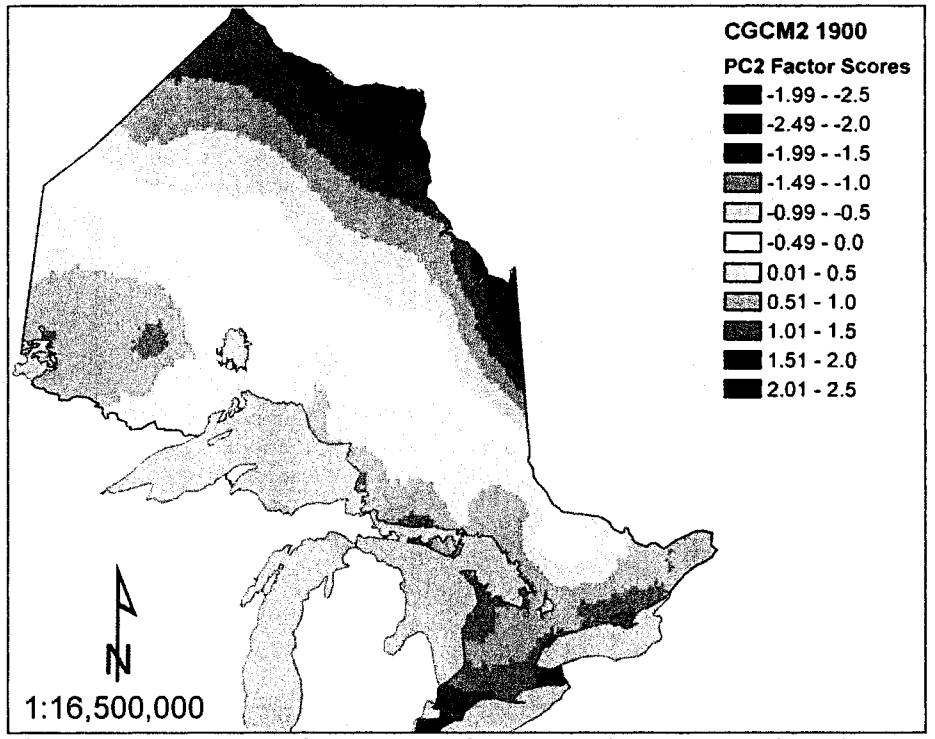

Figure 55. Predicted factor scores for PC2 in the year 1900 based on CGCM2.

PC3 factor scores for CGCM2 1900 (Figure 56) partially resemble those predicted based on 1961-1990 climate normals (Figure 5). However, both grids show a general increase in predicted factor scores from north to south and indicate areas of adaptive similarity between the south and northwest. The area of similarity does not extend as far northward for CGCM2 1900 as for the 1961-1900 grid. CGCM2 1900 predicted factor scores demonstrate east to west variation within the central portion of the province that is anomalous in comparison to the 1961-1990 PC3 factor scores. This pattern may be partially attributable to east-west variation in March Precipitation to the north of the Great Lakes (APPENDIX I). Finally, factor scores are much more variable for CGCM2 1900, which may be attributed to the relatively large variation in April Maximum temperature.

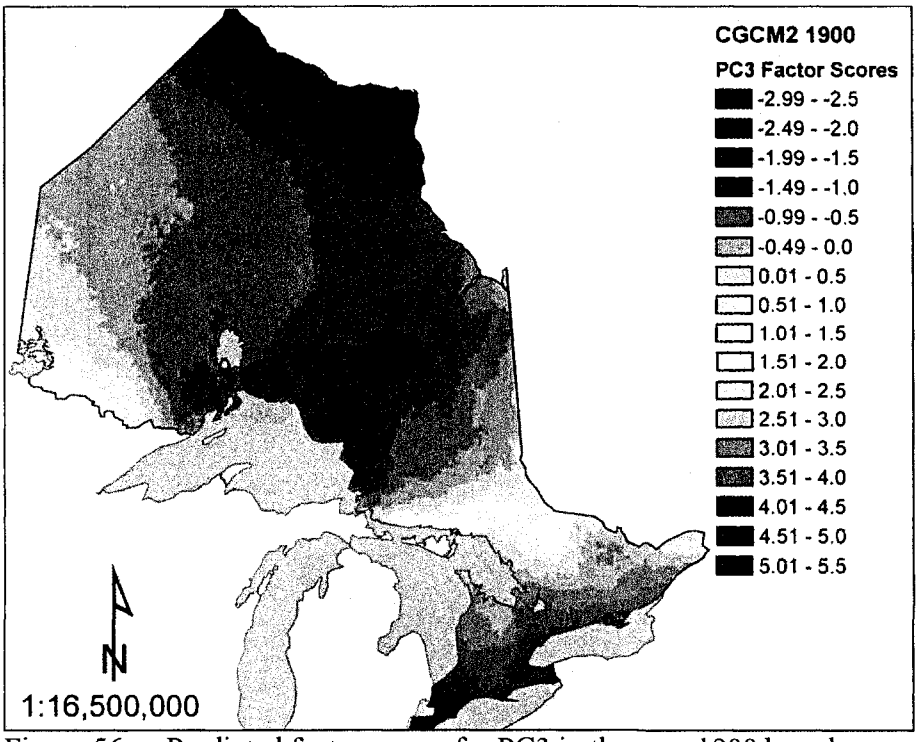

Figure 56. Predicted factor scores for PC3 in the year 1900 based on CGCM2.

Figure 57 to Figure 59 present predicted factor scores for principal components 1 through 3 in the year 1950 based CGCM2. The predicted factor scores for PC1 based on CGCM2 1950 (Figure 57) only marginally resemble predicted PC1 factor scores for 1961-1990 (Figure 3). Both grids indicate a general increase in growth potential from north to south and areas of adaptive similarity between the southern and northwest region. However, the CGCM2 1950 factor scores indicate that the relatively high factor scores of the northwest extend into the northern latitudes of the province, largely due to the influence of August precipitation (APPENDIX I). This creates a east-west pattern of variation, for which factor scores decrease progressively with increasing distance west and east.

CGCM2 1950 predicted factor scores for PC2 (Figure 58) quite closely resemble those for 1961-1990 (Figure 4). Both grids indicate a generally increasing trend from north to south, indicating the latest budflush and budset dates occur for southern sources. An area of similarity between the Ottawa Valley and northwest region is evident, while the area surrounding Lake Nipigon is predicted to have factor scores comparable to those of the far north. A band of relatively low factor scores sweeps northward from the shore of Lake Superior, and scores increase west and east of this band. However, CGCM2 1950 patterns are more strictly east-west oriented in this region than for 1961-1990. This may be attributable to steeper July minimum temperature contours in the northwest and also to the relatively strong east to west variation in October precipitation to the north of the Great Lakes (APPENDIX I).

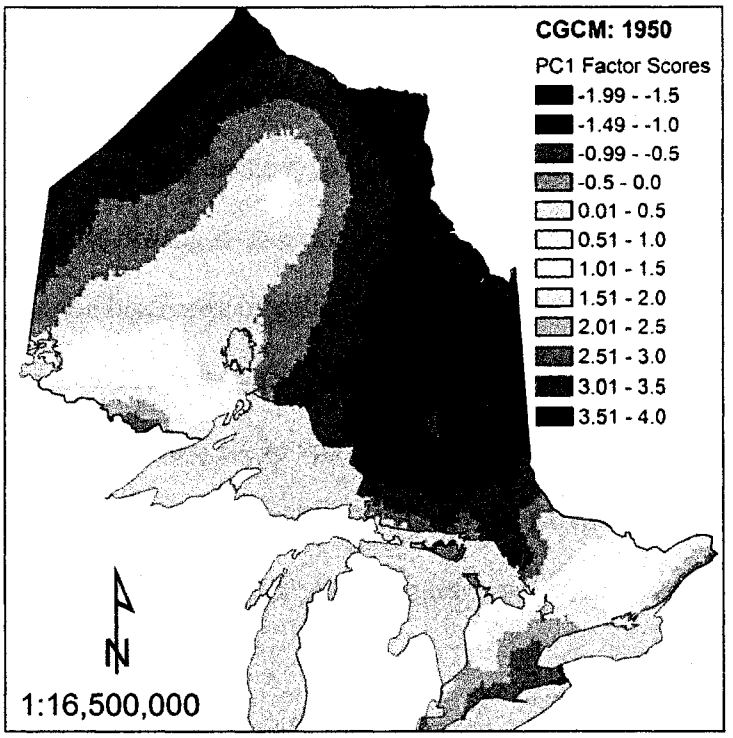

Figure 57. Predicted factor scores for PC1 in the year 1950 based on CGCM2.

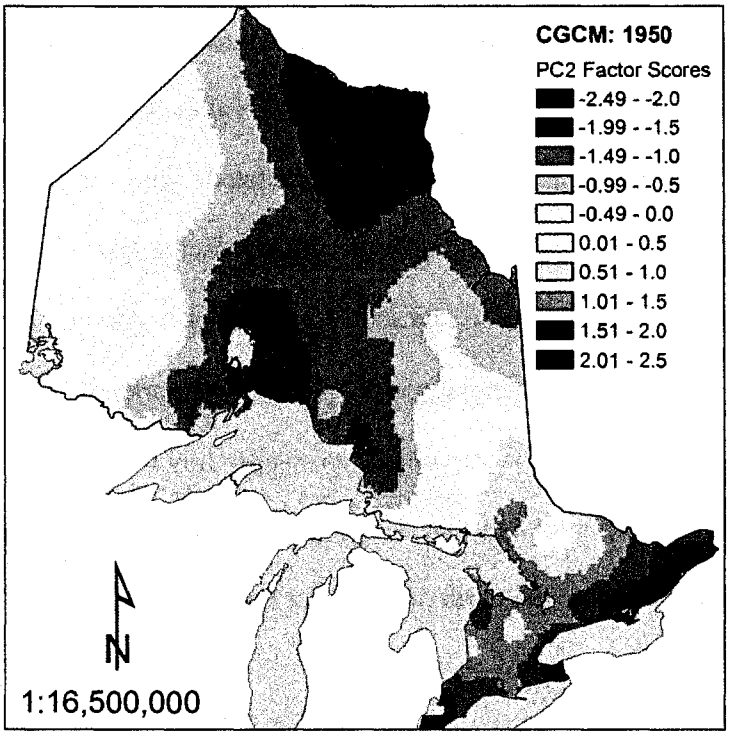

Figure 58. Predicted factor scores for PC2 in the year 1950 based on CGCM2.

Predicted factor scores for PC3 based on CGCM2 1950 (Figure 59) also closely resemble those predicted for 1961-1990 (Figure 5). Both grids indicate a general increase in factor scores from north to south, and the adaptive similarity between the Ottawa Valley region and the northwest is again evident. However the CGCM2 1950 grid indicates an area of relatively low predicted factor scores in the far south that is anomalous in comparison to the 1961-1990 grid. This discrepancy can be explained by differences in March precipitation simulated for CGCM2 1950 in comparison to the 1961-1990 normal (APPENDIX I).

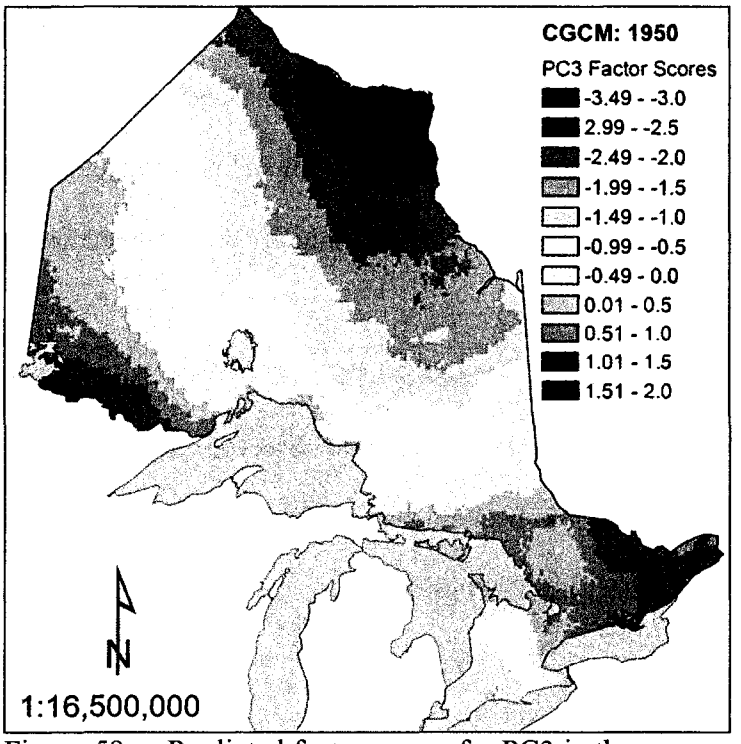

Figure 59. Predicted factor scores for PC3 in the year 1950 based on CGCM2.

Figure 60 to Figure 62 present predicted factor scores for principal components 1 through 3 in the year 1950 based on HADCM3. Predicted factor scores for PC1 based on HADCM3 1950 (Figure 57) rather closely resemble those predicted based on 1961-

1990 climate normals (Figure 3). Factor scores increase from north to south, and are similar between the south and northwest, indicating that sources with the highest growth potential originate from these areas. However, the relatively high factor scores of the northwest region extend further northward for HADCM3 1950, which could be due in part to the relatively high levels of August precipitation in comparison to the 1961-1990 grid (APPENDIX I).

PC2 factor scores (Figure 61) are also quite similar to those predicted based on 1961-1990 climate normals (Figure 4). Budflush and budset dates increase from north to south, with the latest dates occurring for sources in the far south. However, phenological timing varies somewhat more across the range based on HADCM3 1950. Also, the relatively late dates of budflush and budset predicted for the south, and the relatively early dates predicted for the area of Lake Nipigon extend somewhat further northward for HADCM3 1950.

Factor scores predicted for PC3 based on HADCM3 1950 (Figure 62) are nearly identical to those predicted based on 1961-1990 observed climate normals (Figure 5). Factor scores increase from north to south, however, they are more widely variable for HADCM3 1950 than for the 1961-1990 grid.

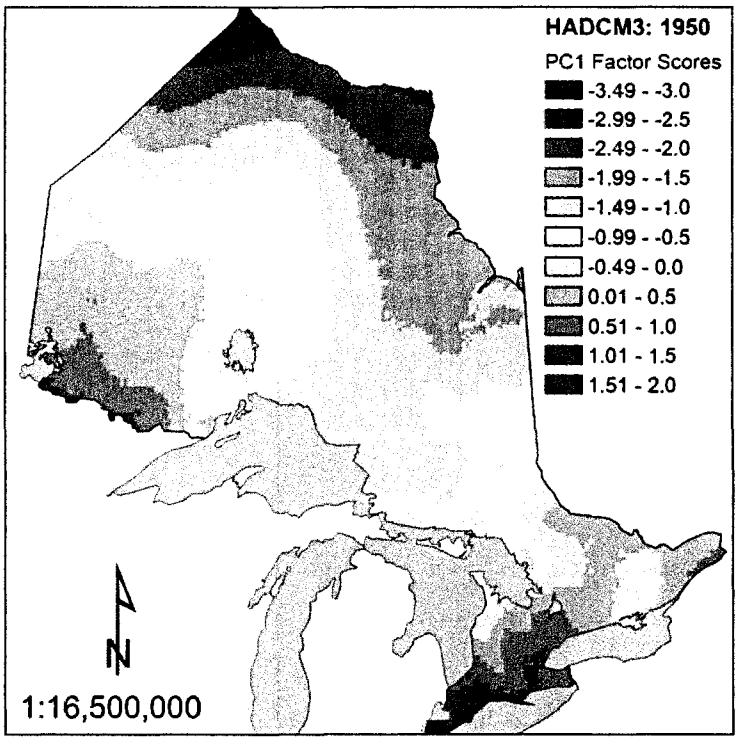

Figure 60. Predicted factor scores for PC1 in the year 1950 based on HADCM3.

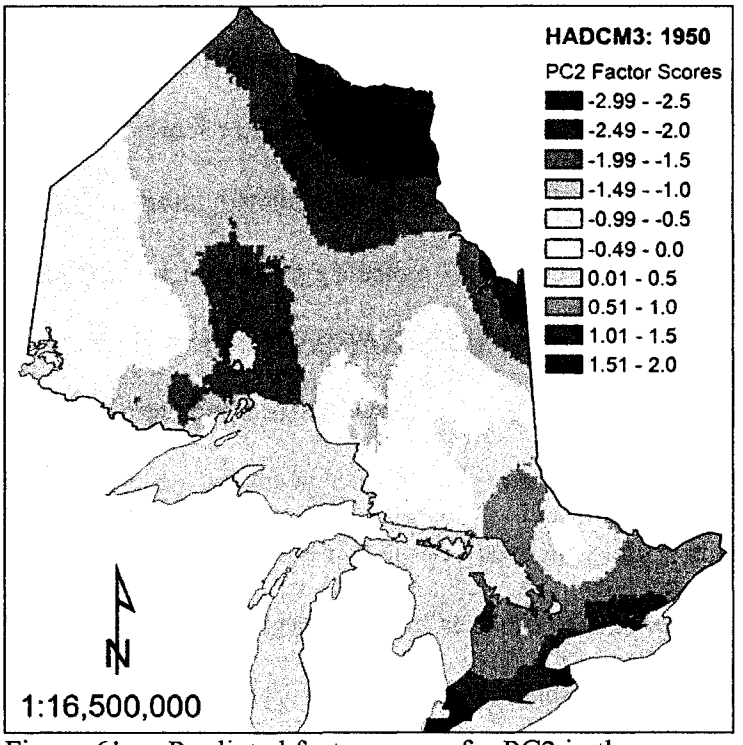

Figure 61. Predicted factor scores for PC2 in the year 1950 based on HADCM3.

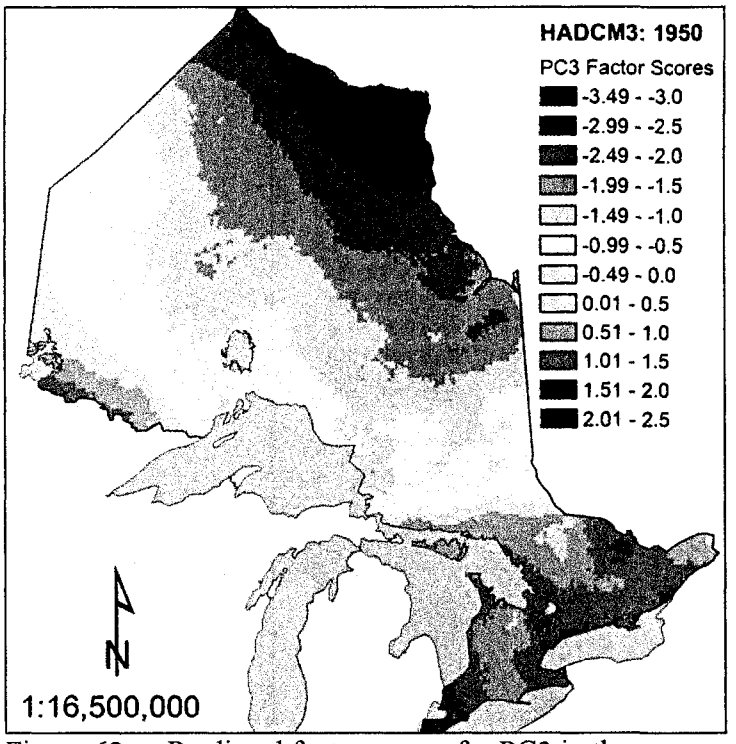

Figure 62. Predicted factor scores for PC3 in the year 1950 based on HADCM3.

Figure 63 to Figure 65 present predicted factor scores for principal components 1 through 3 in the year 1961 based on CSIRO. Predicted factor scores for PC1 based on CSIRO 1961 (Figure 63) only loosely resemble those predicted based on 1961-1990 climate normals (Figure 3). While both grids indicate a general increase in factor scores from north to south, growth potential varies much more widely across the range for CSIRO 1961 than for 1961-1990 normals. The broad contour indicating relatively high growth potential in the central latitudes of the province is anomalous in comparison to the 1961-1990 grid. This is likely the result of the fact that CSIRO 1961 estimates September maximum temperature to be much higher through the mid-latitudes in comparison with the 1961-1990 normal (APPENDIX I). The CSIRO 1961 contours indicate that growth potential in the northwest is relatively low in comparison to the

south, which is contrast to the 1961-1990 grid which indicates that it is relatively similar between the two areas. This inconsistency may be due in part to divergent estimates of August precipitation between CSIRO 1961 and the 1961-1990 normal; the pattern is reversed for CSIRO 1961, indicating that the lowest August precipitation values occur in the northwest.

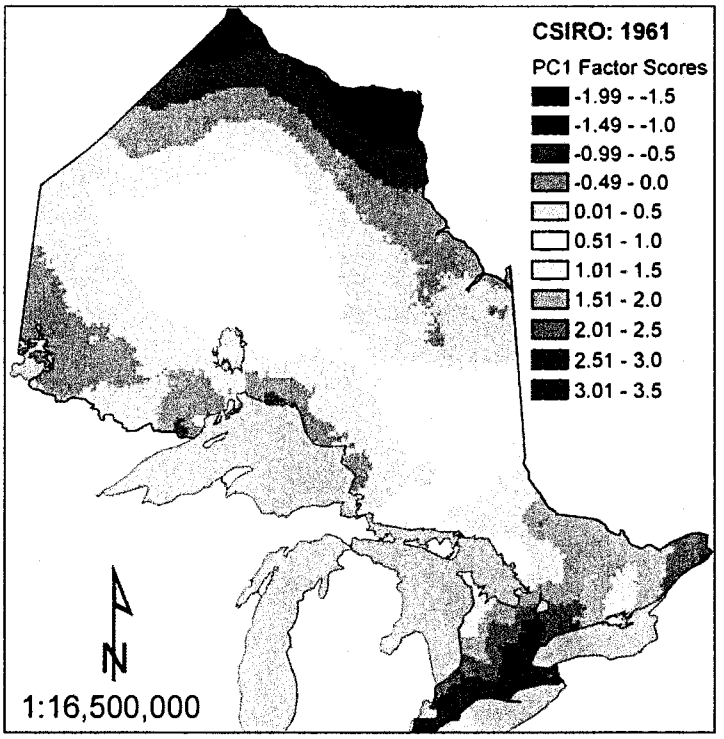

Figure 63. Predicted factor scores for PC1 based on CSIRO modeled climate for the year 1961.

Predicted factor scores for PC2 are relatively similar between CSIRO 1961 (Figure 64) and 1961-1990 (Figure 4) grids. Factor scores generally increase from north to south, indicating that southern sources have the latest dates of both budflush and budset. The area north of Lake Superior is predicted to have relatively low factor scores which extend northwards. However, this band is much narrower for CSIRO 1961 and does not indicate the area of very low factor scores surrounding the perimeter of Lake

Nipigon. This discrepancy is likely the result of divergent patterns of October precipitation between the CSIRO 1961 and 1961-1991 normal grids (APPENDIX I). Factor scores in the northwest region surrounding Lake of the Woods are predicted to be similar to those along the north shore of Lake Huron and the Ottawa Valley.

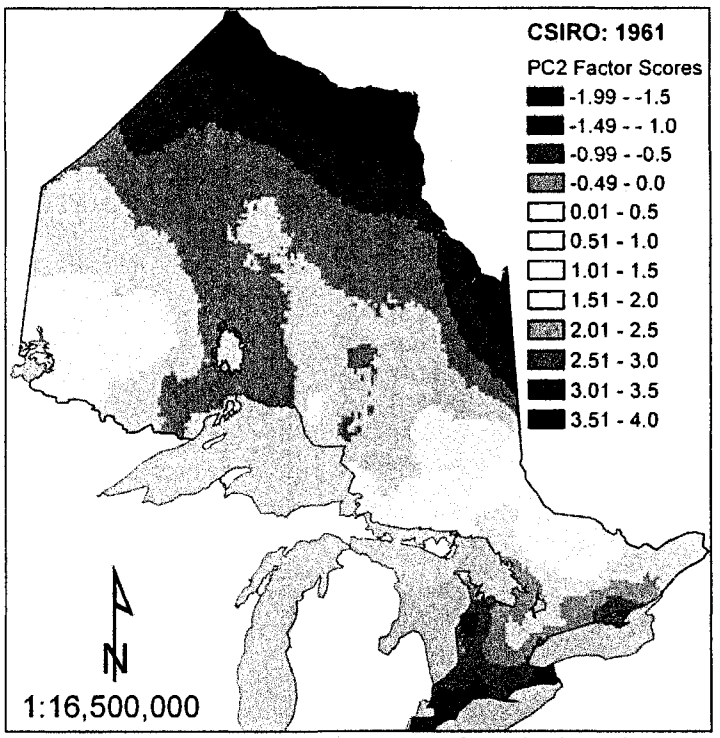

Figure 64. Predicted factor scores for PC2 based on CSIRO modeled climate for the year 1961.

Contours of predicted factor scores for PC3 based on CSIRO 1961 (Figure 65) demonstrate widespread discrepancies when compared to those predicted based on 1961-1990 climate normals (Figure 5). The CSIRO 1961 contours show no clear latitudinal trend; factors scores are intermediate to high in the far north, and highest in the northwest and furthest southern latitudes of the province. The lowest predicted factor scores are predicted in the east along the Quebec border.

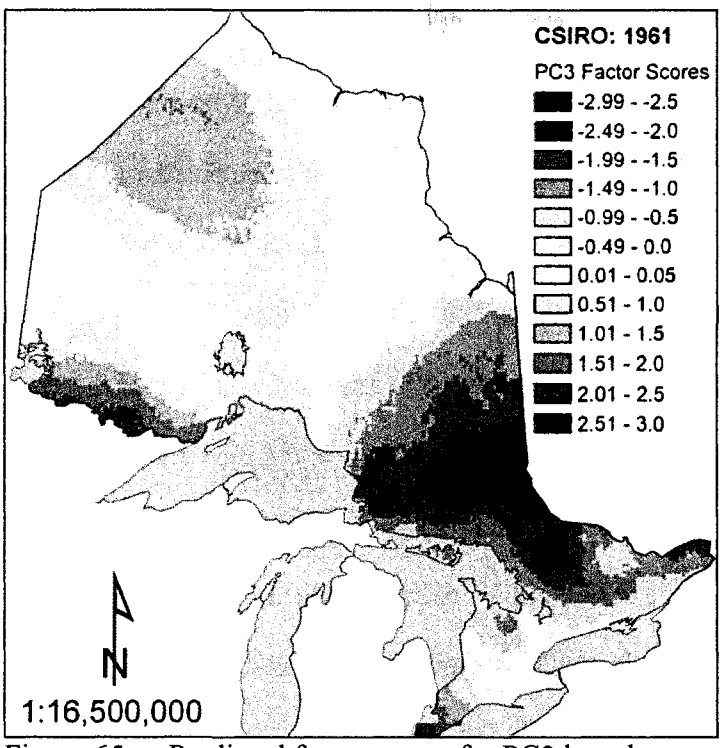

Figure 65. Predicted factor scores for PC3 based on CSIRO modeled climate for the year 1961.

FOCAL POINT SEED ZONE EXAMPLES FOR SIMULATED PAST CLIMATE

Four examples of the 618 focal point seed zones constructed for Ontario are presented for each of the four past climate scenarios in Figure 66 to Figure 81 for CGCM2 1900, CGCM2 1950, HADCM3 1950, and CSIRO 1961, respectively. All zones are based on the 1.0 LSD level of adaptive similarity. These examples utilize four focal points presented in the 1961-1990 seed zone examples (Figure 6 to Figure 9) to allow comparison of patterns of adaptive variation between the simulated past and observed current climate scenarios.

Figure 66 to Figure 69 present the four seed zone examples for the CGCM2 1900 scenario. The 1.0 LSD seed zone for focal point 345 stretches approximately 400 km northeastward from the shore of Lake Nipigon and spans approximately 1.5° of

latitude (Figure 66). Figure 67 indicates that the seed zone for focal point 325 occupies a small area surrounding the focal point just south and west of James Bay that extends approximately 350 km from its western to eastern boundaries. Similar to the previous 2 seed zones, the 1.0 LSD zone for focal point 336 is quite restricted, occupying a narrow latitudinal band in the northwest of the province (Figure 68). This zone extends from the Manitoba border eastward approximately 320 km and from Lake of the Woods north approximately 170 km. In the far north of the province, the seed zone for focal point 584 runs southeast from Hudson Bay (Figure 69). By comparison, this zone is less restricted than the previous 3 zones and is oriented primarily from north to south; it spans approximately 4° latitude and 2° longitude at its widest point.

The 1.0 LSD seed zones based on CGCM2 1900 are much smaller in size and generally do not resemble seed zones developed based on 1961-1990 climate normals (Figure 6 to Figure 11). While the 1961-1990 seed zones generally span several degrees of latitude and are oriented along a northwest-southeast plane, the CGCM2 1900 zones are more latitudinally oriented and span approximately 1.5° latitude. They are generally more comparable in size to the 0.5 LSD zones for 1961-1990. Interestingly, the CGCM2 1900 seed zone for focal point 336 in the northwest does not indicate the adaptive similarity between the northwest and southeast that is demonstrated for the 1961-1990 zone.

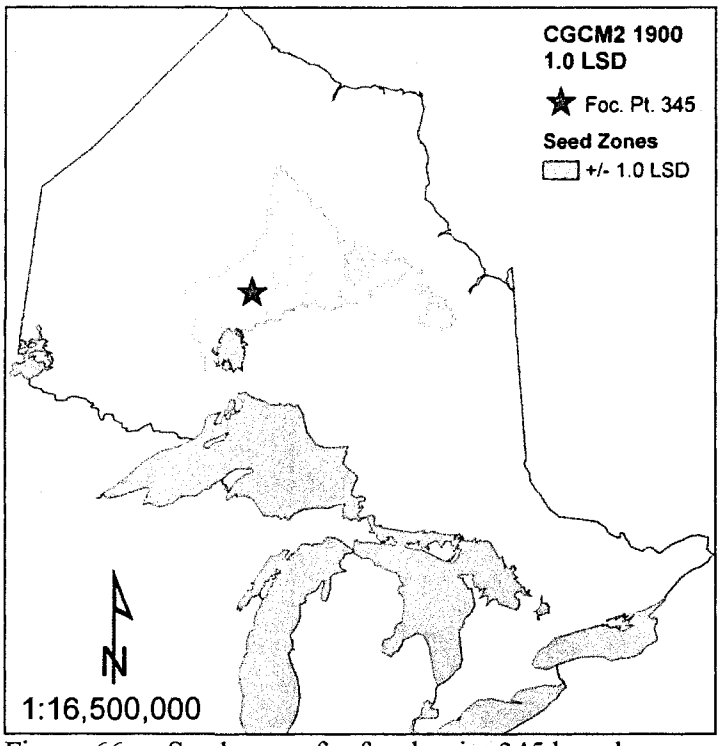

Figure 66. Seed zones for focal point 345 based on CGCM2 for the year 1900.

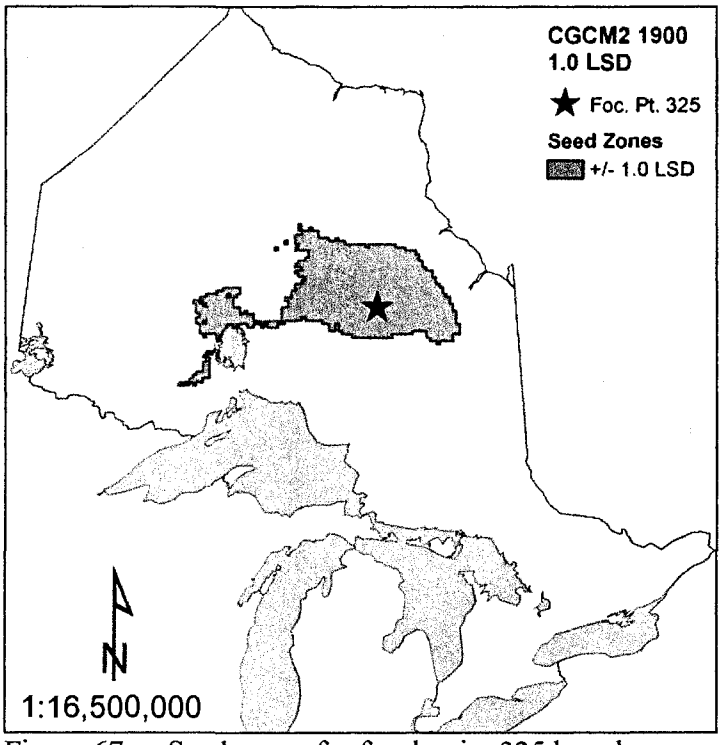

Figure 67. Seed zones for focal point 325 based on CGCM2 for the year 1900.

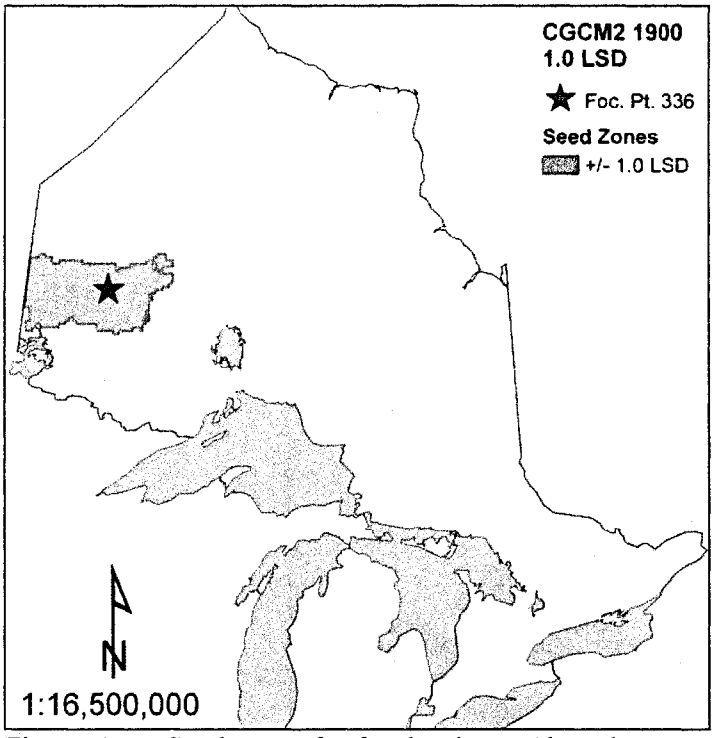

Figure 68. Seed zones for focal point 336 based on CGCM2 for the year 1900.

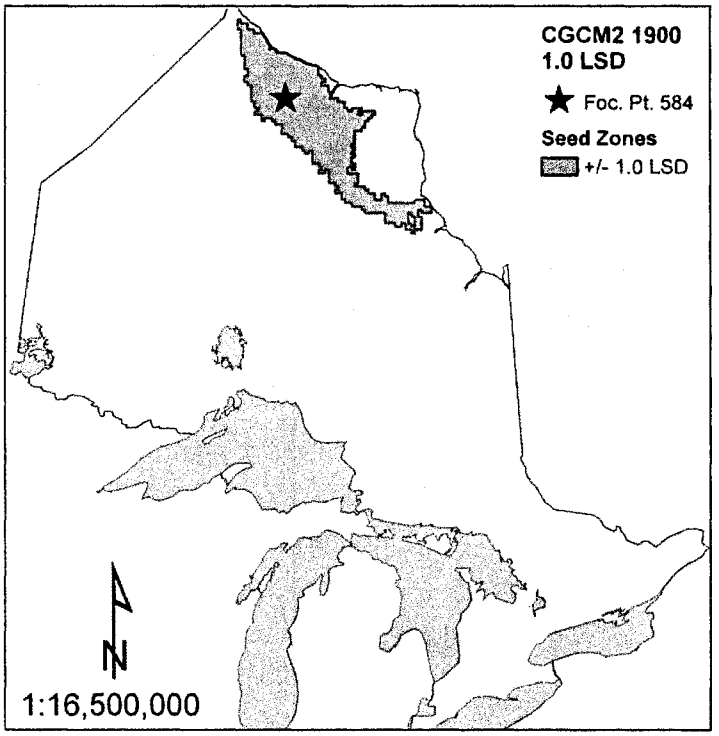

Figure 69. Seed zones for focal point 584 based on CGCM2 for the year 1900.

Figure 70 to Figure 73 present the four seed zone examples for CGCM2 1950 at the 1.0 LSD level of adaptive similarity. The seed zone for focal point 345 north of Lake Nipigon is somewhat circular in form, extending between 140 and 200 km in all directions from the focal point (Figure 70). It runs from approximately 53°N at its furthest point to approximately 49°N, and while it encircles the north shore of Lake Nipigon, it excludes areas to the immediate, west, east, and south.

The 1.0 LSD seed zone indicates two disjunct areas of adaptive similarity for focal point 325 in the northeast (Figure 71). The first area is located in the northeast surrounding the focal point and runs from James Bay southwest approximately 420 km. The second, much smaller area is located in the furthest northwest corner of the province adjacent to Hudson Bay.

Areas of adaptive similarity for focal point 336 are located surrounding the focal point in the northwest, along the north shore of Lake Huron, and the Ottawa Valley (Figure 72). Similar to the previous 2 seed zones, these areas are mostly circular in form. The first area, adjacent to the focal point, runs eastward from the Manitoba border and north from Lake of the Woods while the area to the southeast is composed of 3 much smaller, fragmented zones.

Located in the far north of the province, the seed zone for focal point 584 extends from Hudson Bay southeast to James Bay (Figure 73). Like the CGCM2 1900 zone for the same point, the seed zone for CGCM2 1950 is north-south oriented, spanning approximately 574 km from north to south and 250 km from west to east.

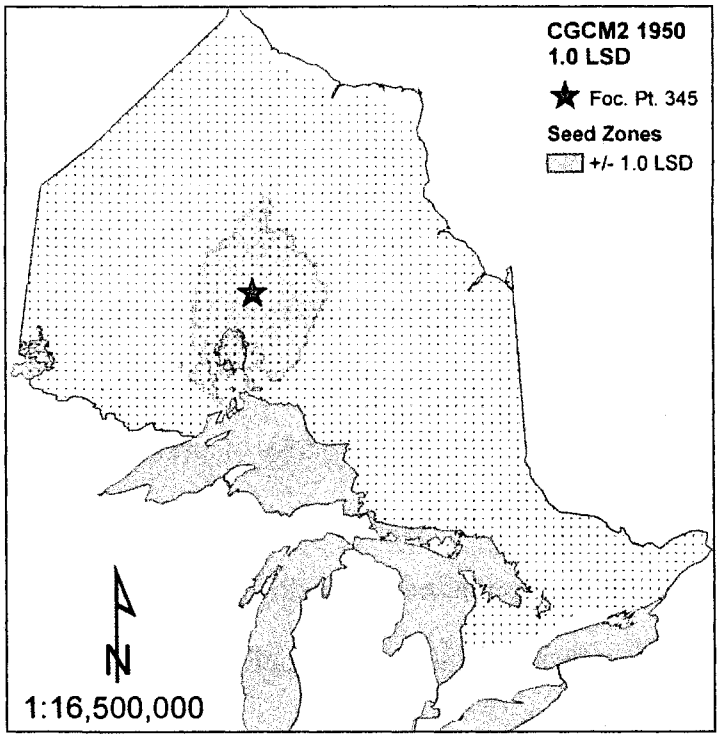

Figure 70. Seed zones for focal point 345 based on CGCM2 for the year 1950.

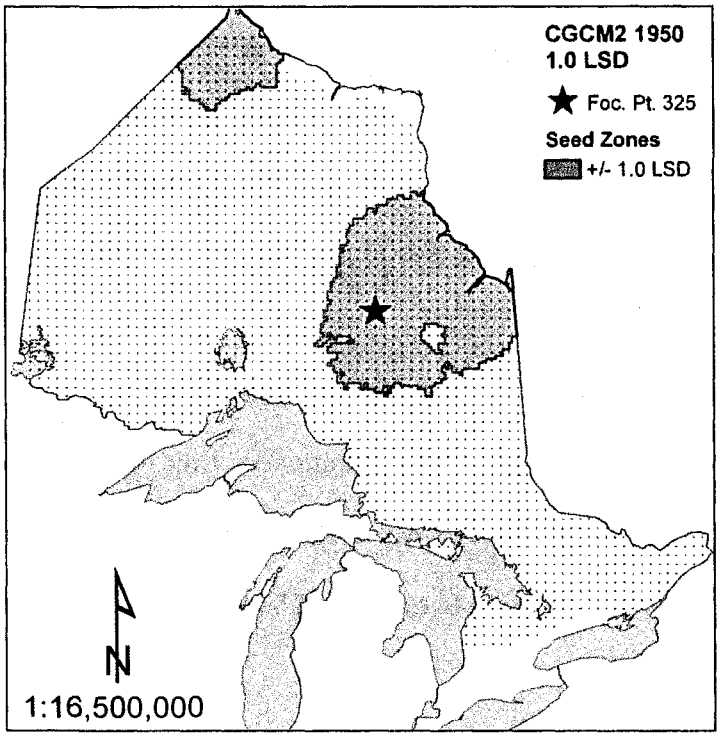

Figure 71. Seed zones for focal point 325, based on CGCM2 for the year 1950.

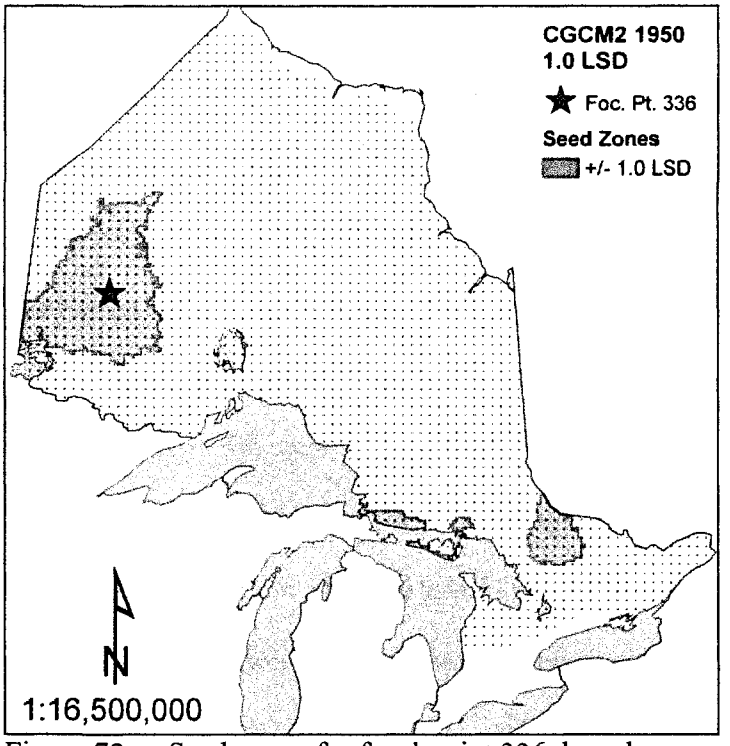

Figure 72. Seed zones for focal point 336, based on CGCM2 for the year 1950.

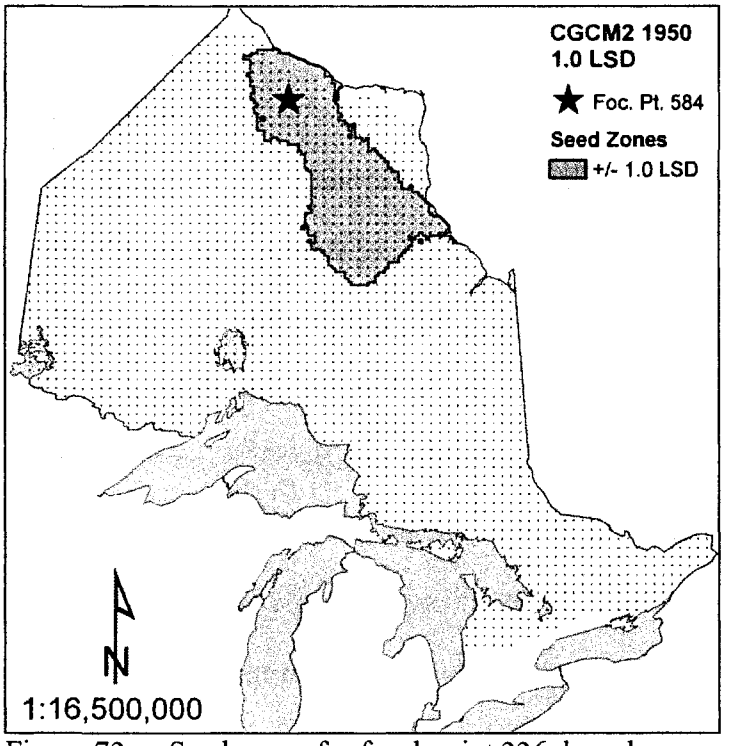

Figure 73. Seed zones for focal point 336, based on CGCM2 for the year 1950.

The CGCM2 1950 seed zones bear limited resemblance to the 1961-1990 seed zones for the same focal points (Figure 6 to Figure 9). While the CGCM2 1950 zones are latitudinally broader than the CGCM2 1900 zones, they are still quite small in comparison to the 1961-1990 zones. The CGCM2 1950 seed zone for focal point 345 occupies approximately 25% of the area as the 1961-1990 zone and does not encompass the southern edge of Lake Nipigon. The seed zone for focal point 325 is similar in size and shape to the 0.5 LSD zone based on 1961-1990 climate normals, but is shifted slightly northward. It bears relatively little resemblance to the 1961-1990 1.0 LSD zone. The 1.0 LSD seed zone for focal point 336 is reasonably similar to the 1.0 LSD zone based on 1961-1990, occupying disjunct areas in both the northwest and southern regions. However, the CGCM2 1950 zone is somewhat smaller. It occupies only the Ottawa Valley area in the south, as compared to the 1961-1990 zone which extends along much of the northern shore of Lake Huron. The CGCM2 1950 seed zone for focal point 584 in the far north is very similar in shape to the 1.0 LSD zone based on 1961-1990, but does not show the same latitudinal orientation.

Figure 74 to Figure 77 present the four seed zone examples for HADCM3 1950 at the 1.0 LSD level of adaptive similarity. The seed zone for focal point 345 indicates a single broad area of adaptive similarity which encompasses the north shore of Lake Superior and Lake Nipigon and extends to approximately 53°N latitude (Figure 74). A rather tiny, disjunct area along the Quebec border is also shown.

The 1.0 LSD seed zone indicates a very broad area of adaptive similarity for focal point 325 (Figure 75Figure 74). This zone runs from approximately 55°N in the west along the Manitoba border, southeast to 49°N along the Quebec border. At its

broadest point in the northeast it spans approximately 4° latitude, but narrows to less than 0.5° along its center.

Focal point 336 in the northwest demonstrates a fairly large area of adaptive similarity that extends from the Manitoba border east approximately 370 km and from Lake of the Woods north 250 km (Figure 76). Another, much smaller area is present along the shore of Lake Superior in the Thunder Bay area. However, the zone notably excludes the area south of Lake of the Woods along the Minnesota Border.

The seed zone for focal point 584 in the far north extends along the shores of Hudson and James Bay, and spans approximately 3° latitude at its widest point (Figure 77).

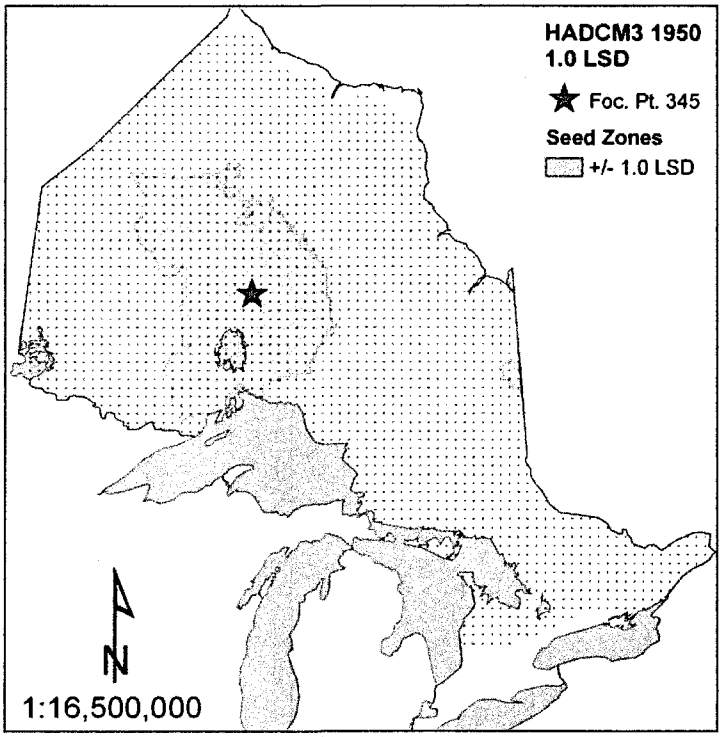

Figure 74. Seed zones for focal point 345, based on HADCM3 for the year 1950.

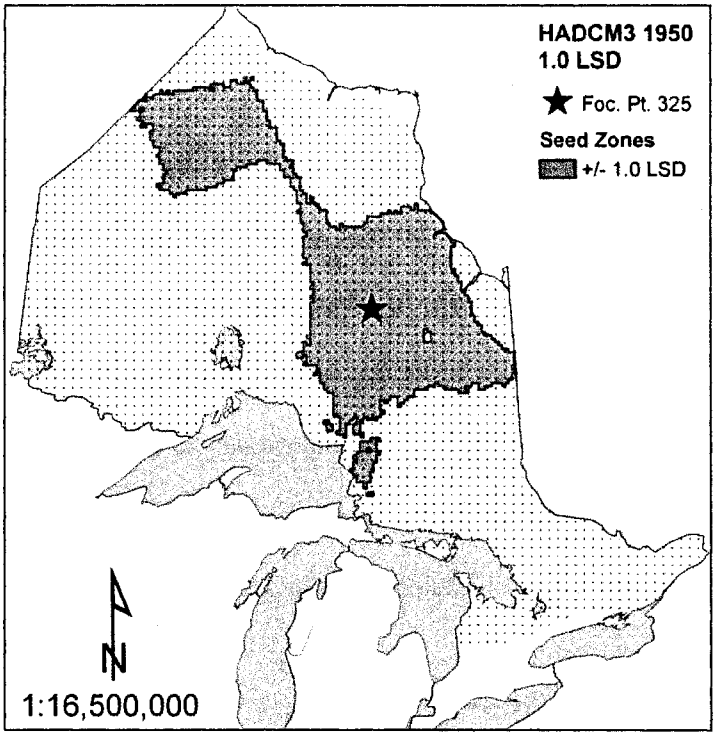

Figure 75. Seed zones for focal point 325, based on HADCM3 for the year 1950.

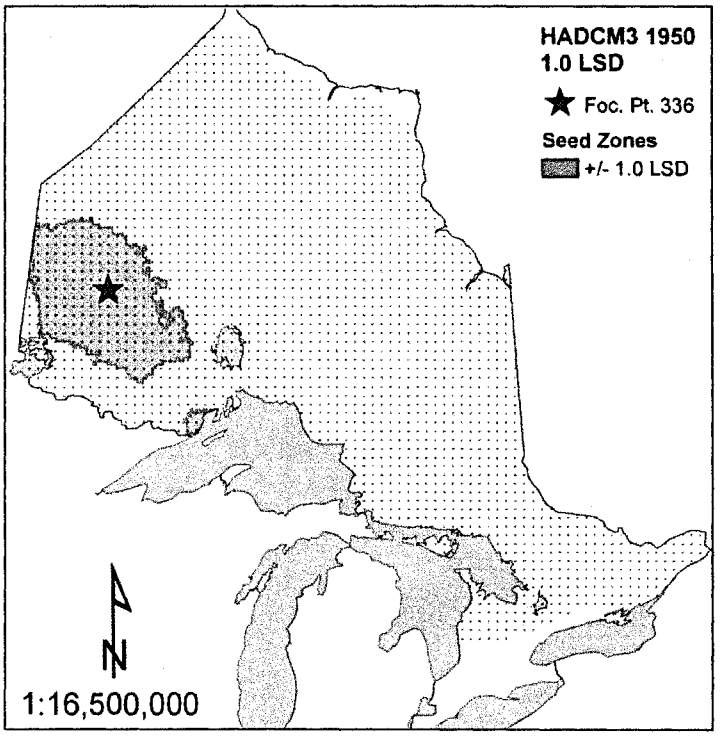

Figure 76. Seed zones for focal point 336, based on HADCM3 for the year 1950.

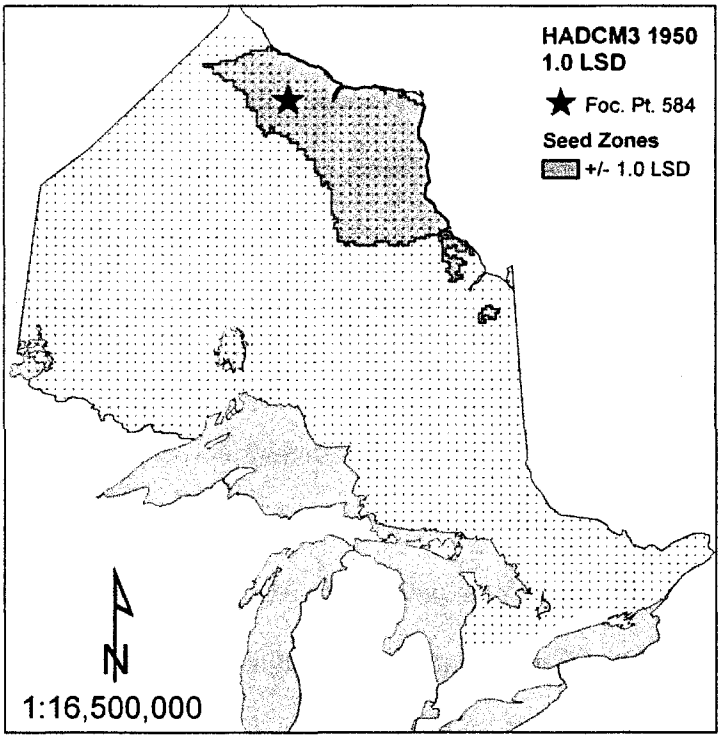

Figure 77. Seed zones for focal point 584, based on HADCM3 for the year 1950.

The HADCM3 1950 seed zones bear moderate resemblance to the 1961-1990 seed zones for the same focal points (Figure 6 to Figure 9). The HADCM3 1950 seed zone for focal point 345 is similar in shape and occupies the same area as the western portion of the 1961-1990 zone. However, the resemblance between the zones is not immediately evident because the HADCM3 1950 zone is severely truncated along its eastern border in comparison the 1961-1990 zone. The seed zone for focal point 325 is also very similar to the analogous 1961-1990 zone, but is comparatively much narrower through its central latitudes. The northwest seed zone for focal point 336 is virtually identical to the 1.0 LSD zone based on 1961-1990 climate normals. However, it does not include the disjunct area in the southern portion of the province. Finally, the 1.0

LSD seed zone for focal point 584 based on HADCM3 1950 is similar in size and shape to the 1961-1990 zone, but extends further southward and not as far westward.

Figure 78 to Figure 81 present the four seed zone examples for CSIRO 1961 at the 1.0 LSD level of adaptive similarity. The broad area of adaptive similarity for focal point 345 extends from the southern shore of Lake Nipigon, northward approximately 520 km and 650 km from west to east (Figure 78).

The seed zone for focal point 325 in the eastern mid-latitudes occupies two discontinuous areas (Figure 79). The first of these areas is oriented primarily from north to south and is located surrounding the focal point in the east. It extends from 48°N at its southernmost point to 53°N at its northernmost point adjacent to James Bay, and spans approximately 5° longitude. The second area of adaptive similarity is formed by a latitudinal band in the northwest of the province that runs from the Manitoba border to the western shore of Lake Nipigon.

Areas of adaptive similarity for focal point 336 are located in the northwest region and along the north shore of Lake Superior (Figure 80). The first and larger area surrounds the focal point in the northwest, running northwards from Lake of the Woods to 53°N latitude and from the Manitoba border east almost to the shore of Lake Nipigon. The second area is oriented north-south, and stretches from the Wawa/Manitowadge area to approximately 52°N.

The seed zone for focal point 584 in the far north stretches from 56°N along the shore of Hudson Bay, southeast to 53°N along the shore of James Bay (Figure 81). A much smaller discontinuous area is located along the western shore of James Bay, just offset from the main zone.

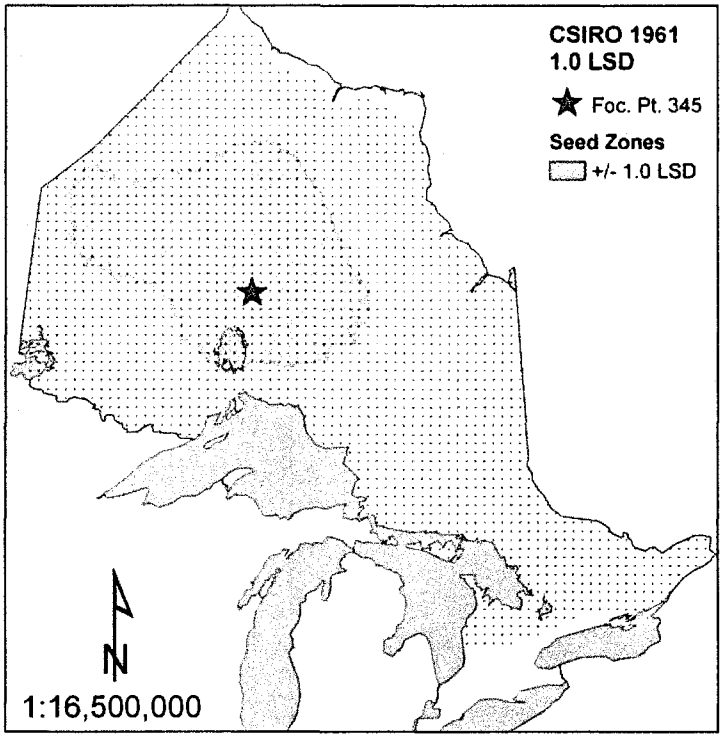

Figure 78. Seed zones for focal point 345, based on CSIRO for the year 1961.

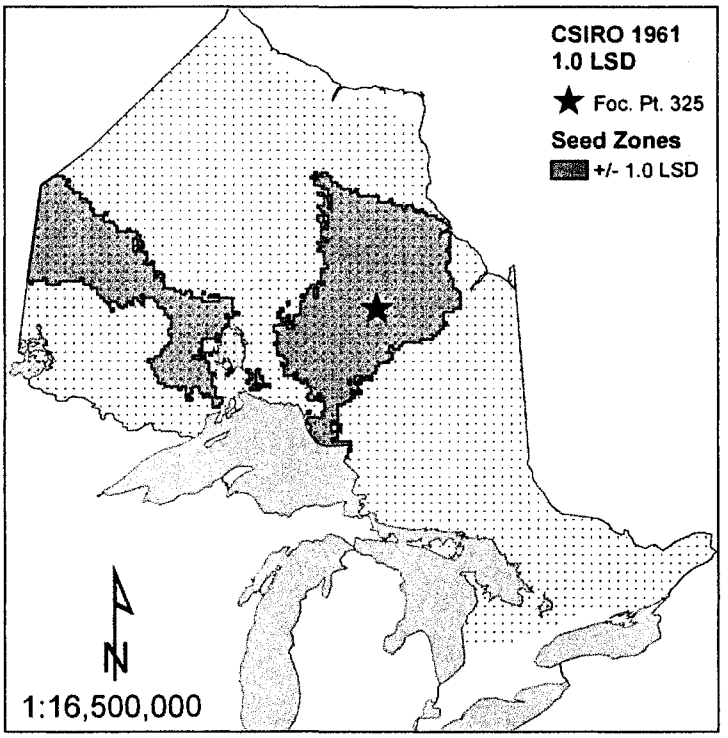

Figure 79. Seed zones for focal point 325, based on CSIRO for the year 1961.

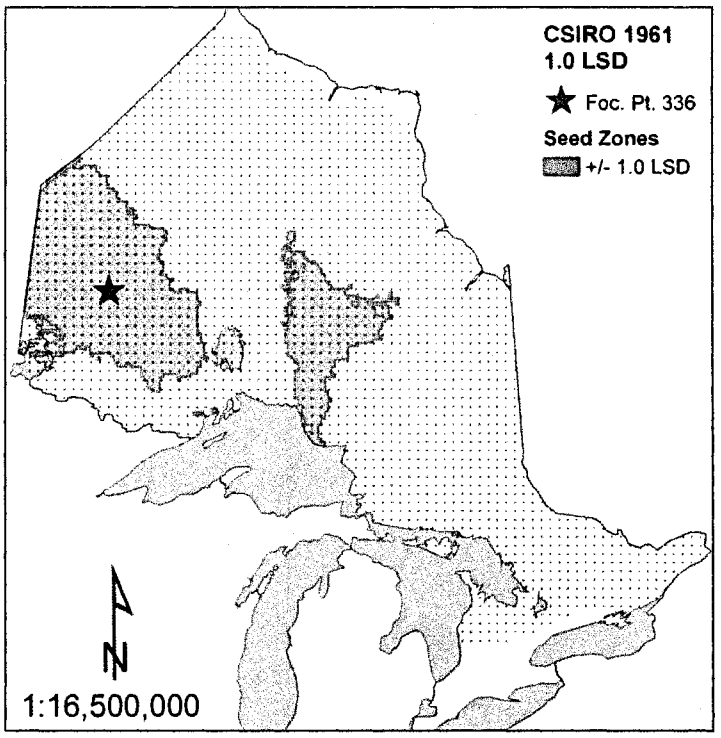

Figure 80. Seed zones for focal point 336, based on CSIRO for the year 1961.

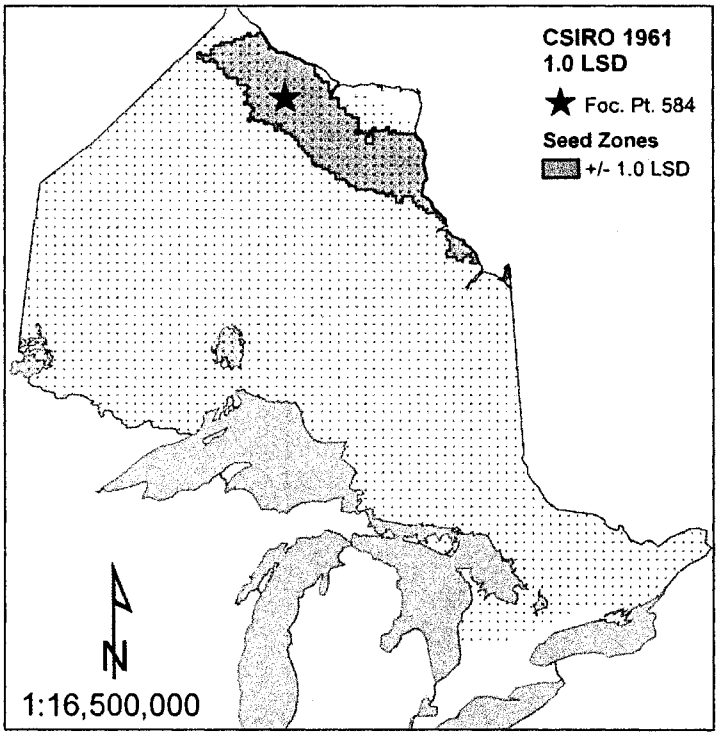

Figure 81. Seed zones for focal point 584, based on CSIRO for the year 1961.

The CSIRO 1961 seed zones bear low to moderate resemblance to the 1961-1990 seed zones for the same focal points (Figure 6 to Figure 9). The seed zone for focal point 345 is similarly broad as the 1961-1990 zone, but extends much farther into the northwest and not nearly as far eastward. It also excludes the area south of Lake Nipigon, in contrast to the 1961-1990 zone which encompasses the entire perimeter. The CSIRO 1961 seed zone for focal point 325 bears the least similarity to the analogous 1961-1990 zone. It is similar in size to the 1961-1990 zone, but is composed of two smaller discontinuous areas instead of one large continuous area. Also, the orientation of the eastern zone is primarily from northeast-southwest, whereas the 1961-1990 zone is oriented from northwest-southeast. It extends much further southward than the 1961-1990 zone. The northwestern portion of the seed zone for focal point 336 is mostly similar to that of the 1961-1990 zone. However, the CSIRO 1961 zone indicates that the second area of adaptive similarity occurs along the north shore of Lake Superior instead of in the Ottawa Valley area. The CSIRO 1961 seed zone for focal point 584 is surprisingly similar to that of the 1961-1990 zone. However, it occupies a somewhat narrower latitudinal range.

PAST BREEDING ZONES

Figure 82 presents the level of coverage that is achieved with 1-10 breeding zones for each of the four past climate estimates. The solutions are presented based on selection from a set of 618 candidate breeding zones constructed at the 1.0 LSD level of adaptive similarity. The first solution-set based on CGCM2 1900 is presented by the green series line, while CGCM2 1950 is presented in purple, HADCM3 1950 is

presented in orange, and CSIRO 1961 is presented in blue. CGCM2 1900 demonstrates the lowest coverage across the range of solutions, with a total coverage of just 67.9% based on 10 breeding zones. CGCM2 1950 also demonstrates a relatively low level of coverage in comparison to the HADCM3 1950 and CSIRO 1961 solutions. Based on 10 optimized breeding zones, the total coverage for CGCM2 1950 is equal to 87.2%. The solutions based on HADCM3 1950 and CSIRO 1961 produced relatively similar coverage, with respective values of 95.2% and 91.7% based on 10 breeding zones.

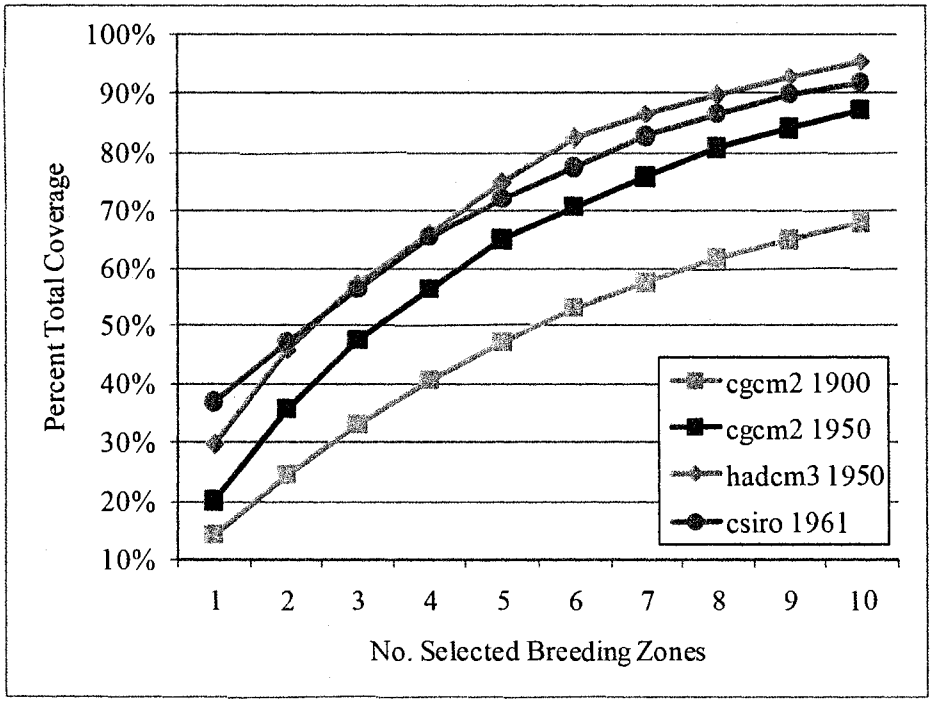

Figure 82. Percent of total area covered with increasing number of breeding zones based on past climate estimates.

Figure 83 to Figure 98 illustrate optimal past breeding zones constructed for CGCM2 1900, CGCM2 1950, HADCM3 1950, and CSIRO 1961, respectively. The solutions are presented based on the allowance of 1 to 4 breeding zones at the 1.0 LSD level of adaptive similarity.

Figure 83 to Figure 86 present the optimal solution for CGCM2 1900 based on 1 to 4 selected breeding zones. The selection of focal point 405 in the center of the province results in a broad zone that covers 14.2% of the total area (Figure 83). Breeding zone 405 stretches from approximately 51°N to between 53 and 55°N.

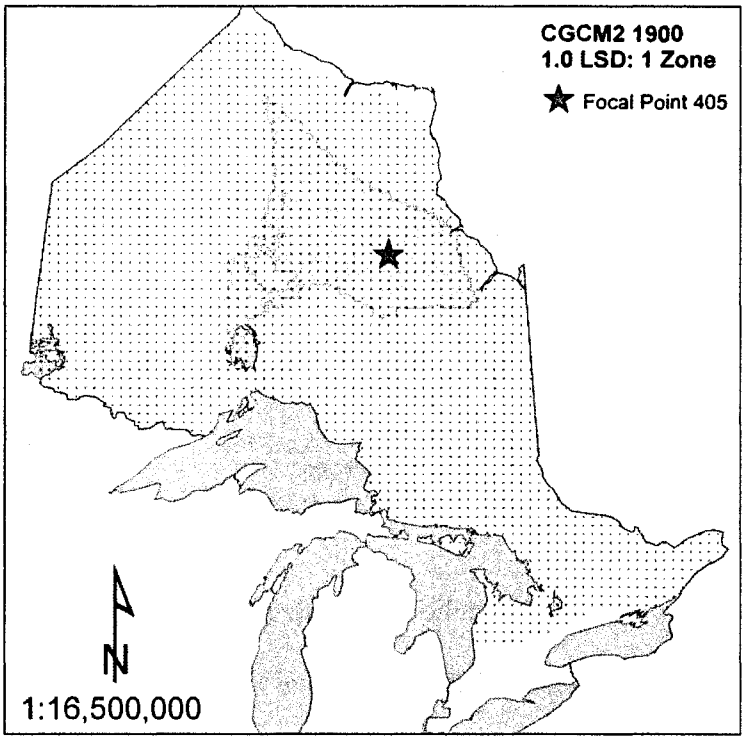

Figure 83. Optimal 1-breeding zone solution based on CGCM2 1900 at the 1.0 LSD level of adaptive similarity.

The optimal 2-zone solution achieves nearly double the coverage as the 1-zone solution with a total coverage of 24.4% (Figure 84). The selection of breeding zone 177 introduces a narrow zone located just to the south of the more broad central zone. The two zones do not overlap. Breeding zone 177 encompasses the north shore of Lake Superior and the area surrounding Lake Nipigon, spanning a broad range of latitudes from approximately 90°W to 82°W.

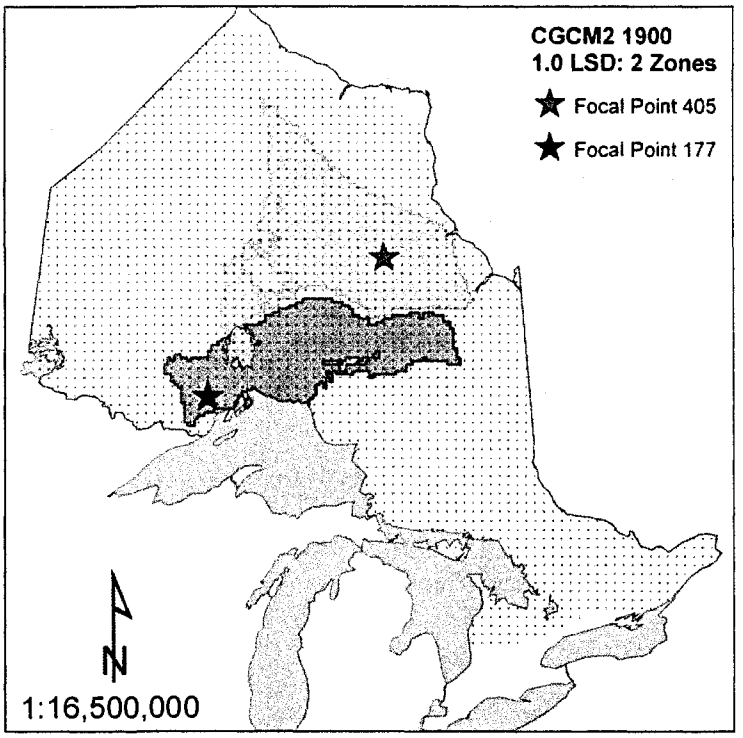

Figure 84. Optimal 2-breeding zone solution based on CGCM2 1900 at the 1.0 LSD level of adaptive similarity.

The selection of focal point 536 in the north increases total coverage to 32.9% for the optimal 3-zone solution (Figure 85). Breeding zone 536 occupies a narrow latitudinal band in the far north of the province close to Hudson and James Bay. The broad central zone expands slightly westward in comparison with the 2-zone solution, while the narrower zone to the south remains unchanged. Overlap between zones is virtually negligible, except for a tiny band along the adjacent borders of zones 402 and 177.

Total coverage for the optimal 4-zone solution reaches 40.5% (Figure 86). Except for the selection of breeding zone 441 in the west, the solution remains unchanged from the 3-zone solution. Breeding zone 441 is latitudinally-restricted,

ranging from 52°N to 53°N along its western edge, to approximately 52°30' to 53°30' along its eastern edge.

The optimal 4-zone solution based on CGCM2 1900 demonstrates somewhat similar zones as the optimal 4-zone solution based on 1961-1990 climate normals (Figure 23). The broad central zone of the CGCM2 1900 solution loosely resembles zone 131 of the 1961-1990 solution, though it is truncated along its eastern and western boundaries and shifted slightly northward. Similarly, northern zone 536 for CGCM2 1900 resembles the northernmost zone (584) for 1961-1990. In contrast, the narrower central zone (177) and western zone (441) for CGCM2 1900 are anomalous when compared to the 1961-1900 solution.

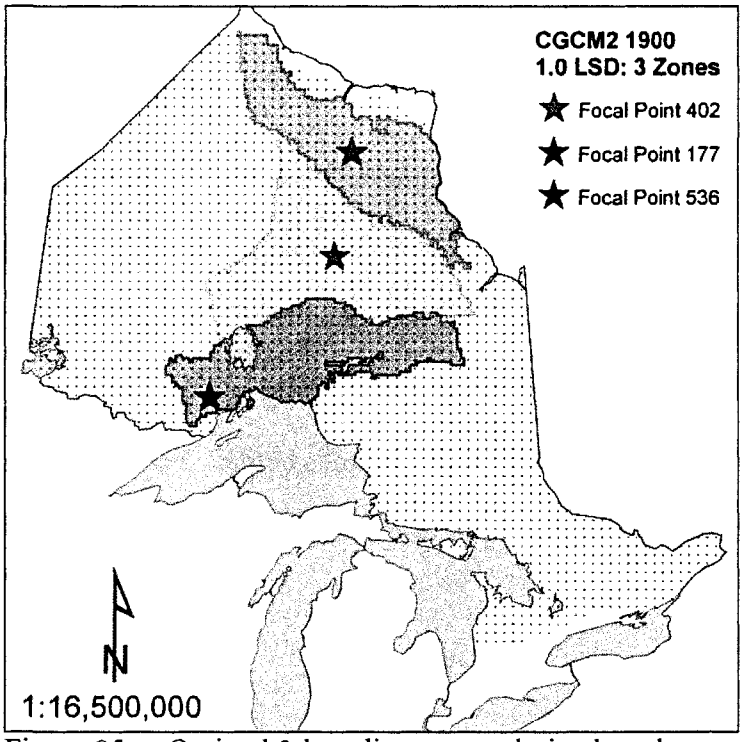

Figure 85. Optimal 3-breeding zone solution based on CGCM2 1900 at the 1.0 LSD level of adaptive similarity.

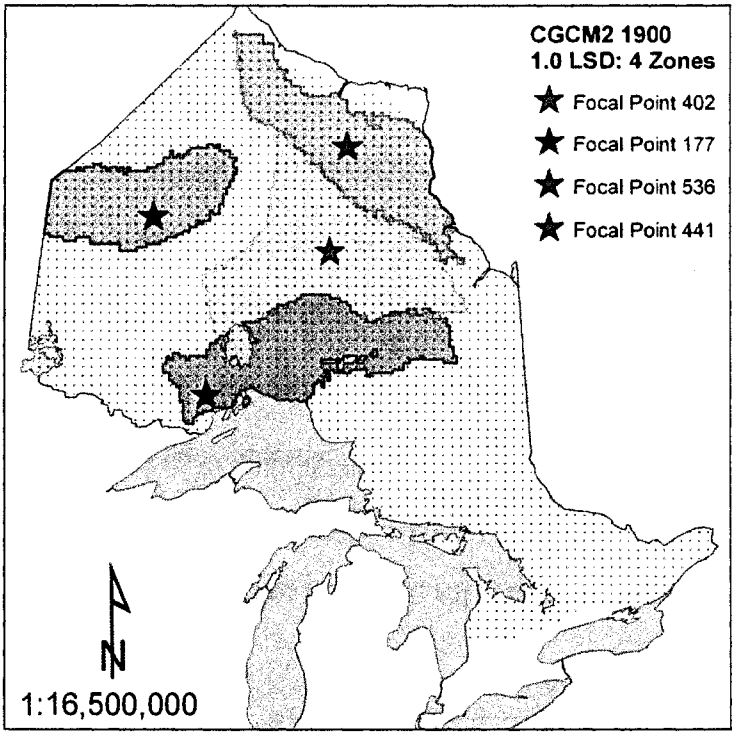

Figure 86. Optimal 4-breeding zone solution based on CGCM2 1900 at the 1.0 LSD level of adaptive similarity.

Figure 87 to Figure 90 present the optimal solution for CGCM2 1950 based on 1 to 4 selected breeding zones. The optimal 1-zone solution produces 19.9% total coverage with the selection of focal point 595. Breeding zone 595 is composed of two broad zones, the first and much smaller of the two is located in the far northwest surrounding the focal point and adjacent to the Manitoba border. The second, much larger zone occupies a roughly circular area in the northeast adjacent to James Bay.

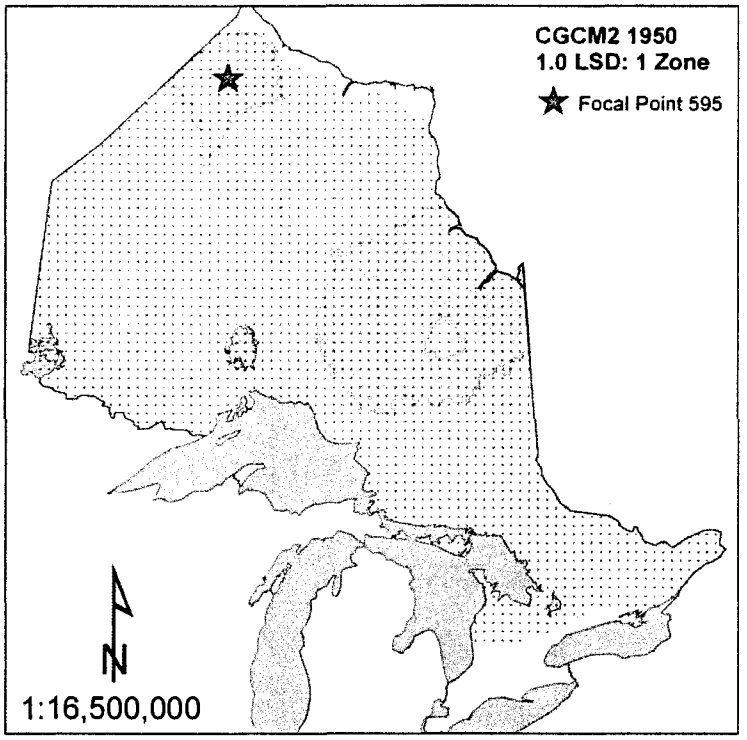

Figure 87. Optimal 1-breeding zone solution based on CGCM2 1950 at the 1.0 LSD level of adaptive similarity.

The selection of focal point 103 in the northeast increases total coverage to 35.5% for the optimal 2-zone solution (Figure 88). Like the previous zone, breeding zone 103 is composed of 2 disjunct portions; the two areas are located just to the south of breeding zone 595 in the northwest and northeast. The area surrounding the focal point is more north-south oriented, spanning approximately 2° longitude and 3° latitude.

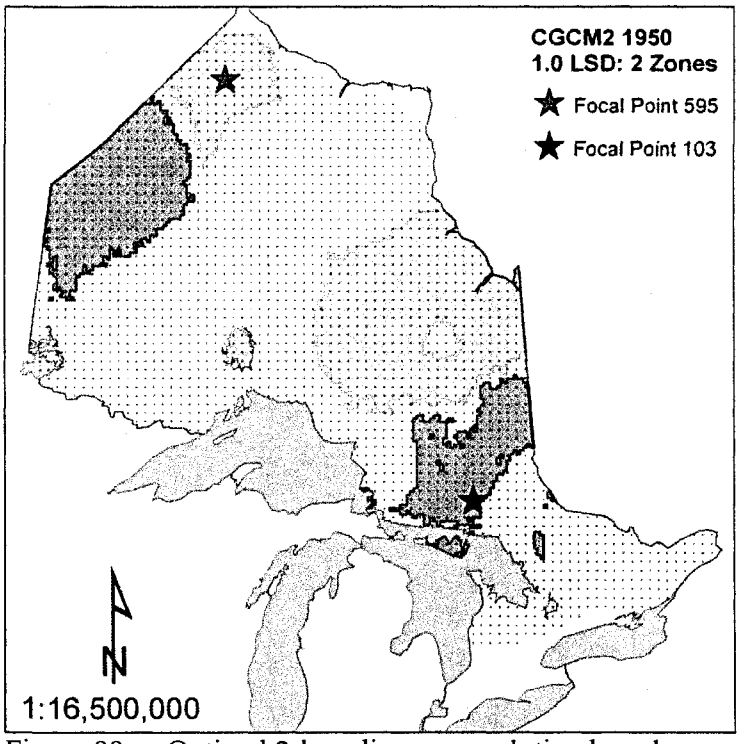

Figure 88. Optimal 2-breeding zone solution based on CGCM2 1950 at the 1.0 LSD level of adaptive similarity.

The total coverage increases to 47.3% with the selection of focal point 397 in the central portion of the province (Figure 89). Though broad on its southern end, breeding zone 397 is also somewhat north-south oriented, running from approximately 50-55°N latitude. This breeding zone noticeably excludes the area immediately north of Lake Nipigon. Overlap between zones is virtually negligible, with only a tiny area of intersection along the adjacent boundaries of zone 397 and zone 595 to the north and east.

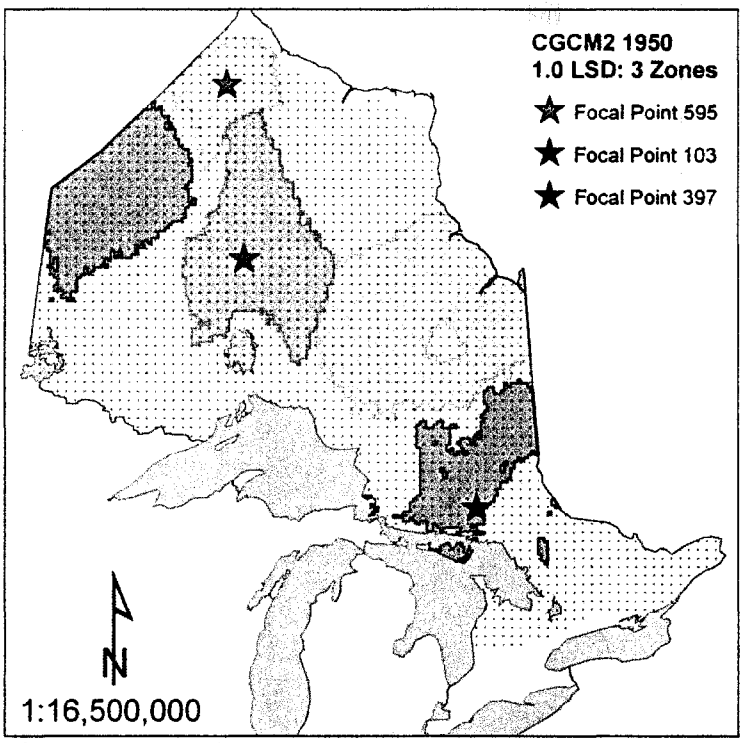

Figure 89. Optimal 3-breeding zone solution based on CGCM2 1950 at the 1.0 LSD level of adaptive similarity.

The selection of breeding zone 399 for the optimal 4-zone solution increases total coverage to 56.3%, but introduces overlap between zones (Figure 90). Breeding zone 399 is located in the far north of the province adjacent to Hudson Bay and overlaps with zone 595 along both its eastern and western boundaries. The large majority of the remaining uncovered area is located in the southern half of the province; virtually the entire northwest and southern regions remain uncovered, while the northeastern region has only moderate coverage.

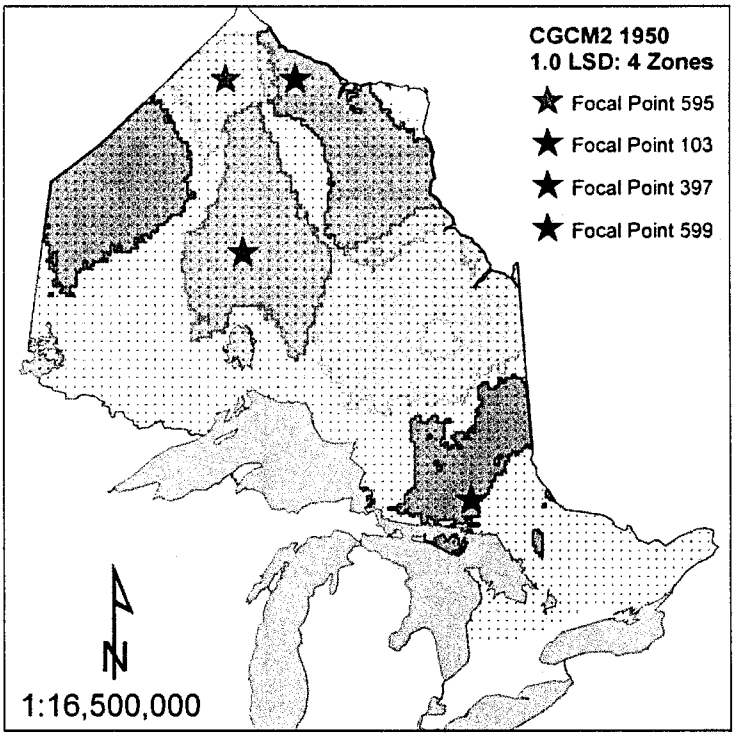

Figure 90. Optimal 4-breeding zone solution based on CGCM2 1950 at the 1.0 LSD level of adaptive similarity.

The optimal 4-zone solution based on CGCM2 1950 bears relatively little similarity with the optimal 4-zone solution based on 1961-1990 climate normals (Figure 23). The northernmost disjunct zone (595) and the central zone (397) are anomalous in comparison to the 1961-1990 solution. The western portion of zone 103 is quite similar to that of zone 75 in the 1961-1990 scenario but is located somewhat further northward. Of the 4 zones selected for the CGCM2 1950 optimization, breeding zone 599 bears the greatest resemblance to the 1961-1900 zones. This zone occupies similar northern latitudes and is similar in shape as the northernmost zone (584) of the 1961-1990 solution. However, the northern zone of the CGCM2 1950 solution is oriented northwest to southeast while the 1961-1990 northern zone is oriented primarily east-west.

Figure 91 to Figure 94 present the optimal solution for HADCM3 1950 based on 1 to 4 selected breeding zones. For the optimal 1-zone solution, the selection of focal point 489 produces a large centralized zone that covers 29.5% of the total area (Figure 91). Breeding zone 489 spans approximately 3° latitude and runs from the area of the focal point in the northwest southeastward to approximately 83°W longitude.

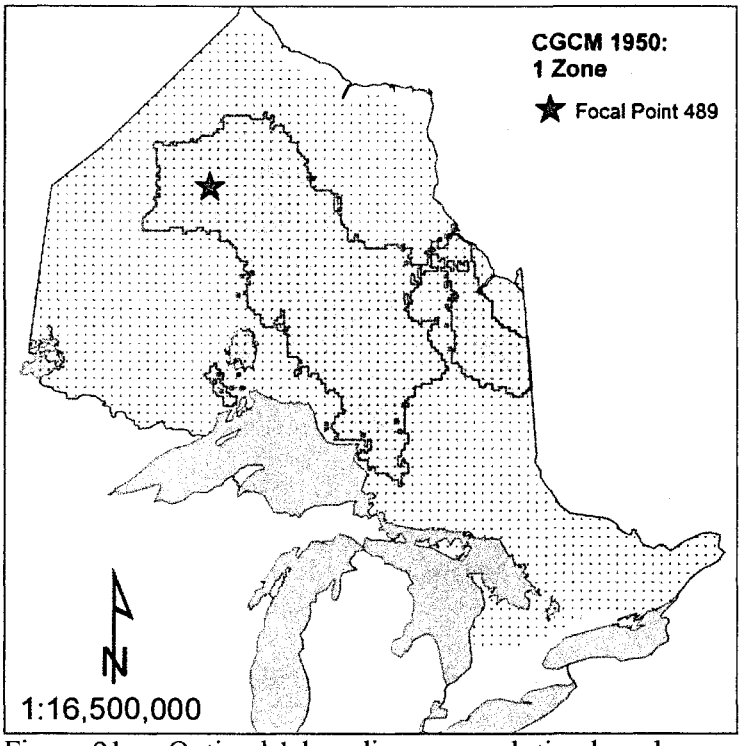

Figure 91. Optimal 1-breeding zone solution based on HADCM3 1950 at the 1.0 LSD level of adaptive similarity.

The selection of focal point 566 increases total coverage to 45.7% for the optimal 2-zone solution (Figure 92). Breeding zone 566 occupies the far north of the province and is oriented along a similar northwest-southeast transect as central zone 465. The two zones overlap slightly near their western and eastern boundaries. In comparison with the optimal 1-zone solution, the central breeding zone has expanded to enclose the western perimeter of Lake Nipigon. However, the central zone still

demonstrates the exclusion of the area immediately to the north and east of Lake Nipigon.

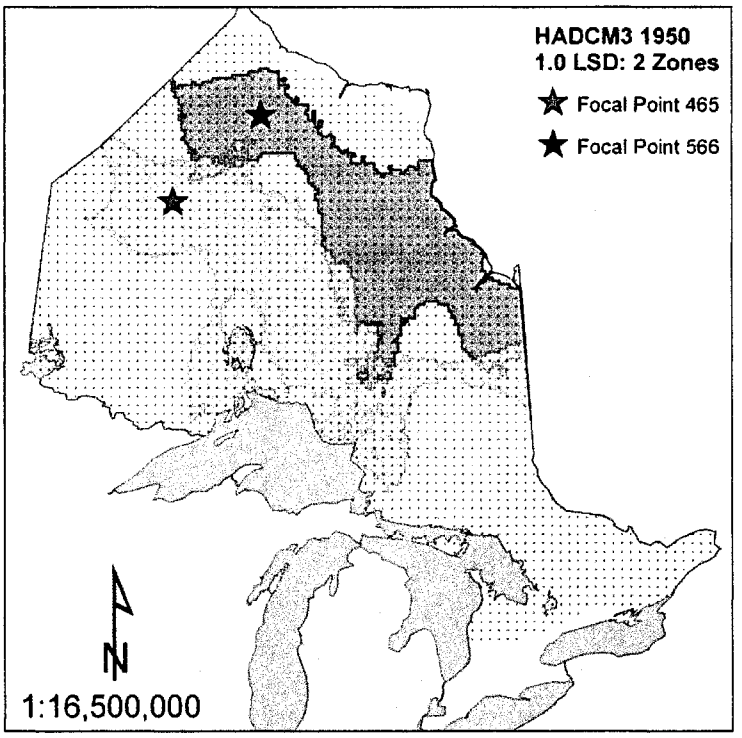

Figure 92. Optimal 2-breeding zone solution based on HADCM3 1950 at the 1.0 LSD level of adaptive similarity.

The selection of focal point 417 in the northwest increases total coverage to 57.3% for the optimal 3-zone solution (Figure 93). Breeding zone 417 stretches south and eastward from the Manitoba border to the area just west and north of Lake Nipigon where it overlaps with the central zone. There is again a notable exclusion of the areas immediately to the north, east, and south of Lake Nipigon. In comparison with the optimal 2-zone solution, the central zone (297) is much narrower along its mid-longitudes and broader along its eastern edge. It also appears the zone has shifted northward slightly. The northern zone (499) is truncated along its western and eastern boundaries and has also shifted northward in comparison with the 2-zone solution.

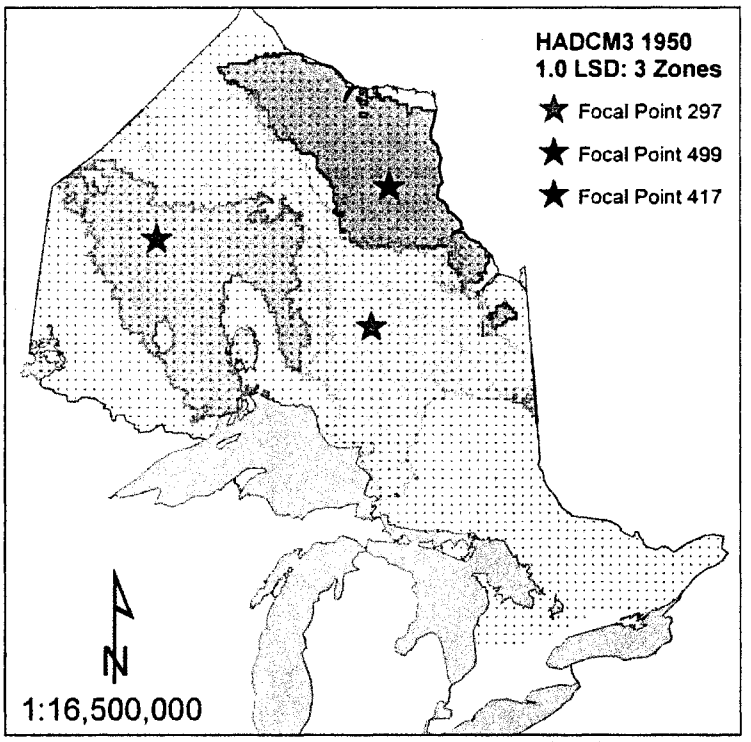

Figure 93. Optimal 3-breeding zone solution based on HADCM3 1950 at the 1.0 LSD level of adaptive similarity.

Total coverage for the optimal 4-zone solution is 66.3% (Figure 94). The selection of focal point 108 greatly increases coverage in the northeast region. Breeding zone 108 is somewhat rounded, stretching from the Wawa area east to Kirkland Lake along the Quebec border, and from and from Hearst, south to Sudbury and North Bay. It also contains a relatively small, disjunct area in the northwest. In comparison with the 3-zone solution, the central zone (374) is much broader through its mid-section, shifts westward, and is truncated along its western boundary. The central zone now encloses the area surrounding Lake Nipigon. The northern zone (566) shifts slightly southward and spans a broader range of longitudes. The western zone (388) shifts slightly southwest and bears little resemblance to that of the 3-zone solution. The western zone

now occupies the area north of Lake of the Woods adjacent to the Manitoba border and does not extend as far eastward.

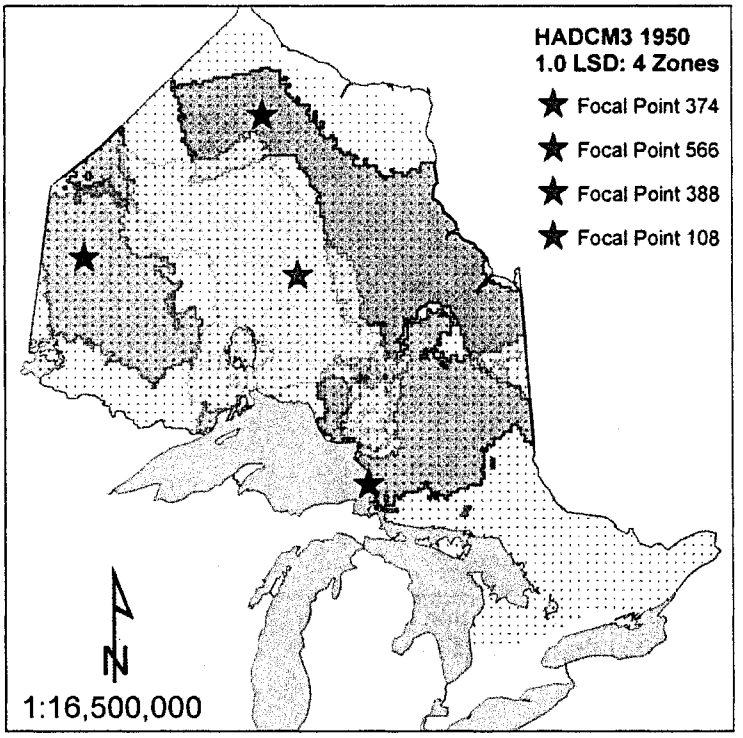

Figure 94. Optimal 4-breeding zone solution based on HADCM3 1950 at the 1.0 LSD level of adaptive similarity.

The optimal 4-zone solution based on HADCM3 1950 bears striking similarity to the optimal 4-zone solution based on 1961-1990 climate normals (Figure 23). The central zone of the HADCM3 solution is similar to that of the 1961-1990 solution, though it is narrower along its western boundary. The northern zone (566) is similar to the mid-northern zone of the 1961-1990 solution (325) but does not extend as far westward. The northwestern zone (388) almost perfectly resembles the northwest zone of the 1961-1990 solution (75) but does not include the disjunct area to the southeast. However, the eastern zone (108) does not have an analogous zone in the 1961-1990 solution.

Figure 95 to Figure 98 present the optimal solution for CSIRO 1961 based on 1 to 4 selected breeding zones. For the optimal 1-zone solution, the selection of focal point 462 produces a very broad zone centered in the northwest that covers 36.7% of the total area (Figure 95). Breeding zone 462 stretches from the Manitoba border eastward in a broad band spanning approximately 5° latitude, to the Nipigon and Cochrane districts.

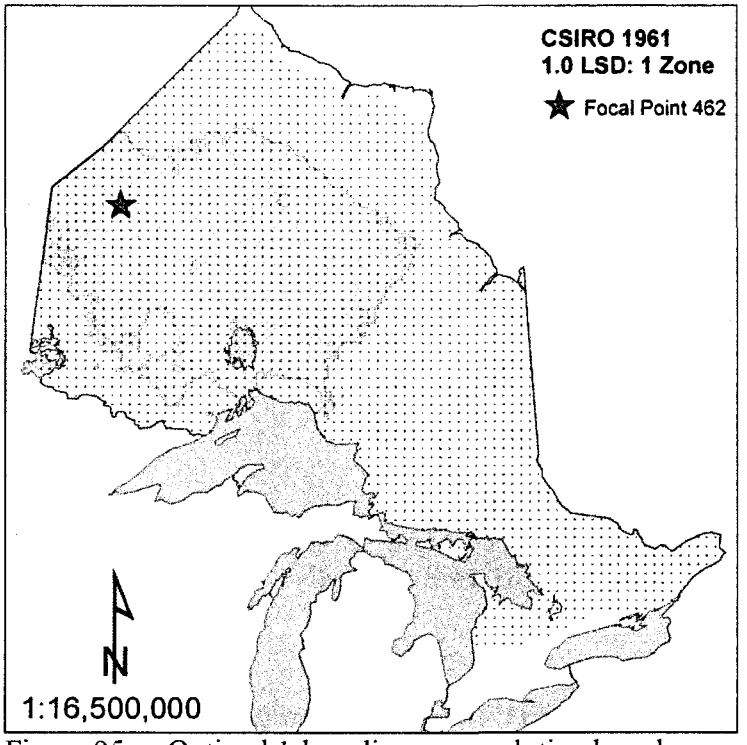

Figure 95. Optimal 1-breeding zone solution based on CSIRO 1961 at the 1.0 LSD level of adaptive similarity.

The selection of focal point 501 to the north increases total coverage to 47.0% for the optimal 2-zone solution (Figure 96). Breeding zone 501 occupies a narrow latitudinal band in the far north of the province and spans from just east of the Manitoba border to the area surrounding James Bay. A small area of overlap between the two zones is evident where they intersect just south of James Bay. In comparison with the 1-zone solution, the broad central zone is quite similar but demonstrates an increased

number of small, uncovered islands within its interior; notably one along the north shore of Lake Nipigon.

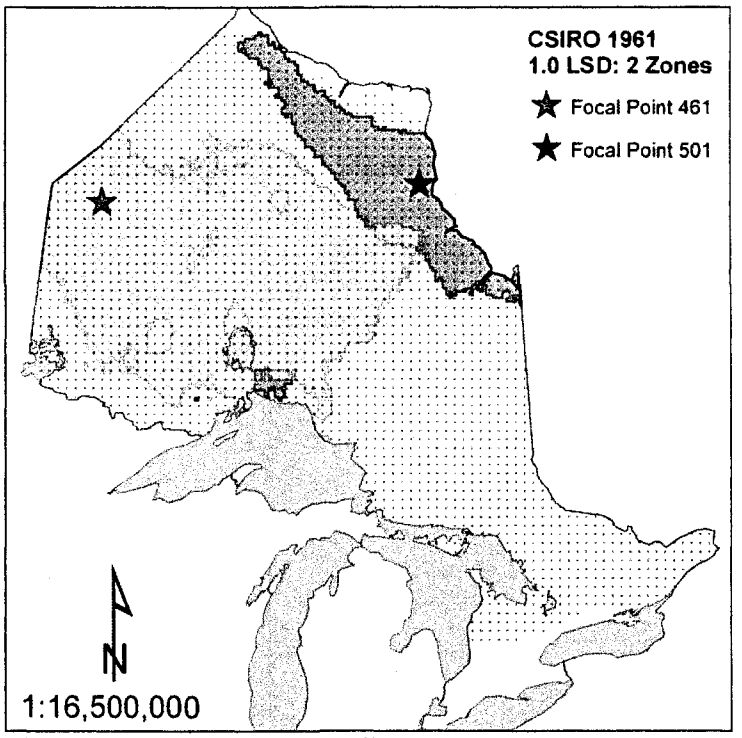

Figure 96. Optimal 2-breeding zone solution based on CSIRO 1961 at the 1.0 LSD level of adaptive similarity.

The selection of focal point 211 in the northeast region increases coverage for the optimal 3-zone solution to 56.3%. Breeding zone 211 spans a latitudinal band composed of 2 disjunct segments. The first of these occupies the area surrounding the focal point in the northeast region, while the second spans from the Manitoba border to the west shore of Lake Nipigon in the northwest region. Significant overlap between zone 211 and the broad central zone is evident. In comparison with the 2-zone solution, the broad central zone is quite similar but does not extend as far south in the west and now includes the area along the north shore of Lake Nipigon. The northern zone remains unchanged.

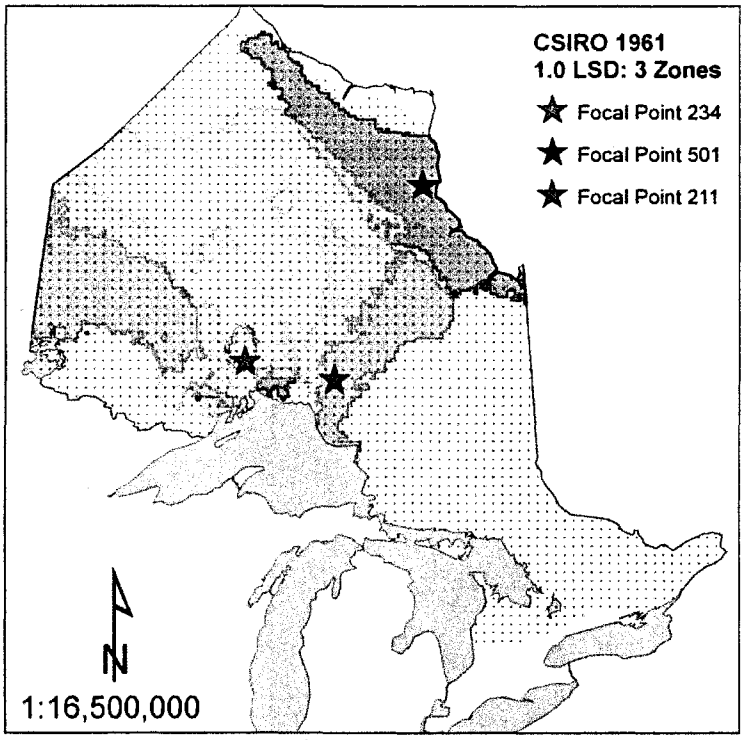

Figure 97. Optimal 3-breeding zone solution based on CSIRO 1961 at the 1.0 LSD level of adaptive similarity.

The optimal 4-zone solution achieves 65.4% total coverage with the selection of focal point 121. Breeding zone 121 covers most of the northeast region, spanning from Sault Ste. Marie northwards to the Timmons and Cochrane area. The broad central (234), northern (501), and northwestern (211) zones are the same as the previous solution. No additional overlap is created by the selection of breeding zone 121.

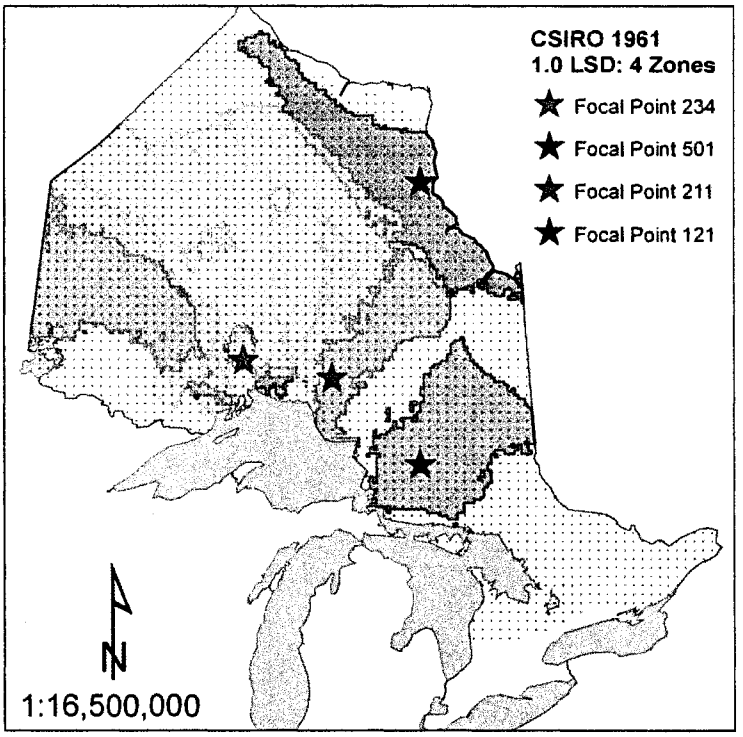

Figure 98. Optimal 4-breeding zone solution based on CSIRO 1961 at the 1.0 LSD level of adaptive similarity.

The optimal 4-zone solution based on CSIRO 1961 bears relatively little similarity to the optimal 4-zone solution based on 1961-1990 climate normals (Figure 23). The northern zone of the CSIRO solution (501) occupies a similar area as zone 325 of the 1961-1990 solution, but is narrower and shifted somewhat further northward. The northeast zone (121) does not have an analogous zone in the 1961-1990 solution. The broad centralized zone (234) of the CSIRO solution bears some resemblance to the broad central zone (131) for 1961-1990, but is much broader and more centered within western Ontario. The narrow latitudinal zone (211) of the CSIRO solution is anomalous and bears little resemblance to any of the 1961-1990 zones.

DISCUSSION

Predicted past and current patterns of principal components are similar, with growth potential, phenological timing, and greenhouse elongation increasing from north to south. However, several of the grids indicate substantial local irregularities in comparison to 1961-1990 factor scores grids, namely CGCM2 1900 and CSIRO 1961.

Focal point seed zones for CGCM2 1900 are much more restricted in comparison to those constructed based on 1961-1990 climate normals. While CGCM2 1950 zones are relatively broader than those of CGCM2 1900, they span only a few degrees of longitude in comparison to the 1961-1990 seed zones which span up to 11° longitude. The HADCM3 1950 seed zones are most similar to those of 1961-1990, generally spanning a similar range of longitude and latitude and are most similar in shape. However, the zone for focal point 345 is extremely truncated along its eastern boundary in comparison with 1961-1990. The CSIRO 1961 seed zones bear the least similarity and indicate several disjunct zones that are anomalous in comparison to 1961-1990 zones.

When compared to 1961-1990 breeding zones, the past scenarios rank in order of similarity: HADCM3 1950 > CSIRO 1961 > CGCM2 1900 > CGCM2 1950. However, when compared to 1961-1990 climate grids, HADCM3 1950 is still most similar but is followed by CGCM2 1950, CGCM2 1900, and CSIRO 1961. It is interesting that the simulated past climate of CSIRO 1961 scenario is the least similar to

that observed for 1961-1990 because the two time periods overlap. Intuitively, one might expect the earliest scenario (CGCM2 1900) to be the least similar because of the greater disparity between the time periods. However, in attempting to explain the observed differences between past simulations and observed normals it is useful to examine the patterns of individual climate variables included in the regressions (APPENDIX I). The large differences in patterns of variation between CSIRO 1961 and 1961-1990 climate normals can be explained by relatively large differences in precipitation patterns, mainly those of August, October, and March. Similarly, differences between CGCM2 1900 and 1961-1990 seed zones can be explained.

It is interesting to note that each of the 3 climate models simulates temperatures accurately; however, there is a great deal of variation in the accuracy with which precipitation is modeled. This is not surprising given that precipitation is relatively much more difficult to predict and is more annually variable than temperature and that most models are shown to predict temperature quite accurately (Covey *et al.* 2003; IPCC 2007b). However, some precipitation variables, such as January precipitation, were simulated more reliably by each of the models than other variables such as October precipitation.

A model validation project in the United Kingdom found that HADCM3 is able to model mean monthly precipitation as well or better than any of the other models, including CSIRO and CGCM2 (Hulme *et al.* 1999). This results of this study would tend to support that finding, given the surprising similarity between the simulated monthly climate data based on HADCM3 in comparison to the observed normals for 1961-1990 (APPENDIX I), and superiority in comparison to CGCM2 and CSIRO. The

authors note some problems with the simulation of April-June precipitation; however, these issues did not affect the results of this study because April-June precipitation was not used to model white spruce performance. The authors note the simulation of precipitation patterns with HADCM3 is better than with CGCM2 but similar to CSIRO. While this may be the case for modeling climate patterns in the UK, the results of this study tend to refute the CSIRO model's accuracy in predicting precipitation in Ontario. The great discrepancy in predicted factor scores based on CSIRO in comparison to the patterns of variation based on observed data suggest large problems in the ability of CSIRO to simulate observed precipitation patterns, at least for those variables used in regressions for the current study.

Lambert and Boer (2001) suggest that there is no single best model; that each model reproduces some aspects of observed climate better than others. However, in this case, the HADCM3 model was superior in simulating most of the 9 climate variables used to model white spruce performance. However, its ability to simulate other climate variables not used in regressions in the current study has not been assessed. This omission suggests that a basic model evaluation such as presented here may need to be conducted for other studies using different climate variables. For example, the relative superiority of HADCM3 in modeling white spruce performance may not apply to black spruce or jack pine if other climate variables are used to simulate their individual patterns of genetic variation.

An important assumption of this analysis is that changes in climate over the past century are minimal, allowing for reasonable comparisons between simulated past climates and recent observed climate normals. However, measurable changes have

occurred over the last hundred years, especially in the last several decades (IPCC 2007b). Thus, comparisons between past simulations and observed normals for 1961-1990 are not entirely equivalent, and even a highly accurate model will probably not simulate a past climate that exactly matches the 1961-1990 normals. However, evaluation is still useful to indicate which of the models is relatively most accurate.

It is probable that the use of annual models contributed to the dissimilarity between past simulations and current climate, because short-term climate simulations are relatively more variable than long-term normals (IPCC 2007b). In contrast, if averages of 30-year simulated climate were used, temperature and precipitation patterns may have been more similar to those observed for the 1961-1990 period.

The ability of the Hadley model to accurately simulate both temperature and precipitation patterns lends great confidence to future predictions based on this model. In fact, the similarity between HADCM3 1950 simulated climate and 1961-1990 observed normals is striking. From the results, it appears that the Hadley model is probably the most reliable in predicting Ontario climate patterns. Predictions based on CGCM2 are probably somewhat reliable, while CSIRO predictions should be treated with caution due to its relatively weak ability to predict temperature and precipitation patterns of in Ontario.

CHAPTER V: WHITE SPRUCE BREEDING ZONES TO COMPENSATE FOR PREDICTED FUTURE CLIMATE CHANGE

INTRODUCTION

Previous chapters were concerned with evaluating the geographic patterns of variation of white spruce in Ontario to determine optimal adaptively-based breeding zones. It is the intention that these zones will ensure that seedlings are only deployed to areas in which they have been demonstrated to be well-adapted. However, rapid climate change over the next century is predicted to lead to significant declines in white spruce growth (Carter 1996; Cherry and Parker 2003; Li *et al.* 1997; Rweyongeza *et al.* 2007) as trees become increasingly maladapted in their planted or native locations. Thus, restructuring of breeding zones with a concomitant reallocation of improved seed sources to those new zones will be required to maintain adequate growth and survival (Rehfeldt *et al.* 1999).

The challenge now becomes one of determining how best to deploy improved seed in the future to ensure that expected gains are realized. Using the previous regression models in combination with future climate data, one can predict future performance patterns to refine existing breeding zones (Rehfeldt 1991). However, a challenge arises in that predictions of future climate are largely uncertain. Numerous models and emissions scenarios have been developed to describe possible future outcomes, but it is unclear which, if any, of these scenarios will hold true in the future. Indeed, the Intergovernmental Panel on Climate Change, composed of top scientists in the field, is reluctant to assign probabilities to any of the scenarios (Betz 2007). Thus, it

is prudent to consider all scenarios as a potential future outcome, and model breeding zones accordingly.

This chapter presents optimized future breeding zones for white spruce based on each of 6 predictions of climate for the period of 2041-2070: CGCM2 A2 & B2, HADCM3 A2 & B2, and CSIRO A2 & B2. These high-resolution models represent the best future climate estimates available for Ontario and have been used in a wide variety of ecological applications (McKenney *et al.* 2006).

The purpose of this chapter was to develop optimal future breeding zones of white spruce for Ontario under six potential climate change scenarios, to avoid deployment of maladapted orchard seed in the future. The results can be used with a modified version of the focal point seed zones program to guide future deployment of improved seed and to determine additional sources for each breeding zone that will be best-suited to future climate conditions.

METHODS

Estimates of future climate for the period 2041-2070 were obtained from Dr. D. McKenney, Great Lakes-St. Lawrence Forestry Centre (McKenney *et al.* 2006b). Ontario-wide grids of 10-km resolution for each of 36 climate variables for each of 6 future climate scenarios were obtained. The future climate scenarios used were CGCM2 A2 & B2, HADCM3 A2&B2, CSIRO A2&B2. The 36 climate variables were the same as those used in previous chapters including: mean monthly maximum and minimum temperature, as well as mean monthly precipitation. Predicted principal components factor scores for each climate scenario were calculated for each gridpoint using the previous regression models, and used to develop focal point seed zone examples as described in the previous chapters. The examples presented herein utilize the same four focal points as previously presented (Chapter IV) to allow comparison between scenarios and time periods. Candidate breeding zones were created for each of the previous 618 focal points for each future scenario and used to determine optimal breeding zones for each potential future climate.

RESULTS

PREDICTED FACTOR SCORES FOR 2041-2070

Factor scores obtained by regression of predicted climate values for CGCM2 A2 & B2, HADCM3 A2 & B2, and CSIRO A2 & B2 for the period of 2041-2070 are presented in Figure 99 to Figure 116.

Figure 99 to Figure 101 present predicted factor scores for principal components 1 through 3 based on CGCM2 A2. The general pattern of PC1 factor scores indicates that growth potential increases from north to south (Figure 99). The contours indicate a similar area of adaptive similarity between the northwest and the southern region as is demonstrated by the 1961-1990 climate normals (Figure 3). A similar area of reduced growth potential stretching north from the shore of Lake Superior is also evident. Growth potential across the range is predicted to be greater than for 1961-1990, due to the increase in September maximum temperature (APPENDIX I). However, the rate of increase is not constant because some areas experience greater warming than others. The range of PC1 factor scores predicted based on CGCM2 A2 is relatively greater than that predicted based on 1961-1990 climate normals, likely due to the increased variability of September maximum temperature values and changes in August precipitation patterns.

Similar to PC1, the grid of predicted factor scores for CGCM2 A2 indicates that factor scores increase from north to south (Figure 100). This pattern indicates that

southern sources continue to be the latest to flush in the spring and to set bud in the fall. However, intermediate to high factor scores in the northwest region indicate that phenological timing is similar in this region as in the Ottawa Valley. The grid of predicted factor scores based on CGCM2 A2 for 2041-2070 is surprisingly similar to that of 1961-1990 observed normals (Figure 4). Geographic patterns of adaptive variation are incredibly similar. However, the CGCM2 A2 grid indicates an increase in factor scores across the range and that the area of similarity between the northwest and Ottawa Valley area is relatively greater. Also, the area of near-minimum factor scores along the north shore of Lake Superior no longer encompasses the entire area of Lake Nipigon.

The contours of predicted factor scores for PC3 based on CGCM2 A2 show a strong latitudinal trend of increase from north to south (Figure 101). The range of predicted factor scores is very broad, ranging from -2.69 in the far north to 4.52 in the extreme southernmost corner of the province. In contrast to PC1 and PC2, factor scores for PC3 in the area immediately surrounding Lake Nipigon are relatively high. In comparison to predicted factor scores based on 1961-1990 normals (Figure 5), the CGCM2 A2 grid shows a much greater range in predicted factor scores, likely due to the increased variability of April maximum temperature and changes in June maximum temperature patterns (APPENDIX I). The area of minimum factor scores in the far north is also much broader based on CGCM2 A2.

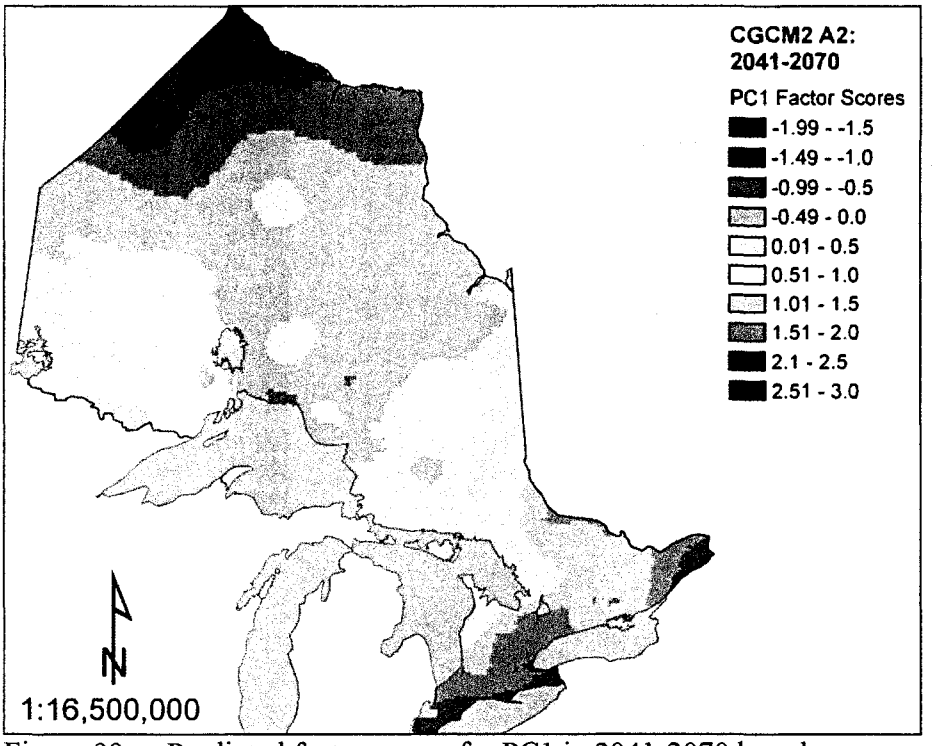

Figure 99. Predicted factor scores for PC1 in 2041-2070 based on CGCM2 A2.

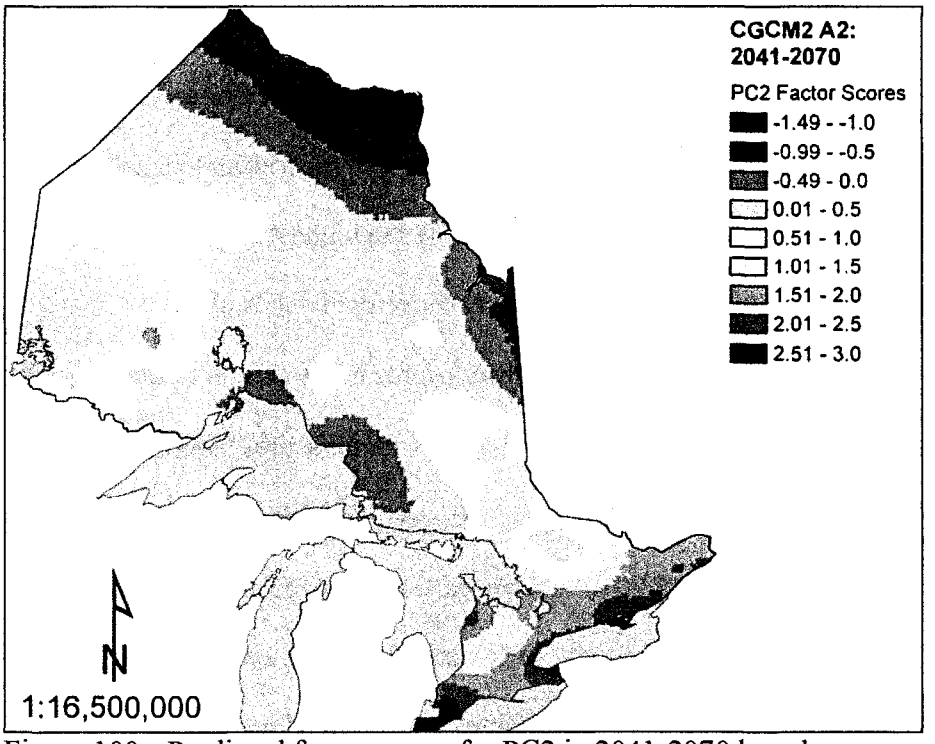

Figure 100. Predicted factor scores for PC2 in 2041-2070 based on CGCM2 A2.

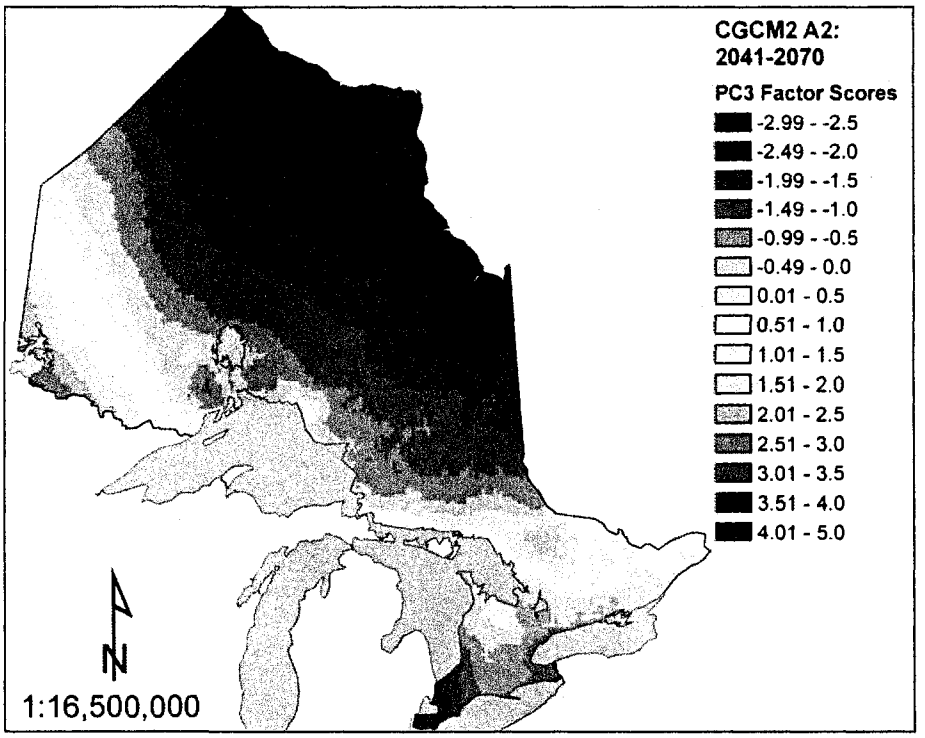

Figure 101. Predicted factor scores for PC3 in 2041-2070 based on CGCM2 A2.

Figure 102 to Figure 104 present predicted factor scores for principal components 1 through 3 based on CGCM2 B2. Predicted factor scores for PC1 indicate a general latitudinal trend of increasing factor scores from north to south, indicating that northwestern and southern sources demonstrate the highest growth potential (Figure 102). Interestingly, the contours indicate two circular islands of relatively high factor scores, and a small irregular island of lower scores in the central to mid-northern latitudes of the province. In comparison to PC1 factor scores based on 1961-1990 normals (Figure 3), the CMCM2 B2 grid indicates that growth potential is greater across the entire province for 2041-2070. However, the area of relatively low factor scores (i.e. -0.49 to 0.0) expands into the more central latitudes of the province instead of being mostly confined to the north. This variation in patterns of growth potential is likely due

to large differences in August precipitation patterns between 1961-1990 and the CGCM2 B2 estimate for 2041-2070 (APPENDIX I).

The contours of predicted factor scores for PC2 based on CGCM2 B2 show a general trend of increase from north to south (Figure 103). Areas of high factor scores in both the northwest and Ottawa Valley area indicate that these sources have similar phenological timing. The band of relatively low scores to the north of Lake Superior indicates that these areas have relatively early dates of budburst and budset. In comparison to predicted factor scores based on 1961-1990 normals (Figure 4), the CGCM2 B2 grid shows increased factor scores across most of the range. Otherwise, the geographic patterns are quite similar.

The grid of predicted factor scores for PC3 indicates a strong latitudinal pattern of increase from north to south (Figure 104). In comparison to the 1961-1990 grid (Figure 5), the CGCM2 B2 grid indicates that the pattern of early greenhouse elongation is much more variable and that factor scores are generally higher across the range. Also, contours across the north are relatively broad, indicating that similar factor scores are achieved over greater latitudinal distances.

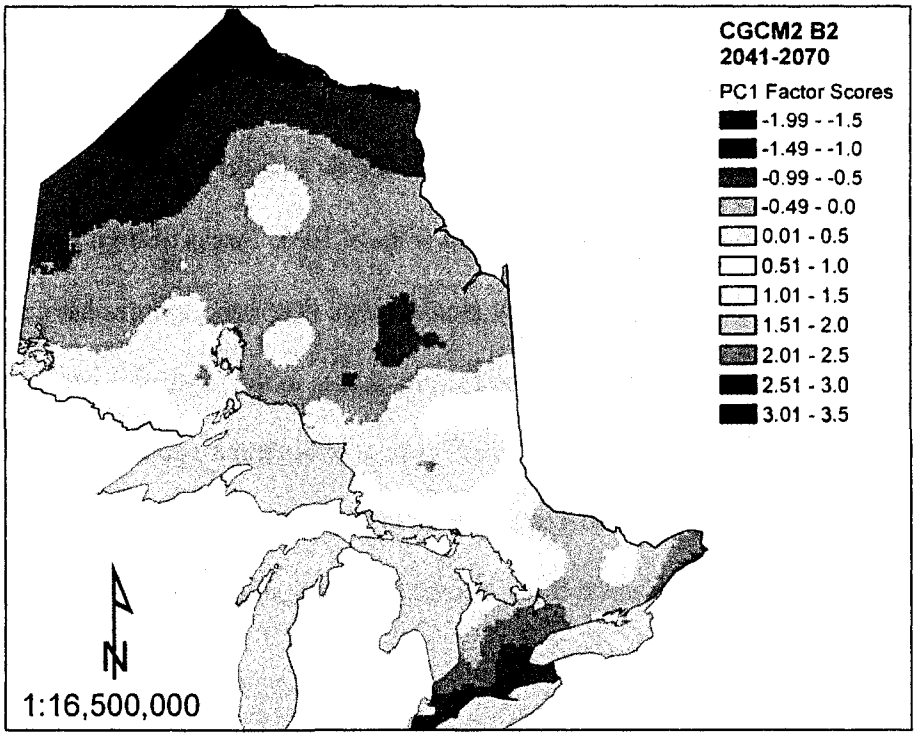

Figure 102. Predicted factor scores for PC1 in 2041-2070 based on CGCM2 B2.

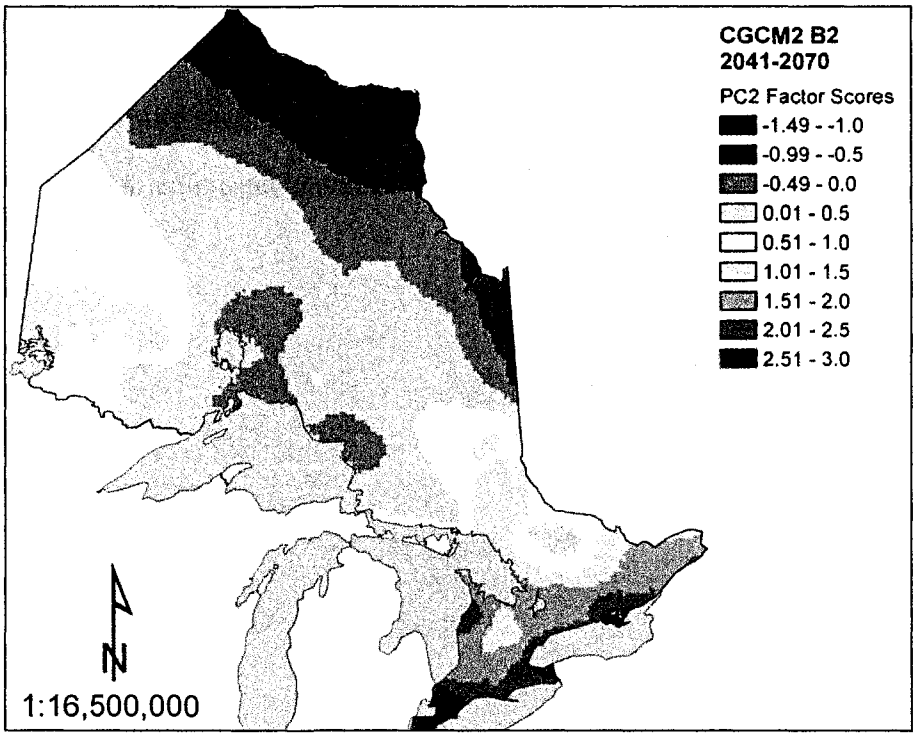

Figure 103. Predicted factor scores for PC2 in 2041-2070 based on CGCM2 B2.

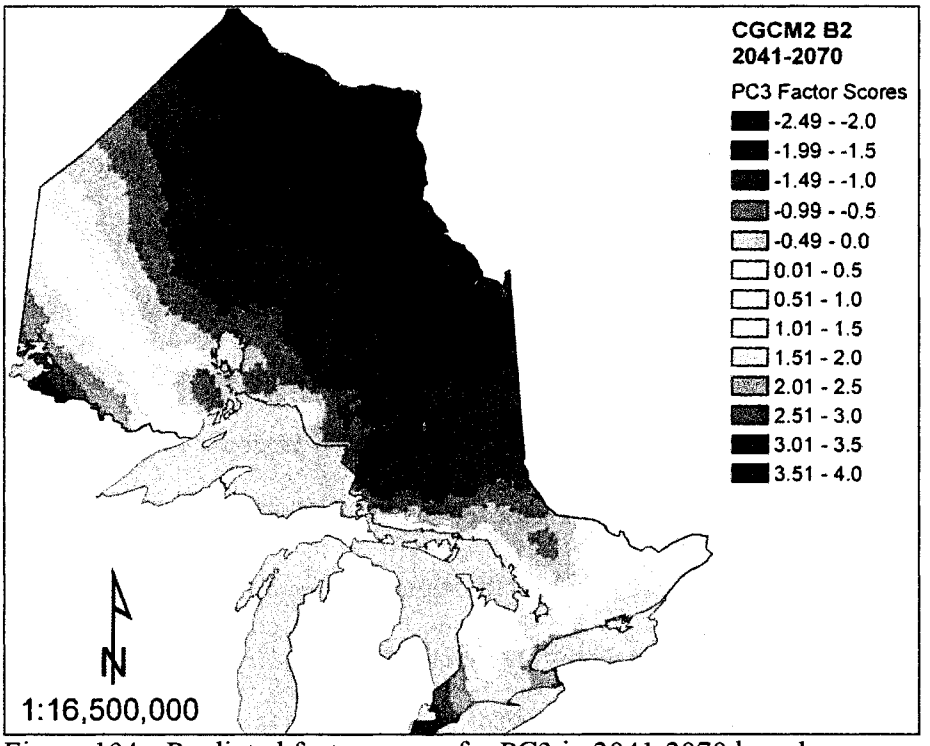

Figure 104. Predicted factor scores for PC3 in 2041-2070 based on CGCM2 B2.

Figure 105 to Figure 107 present predicted factor scores for principal components 1 through 3 based on HADCM3 A2. The contours of predicted factor scores for PC1 show a general trend of increase from north to south (Figure 105). Factor scores for the northwest and southern regions indicate that growth potential is similar for these areas. Contours are irregular in the central latitudes of the province, and demonstrate no clear latitudinal or longitudinal trend; values are highest to the west along the Manitoba border and to the east along the Quebec border. An island of relatively low factor scores is present in this area and another along the north shore of Lake Superior. PC1 factor scores are higher than 1961-1990, ranging from -1.99 to 3.0 SD compared to -2.99 to 2.0 SD. The slight differences between patterns of PC1 factor scores between HADCM3

1950 and 1961-1990 are likely related to changes in the pattern of August precipitation (APPENDIX I).

Patterns of variation in PC2 factor scores for HADCM3 A2 (Figure 106) are generally consistent with those indicated by 1961-1990 climate normals (Figure 4). Factor scores generally increase from north to south, except for along the north shore of Lake Superior where they decrease towards the central latitudes of the province due to the lakeshore effect. However, this effect is much more pronounced for the HADCM3 A2 grid than for 1961-1990. Also, factor scores for 2041-2070 based on HADCM3 A2 are approximately 0.5 SD higher across the range than for 1961-1990.

Predicted PC3 factor scores based on HADCM3 A2 show a general trend of increase from north to south (Figure 107). The exception is once again the area to the north of Lake Superior which shows increasing factor scores with increasing distance from the lakeshore. Another area in the south, stretching from Georgian Bay nearly due south to Lake Erie, also indicates an area of relatively low factor scores. Adaptive similarity between the northwest and southern region is indicated by similar PC3 factor scores. Predicted factor scores based on HADCM3 A2 are similar to those based on 1961-1990 climate normals (Figure 5), but vary somewhat less across the range. Patterns are generally similar between the two grids, except that HADCM3 A2 indicates a relatively wide contour of low factor scores that bulges into the central latitudes of the province from the north.

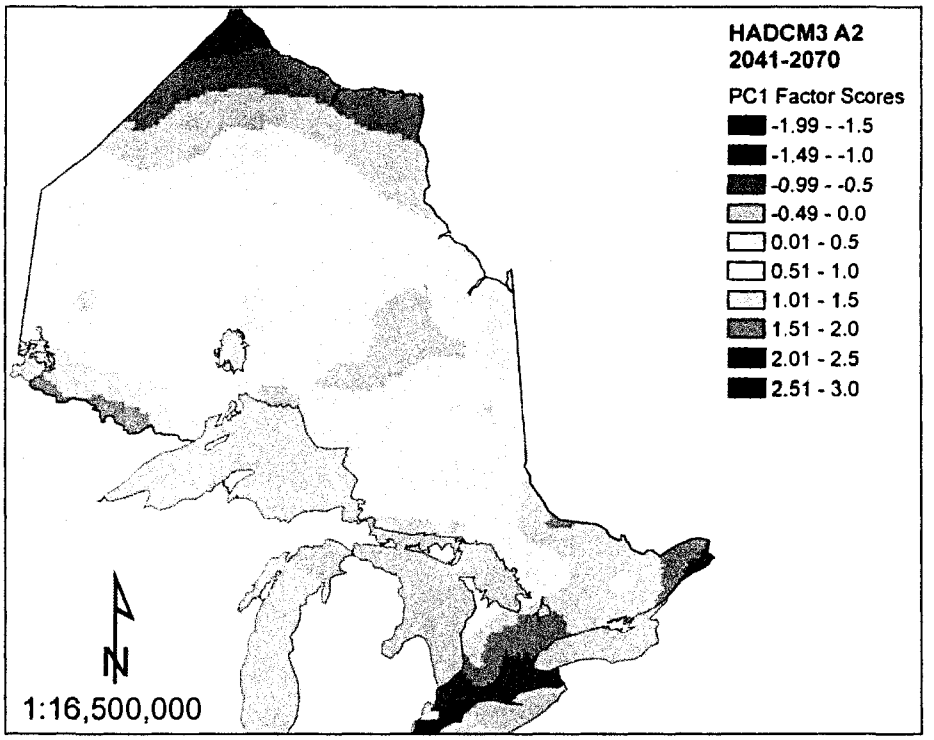

Figure 105. Predicted factor scores for PC1 in 2041-2070 based on HADCM3 A2.

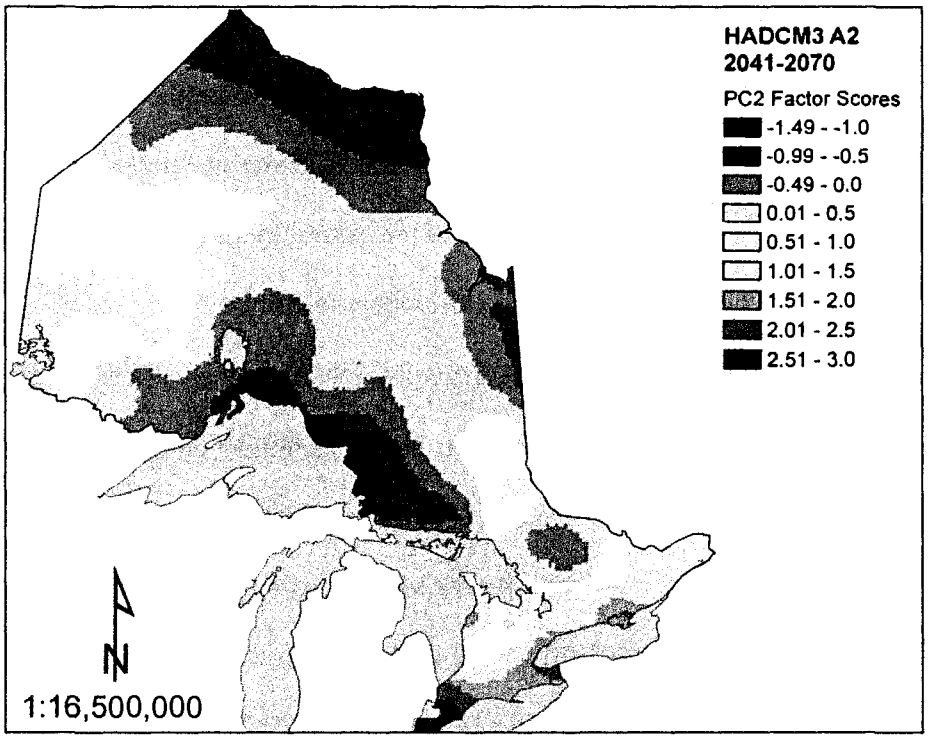

Figure 106. Predicted factor scores for PC2 in 2041-2070 based on HADCM3 A2.

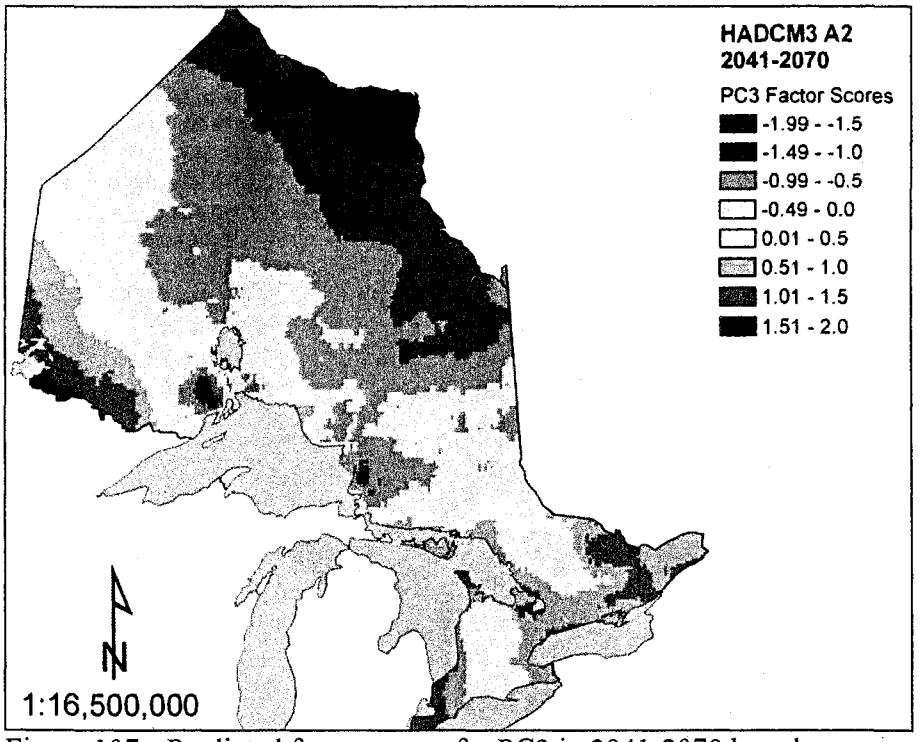

Figure 107. Predicted factor scores for PC3 in 2041-2070 based on HADCM3 A2.

Figure 108 to Figure 110 present predicted factor scores for principal components 1 through 3 based on HADCM3 B2. Contours of predicted factor scores for PC1 indicate mixed latitudinal and longitudinal trends; scores generally increase from north to south but also increase outwards from the central longitudes towards the western and eastern borders (Figure 108). Growth potential is at a minimum in the north of the province and greatest in the northwest and southern regions. The strong east-west trend in the central latitudes of the province is inconsistent with contours of predicted factor scores based on 1961-1990 normals (Figure 3), which show only a weak trend. Also, the variability in predicted factor scores across the range is considerably lower based on HADCM3 B2 than for 1961-1990. Differences are likely the result of varying patterns of January and August precipitation based on HADCM3 B2 and 1961-1990 normals (APPENDIX I) .

Similar to the HADCM3 A2 scenario, patterns of variation in PC2 factor scores for HADCM3 B2 (Figure 109) are generally consistent with those indicated by 1961-1990 climate normals (Figure 4). Factor scores tend to increase from north to south, indicating that southern areas have the latest phenological timing. The area of adaptive similarity between the northwest and Ottawa Valley area is again evident, as is the band of low factor scores to the north of Lake Superior. Factor scores for HADCM3 B2 show a slight increase across the range in comparison to 1961-1990.

Predicted factor scores for PC3 based on HADCM3 B2 indicate minimum factor scores in the far north and intermediate to high scores in the south and northwest (Figure 110). Relatively low factor scores extend further into the central latitudes from the north based on HADCM3 B2 than on 1961-1990 normals (Figure 5). Also the HADCM3 B2 grid indicates lower variability, but higher average factor scores across the range.

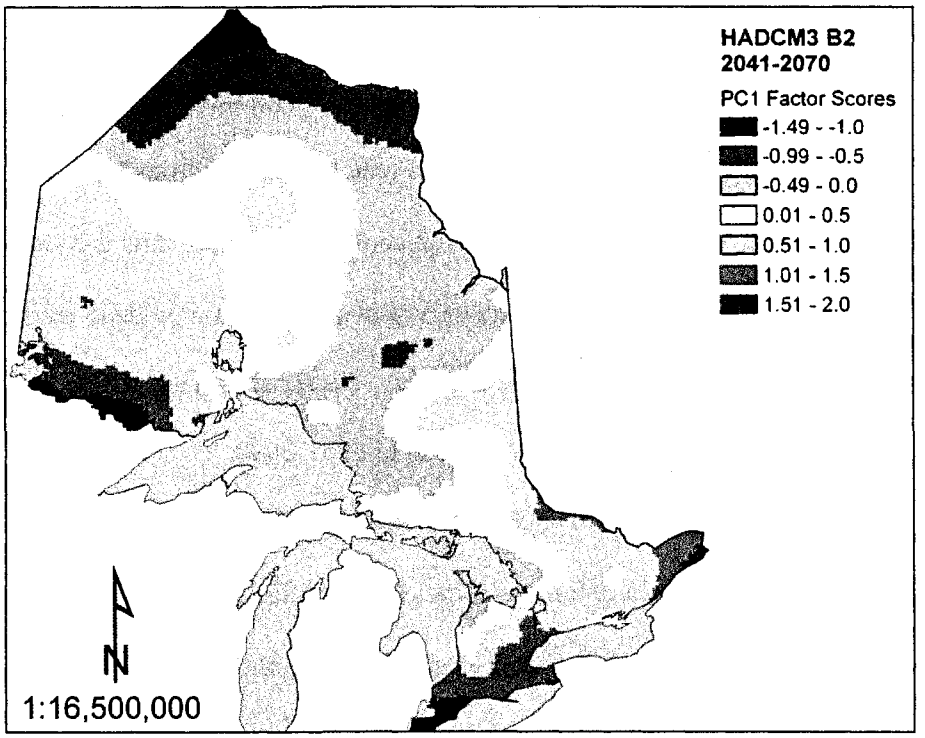

Figure 108. Predicted factor scores for PC1 in 2041-2070 based on HADCM3 B2.

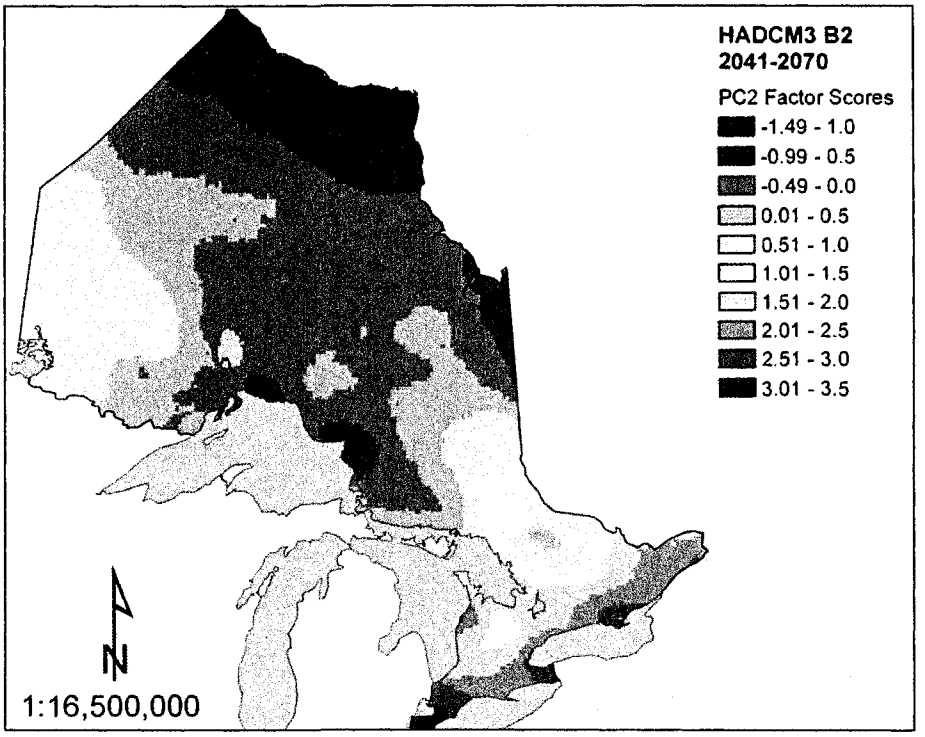

Figure 109. Predicted factor scores for PC2 in 2041-2070 based on HADCM3 B2.

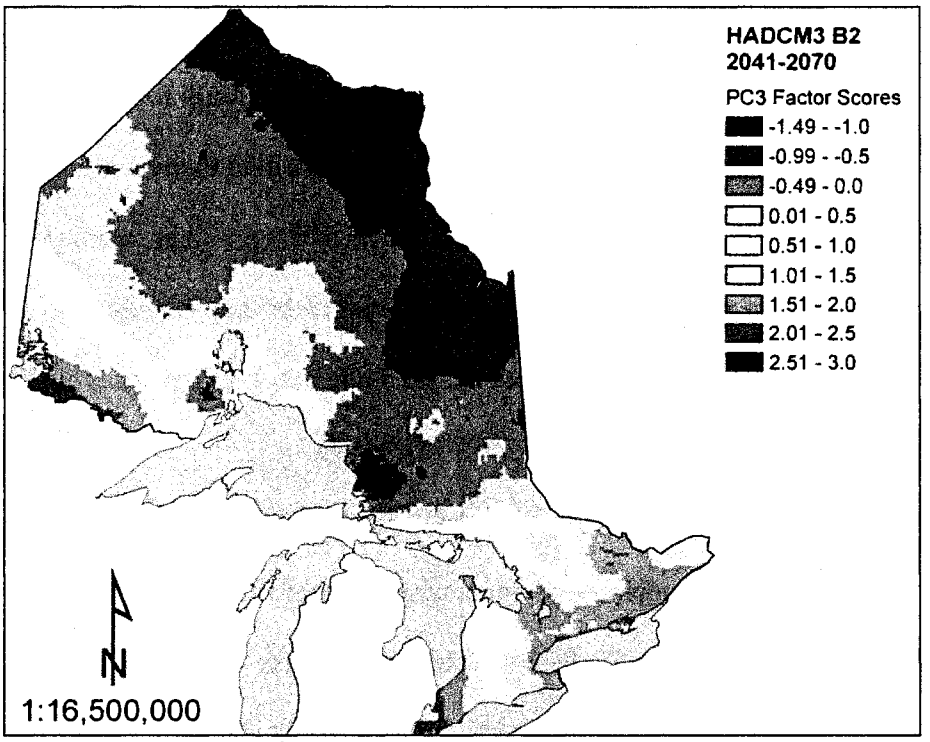

Figure 110. Predicted factor scores for PC3 in 2041-2070 based on HADCM3 B2.

Figure 111 to Figure 113 present predicted factor scores for principal components 1 through 3 based on CSIRO A2. For PC1, factor scores are predicted to increase from north to south (Figure 111). In comparison to factor scores based on 1961-1990 climate normals (Figure 3), scores based on CSIRO A2 do not indicate high growth potential in the northwest. Rather growth potential in the northwest is predicted to be similar to the lower latitudes of the northeast. Also, areas of intermediate to high factor scores in the northwest do not extend as far northward. The area of relatively low factor scores along the shore of Lake Superior extends northward to become continuous with a latitudinal contour in the mid-north. Growth potential is somewhat more variable and generally higher in 2041-2070 for CSIRO A2 than based on 1961-1990 normals.

Predicted factor scores for PC2 show a mixture of latitudinal and longitudinal patterns (Figure 112). Factor scores generally increase from north to south, indicating that budflush and budset occur later for southern latitudes than in the north. A contrasting pattern is apparent in the central latitudes of the province, which indicates that factor scores are at a minimum in the central longitudes intersecting Lake Nipigon and increase outward to the Manitoba and Quebec borders. This pattern is similar for the CSIRO A2 grid in comparison to 1961-1990 (Figure 4).

PC3 factor scores based on CSIRO A2 (Figure 113) show much stronger latitudinal demarcation of adjacent contours when compared to contours based on 1961-1990 climate normals (Figure 5). Factor scores show a clear latitudinal trend of increase from north to south, except in the far south which indicates intermediate factor scores. Scores are at a minimum in the far north adjacent to Hudson Bay and a maximum in the northwest. Adaptive similarity is evident between much of the northwest, northeast, and Ottawa Valley area of the south. Factor scores are generally greater across the range for 2041-2070 than for 1961-1990.

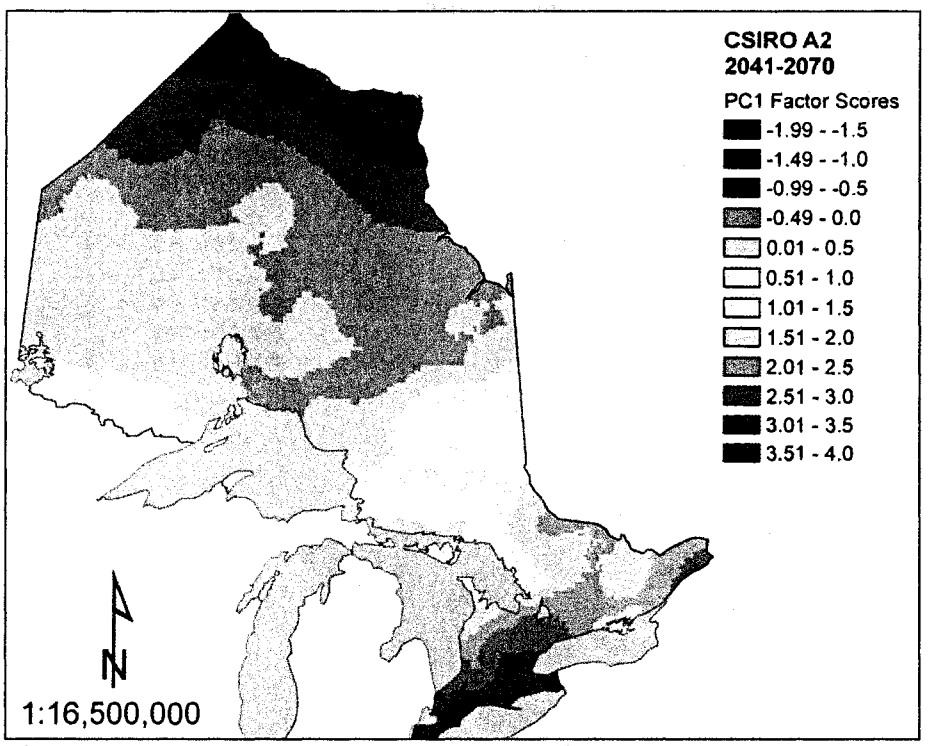

Figure 111. Predicted factor scores for PC1 in 2041-2070 based on CSIRO A2.

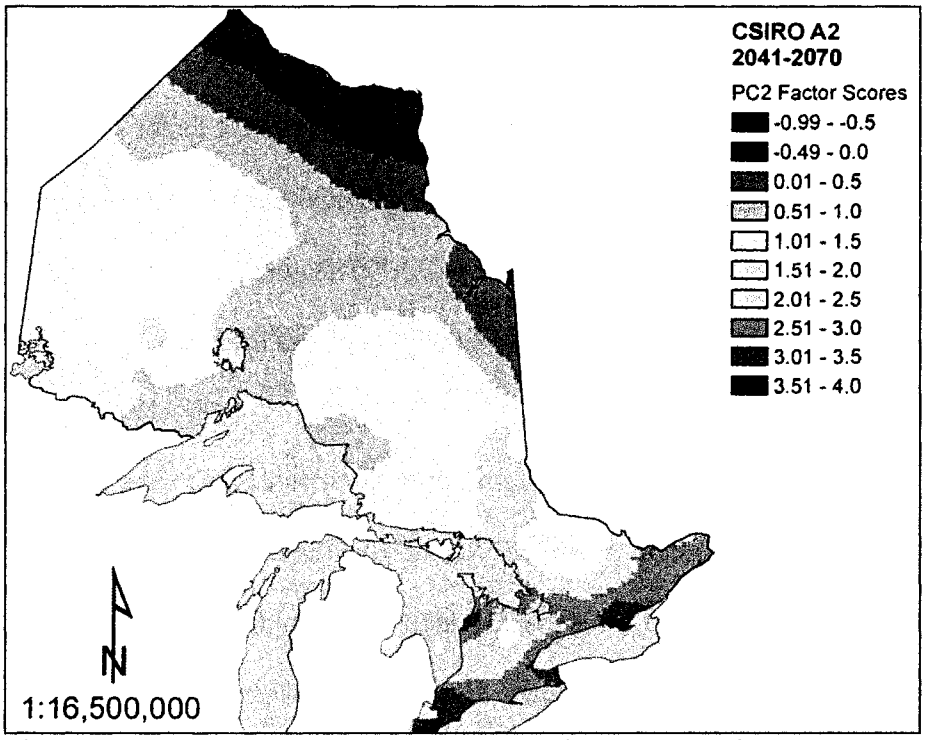

Figure 112. Predicted factor scores for PC2 in 2041-2070 based on CSIRO A2.

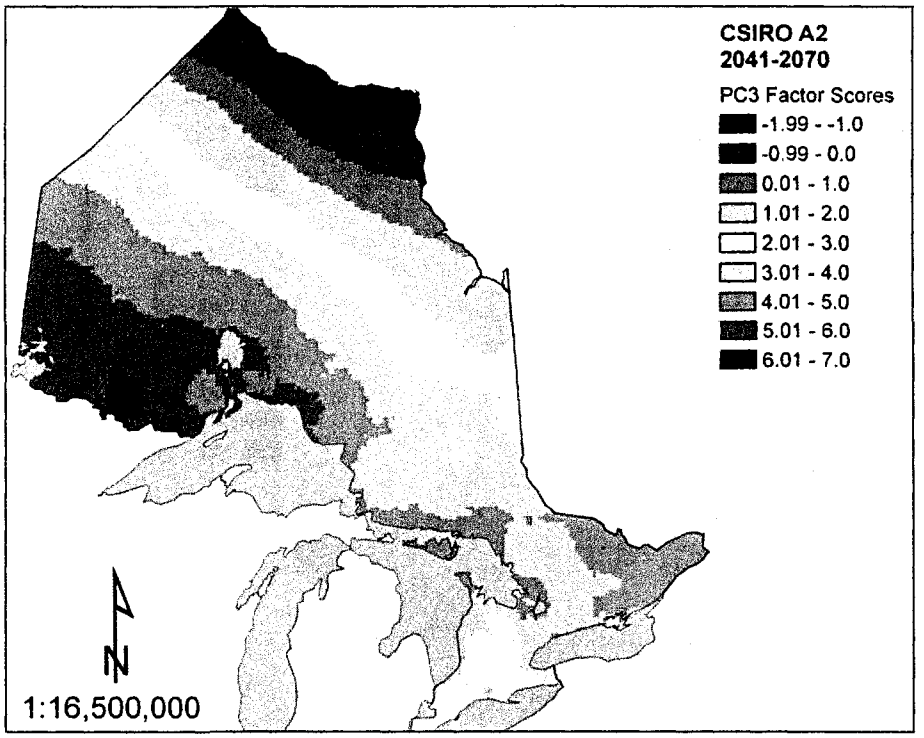

Figure 113. Predicted factor scores for PC3 in 2041-2070 based on CSIRO A2.

Figure 114 to Figure 116 present predicted factor scores for principal components 1 through 3 based on CSIRO B2. Contours of PC1 factor scores are generally broad and show an increase in growth potential from north to south (Figure 114). In contrast to PC1 factor scores for 1961-1990 (Figure 3), scores based on CSIRO B2 are much more variable and are generally higher across the range. Otherwise, patterns are quite similar.

Contours of predicted PC2 factor scores based on CSIRO B2 (Figure 115) are generally quite similar to those based on 1961-1990 climate normals (Figure 4). Contours generally increase from north to south, indicating that northern sources have the earliest dates of budflush and budset. However, the effect of the lakeshore is evident in an area of relatively low factor scores occurring along the north shore of Lake

Superior. Factor scores are similar between northwestern Ontario and the Ottawa Valley area. In comparison to the 1961-1990 PC2 grid, factor scores are generally somewhat higher based on CSIRO B2.

Predicted PC3 factor scores for CSIRO B2 in 2041-2070 (Figure 116) are relatively greater and much more variable than those for 1961-1990 (Figure 5). Scores increase rapidly from north to south; however, an area of intermediate factor scores is evident in the far southeastern corner of the province. In contrast to the 1961-1990 grid that indicates that northwestern Ontario and the Ottawa Valley are adaptively similar, the CSIRO B2 grid indicates that growth potential is somewhat greater in the northwest. Scores range from -2.0 to 6.0 SD across the grid in comparison to -3.0 to 2.5 SD for 1961-1990.

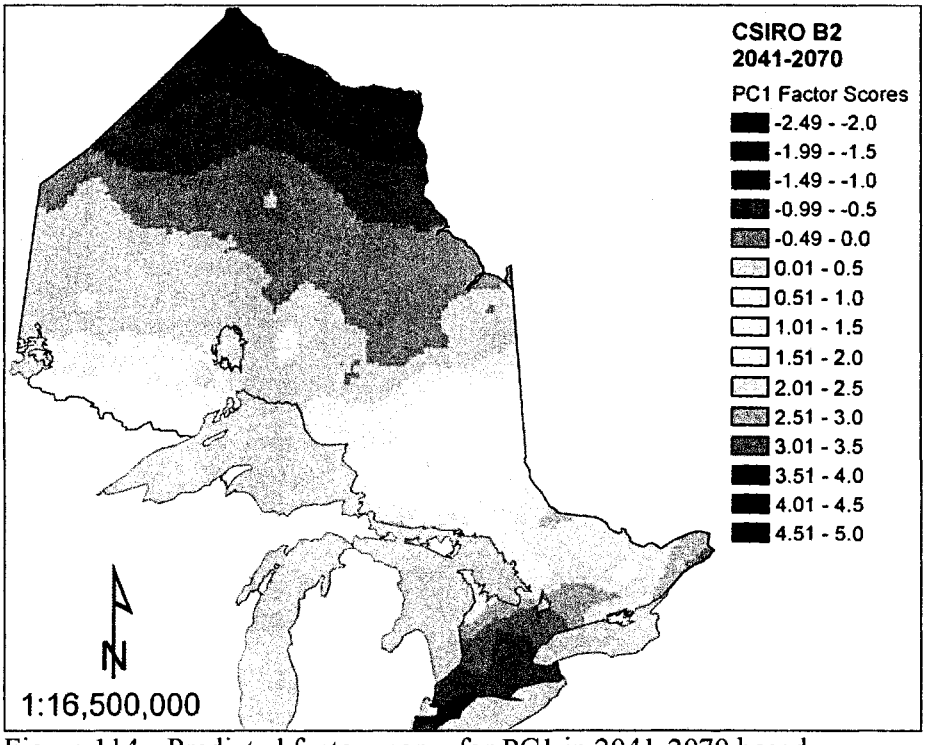

Figure 114. Predicted factor scores for PC1 in 2041-2070 based on CSIRO B2.

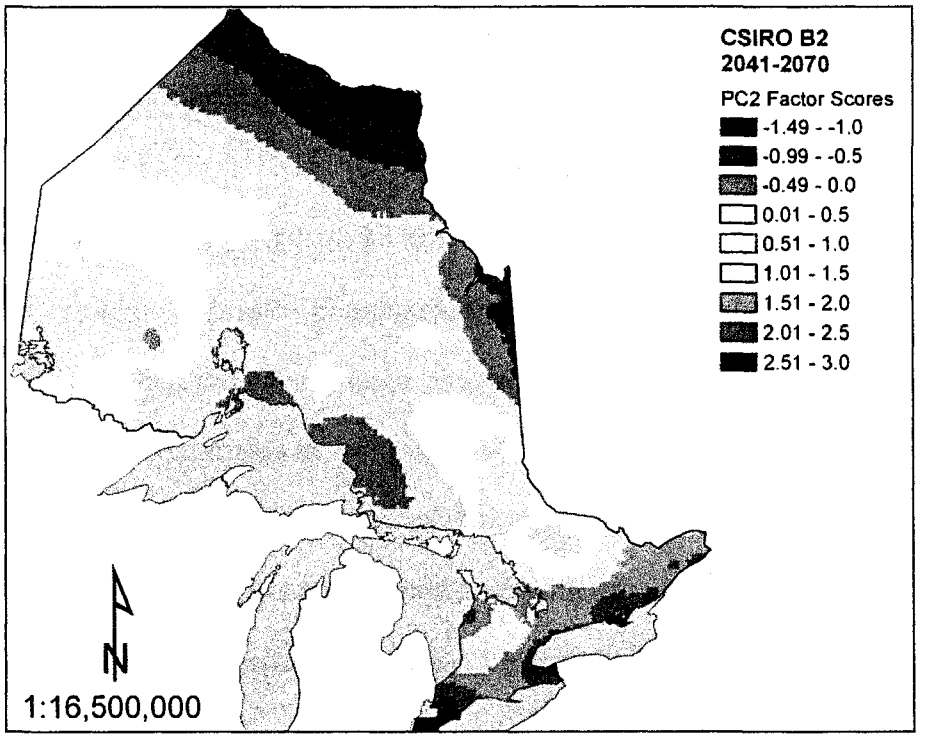

Figure 115. Predicted factor scores for PC2 in 2041-2070 based on CSIRO B2.

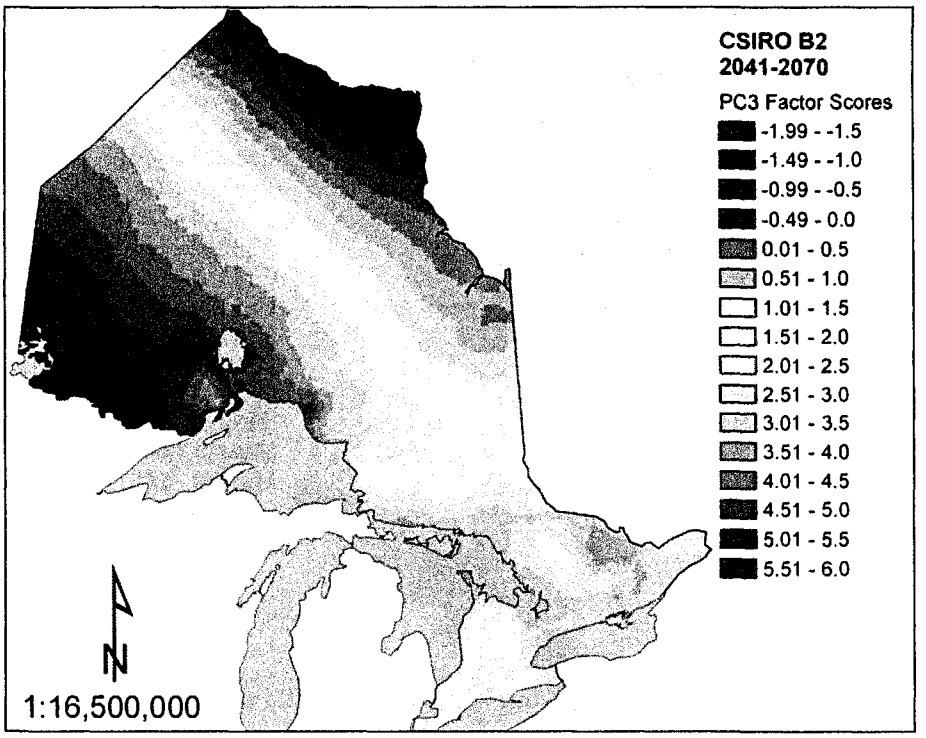

Figure 116. Predicted factor scores for PC3 in 2041-2070 based on CSIRO B2.

FOCAL POINT SEED ZONE EXAMPLES FOR 2041-2070

Four examples of the 618 focal point seed zones constructed for Ontario are presented for each of the six future climate scenarios for 2041-2070. These examples are presented in Figure 117 to Figure 140 for CGCM2 A2 & B2, HADCM3 A2 & B2, and CSIRO A2 & B2, respectively. All zones are based on the 1.0 LSD level of adaptive similarity. The same four focal points presented as past seed zone examples (Figure 66 to Figure 81) were used to allow comparison between past, current, and future climate scenarios.

Figure 117 to Figure 120 present the four seed zone examples for the CGCM2 A2 scenario for 2041-2070. The seed zone for focal point 345 indicates a large area of adaptive similarity in the central latitudes of the province and runs from the Manitoba border southeast to the Sault Ste. Marie and Sudbury districts (Figure 117). It spans approximately 3° latitude at its widest point.

Areas of adaptive similarity for focal point 325 in the northeast occur in a very broad latitudinal band (~ 4°) that stretches northwest from the shore of James Bay (Figure 118). The seed zone also spans a wide range of longitudes; from 81°W to 91°W.

The seed zone for focal point 336 indicates that areas in both the northwest and the east are adaptively similar (Figure 119). The northwest area is a very narrow, semi-latitudinal zone which runs southeastward from the Manitoba border. The eastern area is also quite latitudinally-restricted and occupies an area along the north shore of Georgian Bay and another occupying the whole of Manitoulin Island.

The seed zone for focal point 584 in the far north indicates that areas of adaptive similarity are located along the shore of Hudson Bay (Figure 120). The zone

extends east from the Manitoba border to the shore of James Bay and spans approximately 2° latitude.

The seed zones constructed for the four focal points for 2041-2070 based on CGCM2 A2 bear striking similarity to the 1961-1990 zones for the same points. The zone for focal point 345 is very similar in size, shape and location to the 1961-1990 zone, except that it does not include the area surrounding Lake Nipigon and along the north shore. The seed zone for focal point 325 is also quite similar, but does not extend as far westward. Of the four examples, the seed zone for focal point 336 bears the least similarity to its analogous 1961-1990 zone. The northwest portion is much smaller in comparison to the 1961-1990 1.0 LSD zone; however, it is quite similar to the 0.5 LSD zone. Finally, the CGCM2 A2 and 1961-1990 seed zones for focal point 584 bear virtually no discernable differences.

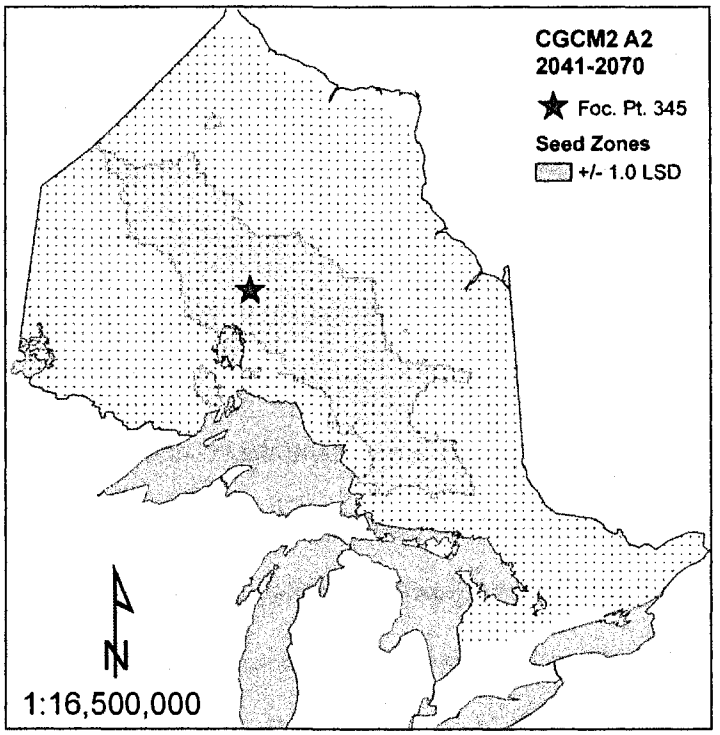

Figure 117. Seed zones for focal point 345, based on CCGM2 A2 for the period 2041-2070.

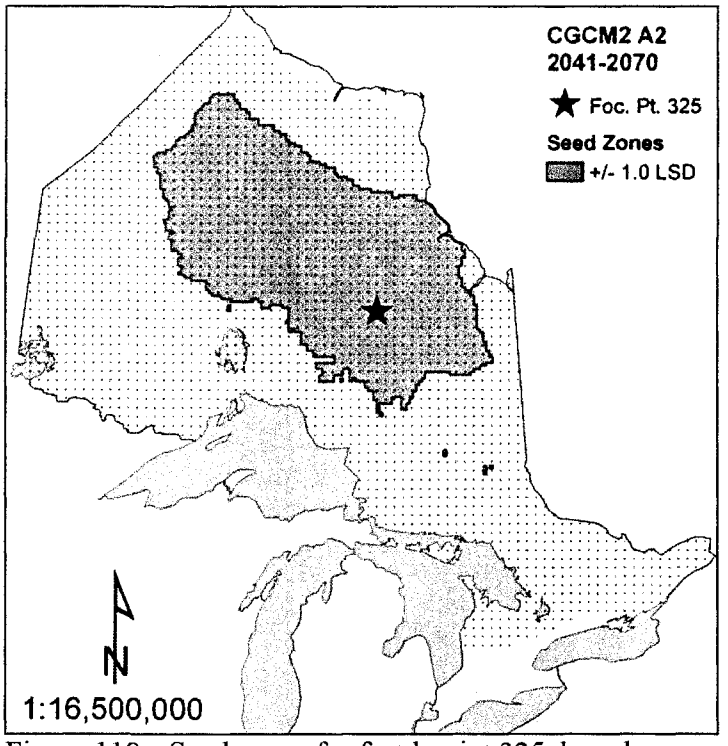

Figure 118. Seed zones for focal point 325, based on CCGM2 A2 for the period 2041-2070.

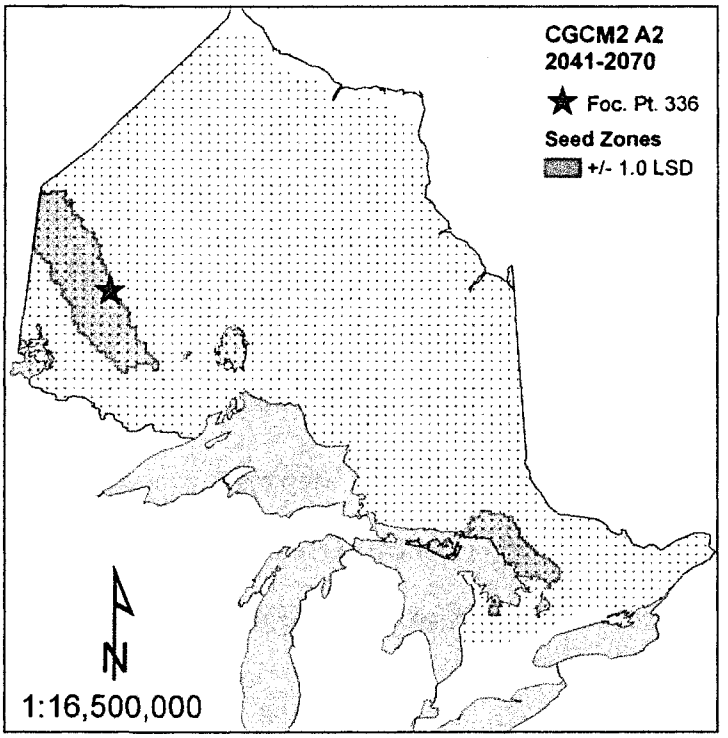

Figure 119. Seed zones for focal point 336, based on CCGM2 A2 for the period 2041-2070.

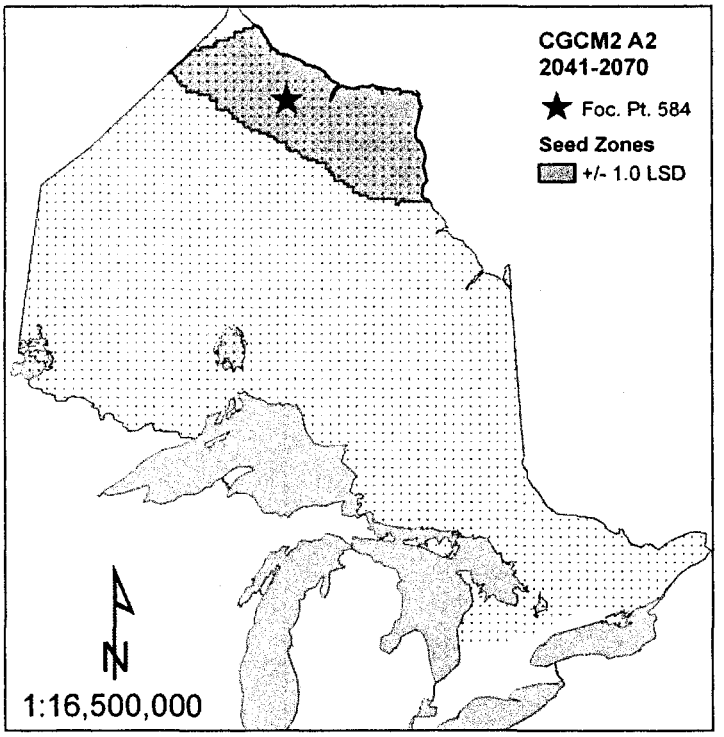

Figure 120. Seed zones for focal point 584, based on CCGM2 A2 for the period 2041-2070.

Figure 121 to Figure 124 present the four seed zone examples based on the CGCM2 B2 scenario for 2041-2070. The seed zone for focal point 345 occupies a large area in the center of the province but excludes several areas along the north shore of Lake Superior (Figure 121). It is similar but somewhat broader and more irregularly shaped in comparison to the zone constructed for the A2 scenario.

The area of adaptive similarity for focal point 325 occupies a broad zone in the center of the province, extending approximately 4° northward from the area just north of Lake Nipigon (Figure 122). It is virtually identical to the CGCM2 A2 zone, except for a small uncovered island within its boundaries and the inclusion of a small disjunct area to the southeast.

The seed zone for focal point 336 is also very similar to its analogous A2 zone, but excludes the area of similarity to the east (Figure 123). However the northwestern portions of the zones are virtually indistinguishable between the A2 and B2 scenarios.

The seed zones constructed for focal point 584 are nearly identical between the CGCM2 A2 and B2 scenarios, except that the B2 seed zone indicates a second, disjunct area of similarity along the shore of James Bay and the Quebec border (Figure 124).

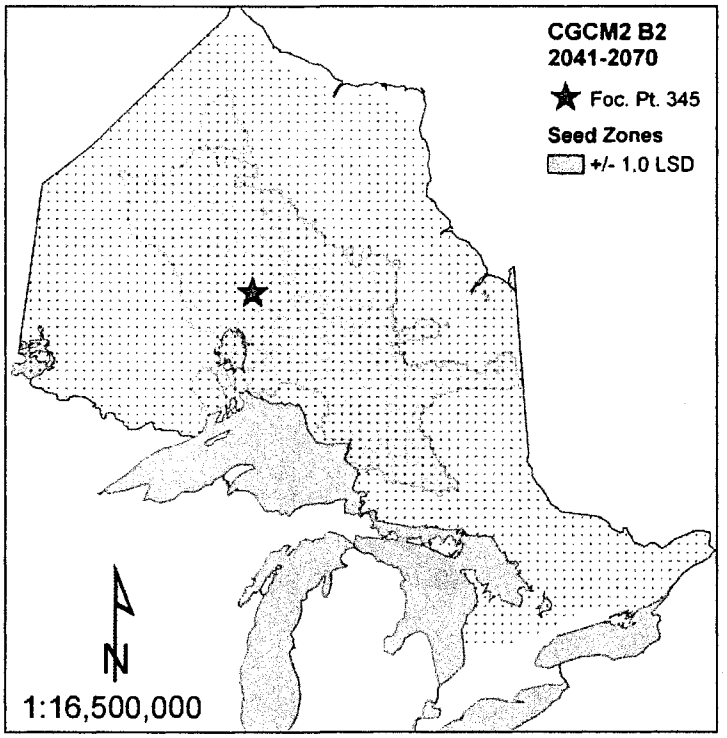

Figure 121. Seed zones for focal point 345, based on CCGM2 B2 for the period 2041-2070.

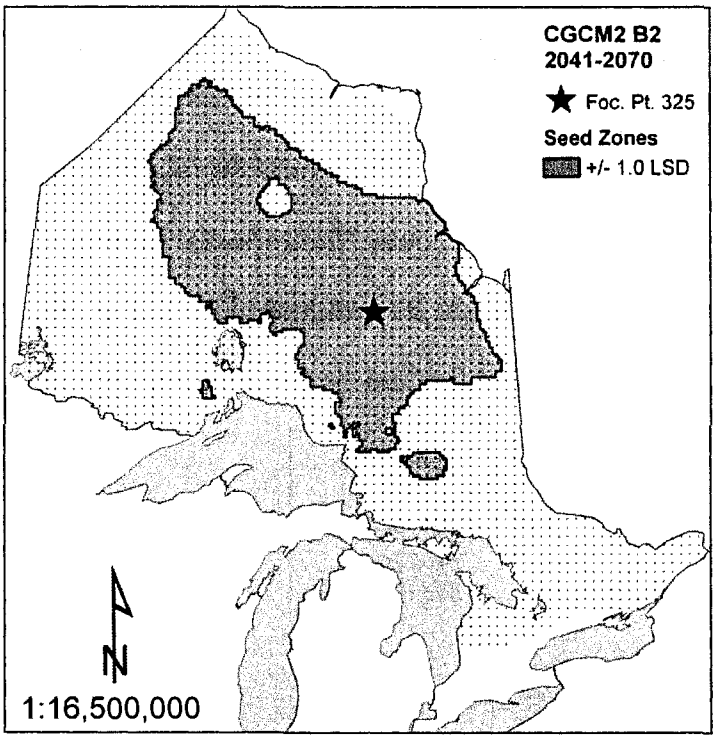

Figure 122. Seed zones for focal point 325, based on CCGM2 B2 for the period 2041-2070.

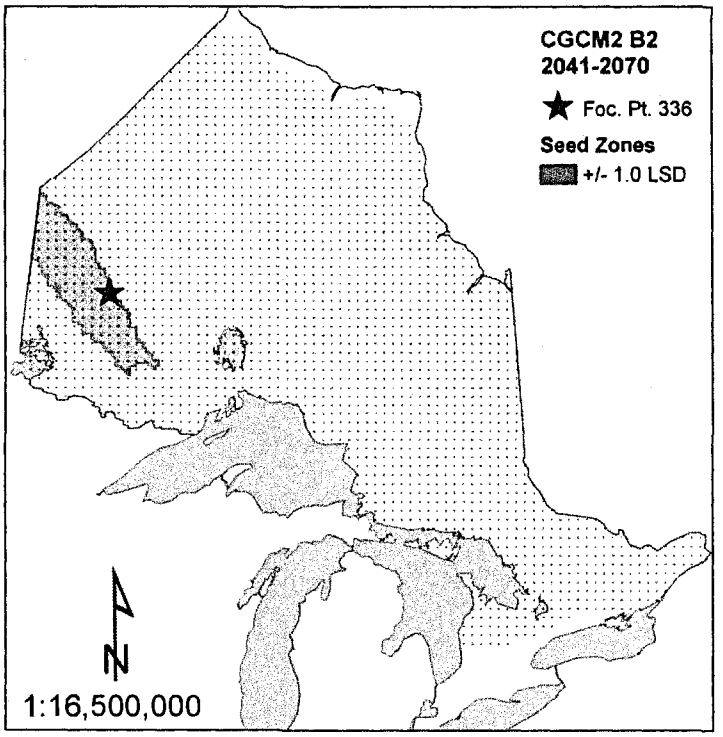

Figure 123. Seed zones for focal point 336, based on CGCM2 B2 for the period 2041-2070.

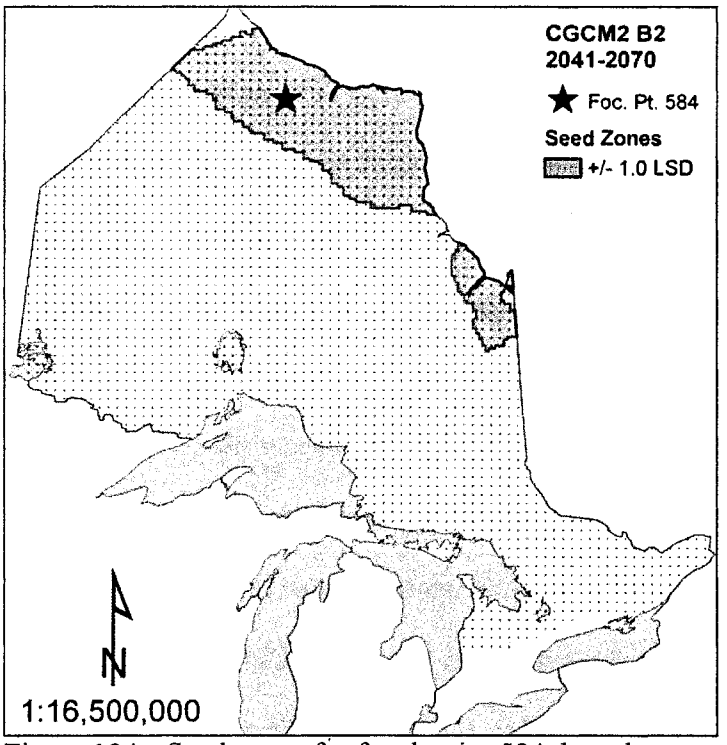

Figure 124. Seed zones for focal point 584, based on CGCM2 B2 for the period 2041-2070.

Figure 125 to Figure 128 present the four seed zone examples based on the HADCM3 A2 scenario for 2041-2070. The seed zone for focal point 345 occupies a very large, irregularly shaped area in the central latitudes of the province (Figure 125). This zone extends across the full width of the province; from the Manitoba border at 53°N, east to the Quebec border at 49°N. The area along the north shore of Lake Superior is conspicuously excluded; however, the area surrounding Lake Nipigon is included. Several much smaller, discontinuous areas of similarity occur in the east.

The seed zone for focal point 325 occupies another very large, irregularly shaped zone in the central latitudes of the province (Figure 126). However, it is somewhat broader than that of the previous focal point. This zone extends from James

Bay west to the Manitoba border along its northern boundary and from the northwestern shore of Lake Nipigon to the Chapleau and Timmins districts on its southern boundary.

The seed zone for focal point 336 indicates areas of adaptive similarity in the northwest, northeast, and southern regions of the province (Figure 127). A single large zone is located in the northwest surrounding the focal point, while several smaller areas occupy the eastern and southern portions of the province.

The seed zone for focal point 584 indicates areas of adaptive similarity in the far north (Figure 128). A moderately large latitudinal zone runs along the shore of Hudson Bay encompassing the focal point, while a second much smaller area of similarity is present along the shore of James Bay to the south.

Seed zones constructed based on HADCM3 A2 bear broad similarity to the analogous zones constructed for 1961-1990 (Figure 6 to Figure 11). The HADCM3 A2 zones are generally similar in size and location to the 1961-1990 zones, but are more irregularly shaped. For example, the seed zone for focal point 345 would be very similar to the 1961-1990 zone were it not for a peninsular protrusion along the northwestern boundary and another along the southeastern edge of the zone. Similarly, the seed zone for focal point 325 resembles the 1961-1990 zone, except for a deep lobe along the southern boundary and a protrusion into the northeast. The HADCM3 A2 zone is also somewhat broader in the east than the 1961-1990 zone. In comparison to 1961-1990, the seed zone for focal point 336 is more fragmented in the east and extends further southward, while the seed zone for focal point 584 includes a small discontinuous area along the shore of James Bay.

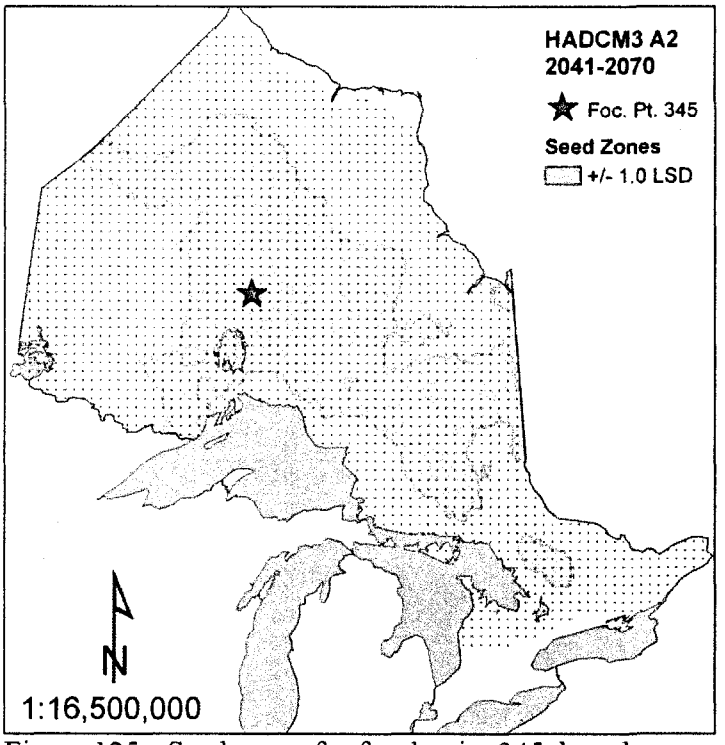

Figure 125. Seed zones for focal point 345, based on HADCM3 A2 for the period 2041-2070.

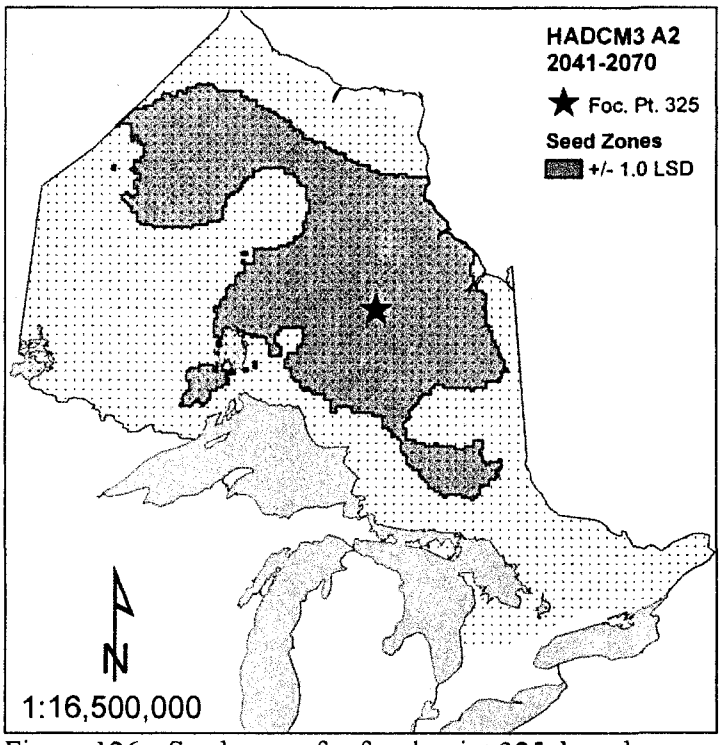

Figure 126. Seed zones for focal point 325, based on HADCM3 A2 for the period 2041-2070.

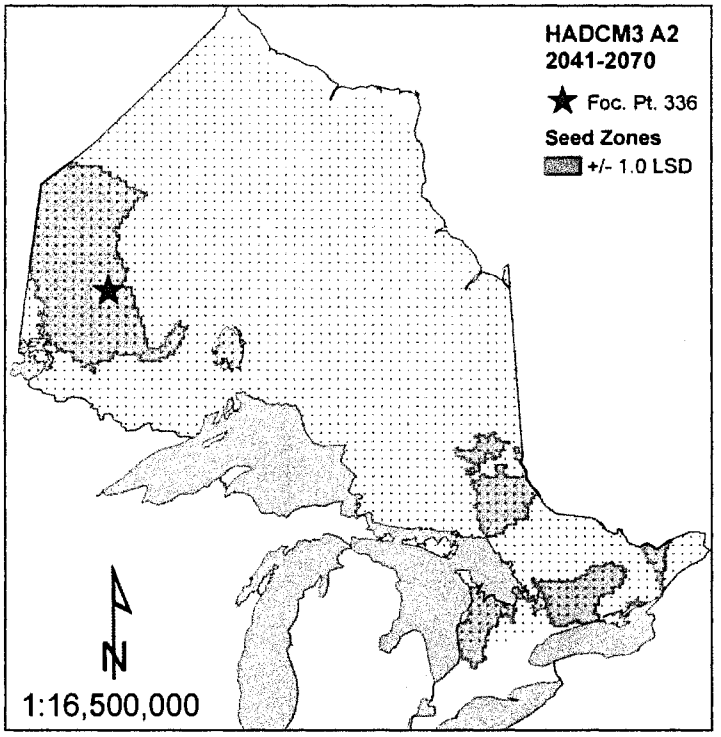

Figure 127. Seed zones for focal point 336, based on HADCM3 A2 for the period 2041-2070.

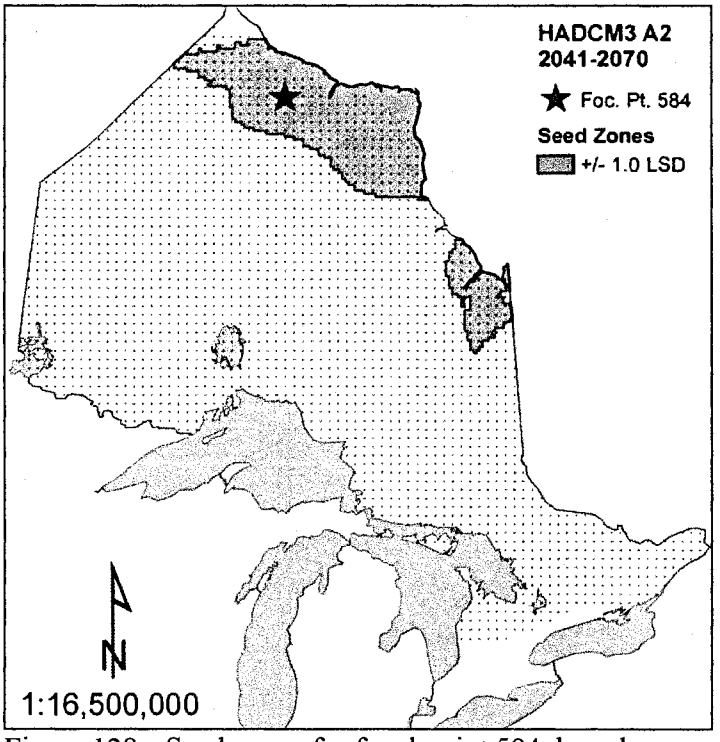

Figure 128. Seed zones for focal point 584, based on HADCM3 A2 for the period 2041-2070.

Figure 129 to Figure 132 present the same seed zone examples based on the HADCM3 B2 scenario for 2041-2070. The HADCM3 B2 seed zones are largely similar to the A2 zones, but are somewhat narrower and extend further south. The seed zone for focal point 345 based on HADCM3 B2 resembles that of the A2 scenario, but includes more of the area along the north shore of Lake Superior, extends further westward, and is narrower in the east (Figure 129). Similarly, the seed zone for focal point 325 based on HADCM3 B2 resembles the A2 zone, but extends further south to encompass more of the area along the shore of Lake Superior (Figure 130). In the east, it extends further southward to the Sault Ste. Marie and Sudbury area. Finally, the seed zones for focal points 336 (Figure 131) and 584 (Figure 132) are similar to their corresponding A2 zones, except that the zone for 584 includes a disjunct area along the shore of Lake Superior, far to the south of the focal point.

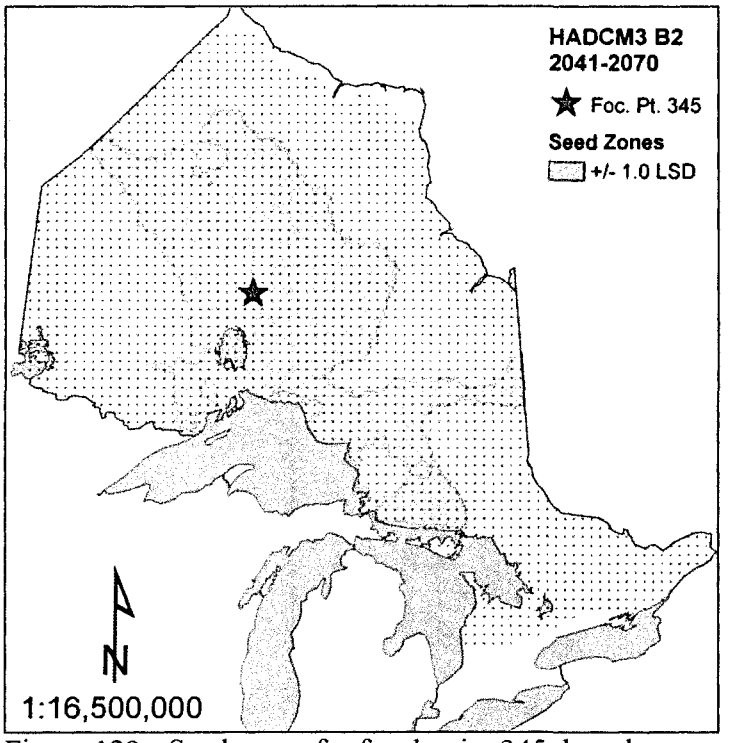

Figure 129. Seed zones for focal point 345, based on HADCM3 B2 for the period 2041-2070.

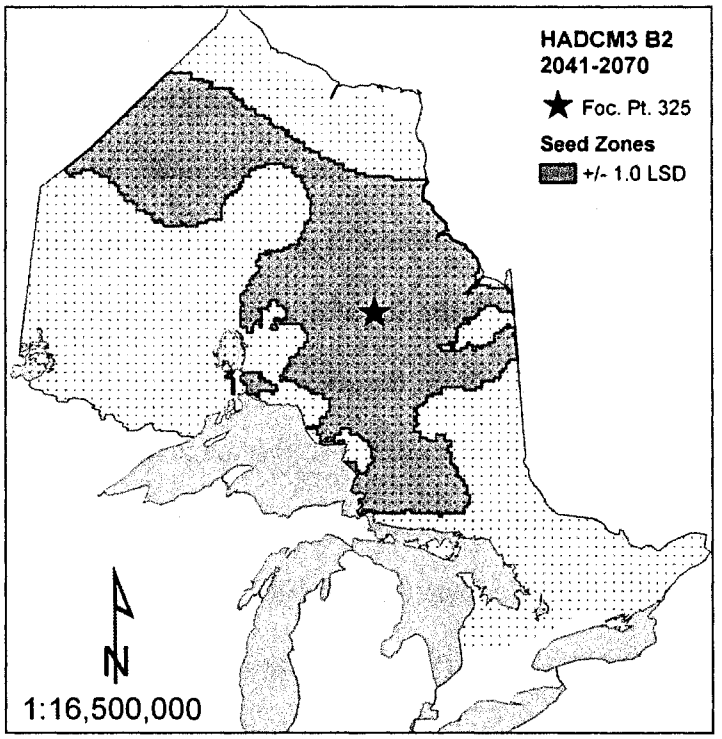

Figure 130. Seed zones for focal point 325, based on HADCM3 B2 for the period 2041-2070.

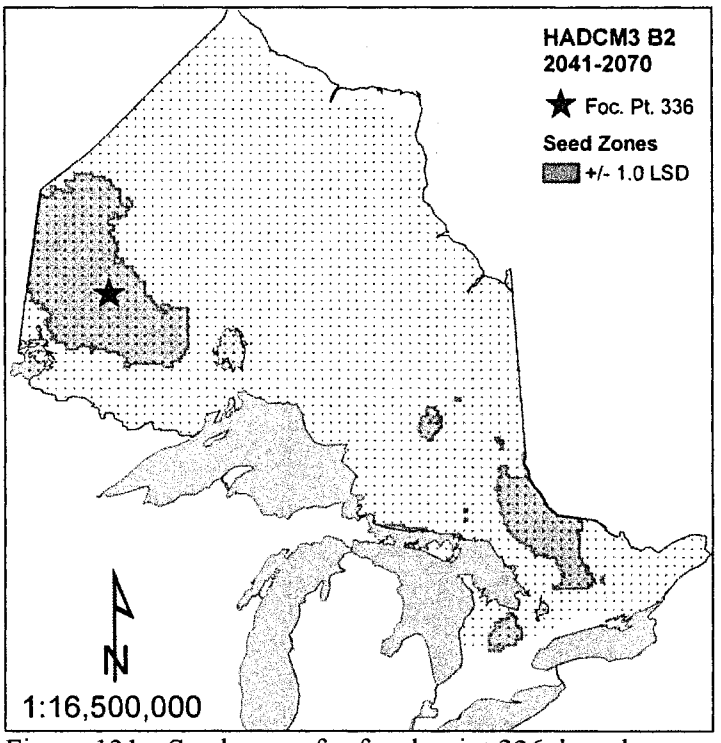

Figure 131. Seed zones for focal point 336, based on HADCM3 B2 for the period 2041-2070.

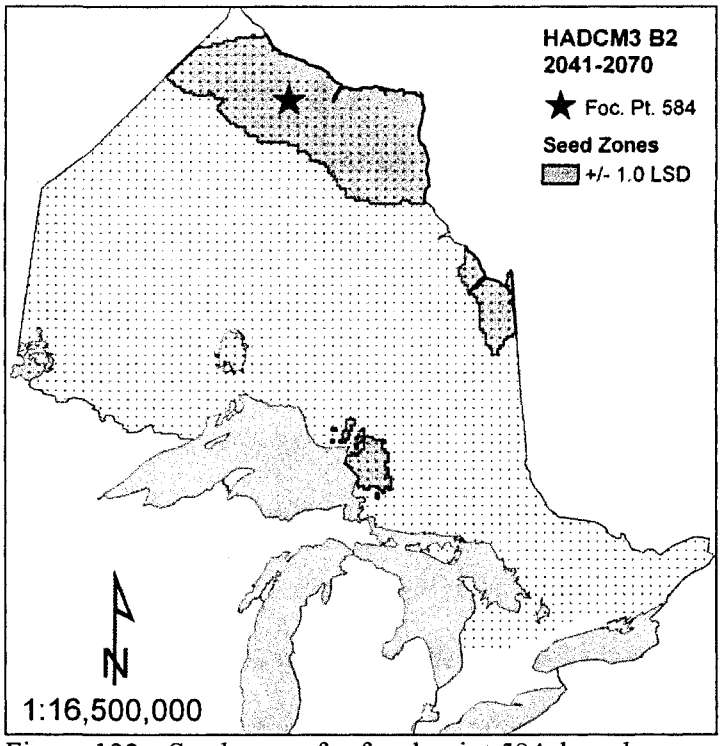

Figure 132. Seed zones for focal point 584, based on HADCM3 B2 for the period 2041-2070.

Figure 133 to Figure 136 present the seed zone examples based on the CSIRO A2 scenario for 2041-2070. The area of similarity for focal point 345 extends in a very narrow latitudinal band northward approximately 2° from the shore of Lake Nipigon (Figure 133). It extends across much of the western and central longitudes of the province; from the Manitoba border southeast to the Wawa area along the north shore of Lake Superior. Similarly, the seed zone for focal point 325 in the east is also quite narrow and extends across a broad range of longitudes (Figure 134). However, it is centered somewhat further northward than the previous zone, stretching from approximately 54°N along the Manitoba border to 49°N along its eastern boundary near the Quebec border. The area of similarity for focal point 336 in the northwest is much broader in comparison (Figure 135); it occupies the area of Lake of the Woods northward approximately 330 km along the Manitoba border and extends west

approximately 385 km. Another tiny area of similarity occurs in the Manitowadge area along the north shore of Lake Superior. In the far north, the seed zone for focal point 584 stretches in a narrow latitudinal band from the Manitoba border, east along Hudson Bay to where it terminates along the western shore of James Bay (Figure 136).

In the central latitudes of the province, the CSIRO A2 seed zones bear little similarity to those constructed based on 1961-1990 climate normals. Although they extend across a similar range of longitudes, the CSIRO A2 zones are extremely latitudinally restricted in comparison to the 1961-1990 zones for focal points 345 and 325. While seed zones for focal points in the northwest (336) and far north (584) are also somewhat narrower, they are generally similar to their corresponding 1961-1990 zones. However, if they were scaled to the same relative intervals, the CSIRO seed zones might bear much greater similarity to those of 1961-1990.

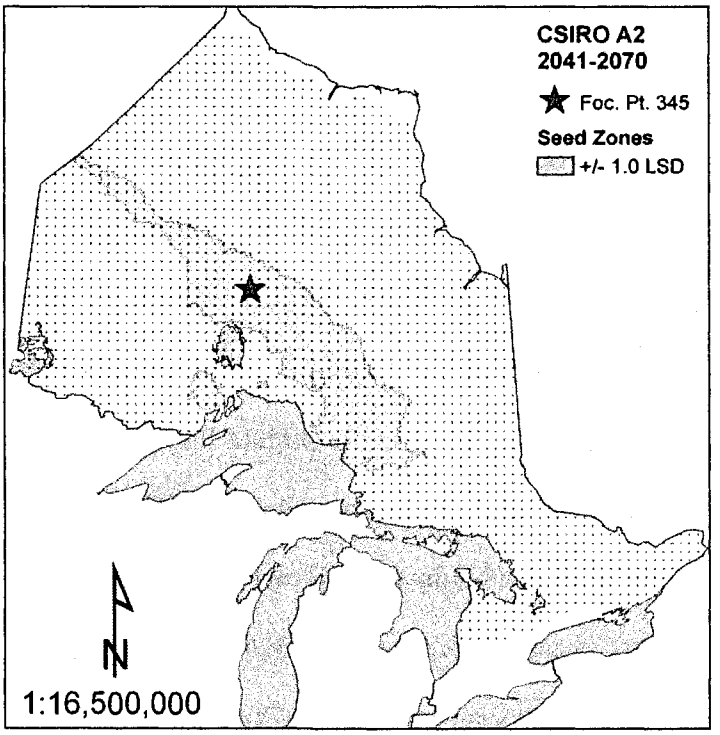

Figure 133. Seed zones for focal point 345, based on CSIRO A2 for the period 2041-2070.

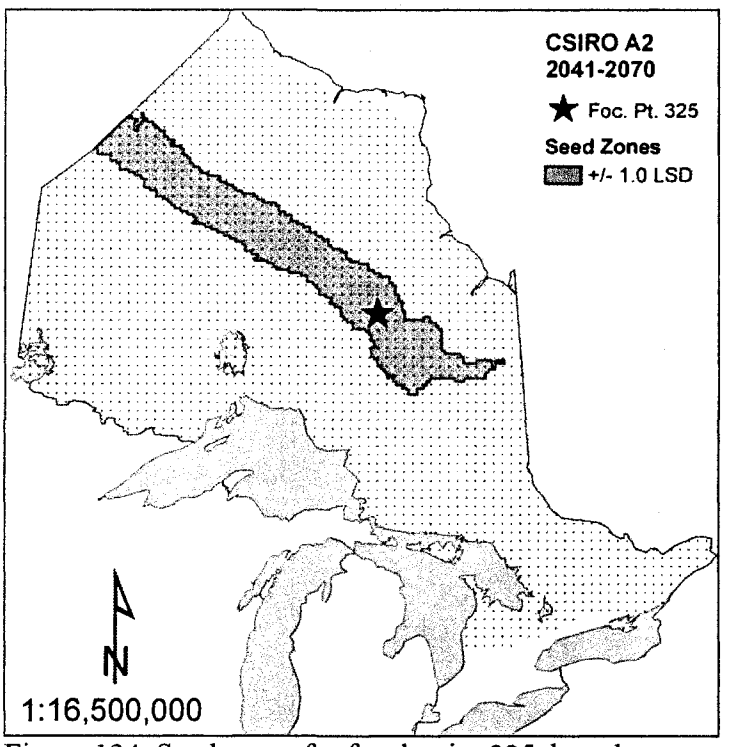

Figure 134. Seed zones for focal point 325, based on CSIRO A2 for the period 2041-2070.

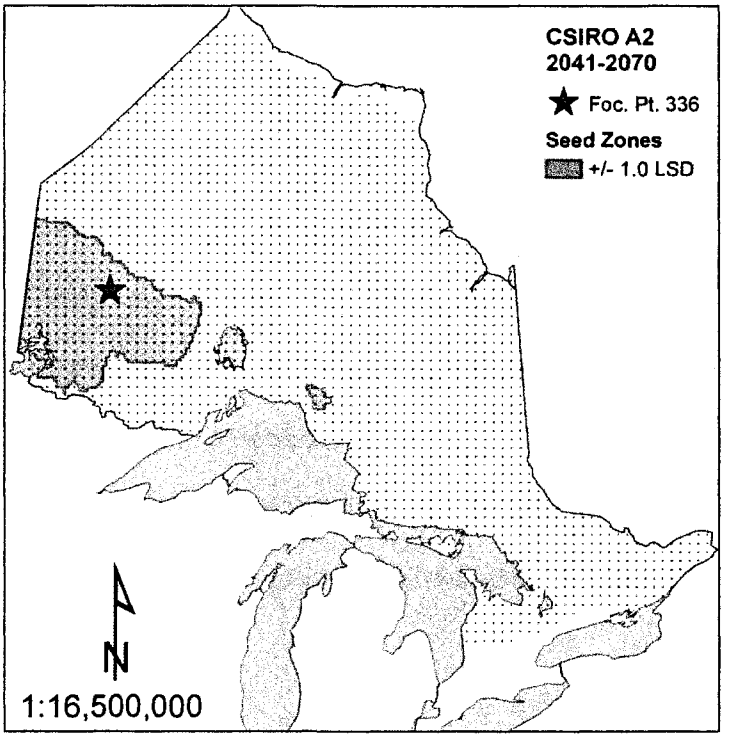

Figure 135. Seed zones for focal point 336, based on CSIRO A2 for the period 2041-2070.

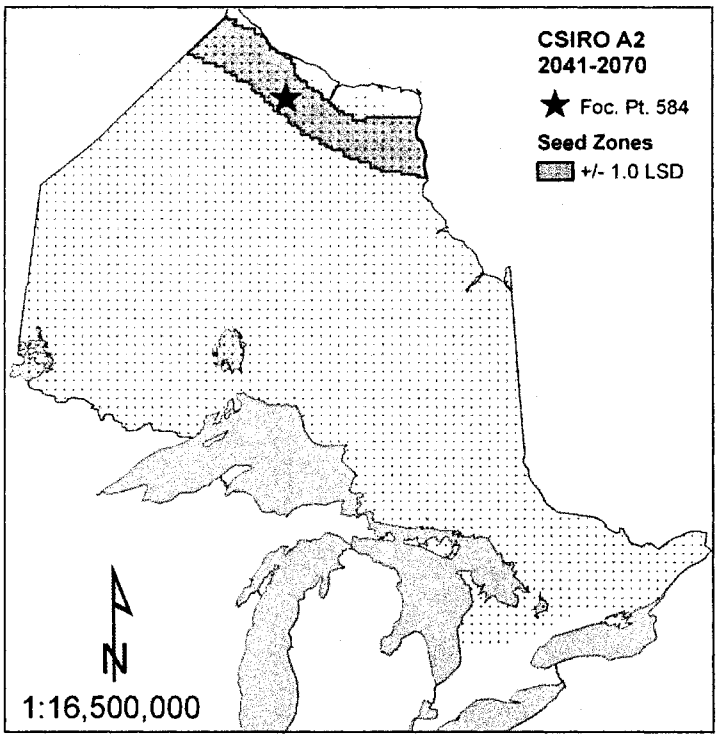

Figure 136. Seed zones for focal point 584, based on CSIRO A2 for the period 2041-2070.

Figure 137 to Figure 140 present the four seed zone examples based on the CSIRO B2 scenario for 2041-2070. Seed zones for the northwestern focal point 336 (Figure 139) and far northern focal point 584 (Figure 140) are virtually identical to those of the A2 scenario. In contrast, seed zones for focal points 345 and 325 vary somewhat from the corresponding A2 zone; they are both located on a steeper northwest-southeast plane (Figure 137 and Figure 138, respectively). The CSIRO B2 seed zone for focal point 345 is centered somewhat further west than the A2 zone, and does not narrow along its western boundary. The seed zone for focal point 325 does not extend as far westward for the B2 scenario, but is otherwise similar to the A2 scenario.

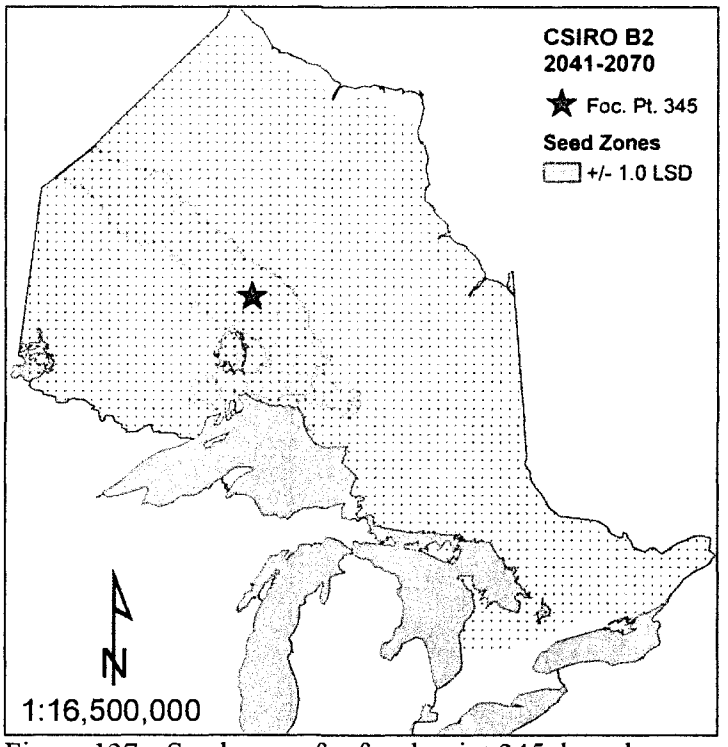

Figure 137. Seed zones for focal point 345, based on CSIRO B2 for the period 2041-2070.

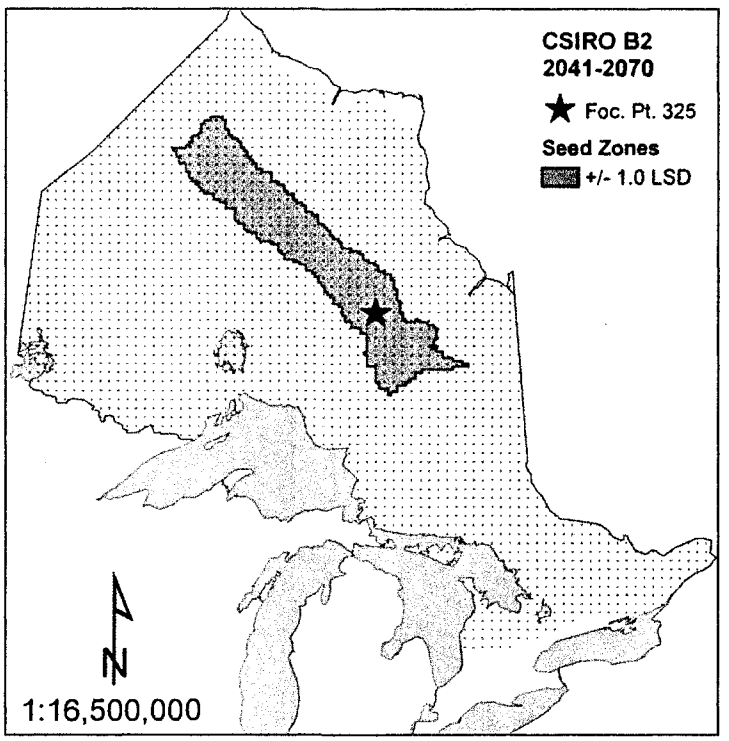

Figure 138. Seed zones for focal point 325, based on CSIRO B2 for the period 2041-2070.

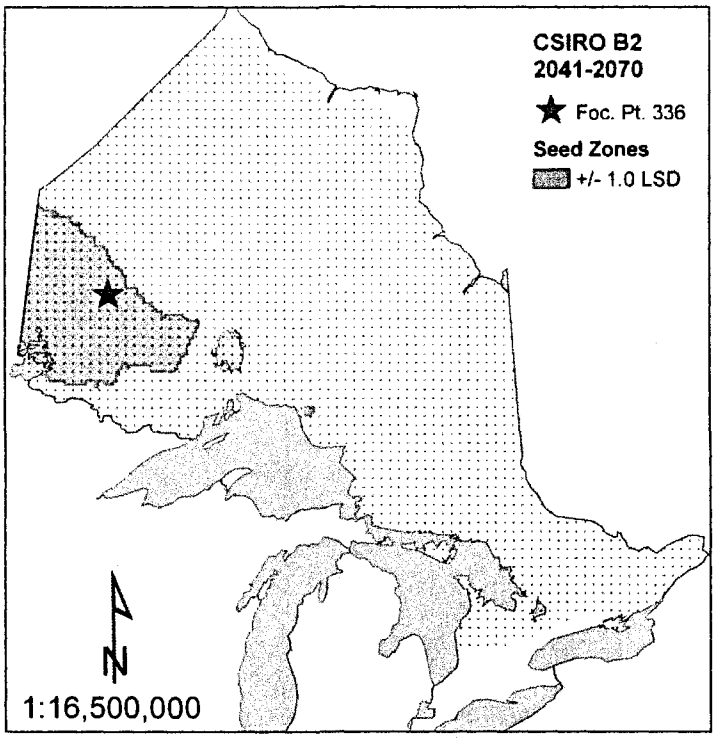

Figure 139. Seed zones for focal point 336, based on CSIRO B2 for the period 2041-2070.

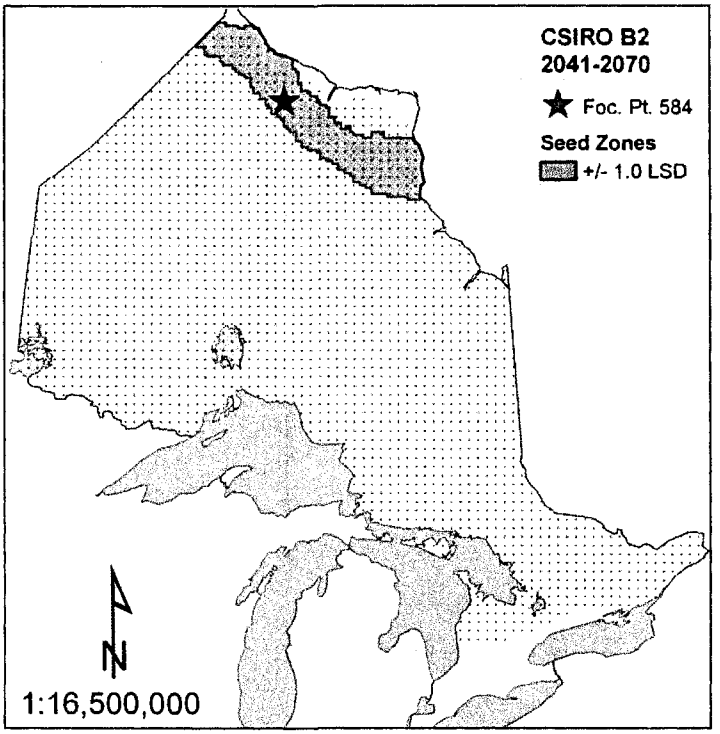

Figure 140. Seed zones for focal point 584, based on CSIRO B2 for the period 2041-2070.

FUTURE BREEDING ZONES FOR 2041-2070

Figure 141 presents the level coverage achieved with 1 through 10 breeding zones for each of the six future climate estimates. The solutions are presented based on selection from a set of 618 candidate breeding zones constructed at the 1.0 LSD level of adaptive similarity. The solution sets based on CGCM2 A2 & B2 scenarios are presented by the green and purple series lines, respectively, while the HADCM3 A2 & B2 scenarios are presented in orange and pink and the CSIRO A2 & B2 scenarios are presented in dark green and blue. The HADCM3 A2 & B2 solution sets produce the highest total coverage, with values of 99.6 and 99.4 % for the optimal 10-zone solutions. In contrast, the CSIRO zones produce the lowest total coverage with values of 92.7 and 87.5 % for the A2 and B2 scenarios, respectively. The CGCM2 A2 & B2 scenarios produce intermediate coverage with values of 99.4 and 92.7% for the 10-zone solution. The A2 emissions scenario produces higher coverage for each of the three models than does the B2 scenario.

In comparison to the 1961-1990 solution, the HADCM3 A2 & B2 scenarios provide relative greater coverage for a given number of zones, requiring only 4 zones to reach 80% full coverage in comparison to 5 zones for the 1961-1990 scenario. The CGCM2 A2 & B2 scenarios provide somewhat less coverage, requiring 6 zones to reach 80% coverage, while the CSIRO A2 & B2 zones provide considerably less coverage, requiring 7 and 8 zones respectively.

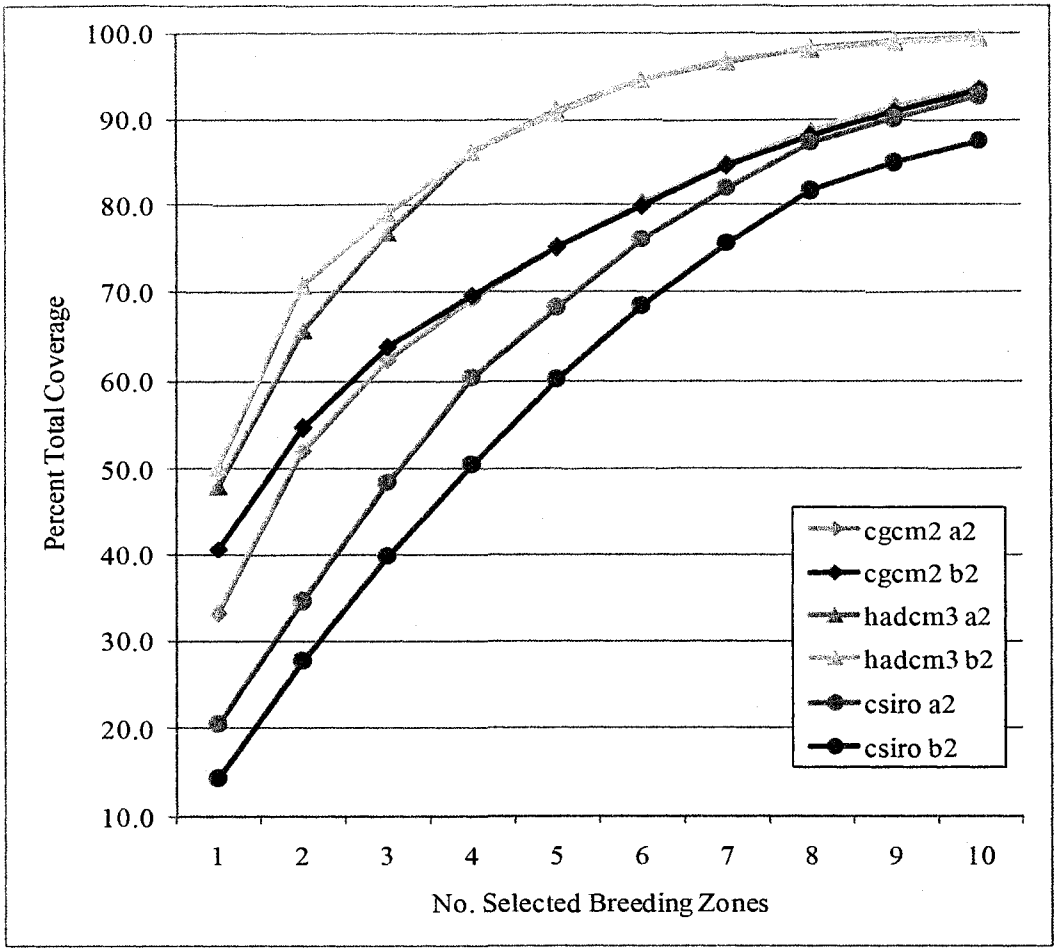

Figure 141. Percent of total area covered with increasing number of breeding zones based on future (2041-2070) climate estimates.

Figure 142 to Figure 176 illustrate optimal future breeding zones constructed for CGCM2 A2 & B2, HADCM3 A2 & B2, AND CSIRO A2& B2, respectively. The solutions are presented to 80% total coverage at the 1.0 LSD level of adaptive similarity.

Figure 142 to Figure 147 present the optimal solution for CGCM2 A2 for 1 through 6 zones, based on the achievement of 80% total coverage. The optimal 1-zone solution results in 33.2% total coverage with the selection of focal point 376 in the center of the province (Figure 142). Breeding zone 376 covers a broad area extending from 51-55°N in the west and from 49-53°N in the east.

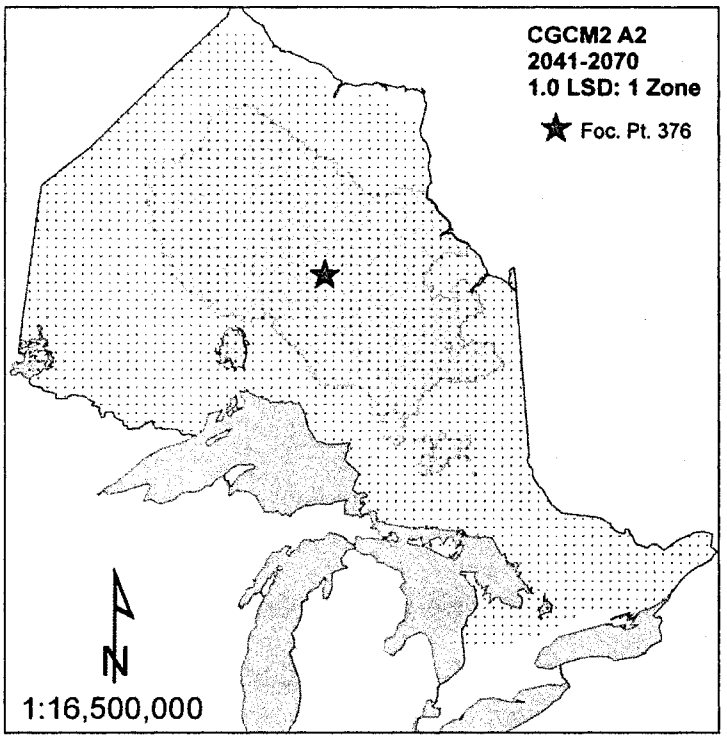

Figure 142. Optimal zones for 2041-2070 based on 1 breeding zone for the CGCM2 A2 scenario.

The selection of focal point 204 increases total coverage to 52.0 % for the optimal 2-zone solution (Figure 143). Breeding zone 204 spans a narrow latitudinal band that runs from the Manitoba border in the northwest, along the north shores of

Lake Superior and Lake Huron to the Sudbury area. In comparison with the 1-zone solution, the broad central zone (548) is similar but has shifted very slightly northward and there is now an uncovered island within its interior. A very small area of overlap occurs along the adjacent boundaries of the two zones.

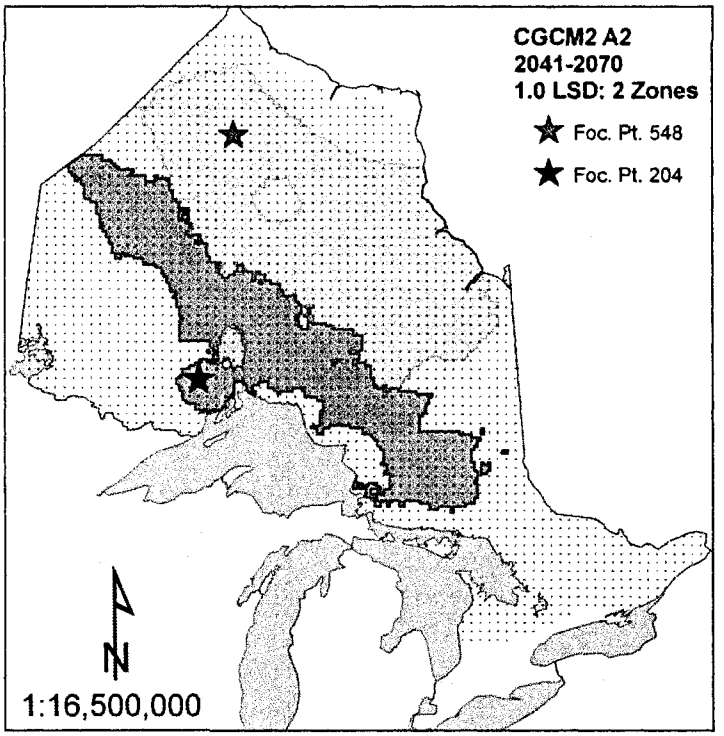

Figure 143. Optimal zones for 2041-2070 based on 2 breeding zones for the CGCM2 A2 scenario.

Total coverage for the optimal 3-zone solution increases to 62.3% with the selection of focal point 229 (Figure 144). Breeding zone 229 spans a very narrow latitudinal and is composed of 2 disjunct portions. The first and larger portion is located surrounding the focal point in the northwest and runs from the Manitoba border southeast to Thunder Bay, while the second is located in the northeast region. In comparison to the 2-zone solution, the selection of breeding 229 has introduced a very

minimal area of overlap where it intersects with the lakeshore zone. The broad central and lakeshore zones remain unchanged in comparison to the optimal 2-zone solution.

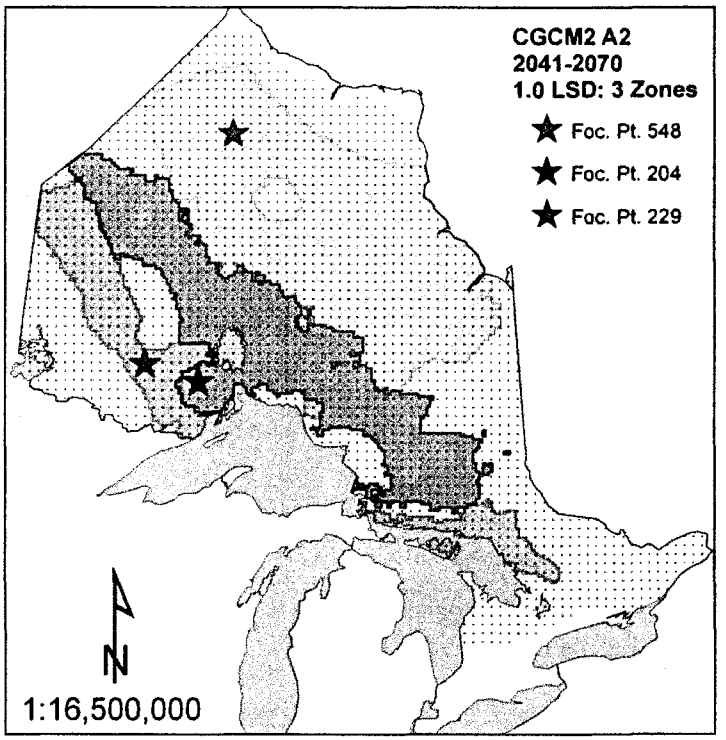

Figure 144. Optimal zones for 2041-2070 based on 3 breeding zones for the CGCM2 A2 scenario.

The selection of focal point 597 in the far north increases total coverage to 69.2% for the optimal 4-zone solution (Figure 145). Breeding zone 597 occupies the far north of the province, stretching from the Manitoba border eastward to James Bay, and from Hudson Bay southward where it overlaps with the central zone (532). In comparison to the optimal 3-zone solution, the central zone is similar but now includes the previously uncovered island within its interior. The lakeshore (315) and northwest (229) zones are similar.

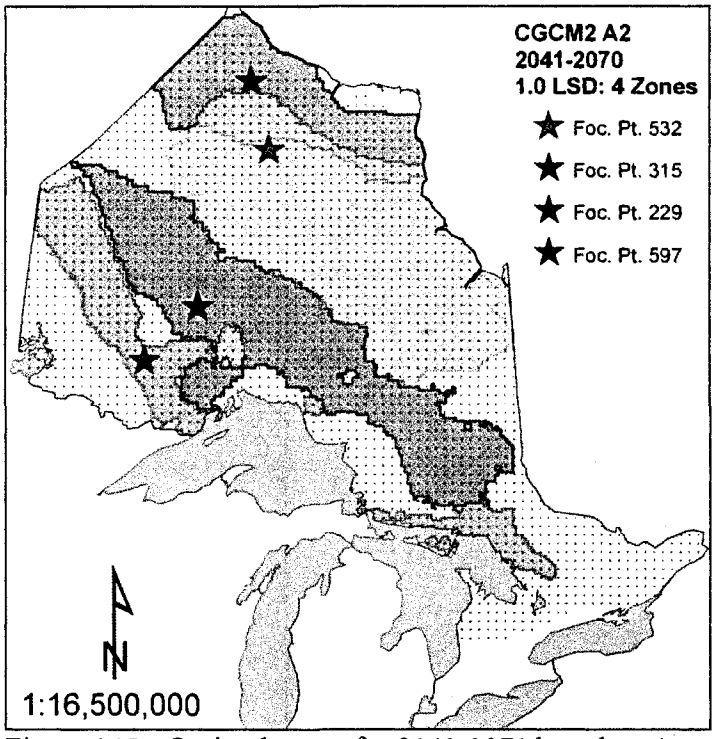

Figure 145. Optimal zones for 2041-2070 based on 4 breeding zones for the CGCM2 A2 scenario.

The optimal 5-zone solution produces 75.0% coverage with the selection of focal point 198 near the Minnesota border (Figure 146). Breeding zone 198 stretches from just north of Lake of the Woods at the Manitoba border southeast to the Atikokan area. Though it contacts with the northwest zone (229) in several places, the southwestern zone (198) does not overlap. The other 4-zones remain unchanged in comparison to the 4-zone solution.

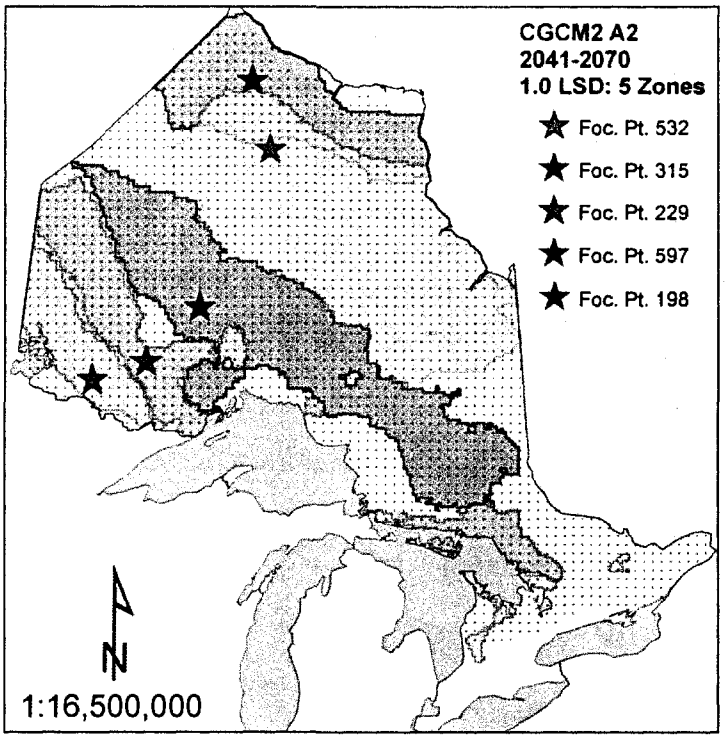

Figure 146. Optimal zones for 2041-2070 based on 5 breeding zones for the CGCM2 A2 scenario.

The optimal 6-zone solution achieves 80.1% coverage with the selection of focal point 314 (Figure 147). Breeding zone 314 occupies 2 narrow, disjunct latitudinal bands. The first of these is located in the northwest region surrounding the focal point where it overlaps with the lakeshore zone (291) while the second is located mostly within the northeast region where it also overlaps. In comparison to the 5-zone solution, the lakeshore zone is much narrower throughout the northwest, while the central (532), northwest (229), far northern, and southwestern (198) zones remain unchanged.

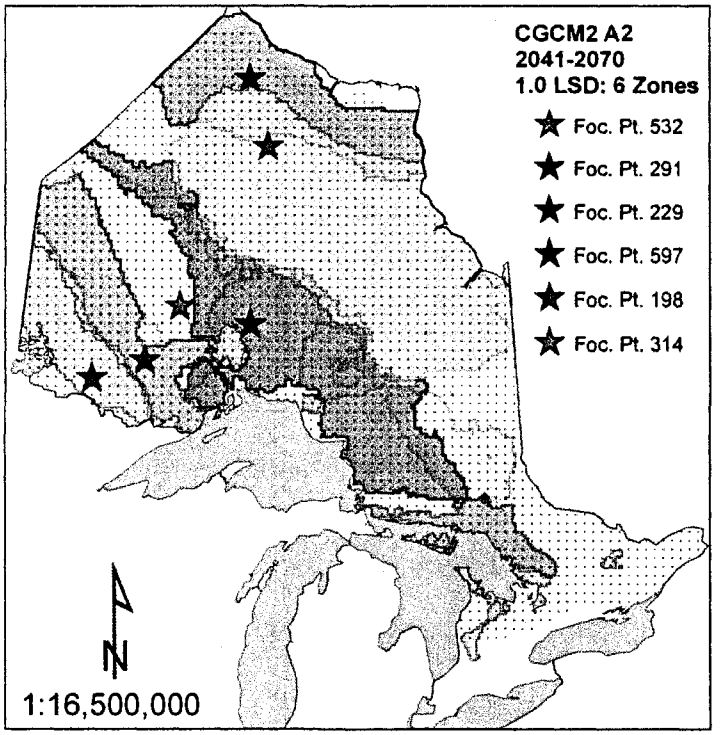

Figure 147. Optimal zones for 2041-2070 based on 6 breeding zones for the CGCM2 A2 scenario.

The optimal 6-zone solution based on CGCM2 A2 indicates that breeding zones for 2041-2070 bear little similarity to those constructed based on 1961-1990 climate normals (Figure 29). It is difficult to distinguish many zones that are comparable between the two scenarios. However, it appears that the northernmost zone (597) for CGCM2 A2 is largely equivalent to the northernmost zone (598) for the 1961-1990 solution. Also, the lakeshore zone (291) vaguely resembles the broad central zone (345) for the current climate but is much narrower and located further south. The relationship, if any, between the remainder of the CGCM2 A2 zones and those constructed for 1961-1990 is unclear.

Figure 148 to Figure 153 present the optimal solution for CGCM2 B2 for 1 through 6 zones, based on the achievement of 80% total coverage. The optimal 1-zone solution results in 40.6% total coverage with the selection of focal point 374 (Figure 148). Breeding zone 374 occupies an area that spans approximately 5-6° latitude in the center of the province and runs from 92°W eastward nearly to the Quebec border. This zone notably excludes the area that runs between the north shore of Lake Superior and Lake Nipigon.

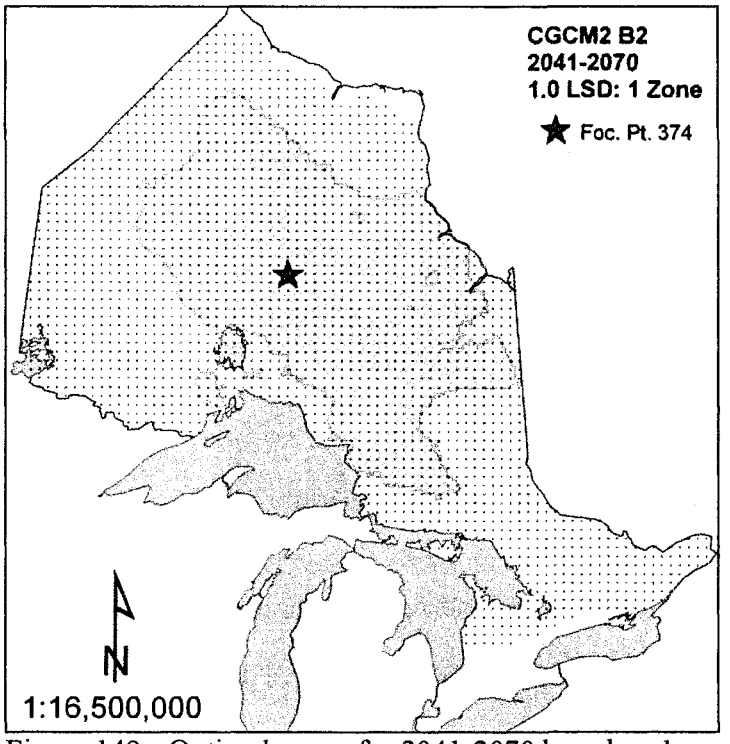

Figure 148. Optimal zones for 2041-2070 based on 1 breeding zone for the CGCM2 B2 scenario.

The selection of focal point 581 in the north increases coverage to 54.6% for the optimal 2-zone solution (Figure 149). Breeding zone 581 occupies a large area in the far north of the province, stretching from the Manitoba border southeast to the Quebec border adjacent to James Bay. In comparison with the 1-zone solution, the large

central zone is similar but its northeastern border does not extend as far northward. There is significant overlap where the northern zone intersects with the central zone along its central longitudes.

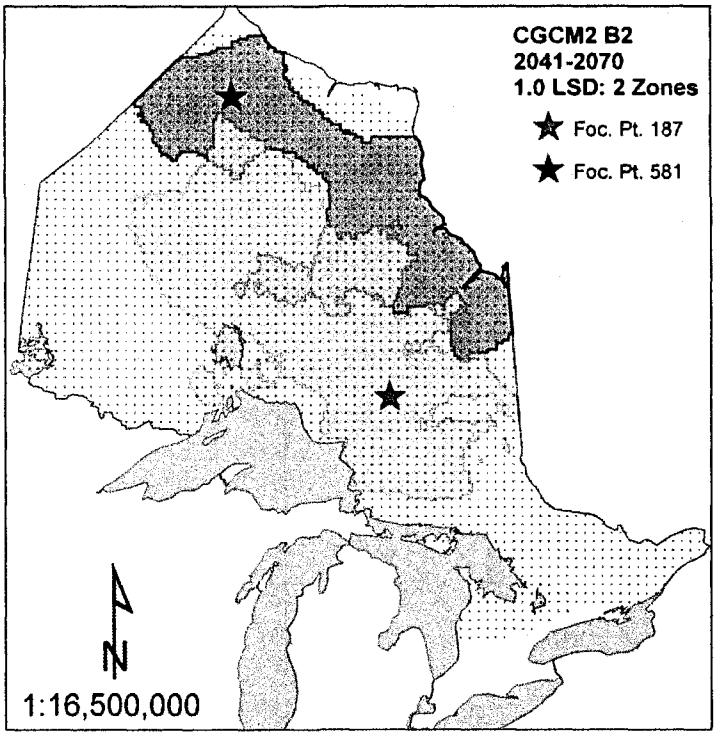

Figure 149. Optimal zones for 2041-2070 based on 2 breeding zones for the CGCM2 B2 scenario.

The total coverage increases to 63.8% percent for the optimal 3-zone solution (Figure 150). Breeding zone 182 stretches from just east of the focal point, along the shore of Lake Superior and northwestwards to the Manitoba border. The central zone (424) is similar in comparison the 2-zone solution, but is broader in the east. The northern zone (583) is also similar but no longer occupies the peninsular area of overlap with the central zone.

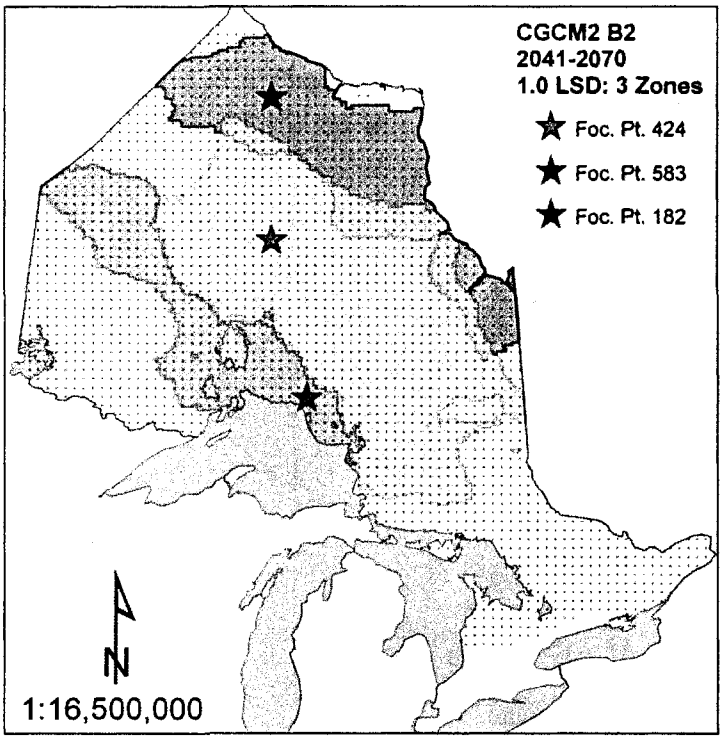

Figure 150. Optimal zones for 2041-2070 based on 3 breeding zones for the CGCM2 B2 scenario.

The selection of focal point 488 increases total coverage to 69.6% for the optimal 4-zone solution (Figure 151). Breeding zone 488 occupies a very broad, segmented area in the central latitudes of the province that overlaps extensively with the other central zone (131). In comparison with the 3-zone solution, the original central zone (131) is deeply incised along its northern border, while the far northern (583) and lakeshore (182) zones remain unchanged.

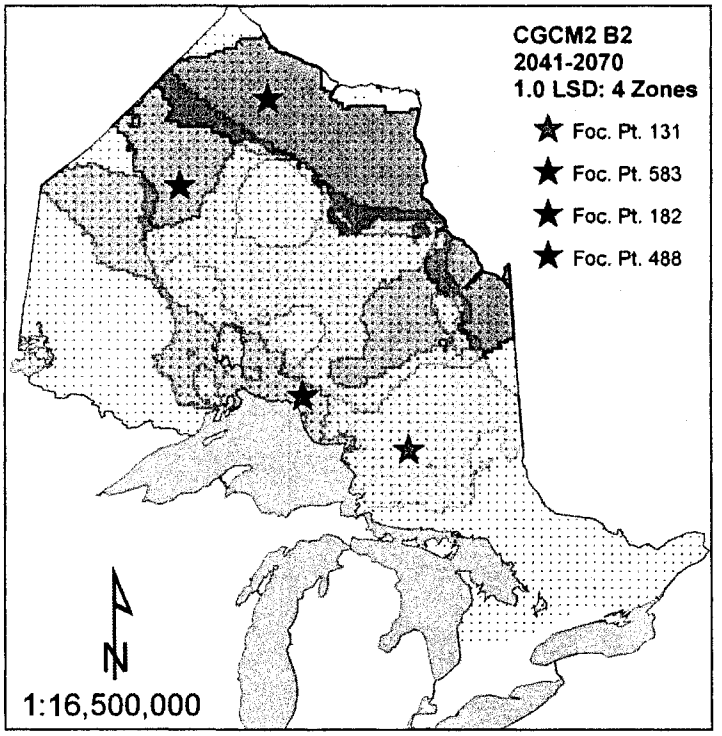

Figure 151. Optimal zones for 2041-2070 based on 4 breeding zones for the CGCM2 B2 scenario.

For the optimal 5-zone solution, the selection of focal point 54 increases total coverage to 75.0% (Figure 152). Breeding zone 54 occupies a narrow area in the northeast region that runs from Sault Ste. Marie east to the Ottawa Valley. Overlap between zone 54 and the adjacent central zone is virtually negligible. The other four zones remain unchanged in comparison to the previous solution.

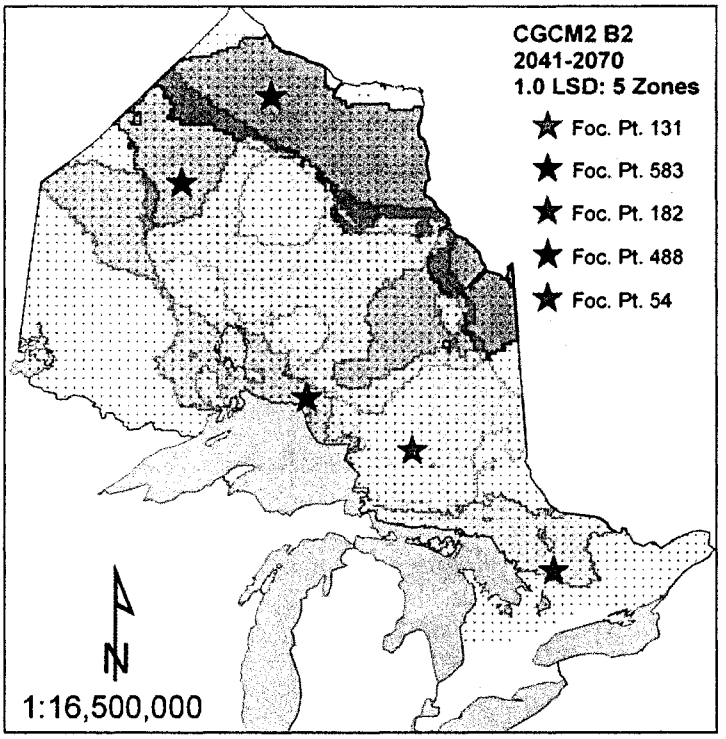

Figure 152. Optimal zones for 2041-2070 based on 5 breeding zones for the CGCM2 B2 scenario.

The selection of focal point 256 in the northwest increases coverage to 79.8% for the optimal 6-zone solution, but otherwise the solution remains unchanged. Breeding zone 256 runs from the Manitoba border southeastward in a narrow latitudinal band to the Fort Frances and Dryden area.

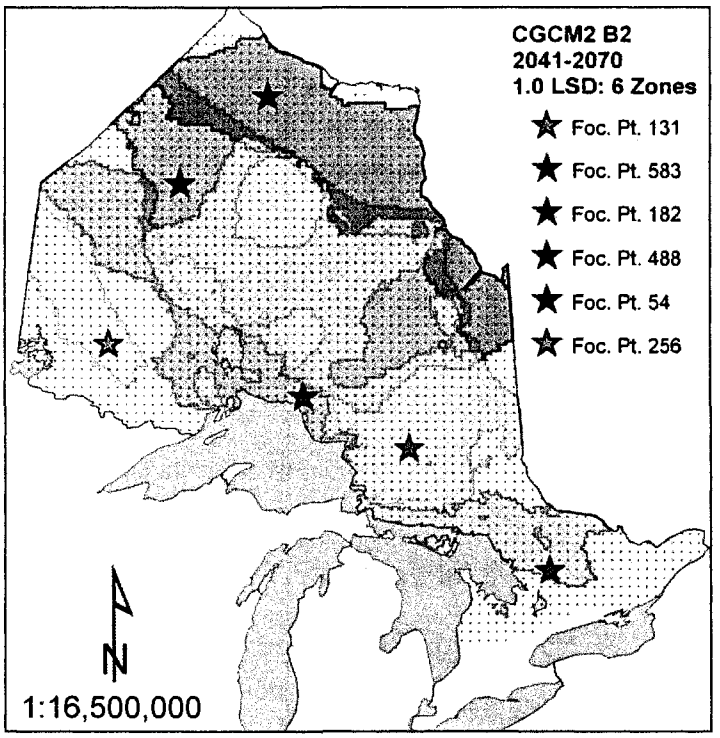

Figure 153. Optimal zones for 2041-2070 based on 6 breeding zones for the CGCM2 B2 scenario.

Like the CGCM2 A2 scenario, the B2 scenario demonstrates little similarity with the optimal zones constructed for 1961-1990 (Figure 29). The boundaries of the breeding zones are largely anomalous, with the exception of the far northern zone (583) which rather closely resembles the northern zone (598) of the 1961-1990 solution. Also the northeastern zone (54) resembles the disjunct northeastern portion of breeding zone 283 that runs along the north shore of Lake Huron for the 1961-1991 solution. It could be that the broad central zones (131,488) are analogous to the central zone (345) for 1961-1991. However, these zones are extremely furrowed and segmented in comparison to 1961-1990.

Figure 154 to Figure 157 present the optimal solution for HADCM3 A2 for 1 through 4 zones, based on the achievement of 80% total coverage. The optimal 1-zone

solution results in 48.0% total coverage with the selection of focal point 401 (Figure 154). Breeding zone 401 stretches from the Manitoba border east to James Bay and the Quebec border. It spans from approximately 52 to 54°N latitude along its western border and from 47 to 52°N along its eastern edge, notably excluding the areas to the immediate north of Lake Superior and Lake Huron.

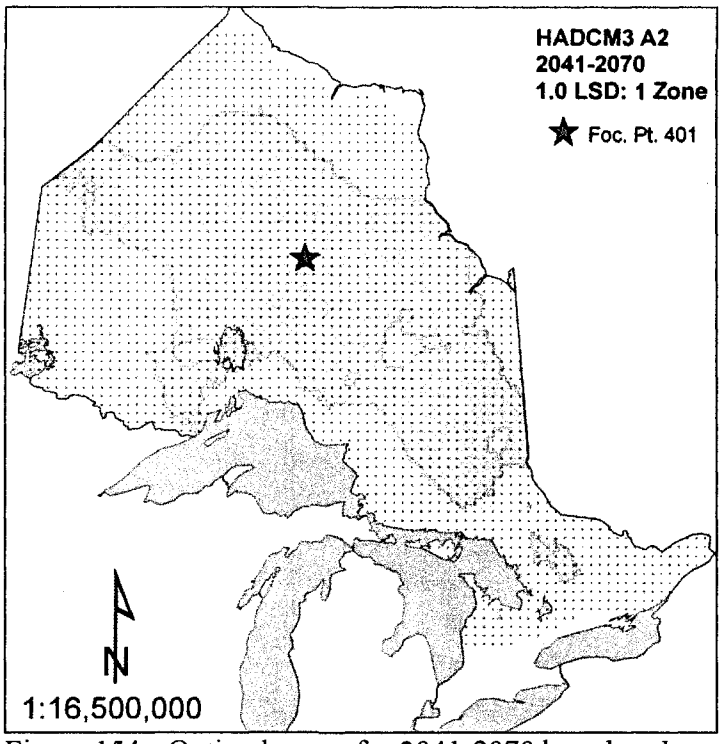

Figure 154. Optimal zones for 2041-2070 based on 1 breeding zone for the HADCM3 A2 scenario.

The selection of focal point 260 increases total coverage to 65.6%, but introduces a significant amount of overlap. Breeding zone 260 is notably fragmented, occupying numerous small or irregular areas throughout northwestern Ontario and the northeast region. One large area is located in the northwest region surrounding the focal point; it runs southeastward from the Manitoba border, terminating along the western shore of Lake Nipigon. A large peninsula extends eastward from this area into the

neighbouring central (216) zone. A second large portion of zone 260 extends from the Timmins/Cochrane area south to the shore of Lake Huron and east to the area surrounding Parry Sound and Bancroft. The central zone (216) is similar when compared to the 1-zone solution, but does not extend as far westward.

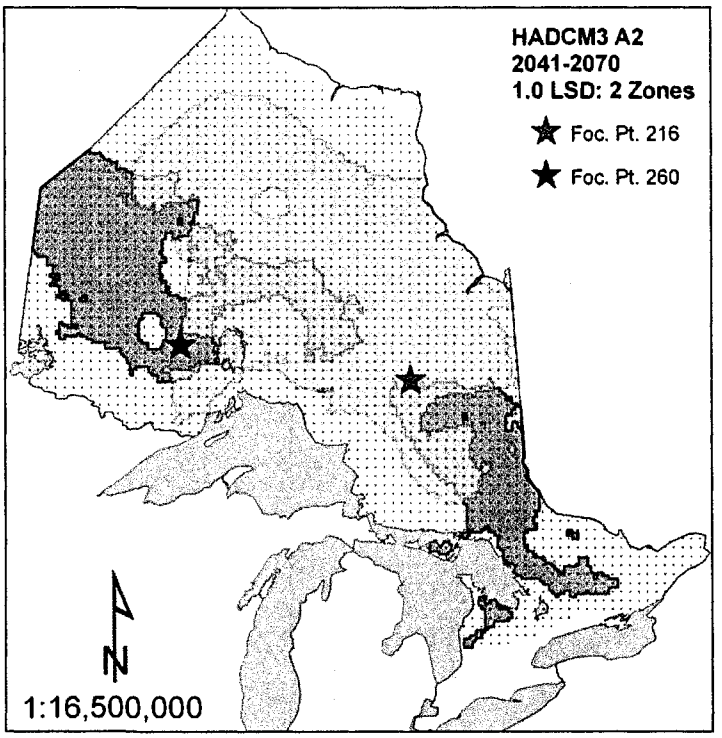

Figure 155. Optimal zones for 2041-2070 based on 2 breeding zones for the HADCM3 A2 scenario.

The optimal 3-zone solution results in 76.7% total coverage with the selection of focal point 566 (Figure 156). Breeding zone 566 occupies much of the far north of the province and overlaps extensively with the central zone (133). It extends from the Manitoba border eastward to James Bay and, from there, south to approximately 49°N latitude. The central zone is similar in comparison to the 2-zone solution, but extends both further west and eastward. The northwestern/northeastern disjunct zone (57) has notably shifted; the northwestern portion is now located further south and no longer

overlaps with the central zone while the northeastern portion has shifted eastward and now covers most of the southern region.

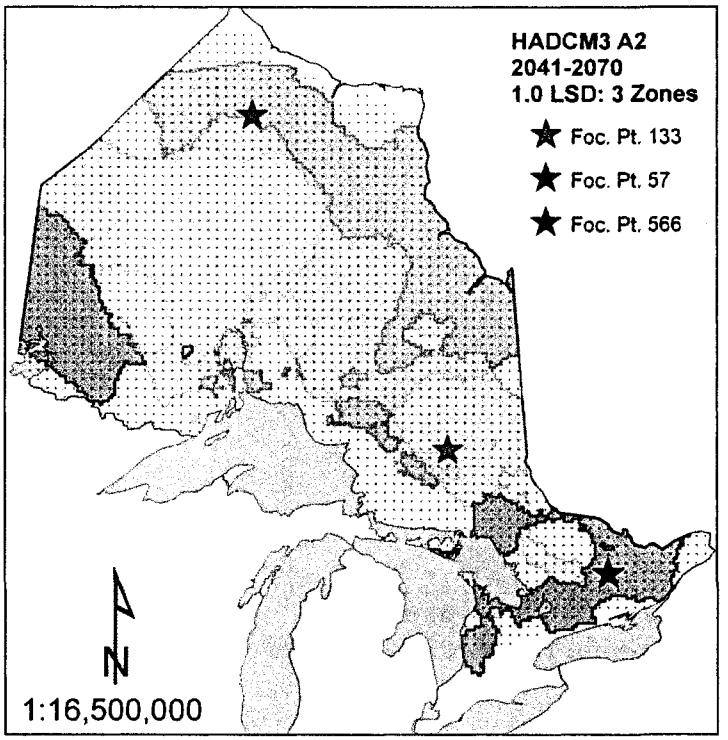

Figure 156. Optimal zones for 2041-2070 based on 3 breeding zones for the HADCM3 A2 scenario.

Total coverage for the optimal 4-zone solution reaches 86.2% with the selection of focal point 102 (Figure 157). Breeding zone 102 extends westward from the focal point near Sudbury and terminates in the area surrounding Thunder Bay. A few moderate areas of overlap between zone 102 and the central (465) zone occur in the central latitudes of the province. The central (465), northwest (57), and far northern (566) zones are similar to the 3-zone solution.

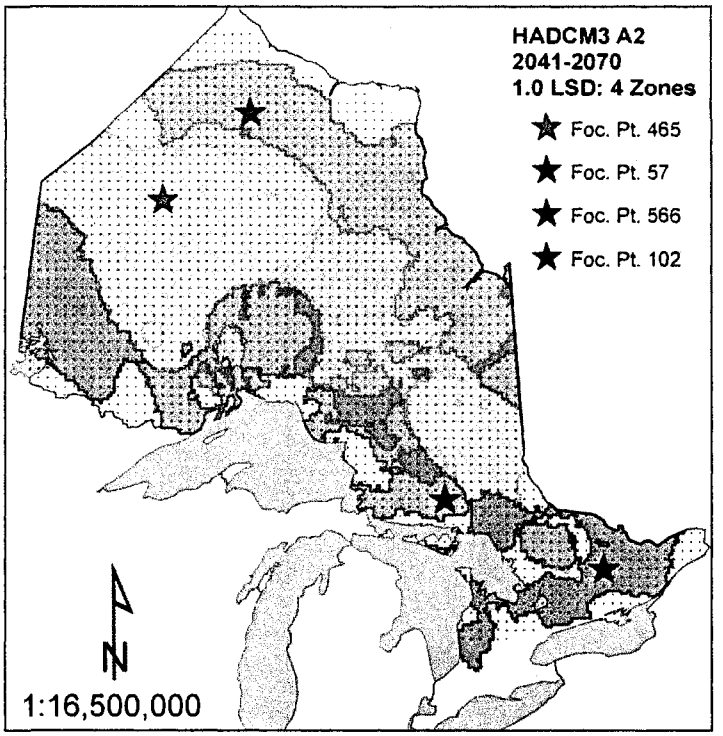

Figure 157. Optimal zones for 2041-2070 based on 4 breeding zones for the HADCM3 A2 scenario.

The breeding zones constructed based on HADCM3 A2 for 2041-2070 bear surprising similarity to the 1961-1990 zones (Figure 23). The northern zone (566) for HADCM3 A2 is similar to breeding zone 325 for the 1961-1990 solution, but is shifted slightly northward. The disjunct breeding zone 57 for CGCM2 A2 is quite similar to the breeding zone 75 for 1961-1990, which also demonstrates a two disjunct areas located in the northwest and southeast . Finally, the central zone (465) for CGCM2 A2 somewhat resembles the central zone (345) of the 1961-1990 scenario, but is located further north and extends across a broader range of longitudes. However, what is interesting is that the 2nd and 3rd zones are added in different order. That is, the 2nd zone added in the HADCM3 A2 scenario is analogous to the 3rd zone added zone in the 1961-1990, while

the 3rd zone added in the HADCM3 A2 scenario is analogous to the 2nd zone added in the 1961-1990 scenario.

Figure 158 to Figure 161 present the optimal solution for HADCM3 A2 for 1 through 4 zones, based on the achievement of 80% total coverage. The optimal 1-zone solution achieves 50.2% coverage with the selection of focal point 403. Breeding zone 403 spans much of the central latitudes of the province, ranging from the north shore of Lake Superior to approximately 55°N latitude. It occupies most of the area ranging from the Manitoba border east to the Quebec border, but noticeably excludes most of the area immediately surrounding Lake Nipigon.

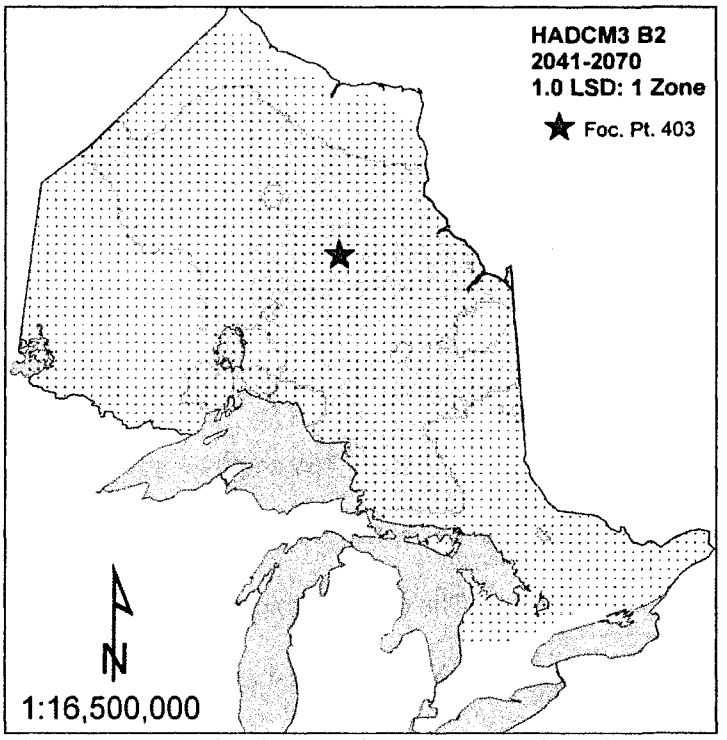

Figure 158. Optimal zones for 2041-2070 based on 1 breeding zone for the HADCM3 B2 scenario.

A total coverage of 70.7% is reached for the optimal 2-zone solution (Figure 159). Breeding zone 65 is notably fragmented, occupying a small area of the southern region surrounding the focal point, a large area of the northeast where it overlaps with

the central zone, and most of the northwest region where it overlaps extensively with the central zone.

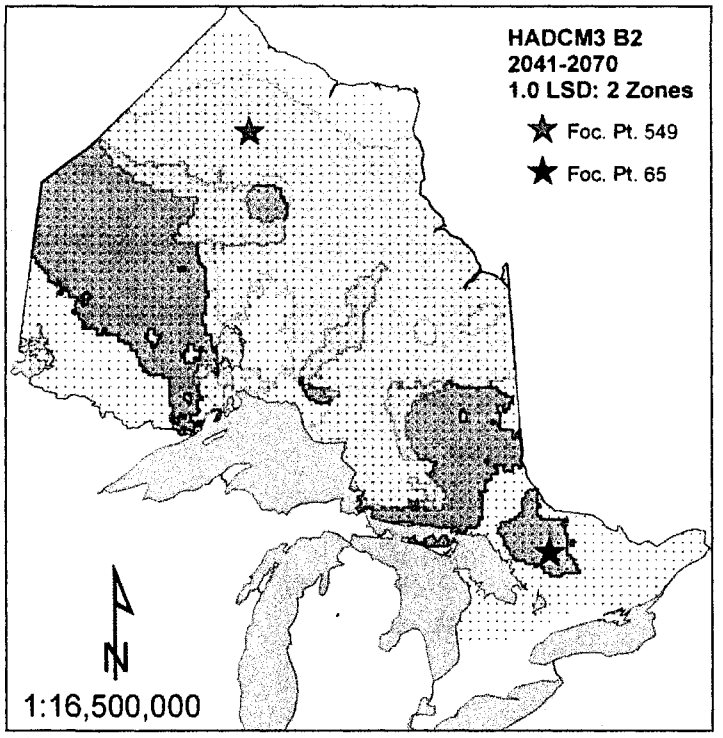

Figure 159. Optimal zones for 2041-2070 based on 2 breeding zones for the HADCM3 B2 scenario.

The selection of breeding zone 597 in the far north increases coverage to 79.0% (Figure 160). Breeding zone 597 runs from Hudson Bay southward to where it overlaps extensively with the northern boundary of the central zone. Two discontinuous areas are also present along the edge of James Bay. The large fragmented zone (78) is similar to the 2-zone solution, but is relatively patchy in the northeast region while the broad central zone is similar.

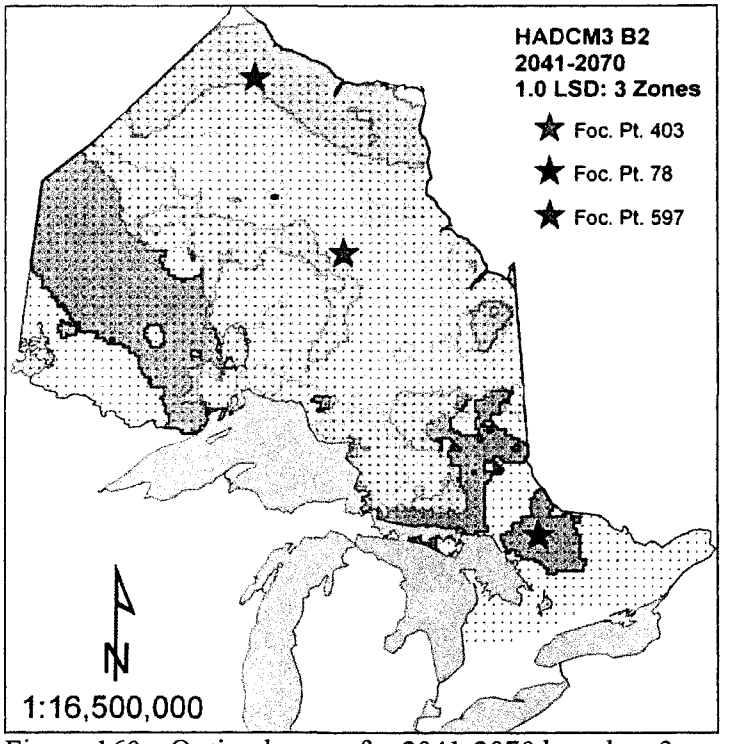

Figure 160. Optimal zones for 2041-2070 based on 3 breeding zones for the HADCM3 B2 scenario.

The optimal 4-zone solution reaches 86.2% coverage with the selection of focal point 279. Breeding zone 279 occupies the furthest southern areas; in the northwest surrounding the focal point near Lake of the Woods, and in the southern region stretching from the Ottawa Valley south the edge of the white spruce range. The large disjunct zone (65) is similar to the 2-zone solution, while the central (403) and northern (597) zones are unchanged.

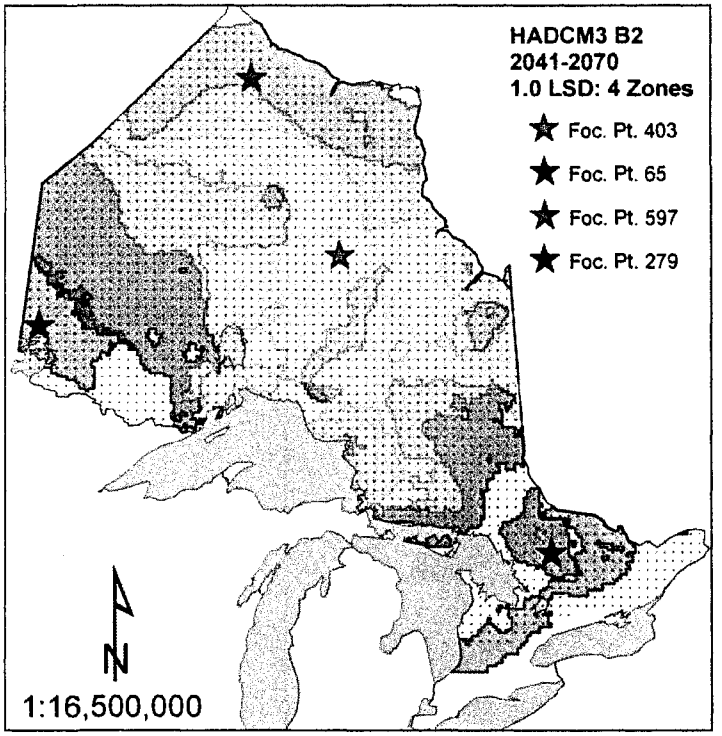

Figure 161. Optimal zones for 2041-2070 based on 4 breeding zones for the HADCM3 B2 scenario.

The four optimal breeding zones constructed based on HADCM3 B2 bear some similarity with 1961-1990 optimum zones (Figure 23to Figure 29). The northernmost (65) zone strongly resembles the northern zone (584) for 1961-1990. The broad central zone (403) is very similar in shape and location, but extends a wider range of latitudes and slightly further eastward than the 1961-1990 central zone (131). Breeding zone 279 is similar to, but somewhat more restricted than the disjunct northwest/southeast zone (75) of the 1961-1900 solution.

Figure 162 to Figure 168 present the optimal solution for CSIRO A2 for 1 through 7 zones, based on the achievement of 80% total coverage (Figure 162). The optimal 1-zone solution produces 20.4% coverage with the selection of focal point 162.

Breeding zone 162 runs in a narrow latitudinal band from the Manitoba border at 52°N, southeast to Sault Ste. Marie at 47°N.

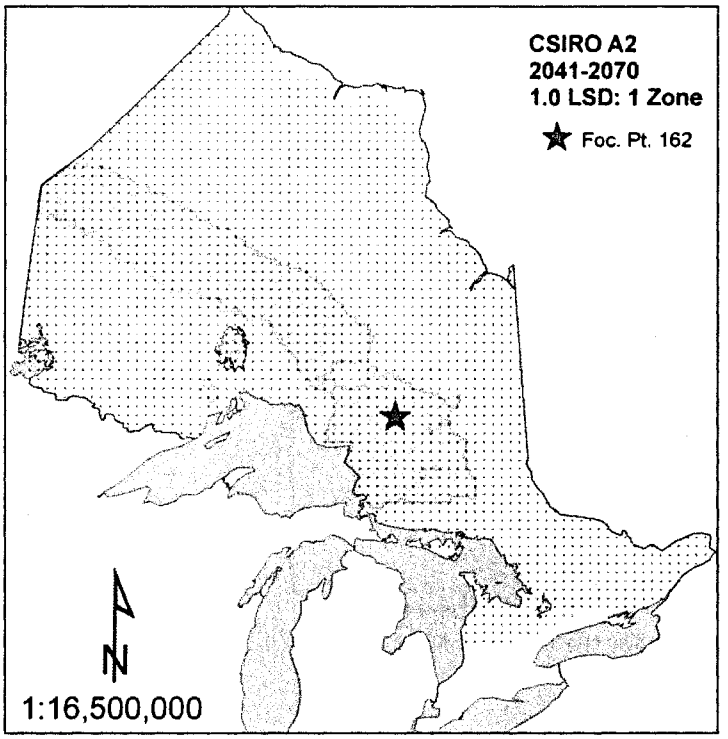

Figure 162. Optimal zones for 2041-2070 based on 1 breeding zone for the CSIRO A2 scenario.

The selection of focal point 230 increases coverage to 34.5% (Figure 163). Breeding zone 230 is located immediately to the south of the first zone and occupies most of the area of the northwest region. It runs from the Manitoba border east to the Thunder Bay area, where it encloses the area immediately surrounding Lake Nipigon. The first zone (162) is the same as for the 1-zone solution. No overlap is present for the optimal 2-zone solution.

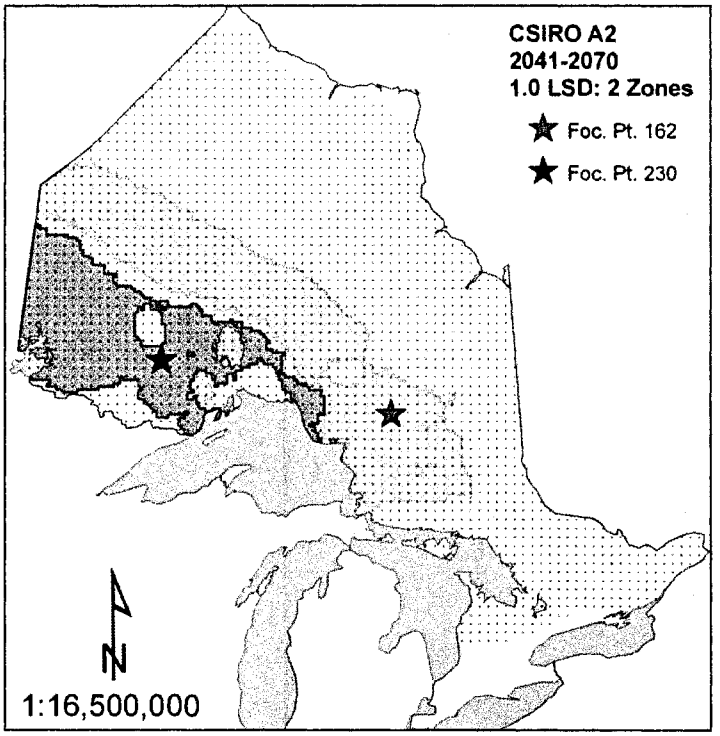

Figure 163. Optimal zones for 2041-2070 based on 2 breeding zones for the CSIRO A2 scenario.

The total coverage reaches 48.3% for the optimal 3-zone solution with the selection of focal point 382 (Figure 164). Breeding zone 382 is also latitudinally-restricted and spans the entire northern width of the province. It runs from 55°N at the Manitoba border, southeast to the shore of James Bay along the Quebec border at 50°N. In comparison to the 2-zone solution, the two zones occupying the northwest region (187,230) are similar and there is still no overlap between zones.

The selection of focal point 377 increases coverage to 60.3% for the optimal 4-zone solution (Figure 165). Breeding zone 377 is located between the previous 2 elongate zones (162, 382) and runs southeast from 54°N to 49°N. It overlaps very slightly along the borders of the two adjacent zones. The other 3 zones are very similar in comparison to the previous solution.

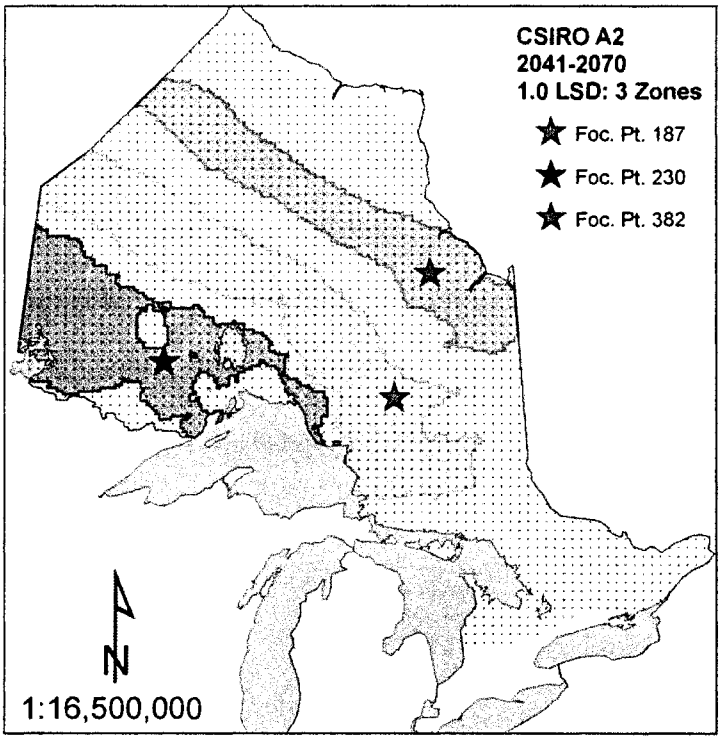

Figure 164. Optimal zones for 2041-2070 based on 3 breeding zones for the CSIRO A2 scenario.

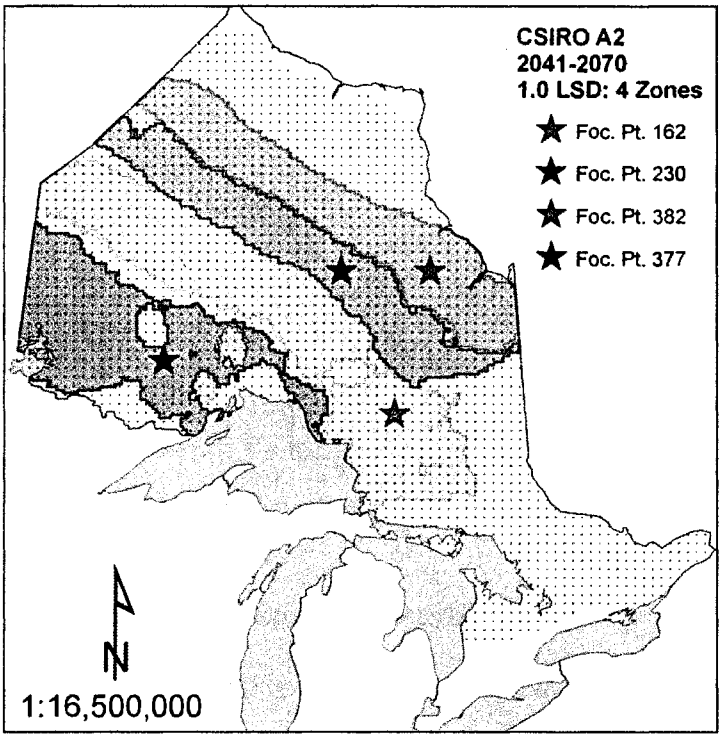

Figure 165. Optimal zones for 2041-2070 based on 4 breeding zones for the CSIRO A2 scenario.

Total coverage for the optimal 5-zone solution is 68.2% with the selection of focal point 103 (Figure 166). Unlike the previous four zones, breeding zone 103 is fairly broad, running from the shore of Lake Huron to the Hearst area. It also occupies a small disjunct area of the southern region. The remaining zones are very similar in comparison with the 4-zone solution. However, the borders of the 3 mid-latitudinal bands (195, 382, and 351) no longer overlap. The border of the first latitudinal zone (185) overlaps slightly with zone 103 in the northeast, and also with zone 230 in the northwest.

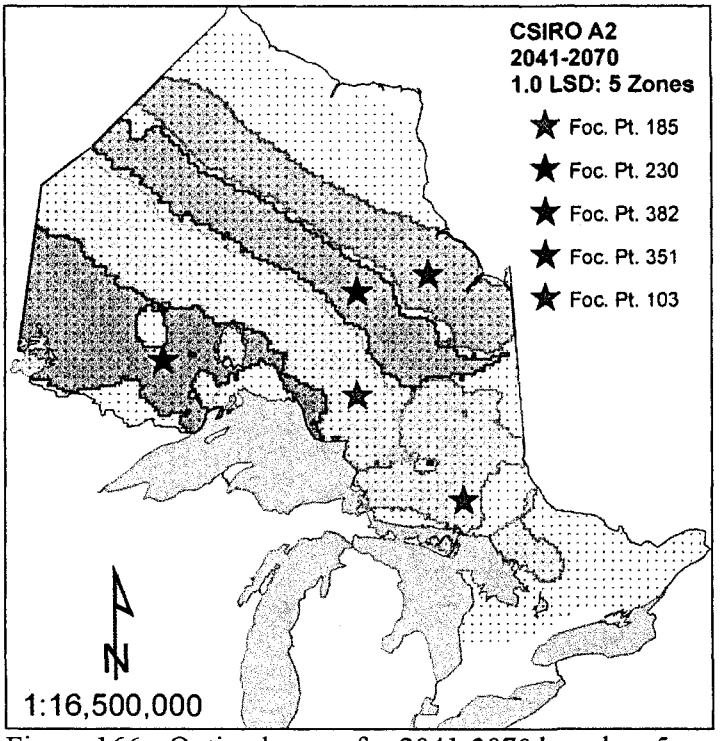

Figure 166. Optimal zones for 2041-2070 based on 5 breeding zones for the CSIRO A2 scenario.

The selection of focal point 457 increases coverage to 75.9% (Figure 167). Breeding zone 457 is located to the immediate north and on the same northwest-southeast orientation as the previous 3 elongate zones. It spans from the Manitoba

border southeast to James Bay. In comparison with the 5-zone solution, breeding zone 216 now excludes a small area in the northwest along the Manitoba border and includes a small, disjunct area in the northeast. The broad northeast zone (63) has expanded to include the previously discontinuous area in the south.

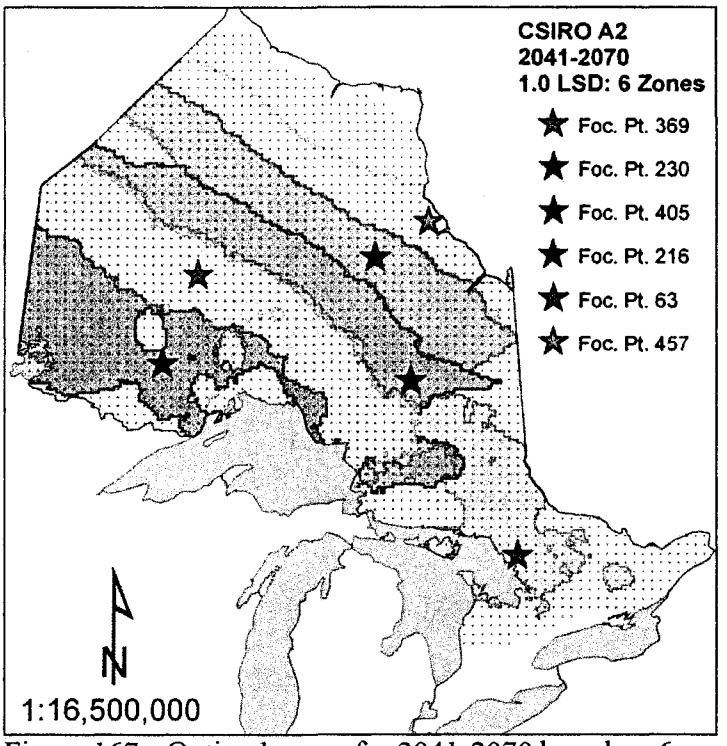

Figure 167. Optimal zones for 2041-2070 based on 6 breeding zones for the CSIRO A2 scenario.

The selection of breeding zone 537 in the far north increases total coverage to 81.9% (Figure 168). Otherwise, the optimal 7-zone solution is virtually identical to the 6-zone solution with the exception of a small increase in overlap between breeding zones 404 and 216.

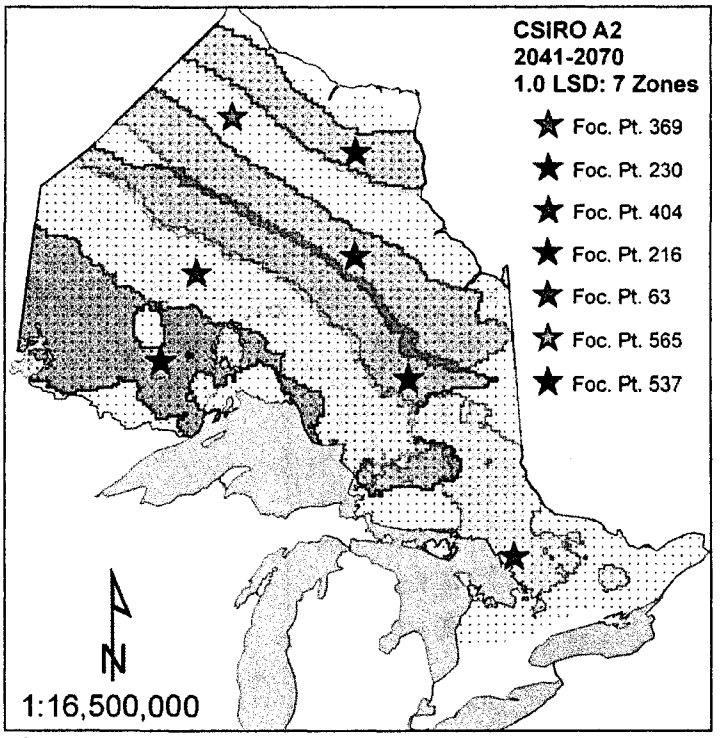

Figure 168. Optimal zones for 2041-2070 based on 7 breeding zones for the CSIRO A2 scenario.

The breeding zones constructed based on CSIRO A2 for 2041-2070 are similar in geographic pattern, but much more latitudinally-restricted in comparison to 1961-1990 zones (Figure 29). The northeast region zone (63) for the CSIRO A2 solution moderately resembles disjunct northeastern zone (146) of the 1961-1990 solution. Zones 369 and 216 combined somewhat resemble the broad central zone (345) of the 1961-1900 solution, while zones 404 and 565 combined resemble the mid-northern zone (508) of the 1961-1990 solution. Zone 537 is similar to, but approximately half as wide as the northern zone (598) of the 1961-1990 solution.

Figure 169 to Figure 176 present the optimal solution for CSIRO B2 for 1 through 8 zones, based on the achievement of 80% total coverage. For the optimal 1-zone solution, the selection of focal point 230 results in 14.3% total coverage (Figure

169). Breeding zone 230 covers much of the western portion of the northwest region, stretching from the Manitoba border east to the Thunder Bay area. Interestingly, the first and second zones are added in reverse order for CSIRO B2 in comparison to CSIRO A2.

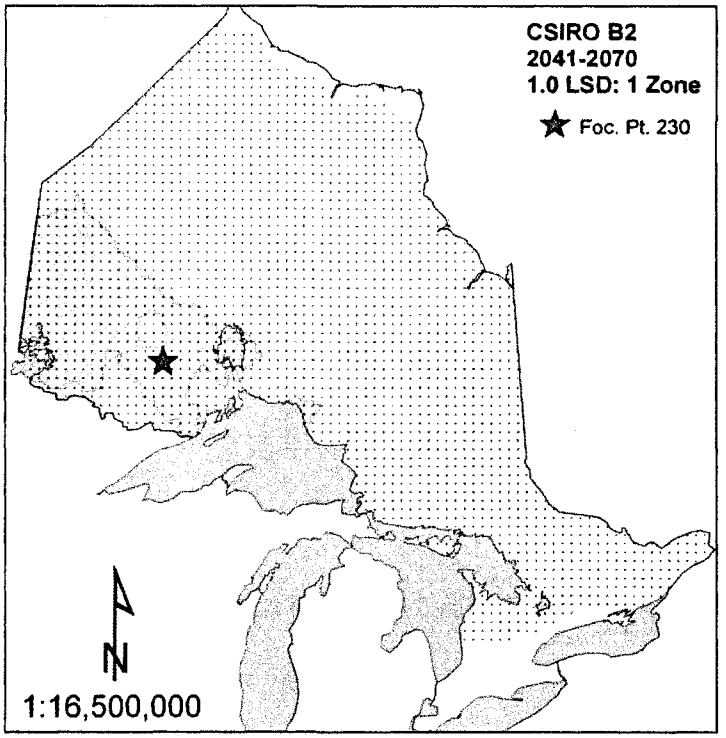

Figure 169. Optimal zones for 2041-2070 based on 1 breeding zone for the CSIRO B2 scenario.

The selection of focal point 370 increases total coverage to 27.6 % for the optimal 2-zone solution (Figure 170). Breeding zone 370 is latitudinally-restricted, spanning approximately 2° latitude along its breadth. This zone runs from approximately 53°N along its western boundary to 49°N in the east. Although the two zones meet along their adjacent borders, they do not appear to overlap.

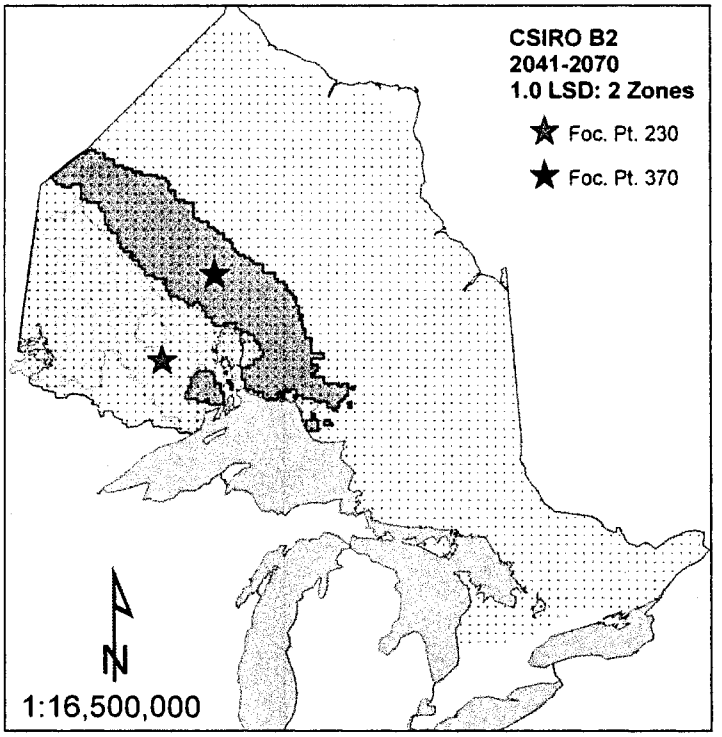

Figure 170. Optimal zones for 2041-2070 based on 2 breeding zones for the CSIRO B2 scenario.

The optimal 3-zone solution reaches 39.7% total coverage with the selection of focal point 495 (Figure 171). Breeding zone 495 is similar in similar in size and shape to zone 370, but is shifted north and eastward. It runs from James Bay northwest approximately 845 km. The other two breeding zones (230, 370) are unchanged from the 2-zone solution.

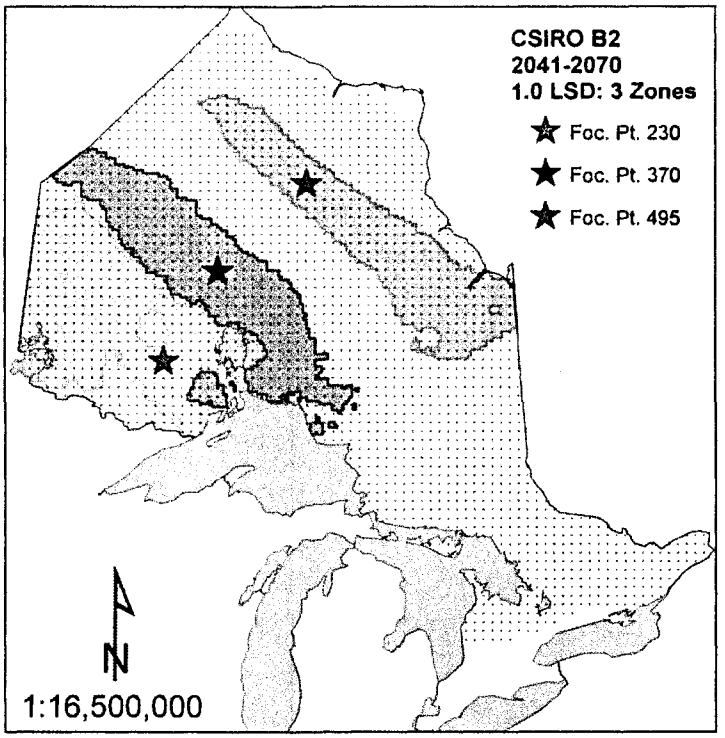

Figure 171. Optimal zones for 2041-2070 based on 3 breeding zones for the CSIRO B2 scenario.

Total coverage for the optimal 4-zone solution increases to 50.4% with the selection of focal point 510 (Figure 172). Breeding zone 510 is located immediately to the south and overlaps slightly with the previous zone (475). Otherwise, the breeding zone locations are very similar to the 3-zone solution. Breeding zone 510 is virtually identical in shape to zone 475, but is shifted just to the southwest. It runs from 92°W along its western border to 82°W along its eastern border.

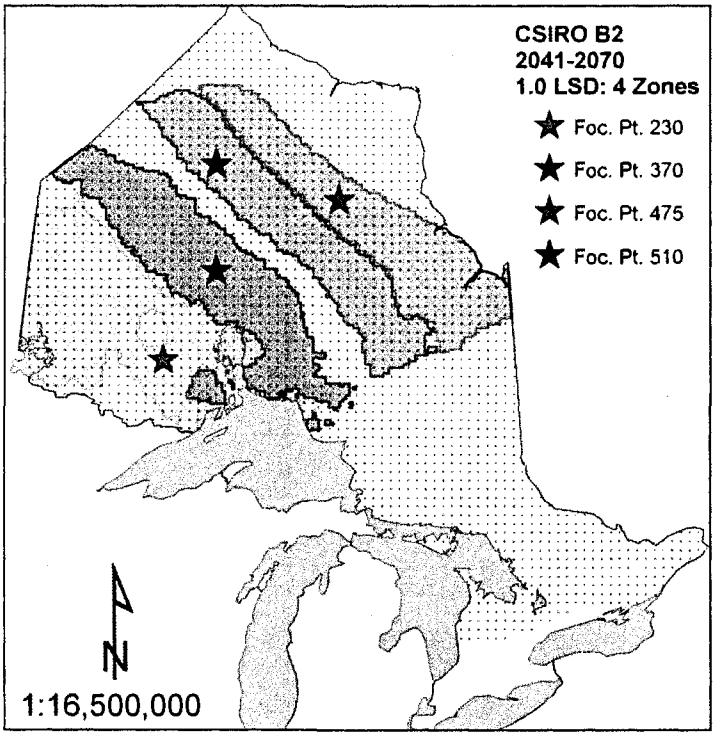

Figure 172. Optimal zones for 2041-2070 based on 4 breeding zones for the CSIRO B2 scenario.

The optimal 5-zone solution reaches 60.0% coverage with the selection of focal point 103 in the northeast (Figure 173). Breeding zone 103 occupies most of the northeast region, and also two discontinuous areas in the southern region. The 4 remaining zones remained unchanged in comparison the optimal 4-zone solution.

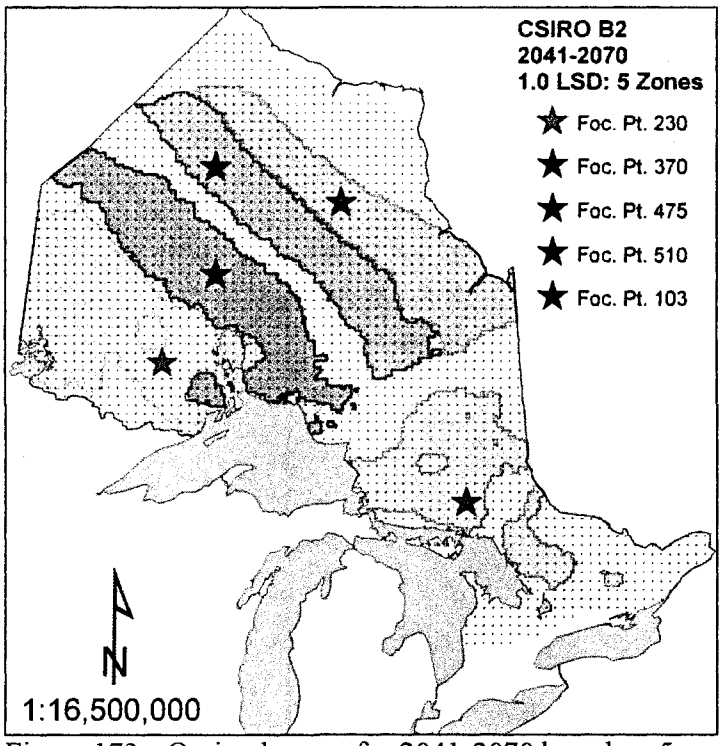

Figure 173. Optimal zones for 2041-2070 based on 5 breeding zones for the CSIRO B2 scenario.

The selection of focal point 423 increases coverage to 68.2% (Figure 174). Breeding zone 423 occupies the previously uncovered area in the central latitudes of the province and is similar in shape and orientation to the other 3 elongate zones. The northern and southern borders of breeding zone 423 overlap very slightly with the two adjacent zones. In comparison with the 5-zone solution, the two northernmost zones have shifted slightly northward. Otherwise, the zones are very similar.

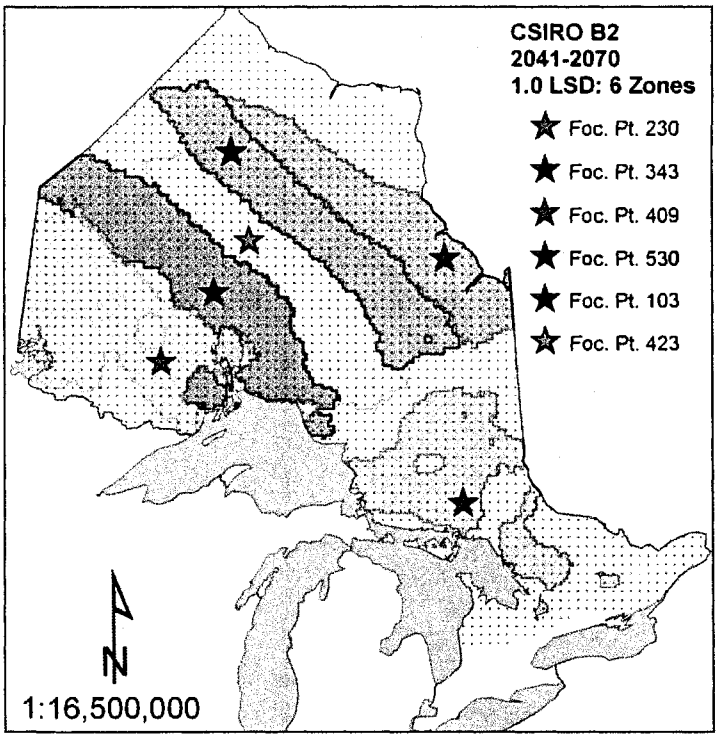

Figure 174. Optimal zones for 2041-2070 based on 6 breeding zones for the CSIRO B2 scenario.

The total coverage reaches 75.5% with the selection of focal point 77 in the south (Figure 175). Breeding zone 77 covers the majority of the area to the north of Lake Huron, and overlaps slightly with the northeast breeding zone (189) along its western border. It is notably fragmented, occupying numerous tiny areas throughout the south. In comparison to the optimal 6-zone solution, the northeast zone is has expanded northward and no longer contains the discontinuous area to the south. The remaining zones are very similar.

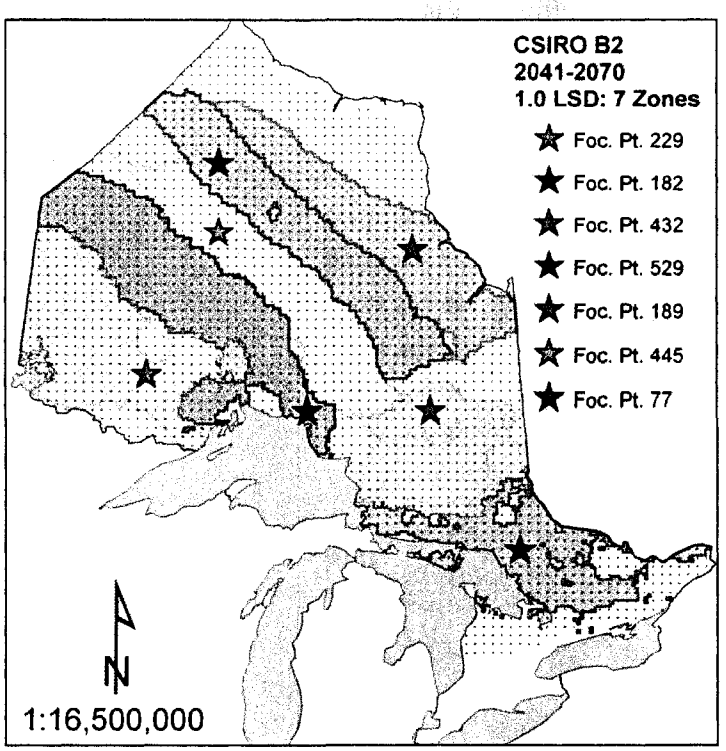

Figure 175. Optimal zones for 2041-2070 based on 7 breeding zones for the CSIRO B2 scenario.

The selection of focal point 584 increases the total coverage to 81.5% for the optimal 8-zone solution (Figure 176). Breeding zone 584 occupies the furthest northern latitudes of the province adjacent to Hudson Bay. The remaining zones are remain unchanged or are largely similar to the 7-zone solution. A small area of overlap is evident along the adjacent boundaries of the two northernmost zones.

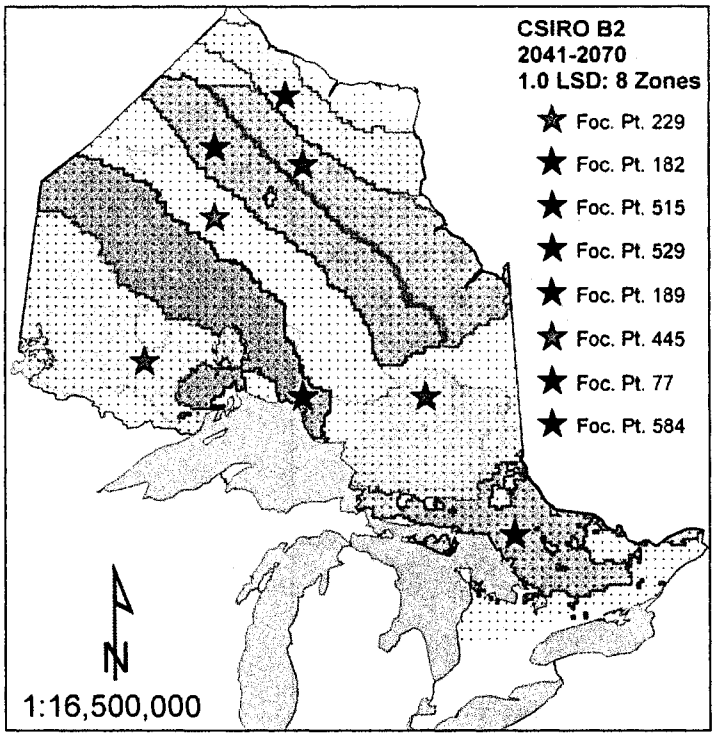

Figure 176. Optimal zones for 2041-2070 based on 8 breeding zones for the CSIRO B2 scenario.

The optimal 8-zone solution based on CSIRO B2 for 2041-2070 bears moderate similarity to breeding zones constructed for 1961-1990 climate (Figure 29). Both solutions indicate a single broad breeding zone can be used to cover most of the northwest region, and select a somewhat round zone to cover most of the northeast. The area immediately north of Lake Huron requires a separate zone, indicating that this area is adaptively dissimilar to the rest of the northeast. Finally, both the CSIRO B2 (2041-2070) and 1961-1990 solutions indicate that a separate breeding zone is required to cover most of the far north adjacent to Hudson Bay. In contrast, the central latitudes of the province indicate very different zone boundaries between the CSIRO B2 and 1961-1990 solutions. The 1961-1990 solution indicates that one broad central zone can be used to cover most of the northwest, while the CSIRO B2 solution indicates that several

very narrow zones are necessary. The CSIRO solution does not indicate that the northwest zone can also be used to cover portions of the northeast and southern regions.

DISCUSSION

Principal components factor scores grids for each of the six scenarios indicate that mean growth potential is expected to increase across the study area by 2041-2070, with increases in temperature ranging from 2.3°C for CGCM2 B2 to 4.6°C for CSIRO A2.

For a given percent of total coverage, fewer breeding zones are required based on the Hadley A2 & B2 scenarios in comparison with CGCM2 and CSIRO (Figure 141). Of the six scenarios studied, Hadley A2 bears the greatest similarity to zones constructed based on 1961-1990 climate normals, and also indicates the greatest average growth potential. Both the A2 and B2 scenarios indicate increases in temperature and precipitation in comparison to 1961-1990 normals. Based on the mean values of regression variables, increases in mean temperature are expected to be 2.9°C for the A2 scenario and 2.8°C for the B2 scenario, while average precipitation is expected to increase by 6.4 and 3.1 mm, respectively.

The CGCM2 model indicates principal components factor scores which are most similar to those of 1961-1990. Temperatures in 2041-2070 are expected to increase by 2.64°C for the A2 scenario and by 2.3°C for the B2 scenario, while precipitation is expected to increase less than 1 mm on average for both scenarios. Breeding zones based on CGCM2 are similar but somewhat narrower than HADCM3 zones, and provide intermediate coverage in comparison to the other 2 models.

In contrast, future breeding zones based on CSIRO are much narrower in comparison to HADCM3 and CGCM2 and bear relatively little similarity to 1961-1990

zones. Estimates of future warming are the most extreme of the 3 models, with predicted average increases of 4.6°C based on the A2 scenario, and increases of 4.0°C based on the B2 scenario. Future precipitation patterns for the A2 and B2 scenarios are variable in comparison with 1961-1990, ranging from a decrease of 9.8 mm for August precipitation to an increase of 8.8 mm for October precipitation, and a decrease 15.4 mm based on February precipitation to 9.0 for January precipitation, respectively. Despite their narrower breadth, the CSIRO are still somewhat similar to HADCM3 and CGCM2 as they occupy much the same areas but generally require 2 zones to represent to an equivalent area in the other 2 scenarios.

It is not surprising that A2 zones are somewhat narrower in comparison with B2 zones for each of the three models, given the greater climatic change predicted by the A2 scenario resulting from a more extreme emissions scenario (Nakicenovic and Swart 2000). However, it is interesting that for each of the three models, optimal solutions based on the A2 scenario achieve relatively greater coverage for a specified number of zones, due to the lesser degree of overlap.

The CGCM2 model indicates the lowest average increases in future temperature of the 3 models examined. Therefore, it appears that the CGCM2 model is the most moderate of the 3 in predicting future temperature increases, followed by HADCM3 with intermediate warming, and CSIRO at the most extreme. This is an interesting result, as the Hadley model generates zones that are broader in comparison to CGCM2 and CSIRO and also bears the greatest similarity to current breeding zones. Iverson and Prasad (2002) reported that the Hadley model was the most moderate of 5 models used to predict species range shifts due to climate change; however, the CGCM2

and CSIRO models were not among those studied. In the current study, HADCM3 and CGCM2 may be considered fairly comparable, as they both indicate similar rates of future warming.

The degree of similarity between current breeding zones and zones developed for CGCM2 and HADCM3 based on the A2 and B2 scenarios is striking. One might expect zones to be widely divergent due to much different predictions of future change based on the various scenarios. However, the contour maps for each of the 9 variables used to predict performance indicate that, while the climate in a particular area may differ by several degrees between these scenarios, broad-scale climatic patterns are generally similar. This tends to support the widely noted observation that the majority of models are accurate in evaluating large-scale climatic processes but are relatively limited in their ability to reproduce regional climatic variation (IPCC 2007b). Thus, the transition from current to future breeding programs may be relatively straightforward, as only the CSIRO zones indicate that a widespread restructuring of breeding zones may be necessary. However, it is important to note that, despite having similar boundaries, the breeding zones of the future will be associated with much different expectations of white spruce performance.

The predicted increase in growth potential across the study area is in contrast to previous studies reporting that white spruce growth is expected to decrease due to climate change (Andalo *et al.* 2005; Cherry and Parker 2003; Rweyongeza *et al.* 2007). Transfer models used to predict growth of white spruce in Quebec indicated that under scenarios of 1° and 4°C of warming, height and diameter growth are predicted to decrease significantly (Andalo *et al.* 2005), while similar models for Ontario indicate

that productivity is expected to decrease with 3°C warming for all but the northernmost provenances (Cherry and Parker 2003). Rweyongeza *et al.* (2007) found that growth will either increase or decrease depending on provenance location; central sources were predicted to be most negatively affected, followed by southern sources, while northern sources were expected to benefit from increased temperatures.

The disagreement between this and previous studies can be explained by the different approaches used to model white spruce response to climate. While the previous studies used quadratic functions (Andalo *et al.* 2005; Cherry and Parker 2003; Rweyongeza *et al.* 2007), the current study uses linear regression models. The use of quadratic functions inherently implies that there is some optimum temperature above or below which growth decreases (Matyas 1994; Raymond and Lindgren 1990). However, the use of linear models implies that growth does not demonstrate any specific optimum within the range of temperatures examined, but increases or decreases constantly. The positive coefficient of September maximum temperature used to predict PC1 factor scores implies that increased temperature is always expected to increase growth if precipitation does not become limiting. Thus, all future climate scenarios indicate an increase in growth potential in comparison with current climate conditions because precipitation remains adequate.

The results of the previous studies imply that the use of linear growth models may somewhat oversimplify the relationship between growth and climate across some parts of the range, and that predictions of increased growth should be treated with some caution when applied to southern and central sources (Andalo *et al.* 2005; Cherry and Parker 2003; Rweyongeza *et al.* 2007). However, linear models were considered

preferable for the current study because they allow the use of multiple climatic predictor variables. In contrast, quadratic models are fundamentally constrained to a maximum of 1 or 2 predictor variables (Raymond and Lindgren 1990) and, thus, may not account for all important climate variables.

It is possible that predictions of future growth potential may not be fully realized due to the increased likelihood of spring frost damage in the future. Cannell and Smith (1986) found that increased spring temperatures corresponded with earlier flushing dates and a greater risk of frost damage in Britain, as temperatures on the date of budflush were generally colder than on historical flushing dates. Beuker and Koski (1997) found that budflush dates were at least 10 days earlier in years with early springs when compared to years with relatively late springs. Thus, a greater risk of spring frost damage may be expected for scenarios which indicate earlier phenology. Even when dates of spring budflush remain constant, climate change may lead to decreased growth if early frost events are more frequent and extreme (Andalo *et al.* 2007; Beuker and Koski 1997).

The reliability of future breeding zones depends both on the accuracy of future climate predictions (Cherry and Parker 2003) and on the validity of the models used to predict performance (Rehfeldt 1991). There is a great deal of uncertainty in predicting future climate as a result of disagreement in scenarios of future greenhouse gas emissions, and because each of the models yields slightly different results (McKenney *et al.* 2007). Thus, the future zones are only as accurate as the climate models used to construct them. The IPCC (2007b) notes that there is a great deal more uncertainty in future precipitation estimates than in temperature. Given that 6 of 9 climate variables

used to describe adaptive variation of white spruce are based on precipitation, the seed zones presented here will inherently be subject to more uncertainty than if zones were constructed based on temperature alone. Thus, future breeding zones were modeled at the 1.0 LSD level to provide a more generalized illustration of future zone boundaries.

Regression models are only valid assuming that the relationship between climate and performance does not change in the future (Rehfeldt 1991). If one of the variables becomes more limiting, or some other climatic factor that is not considered becomes limiting, then the accuracy of predictions will be compromised. The validity of the regression models in predicting performance under future climate cannot be readily examined without the use of greenhouse or growth chamber trials simulating future conditions. However, the model presented here provide reasonable means of evaluating shifts in future breeding zones in the absence of such tests.

It is important to understand that, by this approach, the focal points no longer represent the location of a seed orchard that can be used to regenerate the surrounding zone, nor do the breeding zones represent areas of similarity from which adapted seed can be collected for inclusion within the breeding program. Rather, the focal points represent the center of a climate zone where future performance is expected to be similar based on similarity of temperature and precipitation patterns. Thus, the determination of seed sources that are adequately pre-adapted to the environments of future zones is a task that must be considered separately.

Xiao (2005) presented a method of using the focal point seed zones procedure to determine the present location of seed sources expected to be adequately pre-adapted to future regeneration sites. This method uses the predicted future climate at the

planting location (focal point) to determine seed sources that currently originate from similar environments. Because these sources have evolved under conditions similar to those predicted to occur at the focal point, they are assumed to be adequately pre-adapted. Suitable future planting sites can be determined using a similar procedure; the current climate at seed source origin is determined and GIS is used to locate areas with similar future climates.

Using this approach, Xiao (2005) found that well-adapted seed sources are generally located south or southeast of future planting locations. A similar pattern has been shown for other boreal species including black spruce (Riddell 2004) and jack pine (Thomson and Parker 2008), indicating that the best future planting locations will shift northward several degrees, while best-matched future sources originate from south of future regeneration sites.

It is, therefore, reasonable to assume that white spruce seed sources for future breeding zones will come from zones which currently lie to the south. Similarly, seed from current 1st and second generation orchards could be used to provide high performance, well-adapted stock to more northern zones in the future. Thus, much of the investments in current breeding programs can be salvaged by deploying improved seed to locations in which it will be adequately adapted to future conditions. However, over the long term as orchard productivity begins to decline due to climate change, additional sources of seed will be necessary. Therefore, adaptively matched seed for future zones can be identified using the approach of Xiao (2005) and incorporated into breeding programs.

Within areas identified as adaptively similar, factor scores on the first principal component axis can be used to determine sources with the highest growth potential (Parker 1992). Alternatively, population response functions can be used to determine the fastest-growing sources (Lesser 2005) or sources with the greatest range of environmental tolerance (Rehfeldt 1990). Thus, the location of top-performing provenances/families can be estimated before the breeding program is established.

One of the disadvantages of the current methodology is that adaptive matches between present and future climates are not readily apparent; one must return to the grids of principal components factor scores for current and future scenarios to make such a determination. However, a relatively straightforward modification to the focal point seed zones program could be used to accomplish this. For each focal point, future factor scores could be retrieved and used to locate similar areas on current factor scores grids, which could then be intersected to generate an adaptive match.

Although future breeding zones were constructed for the entire area of Ontario, these zones probably do not accurately reflect the extent of white spruce management in the future. Climate envelope studies of white spruce indicate that the range will shift northward over the next century (Thiberville and Parker 2007). Thus, despite factor score grids indicating high growth potential in the southern parts of the range, it is possible that these areas will be unsuitable or marginal in 2041-2070 because they may exceed the environmental tolerance limits of the species. Even if southern areas continue to offer suitable habitat, adapted seed sources may not be available, as seed sources would have to be collected from further south, outside of the species range (Xiao 2005). In contrast, more favorable conditions in the far north may allow white spruce

management to extend much further northward in the future (Cherry and Parker 2003; Rweyongeza *et al.* 2007).

The IPCC's unwillingness to assign probabilities to predictions of climate based on various models and emissions scenarios makes it difficult to suggest any one of the solutions for implementation; rather, the IPCC recommends considering each of the scenarios as equally probable. Thus, the ultimate design of future breeding zones will depend on the refinement of general circulation models, as well as more accurate predictions of the likely scenario of greenhouse gas emissions. However, as more accurate predictions of future warming become available, the zones can reevaluated and additional sources can be incorporated into breeding programs if necessary.

CONCLUSION

The delineation of current optimal breeding zones in Ontario represents an important step in ensuring adequate growth and survival of improved white spruce seedlings. The benefit of such zones can be realized through an increase in both forest productivity and forest health, which may provide greater resistance against pests and disease that are likely to be more frequent under climate change. When and if the results presented herein are used to implement fixed breeding zones in Ontario, optimal seed sources for each breeding zone can be determined. While one could select from the fastest growing sources within each zone, it may be more prudent to select sources with greater breadth of suitable habitats that may perform well under a variety of future climate change scenarios.

Future breeding zones provide critical insights as to how patterns of adaptive variation may shift over the next several decades due to climate change. While it is yet unclear which, if any of these future scenarios may be ultimately realized, the results indicate that changes in forest management practices will be necessary to maintain adaptation of white spruce seedlings. When used with the focal point seed zones approach, these zones provide an excellent means of determining genotypes that will be best adapted for deployment within each zone. This approach can therefore be used to determine sources for inclusion into current breeding programs which may be bred with current stock to produce genotypes adapted to interim climates. As more reliable

estimates of future climate become available, the breeding zones can be readily refined using the methods presented herein.

LITERATURE CITED

Aitken, S.N., S. Yeaman, J.A. Holliday, T. Wang, and S. Curtis-McLane. 2008. Adaptation, migration, or extirpation: climate change outcomes for tree populations. Evolutionary Applications. 1:95-111.

Andalo, C., J. Beaulieu, and J. Bosquet. 2005. The impact of climate change on growth of local white spruce populations in Quebec, Canada. Forest Ecology and Management. 205:169-182.

Beaulieu, J. M. Perron, and J. Bousquet. 2004. Multivariate patterns of adaptive genetic variation and seed source transfer in *Picea mariana*. Can. J. For. Res. 34:531-545.

Becker, H.F. 1961. Oligocene Plants from the Upper Ruby River Basin, South-western Montana. The Geological Society of America, New York, NY. 127 pp.

Bennuah, S.Y., T. Wang, and S.N. Aitken. 2002. Genetic analysis of the *Picea sitchensis* x *glauca* introgression zone in British Columbia. Forest Ecology and Management. 197: 65-77.

Betz, G. 2007. Probabilities in climate policy advice: a critical comment. Climatic Change. 85: 1-9.

Beuker, E., and V. Koski. 1997. Adaptation of tree populations as reflected by aged provenance tests PP 103-108 *in* Matyas, C. (ed.) Perspectives of forest genetics and tree breeding in a changed world. IUFRO Word Series Vol. 6. IUFRO Secretariat, Vienna, Austria. 158 pp.

Van Buijtenen, J.P. 1992. Fundamental genetic principles pp 29-68 *in* Fins, L., S. Friedman and J. Brotschol (eds.) Handbook of Quantitative Forest Genetics. Kluwer Academic Publishers, Boston, Mass. 402 pp.

Campbell, R.K. 1979. Genecology of Douglas-fir in a watershed in the Oregon cascades. Ecology. 60:1036-1050.

Campbell, R.K. 1986. Mapped genetic variation of Douglas-fir to guide seed transfer in southwest Oregon. Silvae Genetica. 35: 85-96.

Campbell, R.K., and F.C. Sorensen. 1978. Effect of test environment of expression of clines and delimitation of seed zones in Douglas-fir. Theor. Appl. Genet. 51:233-246.

Cannell, M.G., and R.I. Smith. 1986. Climatic warming, spring budburst and frost damage on trees. J. Appl. Ecol. 23:177-191.

Carter, K.K. 1996. Provenance tests as indicators of growth response to climate change in 10 north temperate species. Can. J. For. Res. 26:1089-1095.

Chatterjee, S., and B. Price. 1977. Regression analysis by example. John Wiley & Sons, Inc., New York, NY.

Cherry, M., and W.H. Parker. 2003. Utilization of genetically improved stock to increase carbon sequestration. Forest Research Report No. 160. Queen's Printer for Ontario, Sault ste. Marie, ON. 15 pp.

Corriveau, A., J. Beaulieu, and F. Mothe. 1987. Wood density of natural white spruce populations in Quebec. Can. J. For. Res. 17:675-682.

Covey, C., K.M. AchutaRao, U. Cubasch, P. Jones, S.J. Lambert, M.E. Mann, T.J. Phillips, K.E. Taylor. 2003. An overview of results from the coupled model intercomparison project (CMIP). Global and Planetary Change. 37:103-133.

Crowe, Kevin A, and W.H. Parker. 2005. Provisional breeding zone location modeled as a maximal covering location problem. Can. J. For. Res. 35:1173-1182

Crowe, K.A., and W.H. Parker. 2008. Using portfolio theory to guide reforestation and restoration under climate change scenarios. Climatic Change. In press.

Daubenmire, R. 1974. Taxonomic and ecologic relationships between Picea glauca and Picea engelmannii. Can. J. For. Res. 52: 1545-1560.

Davis, M.B., and R.G. Shaw. 2001. Range shifts and adaptive responses to quaternary climate change. Science. 292:673-679.

ESRI. 2006. ArcGIS Desktop 9.2. ESRI Inc., Redlands, CA.

Etterson, J.R., and R.G. Shaw. 2001. Constraint to adaptive evolution in response to global warming. Science. 294:151-154.

Flato, G.M. and G.J. Boer. 2001. Warming asymmetry in climate change simulations. Geophysical Research Letters. 28: 195-198.

Furnier, G.R., C.A. Mohn, and M.A. Clyde. 1991. Geographic patterns of variation in allozymes and height growth in white spruce. Can. J. For. Res. 21:707-712.

Gordon, C., C. Cooper, C.A. Senior, H. Banks, J.M. Gregory, T.C. Johns, J.F.B. Mitchell, R.A. Wood. 2000. The simulation of SST, sea ice extents and ocean heat transport in a version

of the Hadley Centre coupled model without flux adjustments. Climate Dynamics. 16:147-168.

Gordon, H.B, and S.P. O'Farrell. 1997. Transient climate change in the CSIRO coupled model with dynamic sea ice. Monthly Weather Review. 125:875-907.

Hamann, A., M.P. Koshy, G. Namkoong, and C.C. Ying. 2000. Genotype x environment interactions in *Alnus rubra*: developing seed zones and seed-transfer guidelines with spatial statistics and GIS. Forest Ecology and Management. 136:107-119.

Hills, G.A. 1959. A ready reference to the description of the land of Ontario and its productivity. Preliminary Report. Ontario Department of Lands and Forests, Division of Research, Toronto, ON. 34 pp.

Hofgaard, A., J. Tardif, and Y. Bergeron. 1999. Dendroclimatic response of *Picea mariana* and *Pinus banksiana* along a latitudinal gradient in the eastern Canadian boreal forest. Can. J. For. Res. 29:1333-1346.

Hulme, M., T. Osborn, J. Jones, K. Briffa, and P. Jones. 1999. Climate observations and GCM validation. Draft Report. Climatic Research Unit Norwich. 70 pp.

IPCC. 2007a. Climate Change 2007: Synthesis Report. Cambridge University Press, Cambridge, UK. 52 p.

IPCC. 2007b. Climate Change 2007: The Physical Science Basis. Cambridge University Press, Cambridge, UK. 996 p.

Iverson, L.R., and A.M. Prasad. 2002. Potential redistribution of tree species habitat under five climate change scenarios in the eastern US. Forest Ecology and Management. 155:205-222.

Iverson, L.R., A.M. Prasad, S.N. Matthews, and M. Peters. 2008. Estimating potential habitat for 134 eastern US tree species under six climate scenarios. Forest Ecology and Management 254:390-406.

Jaramillo-Correa, J.P., J. Bosquet, and J. Beaulieu. 2001. Contrasting evolutionary forces driving population structure at expressed sequence tag polymorphisms, allozymes, and quantitative traits in white spruce. Molecular Ecology. 10:2729-2740.

Khalil, M.A.K. 1985. Genetic variation in eastern white spruce (*Picea glauca* (Moench) Voss) populations. Can. J. For. Res. 15:444-452.

Lambert, S.J., and G.J. Boer. 2001. CMIP1 evaluation and intercomparision of coupled climate models. Climate Dynamics. 17:83-106.

Lempert, R., N. Nakicenovic, and M. Schlesinger. 2004. Characterizing climate change uncertainties for decision-makers. Climatic Change. 65:1-9.

Lenihan, J.M., and R.P. Neilson. 1995. Canadian vegetation sensitivity to climatic change at three organizational levels. Climatic Change. 30:27-56.

Lesser, M. 2005. Genecology, patterns of adaptive variation and a comparison of focal point seed zone development methodologies for white spruce (*Picea glauca*). MScF Thesis, Lakehead University, ON. 259 pp.

Lesser, M.R. and W.H. Parker. 2004. Genetic variation in *Picea glauca* for growth and phenological traits from provenance tests in Ontario. Silvae Genetica. 53:141-148.

Lesser, M.R, and W.H. Parker. 2006. Comparison of canonical correlation and regression based focal point seed zones of white spruce. Can. J. For. Res. 36:1572-1586.

Li, P., Beaulieu, J., and J. Bosquet. 1997. Genetic structure and patterns of genetic variation among populations in eastern white spruce (*Picea glauca*). Can. J. For. Res. 27:189-198.

Li, P., A. Corriveau, and J. Bosquet. 1993. Genetic variation in juvenile growth and phenology in a white spruce provenance-progeny test. Silvae Genetica. 42:52-60.

Lindgren, D. and C.C. Ying. 2000. A model integrating seed source adaptation and seed use. New Forests 20:87-104.

Matyas, C. 1994. Modeling climate change effects with provenance test data. Tree Physiology. 14:797-804.

Matyas, C. 1997. Effects of environmental change on the productivity of tree populations pp 109-121 *in* Matyas, C. (ed.) Perspectives of Forest Genetics and Tree Breeding in a Changing World. IUFRO Word Series Vol. 6. IUFRO Secretariat, Vienna, Austria. 158 pp.

Matyas, C., and C.W. Yeatman. 1992. Effect of geographical transfer on growth and survival of jack pine (*Pinus banksiana* Lamb.) populations. Silvae Genetica. 41:370-375.

McKenney, D., P. Papadopol, K. Lawrence, K. Campbell, and M. Hutchinson. 2007. Customized spatial climate models for Canada. Frontline Technical Note No. 108. Canadian Forest Service, Great Lakes Forestry Centre, Sault Ste. Marie, ON. 7 pp.

McKenney, D.W., J.H. Pedlar, K. Lawrence, K. Campbell, and M.F. Hutchinson. 2007. Potential impacts of climate change on the distribution of North American Trees. BioScience.57:939-948.

McKenney, D., D. Price, P. Papadopol, M. Siltanen, and K. Lawrence. 2006. High-resolution climate change scenarios for North America. Frontline Technical Note No. 107. Canadian Forest Service, Great Lakes Forestry Centre Sault Ste. Marie, ON. 5 pp.

Mohn, C.A., D.E. Reimenschneider, W. Cromell, and L.C. Peterson. 1976. A white spruce progeny test-seedling seed orchard pp 98-107 *in* 12th Lake States Forest Tree Improvement Conference. Chalk River, Ontario: USDA Forest Service North Central Forest Experiment Station, General Tech. Report NC-26.

Morgenstern, E.K. 1996. Geographic Variation in Forest Trees. UBC Press, Vancouver, BC. 208 pp.

Morgenstern, E.K., and P. Copis. 1999. Best white spruce provenances in Ontario. Information Report ST-X-16. Natural Resources Canada.

Nakicenovic, N., and R. Swart. 2000. Special Report on Emissions Scenarios: A Special Report of Working Group III of the Intergovernmental Panel on Climate Change. Cambridge University Press, New York, NY.

Nienstadt, H. 1985. Inheritance and correlations of frost injury, growth, flowering, and cone characteristics in white spruce, *Picea glauca* (Moench) Voss. Can. J. For. Res. 15:498-504.

Nienstadt, H., and D.E. Riemenschneider. 1985. Changes in heritability estimates with age and site in white spruce, *Picea glauca* (Moench) Voss. 1985. Silvae Genetica. 34:34-41.

Nienstadt, H, and A. Teich. 1972. Genetics of White Spruce. For. Serv. Res. Pap. WO-15. USDA.

O'Neill, G.A., and S.N. Aitken. 2004. Area-based breeding zones to minimize maladaptation. Can. J. For. Res. 34:695-704.

Park, Y.S., D.P. Fowler, and J.F. Coles. 1984. Population studies in white spruce. II. Natural inbreeding and relatedness among neighbouring trees. Can. J. For. Res. 14:909-913.

Parker, W.H. 1992. Focal point seed zones: site-specific seed zone delineation using geographic information systems. Can. J. For. Res. 22:267-271.

Parker, W.H. 2000. Rates of change of adaptive variation in *Picea mariana* visualized by GIS using a differential systematic coefficient. New Forests. 20:259-276.

Parker, W.H. 2008. Intraclass correlation coefficients of jack pine, black spruce, and white spruce from Canadian Forestry Service range-wide provenance tests. Unpublished Data.

Parker, W.H., and K.A. Crowe. 2005. Adjustments to seed source selections and breeding zones to compensate for predicted climate change in Ontario. Proposal to the Enhanced Forest Productivity Science Program. 13 pp.

Parker, W.H., and A. van Niejenhuis. 1996a. Seed zone delineation for jack pine in the former northwest region of Ontario using short-term testing and geographic information systems. Tech. Rep. NODA/NFP TR-35. Nat. Res. Can., Canadian Forestry Service, Great Lakes Forestry Centre, Sault Ste. Marie, ON. 34 pp.

Parker, W.H., and A. van Niejenhuis. 1996b. Regression-based focal point seed zones for *Picea mariana* from northwestern Ontario. Can. J. Bot. 74:1227-1235.

Pollard, D.F., and C.C. Ying. 1979. Variance in flushing among and within stands of seedling white spruce. Can. J. For. Res. 9:517-521.

Pope, V.D., M.L. Gallani, P.R. Rowntree, and R.A. Stratton. 2000. The impact of new physical parameterizations in the Hadley Centre climate model: HadCM3. Climate Dynamics. 16:123-146.

Rajora, O.P., and B.P. Dancik. 2000. Population genetic variation, structure, and evolution in Engelmann spruce, white spruce, and their natural hybrid complex in Alberta. Can. J. For. Res. 78:768-780.

Raymond, C.A., and D. Lindgren. 1990. Genetic flexibility - A model for determining the range of suitable environments for a seed source. Silvae Genetica. 39:112-120.

Rehfeldt, G.E. 1982. Differentiation of Larix occidentalis populations from the northern Rocky Mountains. Silvae Genetica. 31:13-19.

Rehfeldt, G.E. 1983a. Adaptation of *Pinus contorta* populations to heterogeneous environments in northern Idaho. Can. J. For. Res. 13:405-411.

Rehfeldt, G.E. 1983b. Transfer guidelines for Douglas-fir in central Idaho. USDA Research Note INT-337. USDA, Ogden, UT. 3pp.

Rehfeldt, G.E. 1983c. Seed transfer guidelines for Douglas-fir in western Montana. USDA Research Note INT-329. USDA, Ogden, UT.

Rehfeldt, G.E. 1984. Microevolution of conifers in the northern Rocky Mountains: a view from common gardens pp132-146. *in* R.M. Lanner (ed.) Proceeding of the 8th North American Forest Biology Workshop. Utah State University, Logan, UT.

Rehfeldt, G.E. 1990. Adaptability versus zone size: continuous zones for the Rocky Mountains (USA). Joint Meeting of Western Forest Genetics Association and IUFRO Working Parties. S 2.02-5, 06, 12, and 14. Olympia, Washington. 11 pp.

Rehfeldt, G. E. 1991. A model of genetic variation for *Pinus ponderosa* in the Inland Northwest (U.S.A.): applications in gene resource management. Can. J. For. Res. 21:1491-1500.

Rehfeldt, G.E., C.C. Ying, D.L. Spittlehouse, and D.A. Hamilton. 1999. Genetic responses to climate in Pinus contorta: niche breadth, climate change, and reforestation. Ecological Monographs. 69:375-407.

Riddell, C.L. 2004. Climate change and black spruce: implications for future forests in Ontario. HBScF Thesis. Lakehead university, Thunder Bay, ON. 107 pp.

Risbey, J.S., and M. Kandlikar. 2007. Expressions of likelihood and confidence in the IPCC uncertainty assessment process. Climatic Change. 85:19-31.

Rivington, M., D. Miller, K.B. Matthews, G. Russell, and G. Buchan, K. Bellochi. 2008. Evaluating regional climate model estimates against site-specific observed data in the UK. Climatic Change. 88:157-158.

Roberds, J.H., and G. Namkoong. 1989. Population selection to maximize value in an environmental gradient. Theor. Appl. Genet. 77:128-134.

Rweyongeza, D.M., R.-C. Yang, N.K. Dhir, L.K. Barnhardt, and C. Hansen. 2007. Genetic variation and climatic impacts on survival and growth of white spruce in Alberta, Canada. Silvae Genetica. 56:117-127.

SAS Institute Inc. 2000. SAS System for Windows. SAS Institute Inc., Cary, N.C.

Schmidtling, R.C. 1994. Use of provenance tests to predict response to climatic change: loblolly pine and Norway spruce. Tree physiology. 14:805-817.

Taylor, T.M.C. 1959. The taxonomic relationship between *Picea glauca* (Moench) Voss and *Picea englemanii* Parry. Madrono. 15:111-115.

Thiberville, M., and W.H. Parker. 2007. 2050 Ontario tree distributions. http://flash.lakeheadu.ca/ontariotreesl.htm (accessed June 14, 2008).

Thomson, A.M. 2006. Implication of climate change for jack pine in Ontario and the Lake States: Identification of seed sources to compensate for loss of height growth. HBScF Thesis. Lakehead University, Thunder Bay. 161 pp.

Thomson, A.M., and W.H. Parker. 2008. Boreal forest provenance tests used to predict optimal growth and response to climate change. 1. Jack pine. Can. J. For. Res. 38:157-170.

van Buijtenen, J.P. 1992. Fundamental genetic principles pp 29-68 *in* Fins, L., S.T. Friedman, and J.V. Brotschol. (eds.) Handbook of Quantitative Forest Genetics. Kluwer Academic Publishers, Norwell, MA. 403 pp.

Wang, T., A. Hamann, A. Yanchuk, G.A. O'Neill, and S.N. Aitken. 2006. Use of response function in selecting lodgepole pine populations for future climates. Global Change Biology. 12:2404-2416.

Wilkinson, R.C., J.W. Hanover, J.W. Wright, and R.H. Flake. 1971. Genetic variation in the monoterpene composition of white spruce. Forest Sci. 17:83-90.

Xiao, B. 2005. Present and future focal point seed zones for jack pine in northwestern Ontario. M.Sc.F. Thesis. Lakehead University, Thunder Bay, ON. 208 pp.

Ying, C.C., and E.K. Morgenstern. 1979. Correlations of height growth and heritabilities at different ages in white spruce. Silvae Genetica. 28:181-185.

Yu, Q., D-Q. Yang, S.Y. Zhang, J. Beaulieu, and I. Duchense. 2003. Genetic variation in decay resistance and its correlation to wood density and growth in white spruce. Can. J. For. Res. 33:2177-2183.

Zhang, S.Y., Q. Yu, and J. Beaulieu. 2004. Genetic variation in veneer quality and its correlation to growth in white spruce. Can. J. For. Res. 34:1311-1318.

APPENDIX I: CLIMATE GRIDS USED TO PREDICT PRINCIPAL COMPONENTS FACTOR SCORES

OBSERVED NORMALS FOR 1961-1990

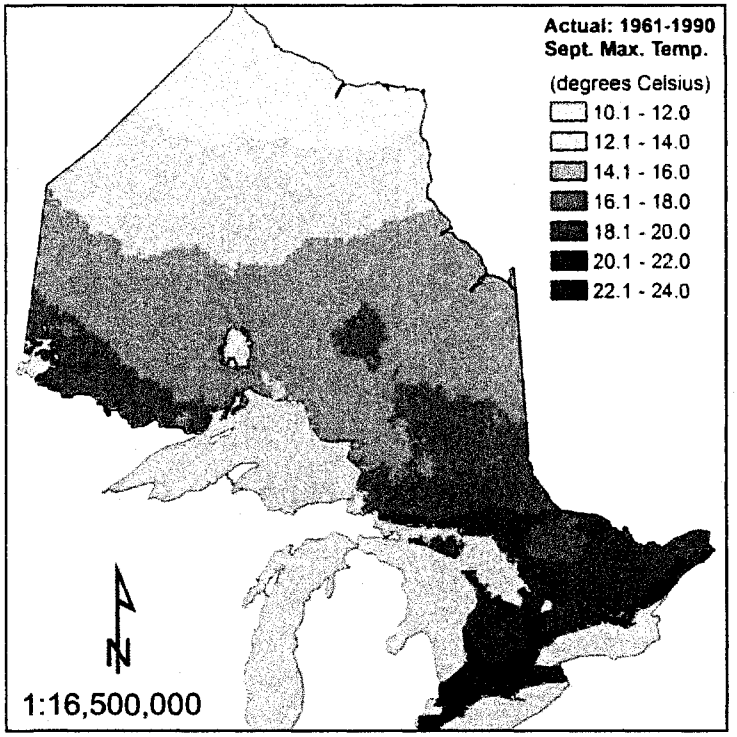

September maximum temperature based on 1961-1990 climate normals.

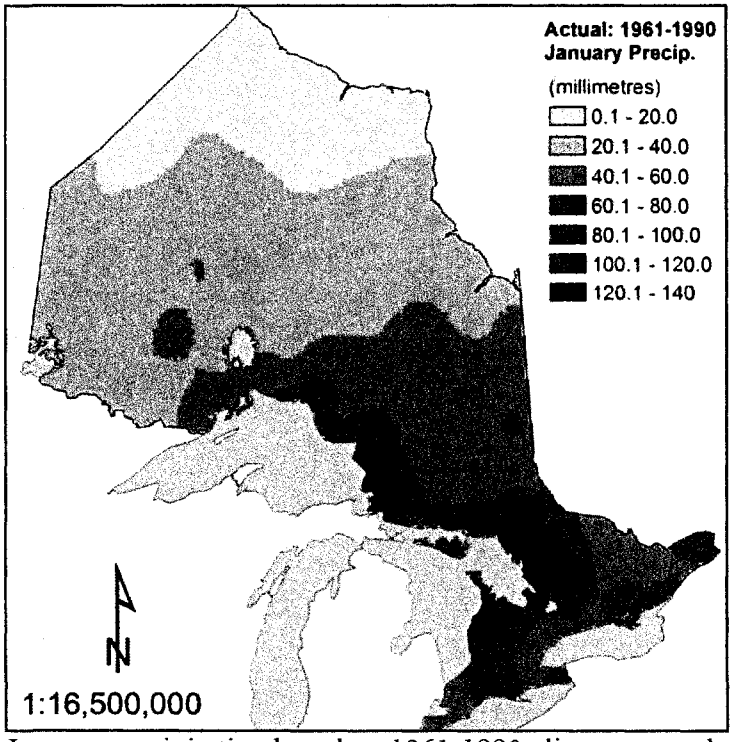

January precipitation based on 1961-1990 climate normals.

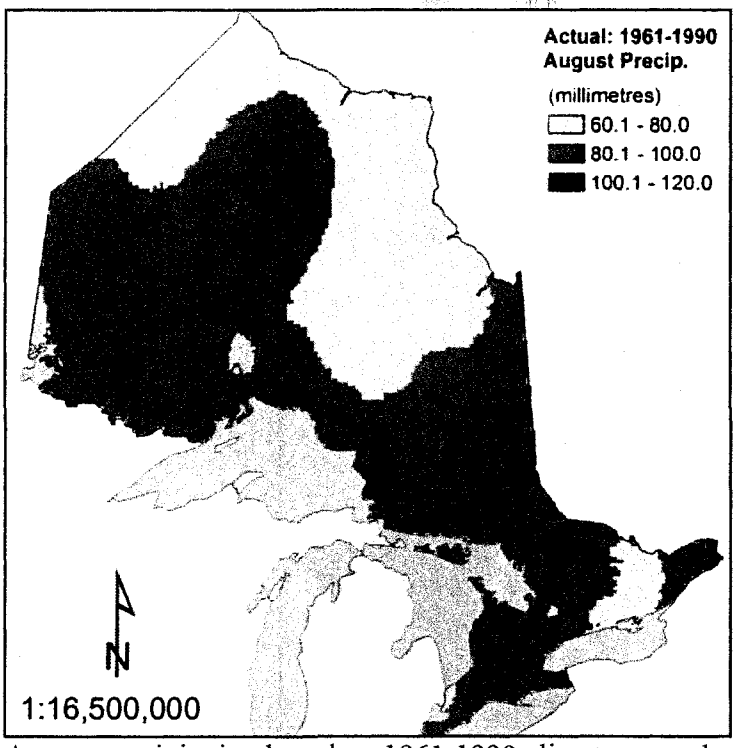

August precipitation based on 1961-1990 climate normals.

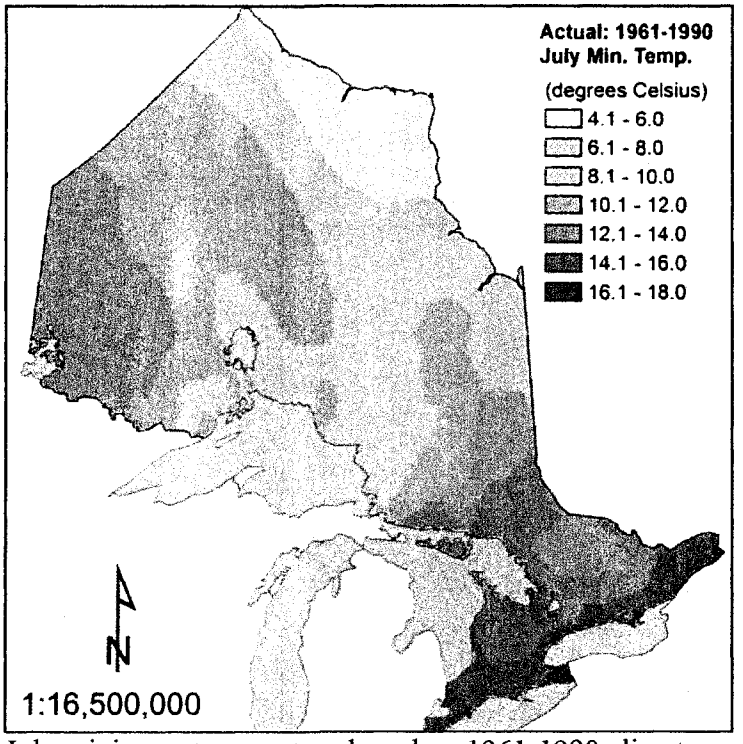

July minimum temperature based on 1961-1990 climate normals.

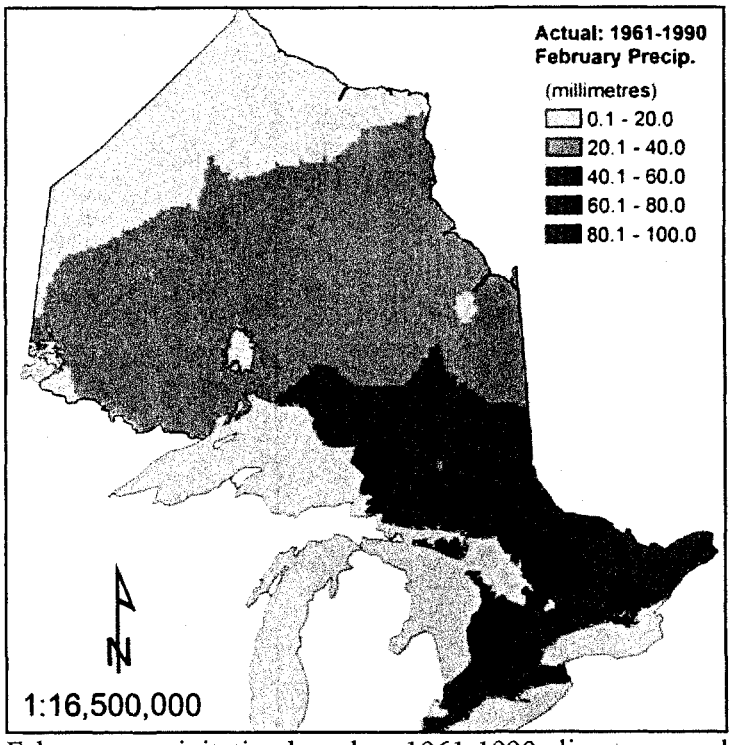

February precipitation based on 1961-1990 climate normals.

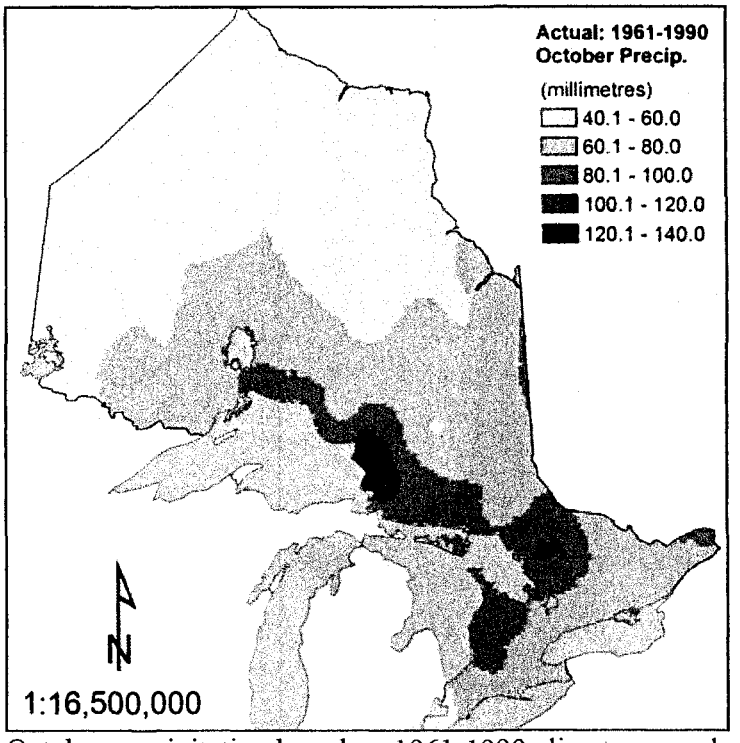

October precipitation based on 1961-1990 climate normals.

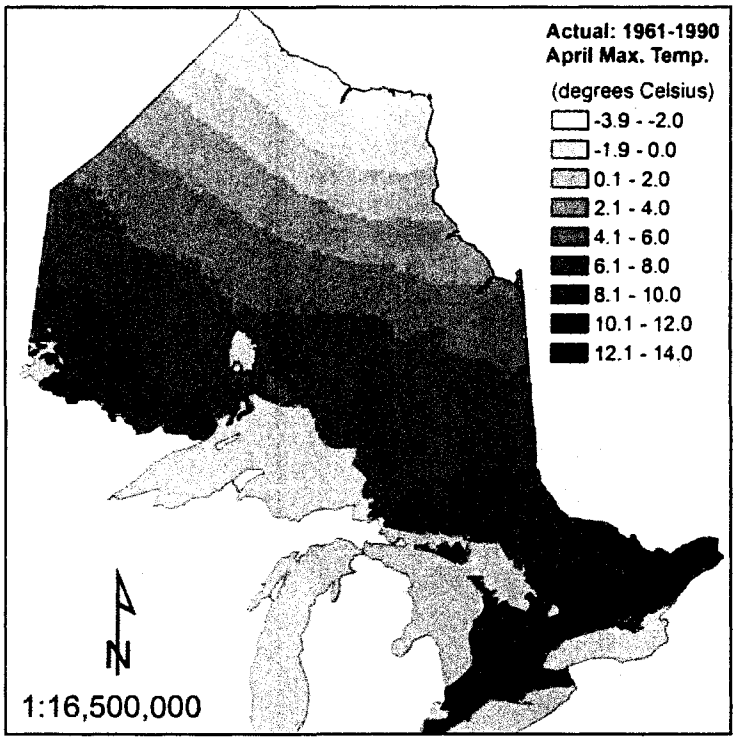

April maximum temperature based on 1961-1990 climate normals.

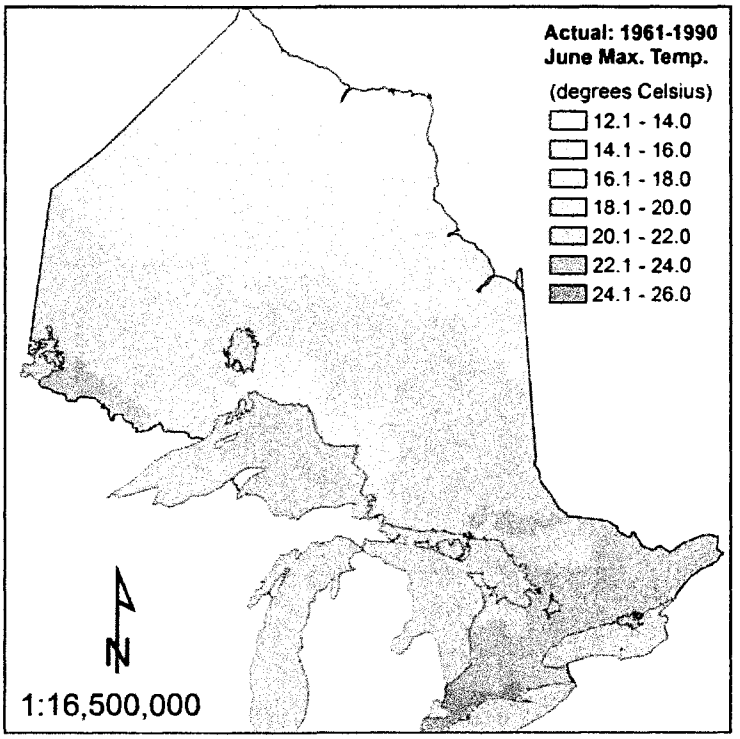

June maximum temperature based on 1961-1990 climate normals.

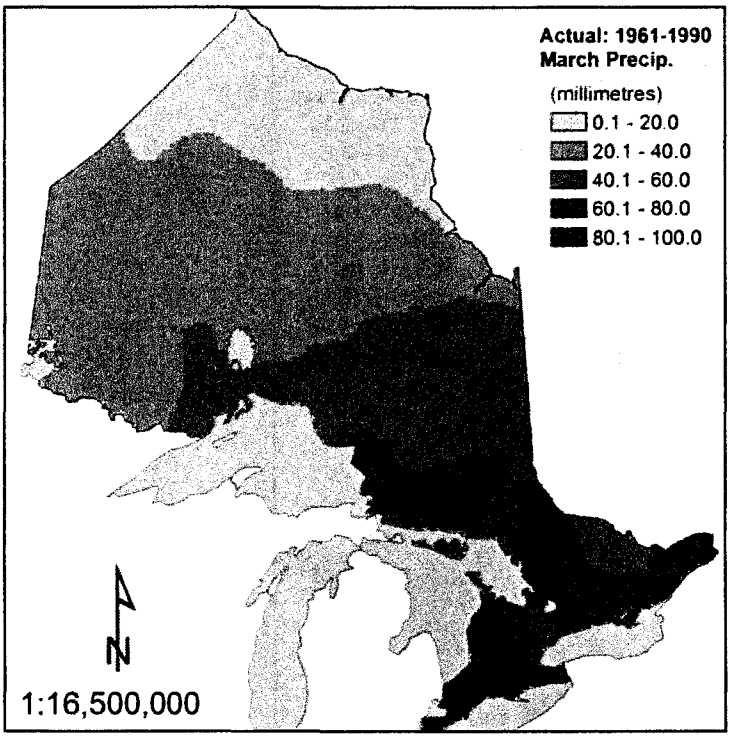

March precipitation based on 1961-1990 climate normals.

CGCM2: 1900

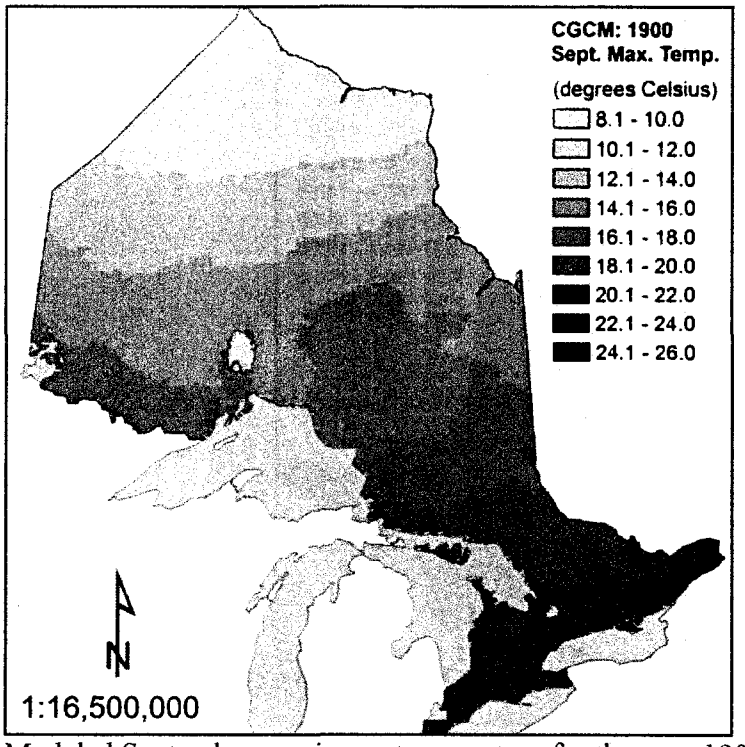

Modeled September maximum temperature for the year 1900 based on CGCM2.

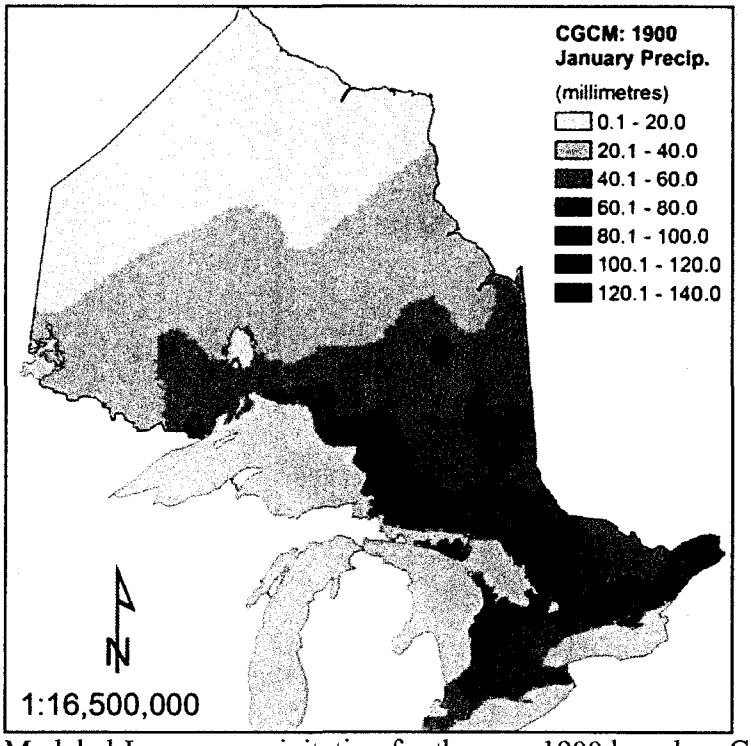

Modeled January precipitation for the year 1900 based on CGCM2.

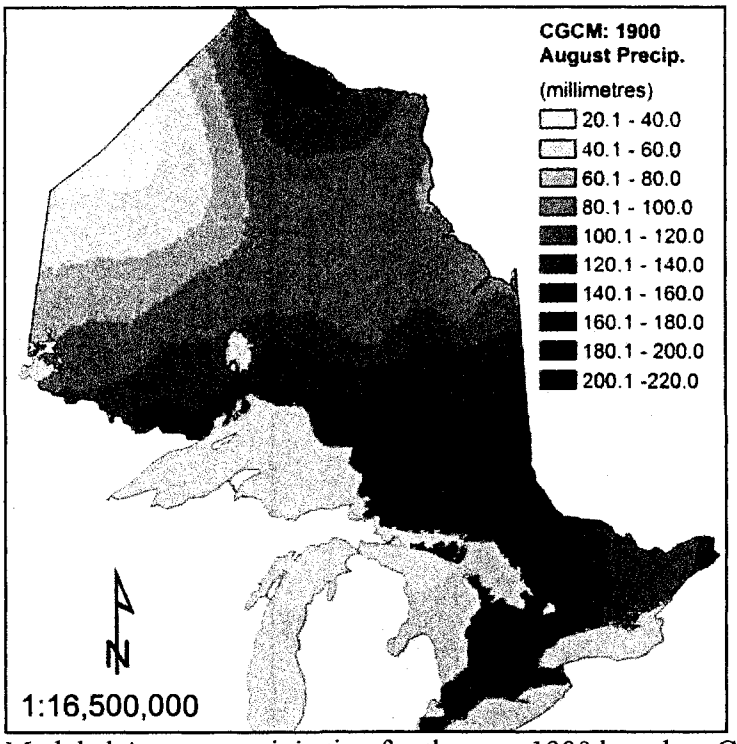

Modeled August precipitation for the year 1900 based on CGCM2.

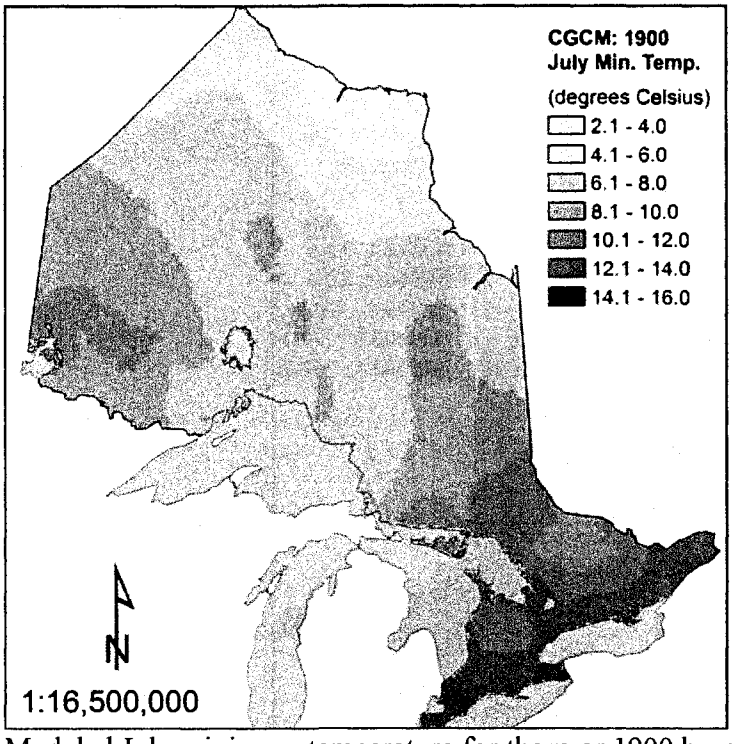

Modeled July minimum temperature for the year 1900 based on CGCM2.

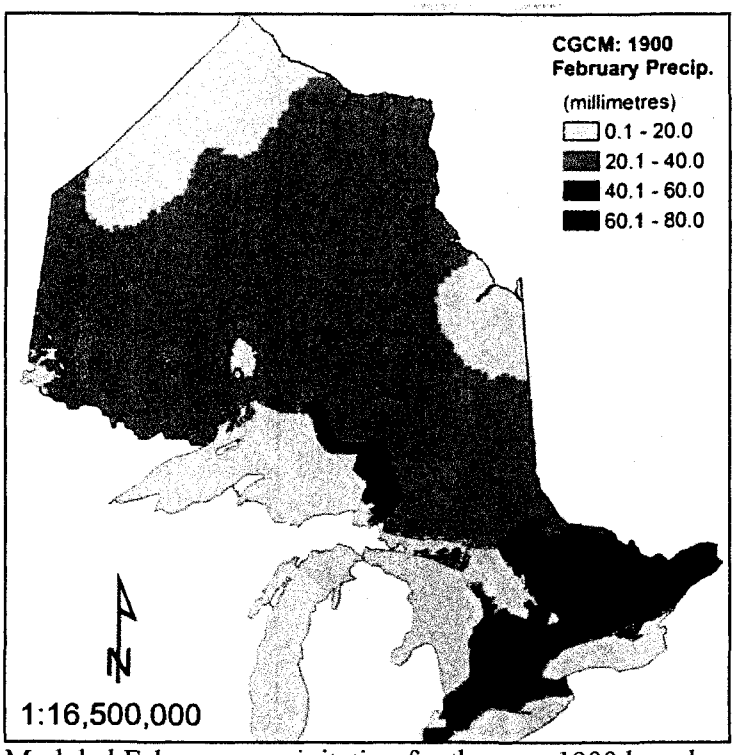

Modeled February precipitation for the year 1900 based on CGCM2.

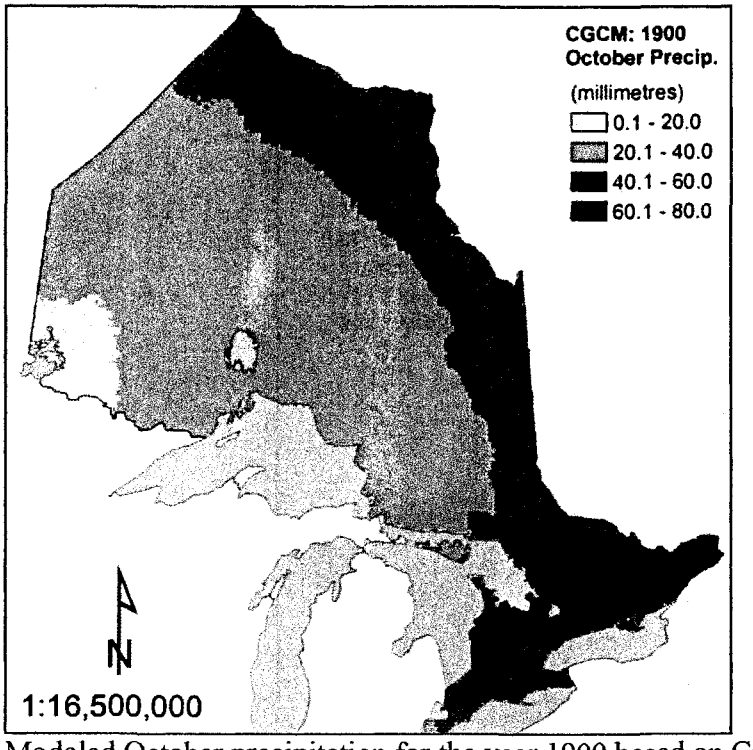

Modeled October precipitation for the year 1900 based on CGCM2.

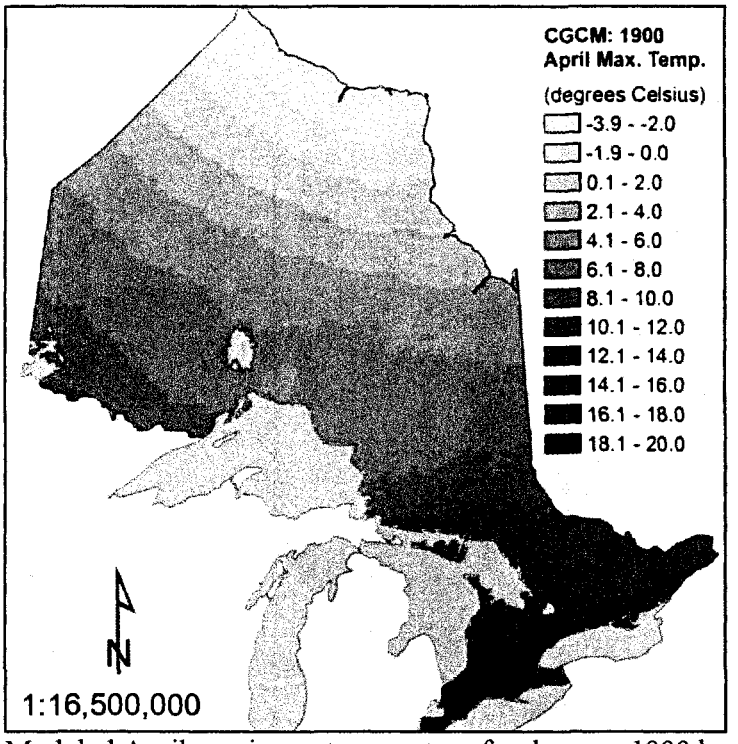

Modeled April maximum temperature for the year 1900 based on CGCM2.

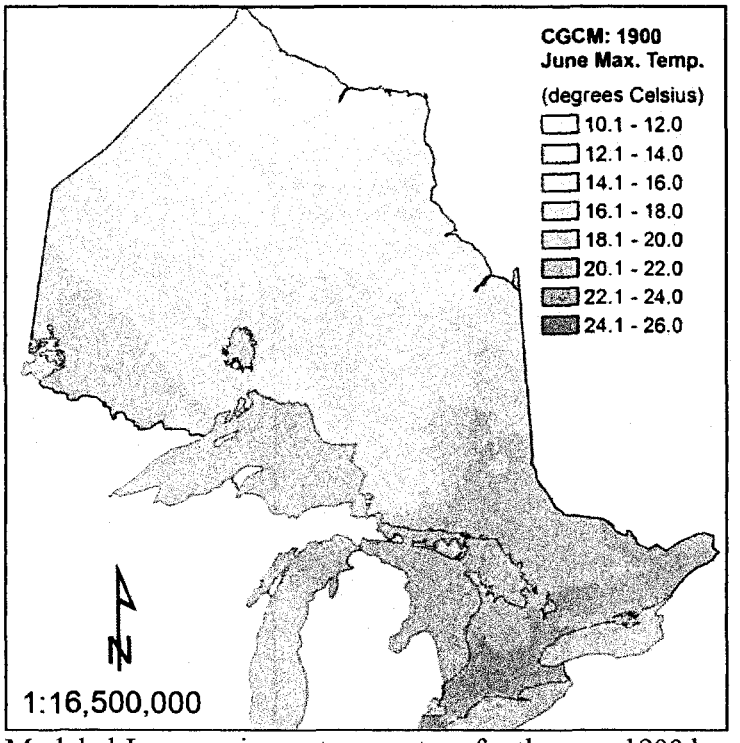

Modeled June maximum temperature for the year 1900 based on CGCM2.

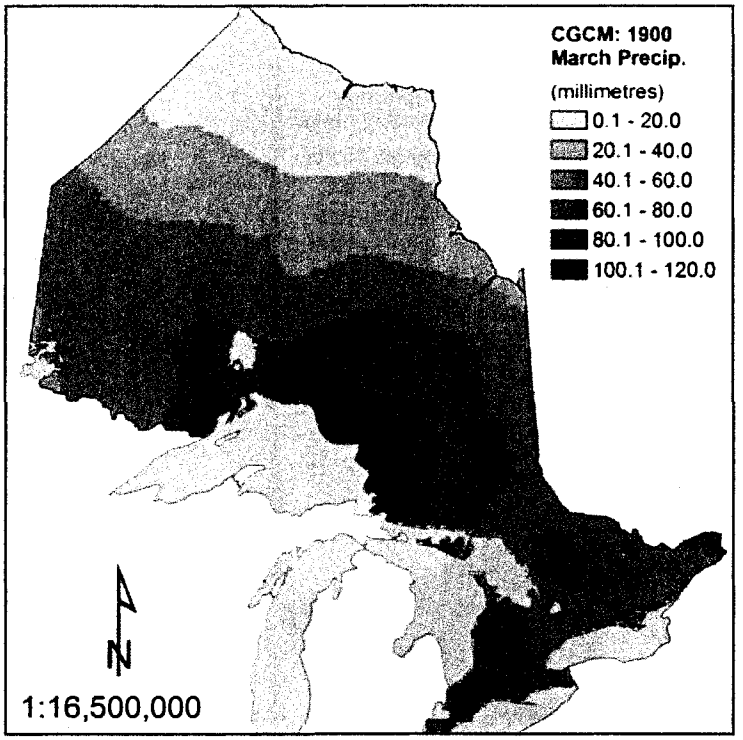

Modeled March precipitation for the year 1900 based on CGCM2.

CGCM2: 1950

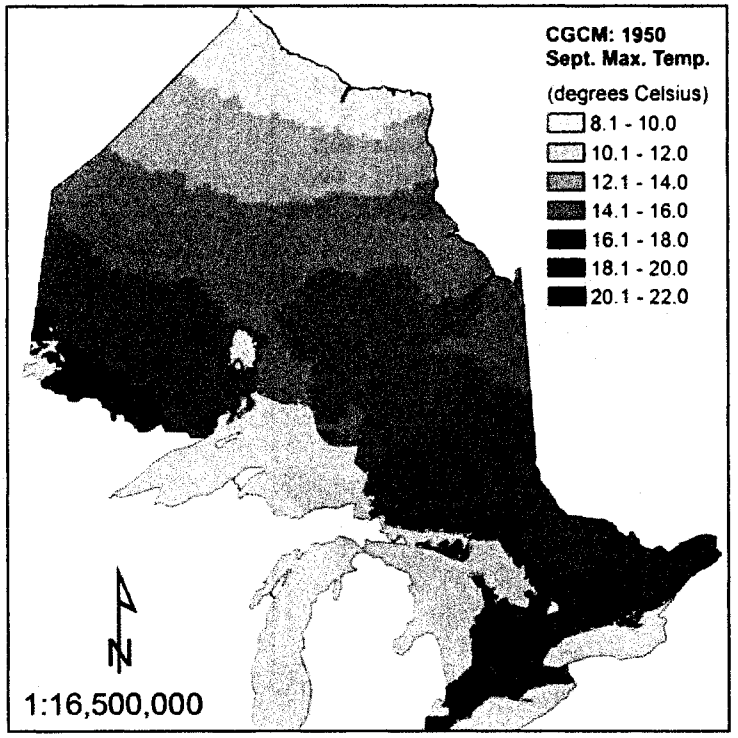

Modeled September maximum temperature for the year 1950 based on CGCM2.

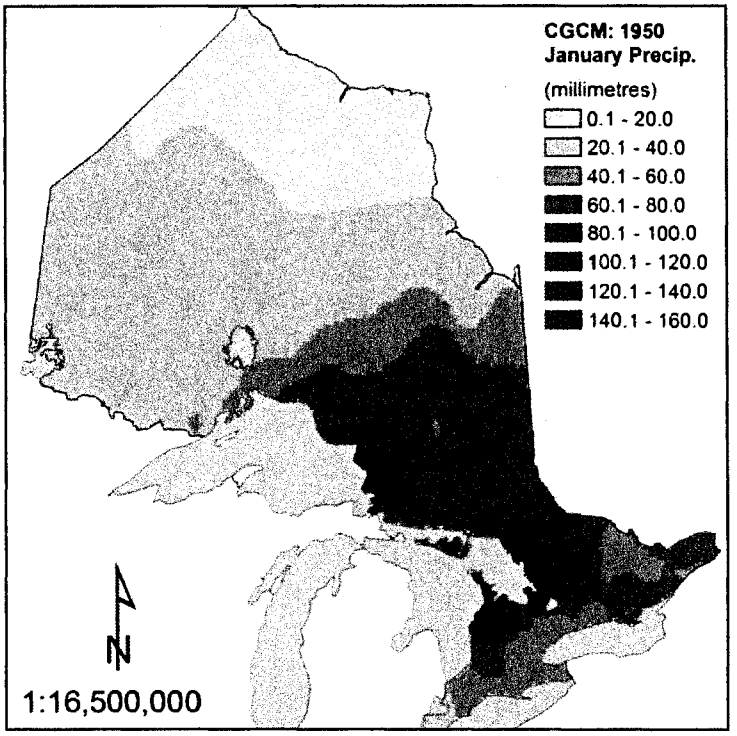

Modeled January precipitation for the year 1950 based on CGCM2.

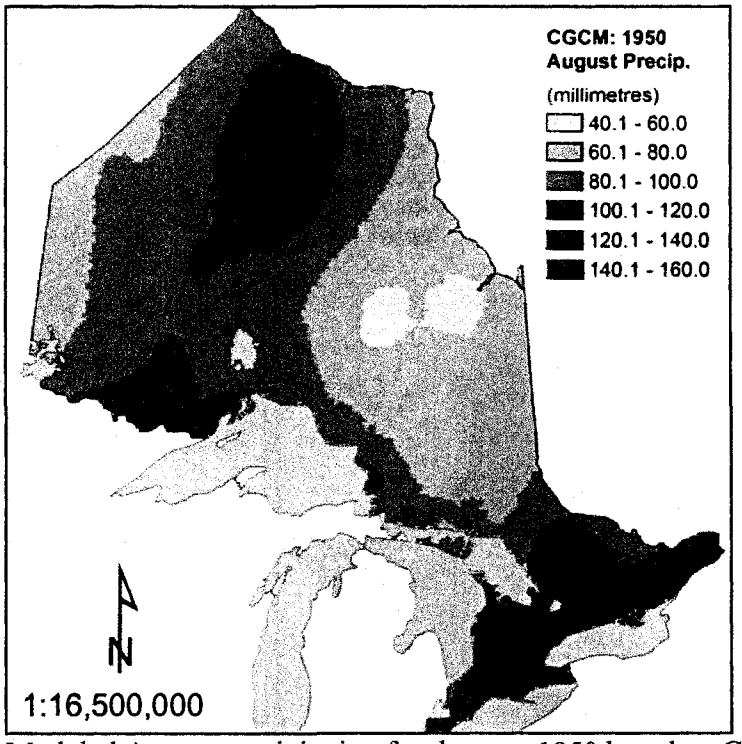

Modeled August precipitation for the year 1950 based on CGCM2.

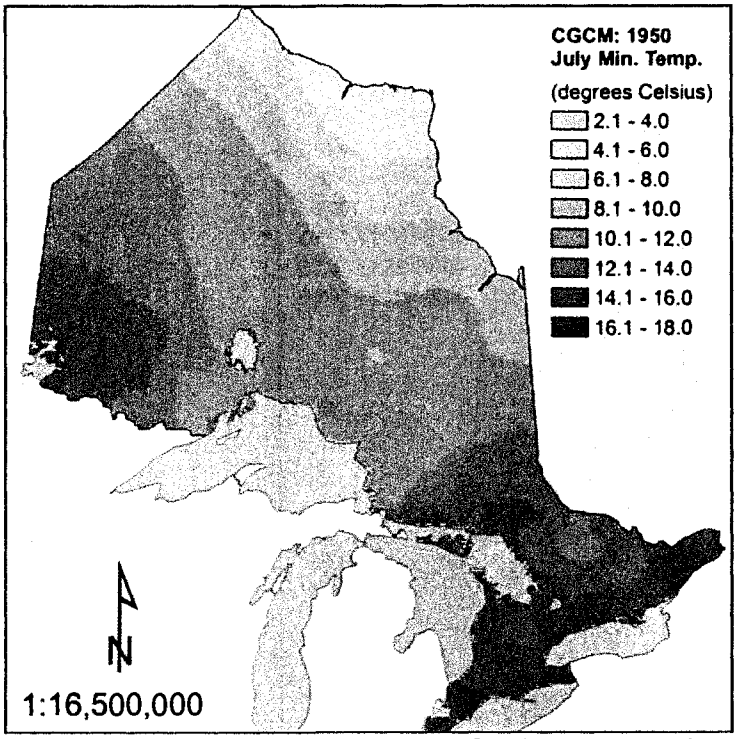

Modeled July minimum temperature for the year 1950 based on CGCM2.

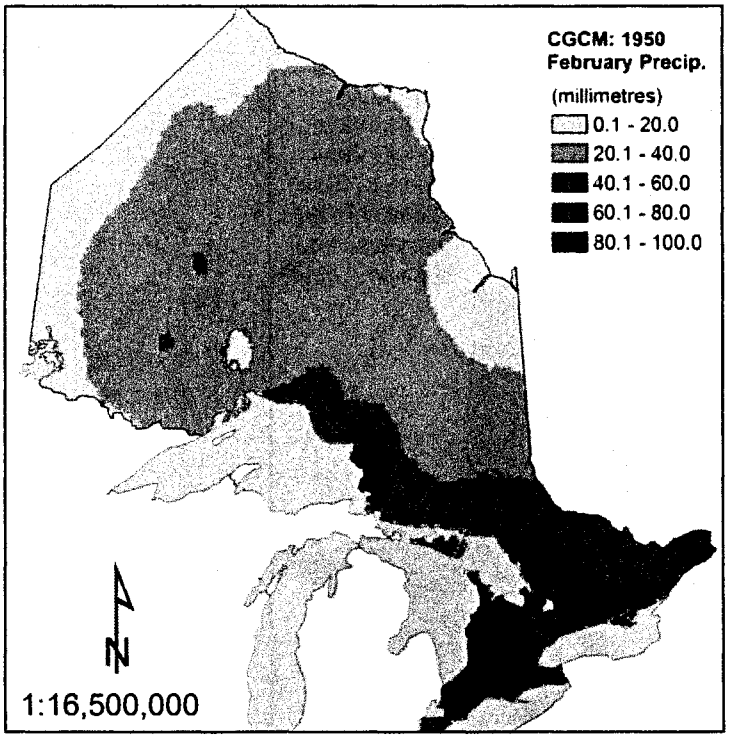

Modeled February precipitation for the year 1950 based on CGCM2.

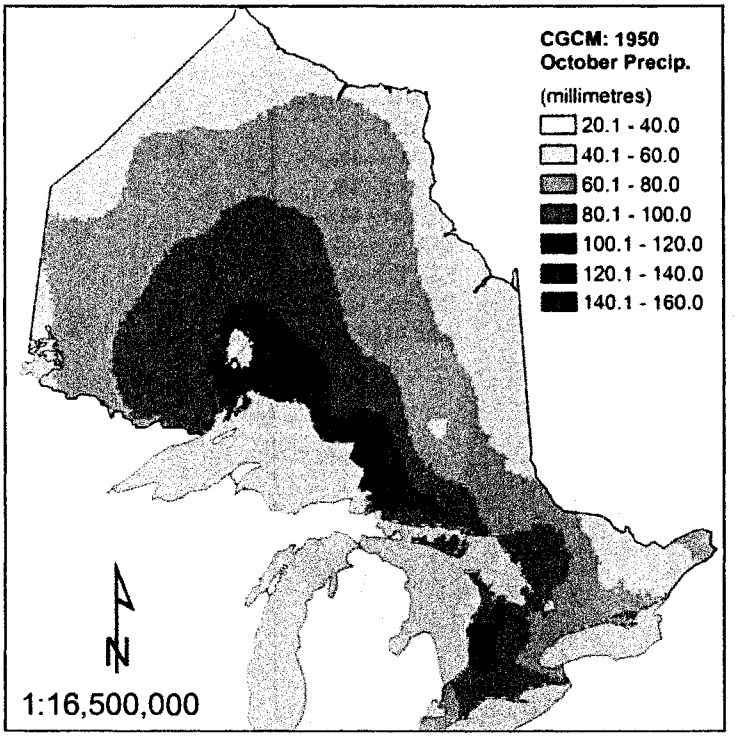

Modeled October precipitation for the year 1950 based on CGCM2.

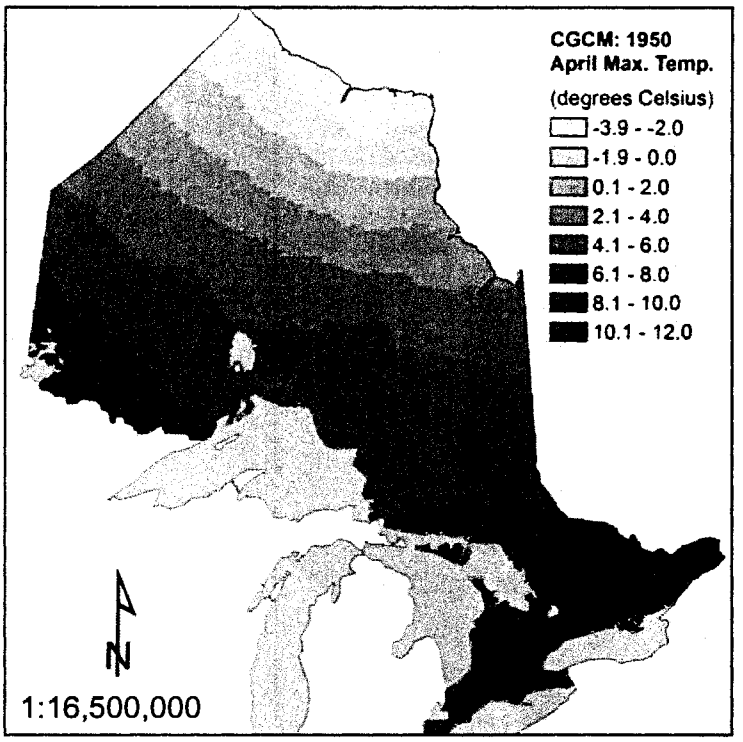

Modeled April maximum temperature for the year 1950 based on CGCM2.

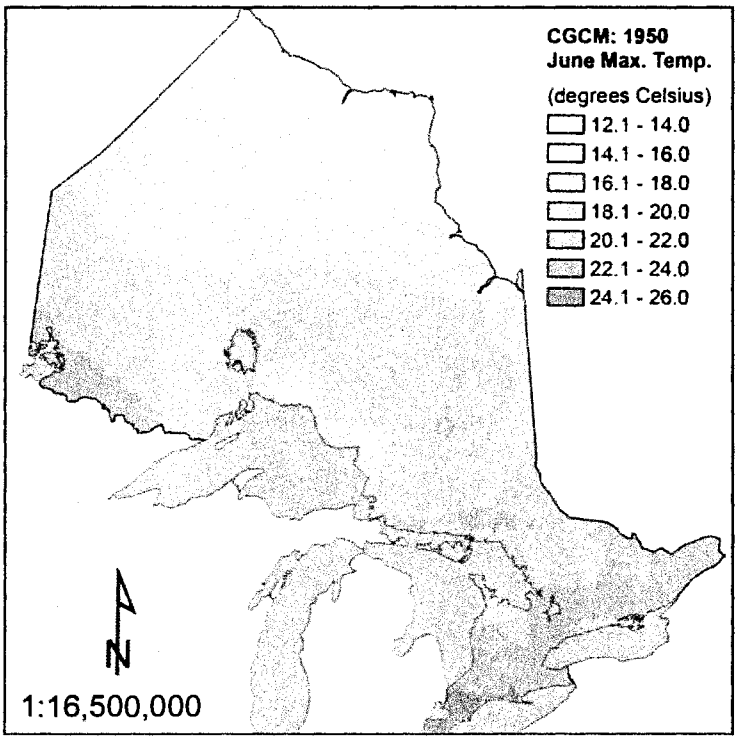

June maximum temperature for the year 1950 based on CGCM2.

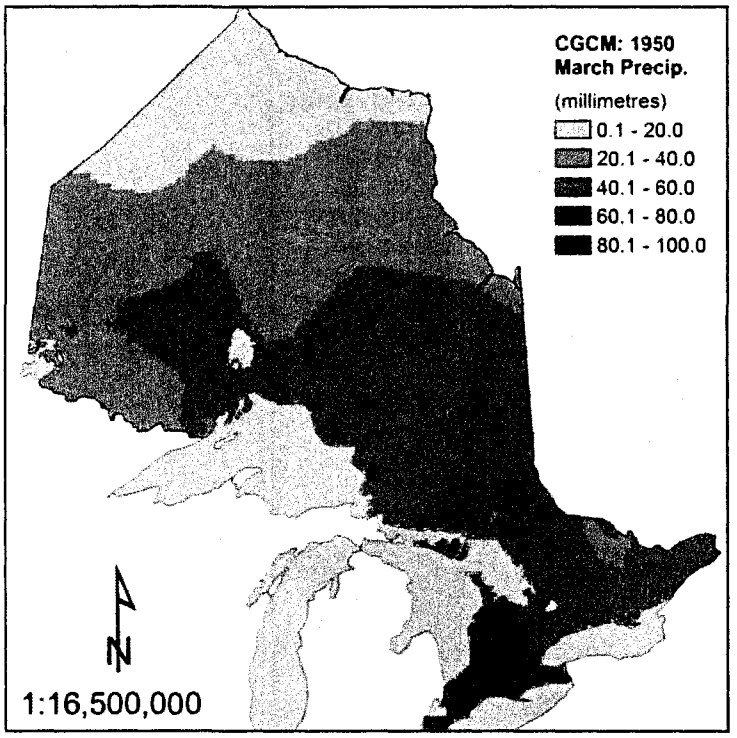

Modeled March precipitation for the year 1950 based on CGCM2.

HADCM3 1950

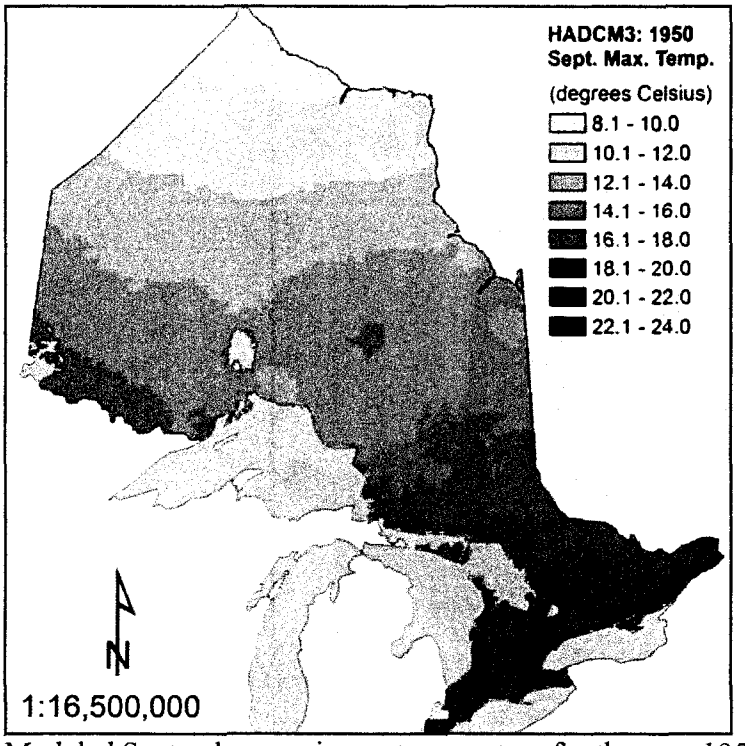

Modeled September maximum temperature for the year 1950 based on HADCM3.

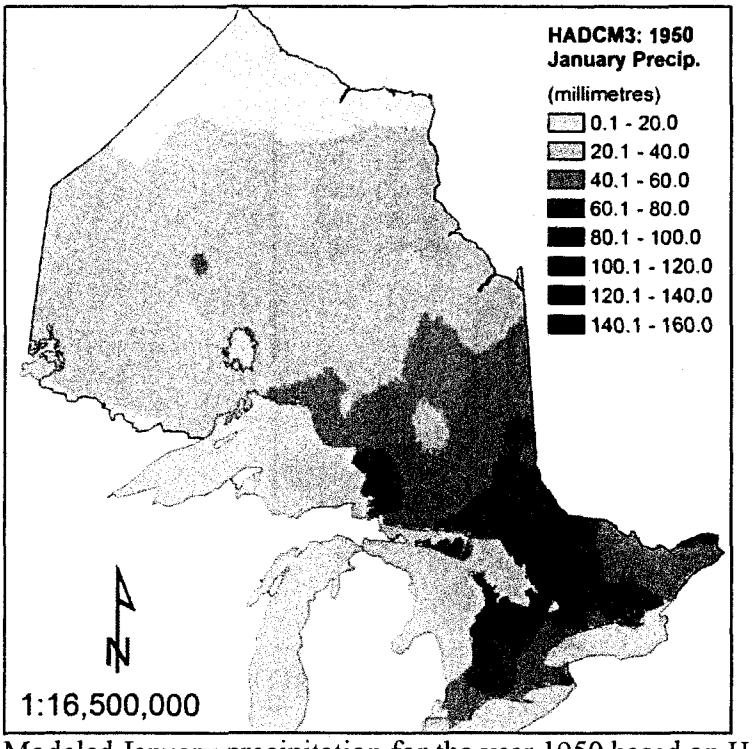

Modeled January precipitation for the year 1950 based on HADCM3.

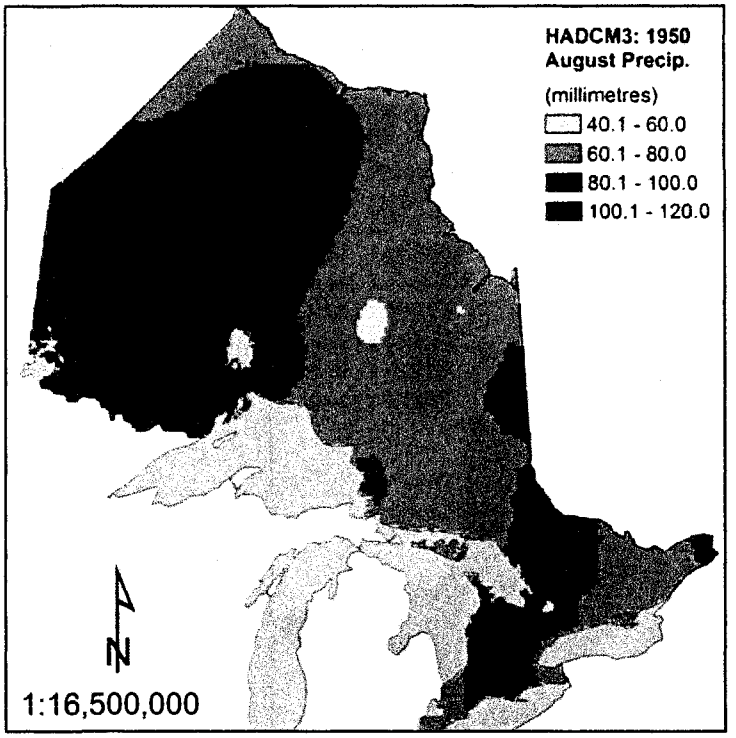

Modeled August precipitation for the year 1950 based on HADCM3.

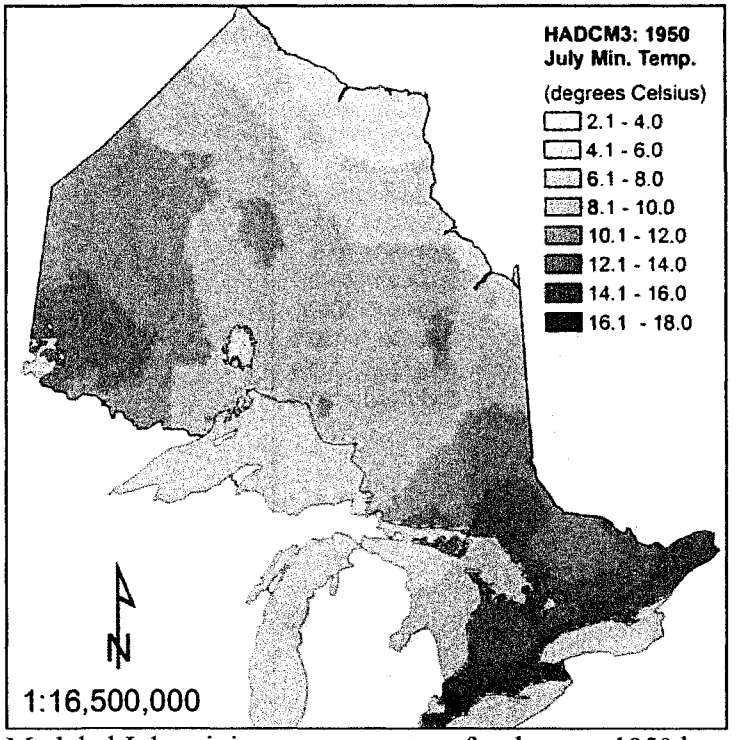

Modeled July minimum temperature for the year 1950 based on HADCM3.

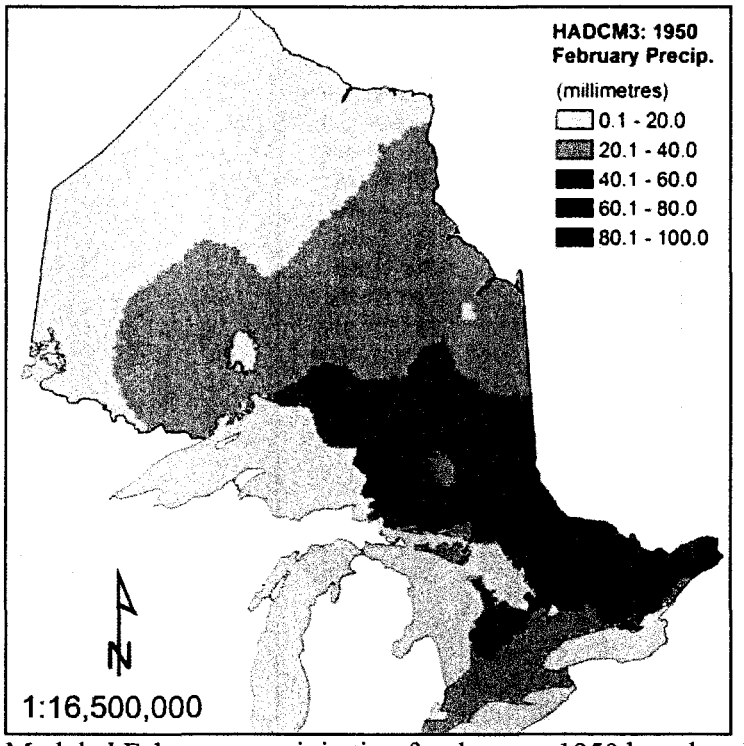

Modeled February precipitation for the year 1950 based on HADCM3.

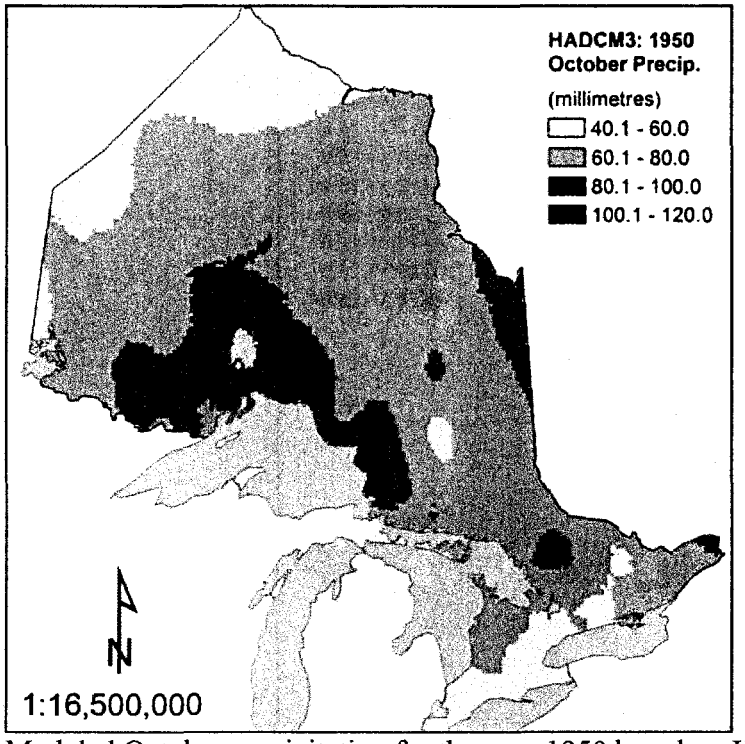

Modeled October precipitation for the year 1950 based on HADCM3.

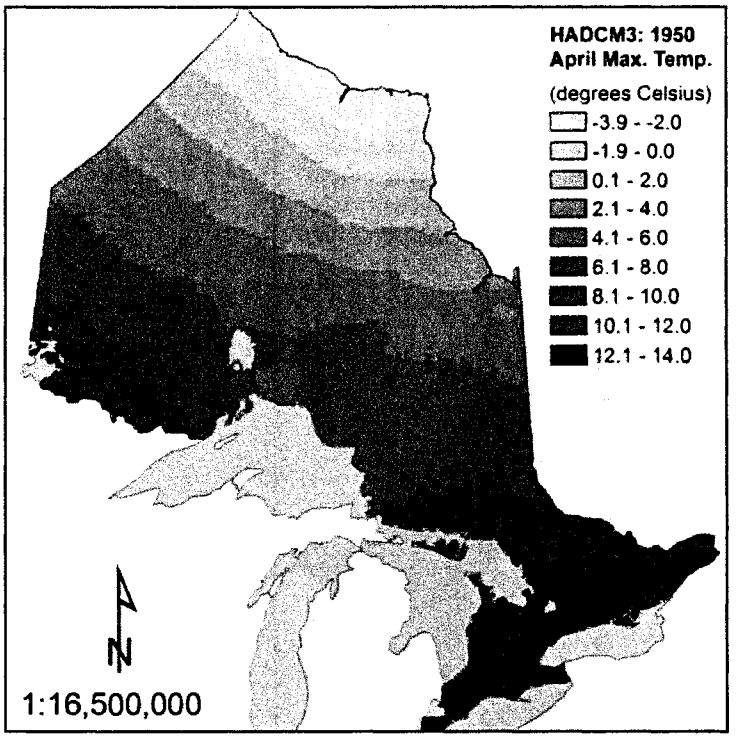

Modeled April maximum temperature for the year 1950 based on HADCM3.

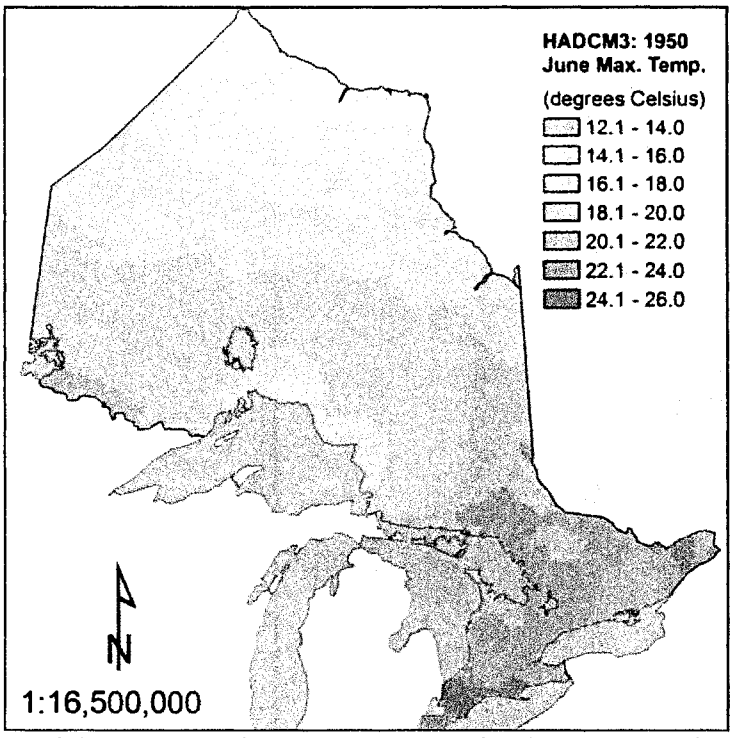

Modeled June maximum temperature for the year 1950 based on HADCM3.

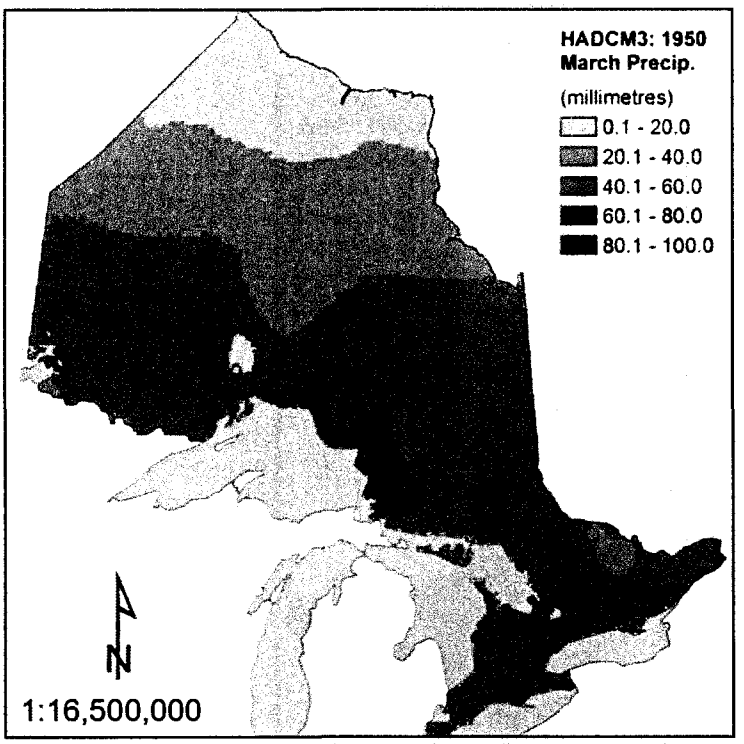

Modeled March precipitation for the year 1950 based on HADCM3.

CSIRO 1961

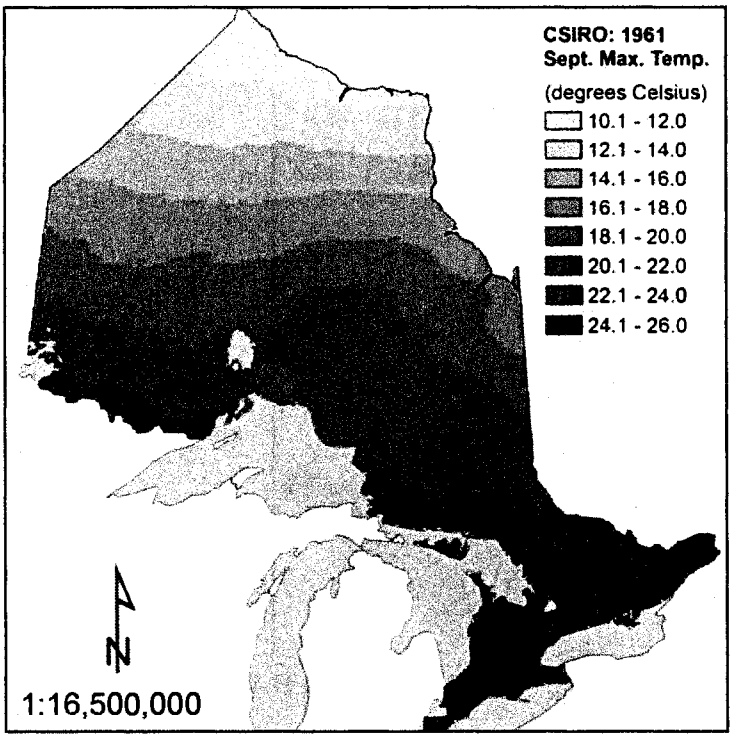

Modeled September maximum temperature for the year 1961 based on CSIRO.

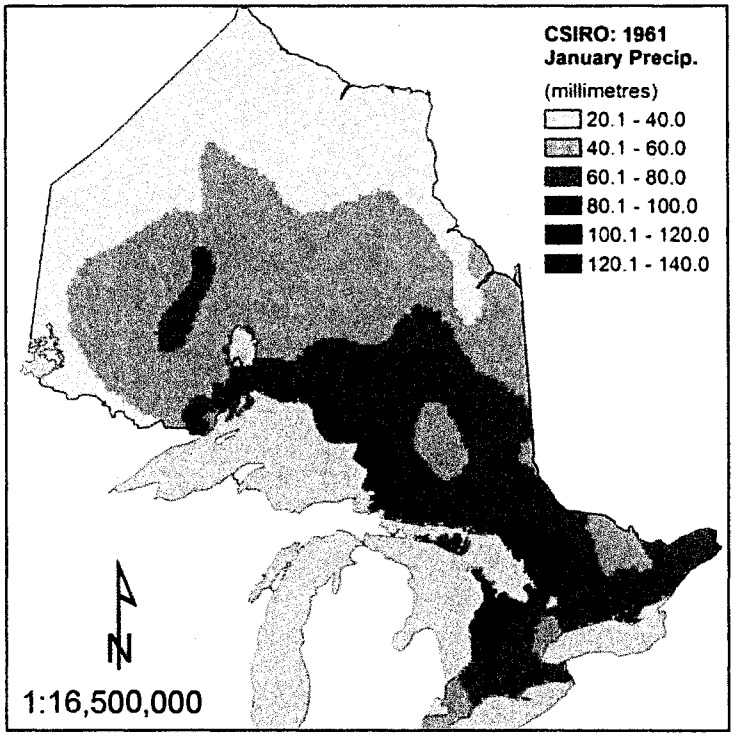

Modeled January precipitation for the year 1961 based on CSIRO.

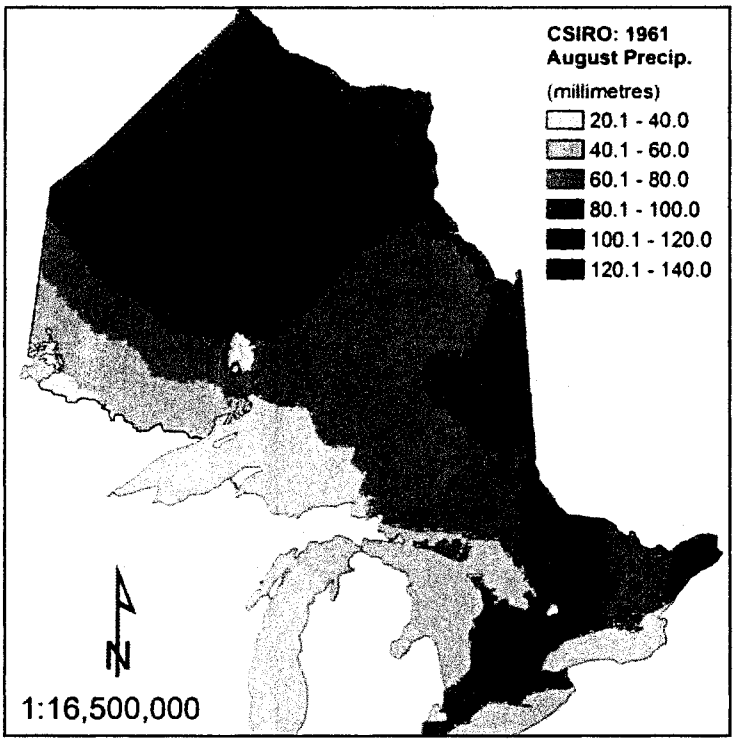

Modeled August precipitation for the year 1961 based on CSIRO.

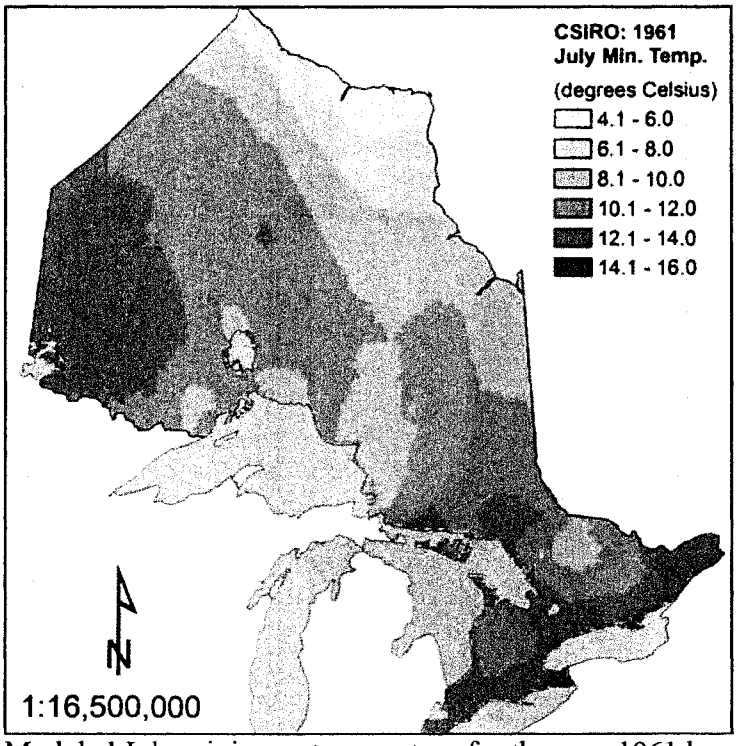

Modeled July minimum temperature for the year 1961 based on CSIRO.

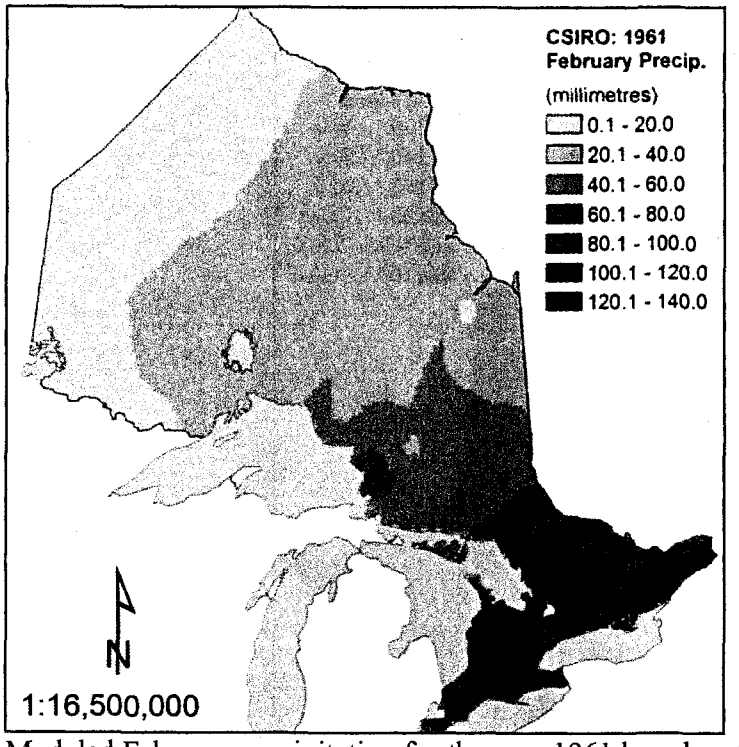

Modeled February precipitation for the year 1961 based on CSIRO.

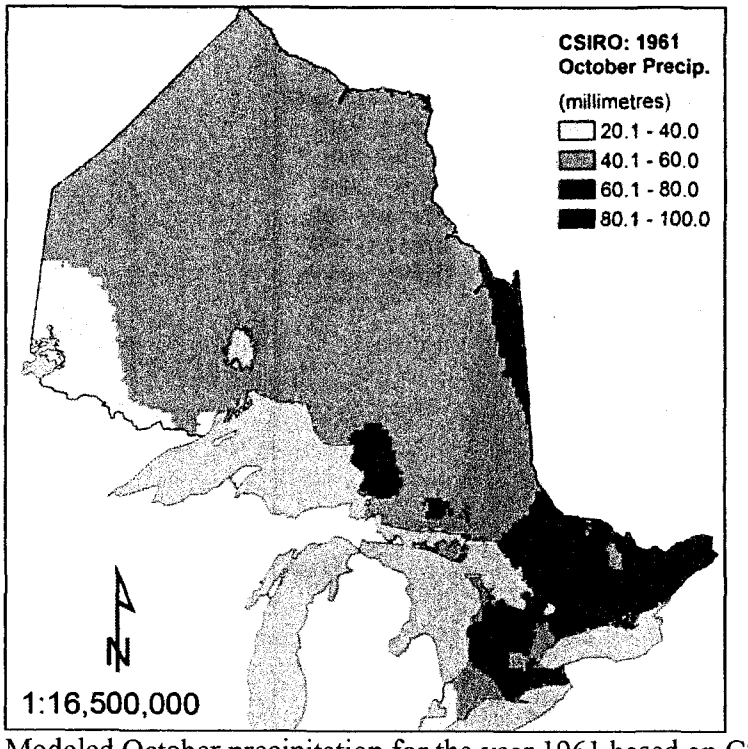

Modeled October precipitation for the year 1961 based on CSIRO.

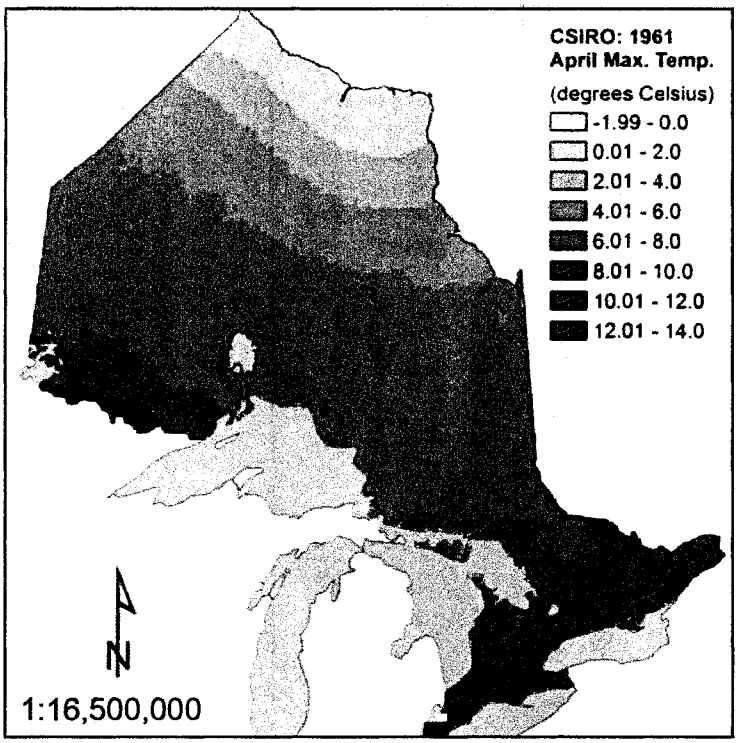

Modeled April maximum temperature for the year 1961 based on CSIRO.

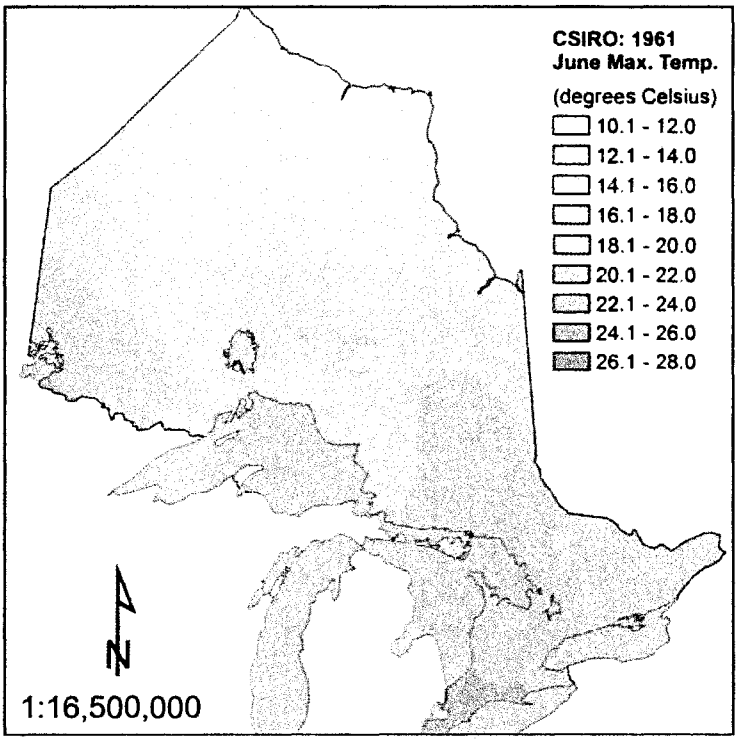

Modeled June maximum temperature for the year 1961 based on CSIRO.

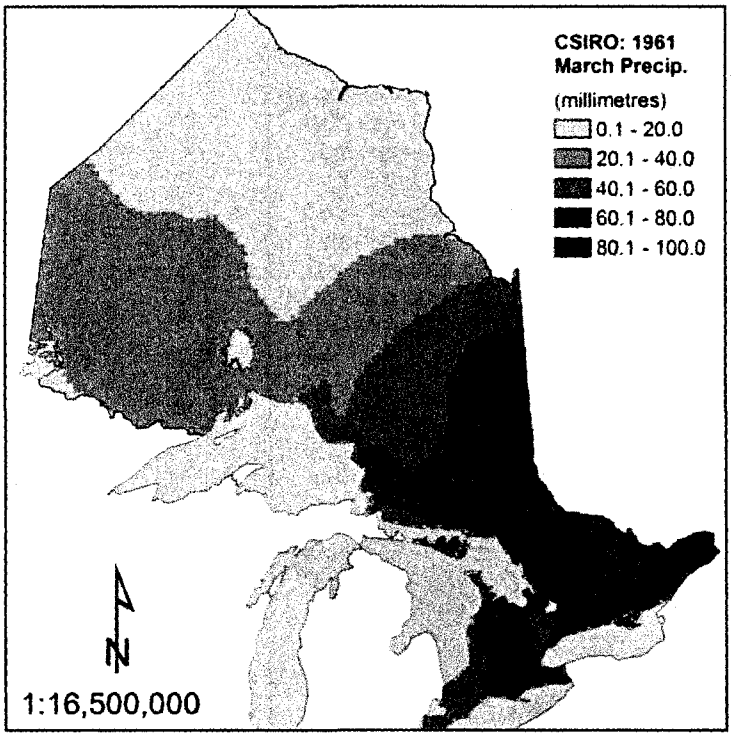

Modeled March precipitation for the year 1961 based on CSIRO.

CGCM2 A2: 2041-2070

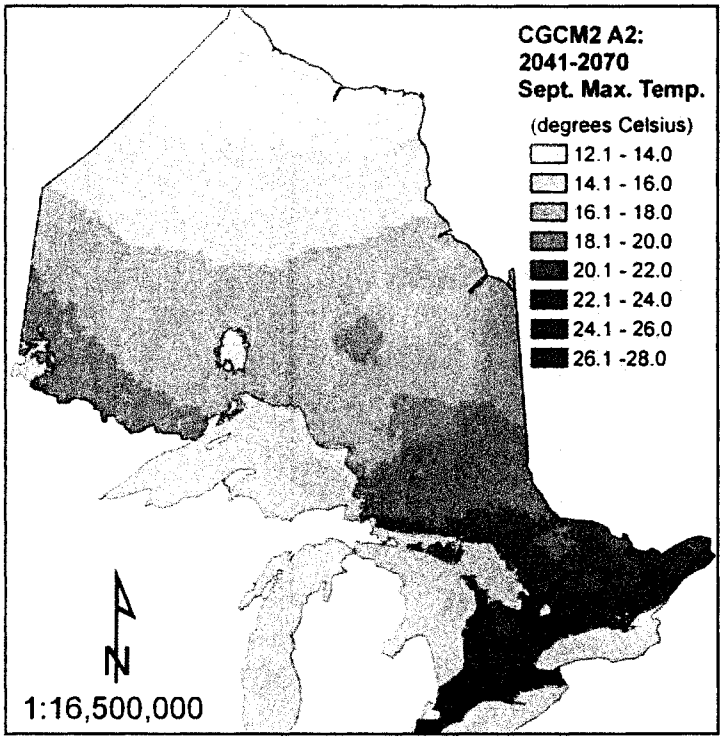

Predicted September maximum temperature for 2041-2070 based on CGCM2 A2.

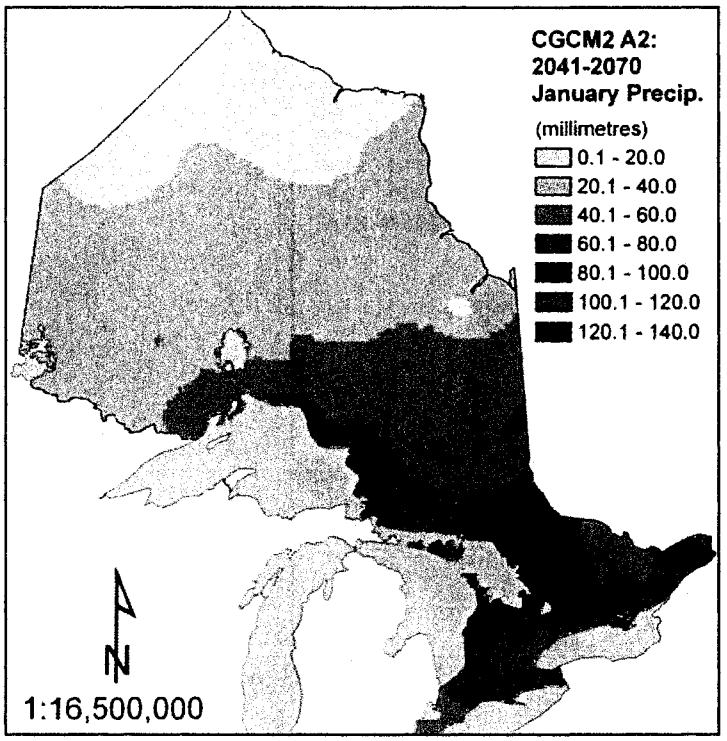

Predicted January precipitation for 2041-2070 based on CGCM2 A2.

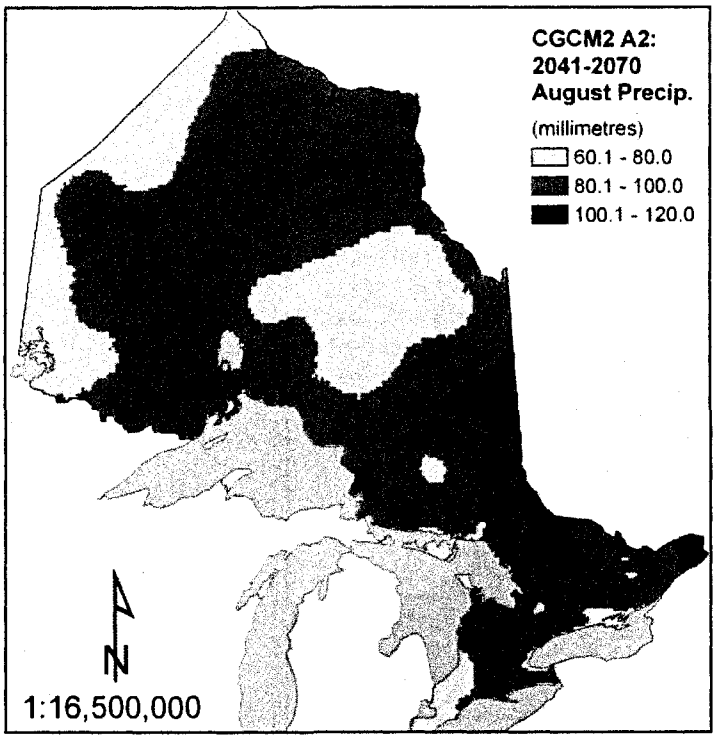

Predicted August precipitation for 2041-2070 based on CGCM2 A2.

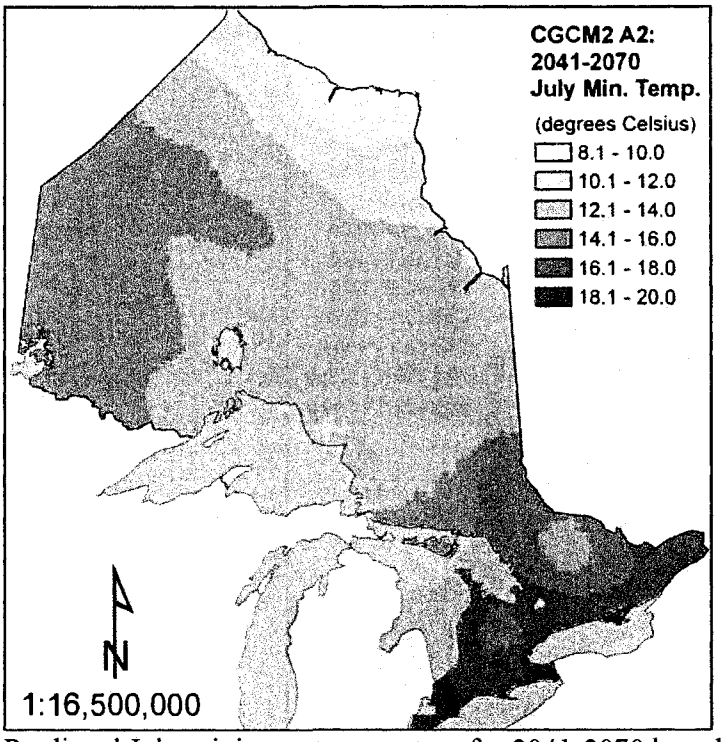

Predicted July minimum temperature for 2041-2070 based on CGCM2 A2.

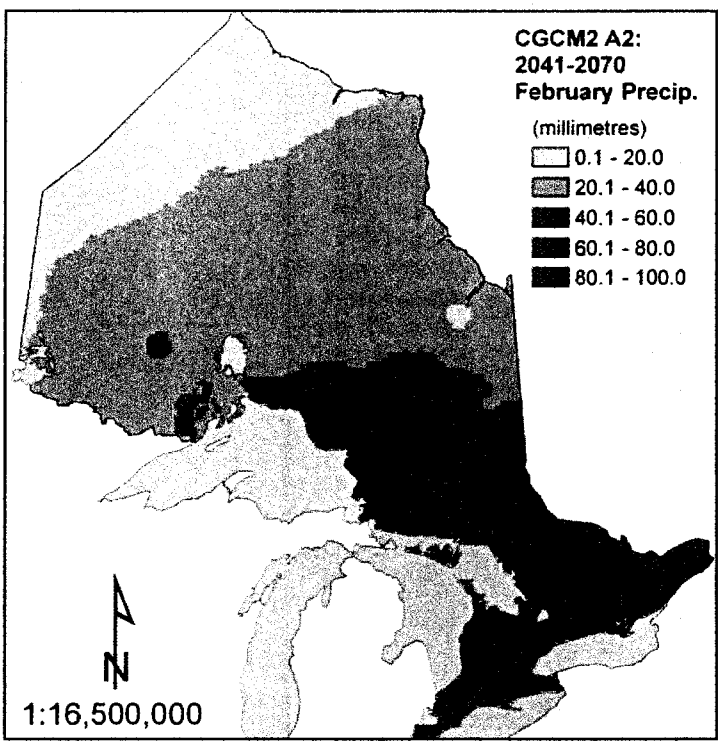

Predicted February precipitation for 2041-2070 based on CGCM2 A2.

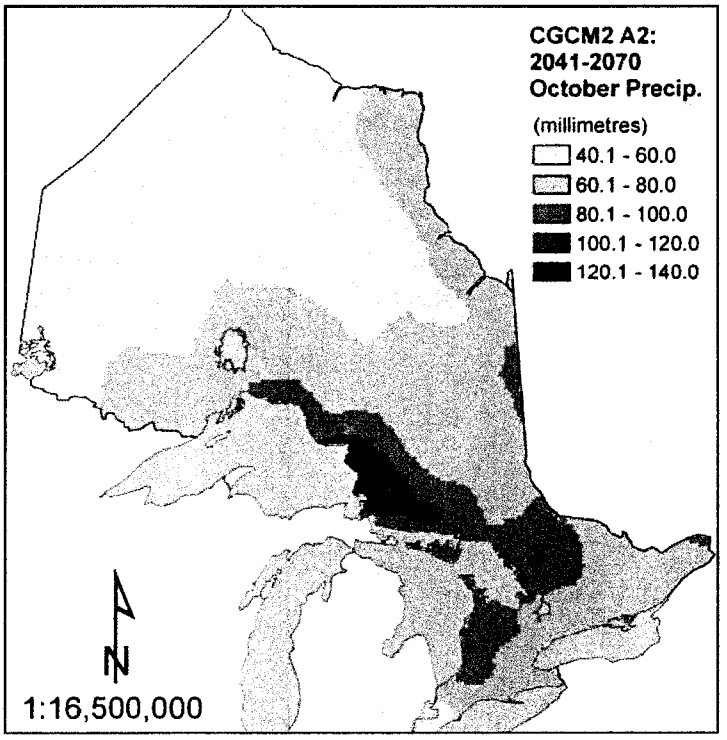

Predicted October precipitation for 2041-2070 based on CGCM2 A2.

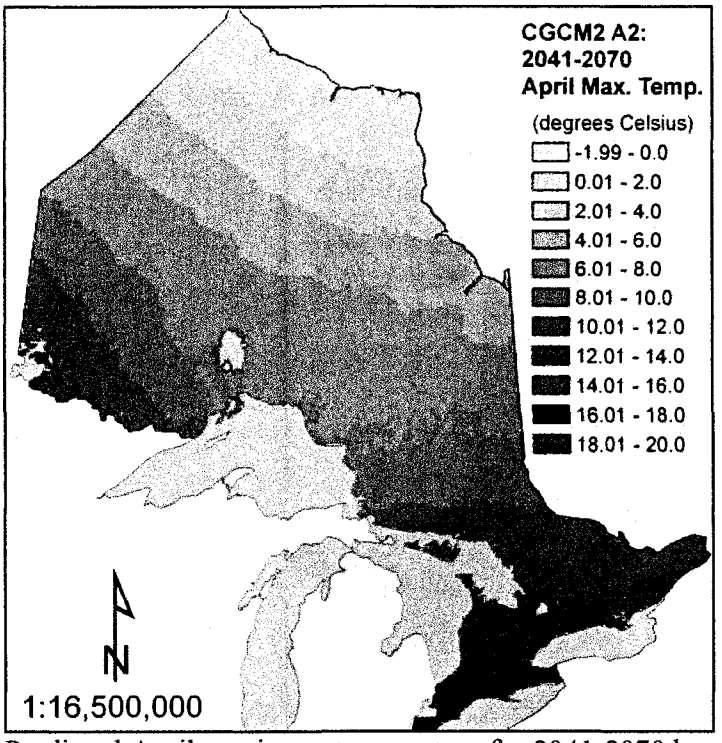

Predicted April maximum temperature for 2041-2070 based on CGCM2 A2.

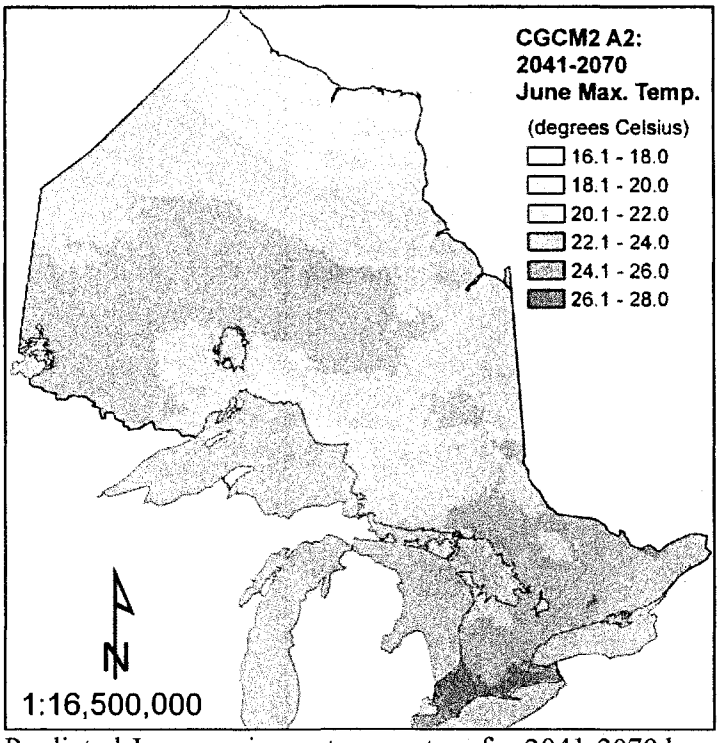

Predicted June maximum temperature for 2041-2070 based on CGCM2 A2.

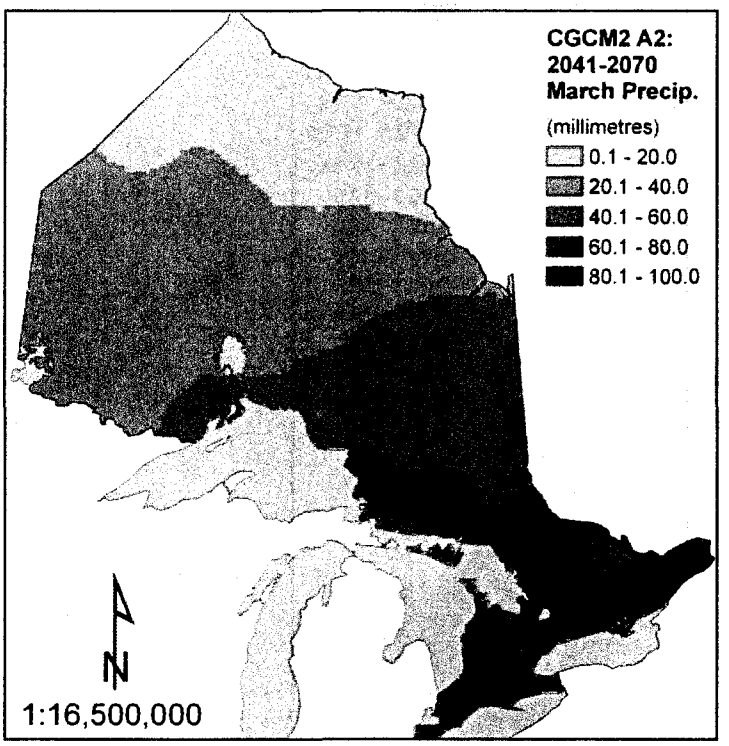

Predicted March precipitation for 2041-2070 based on CGCM2 A2.

CGCM2 B2: 2041-2070

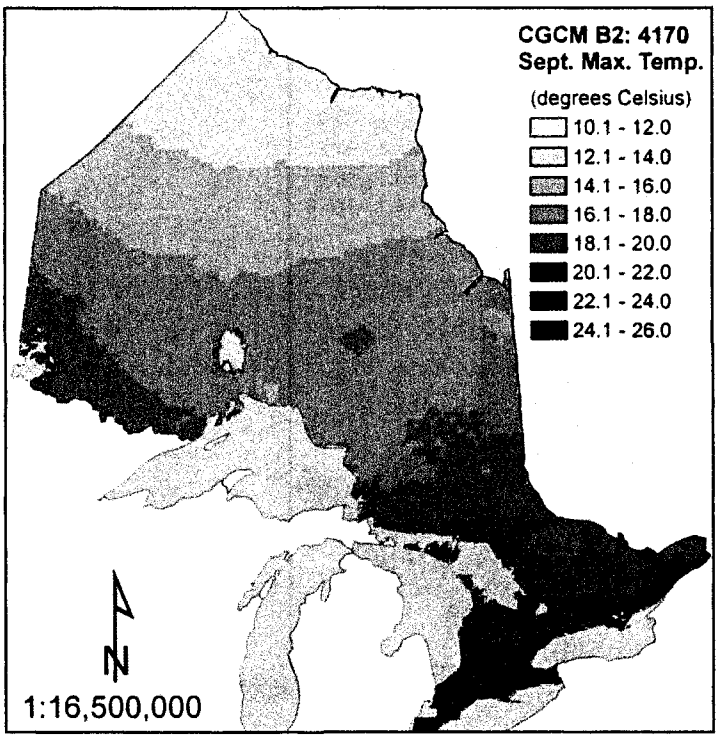

Predicted September maximum temperature for 2041-2070 based on CGCM2 B2.

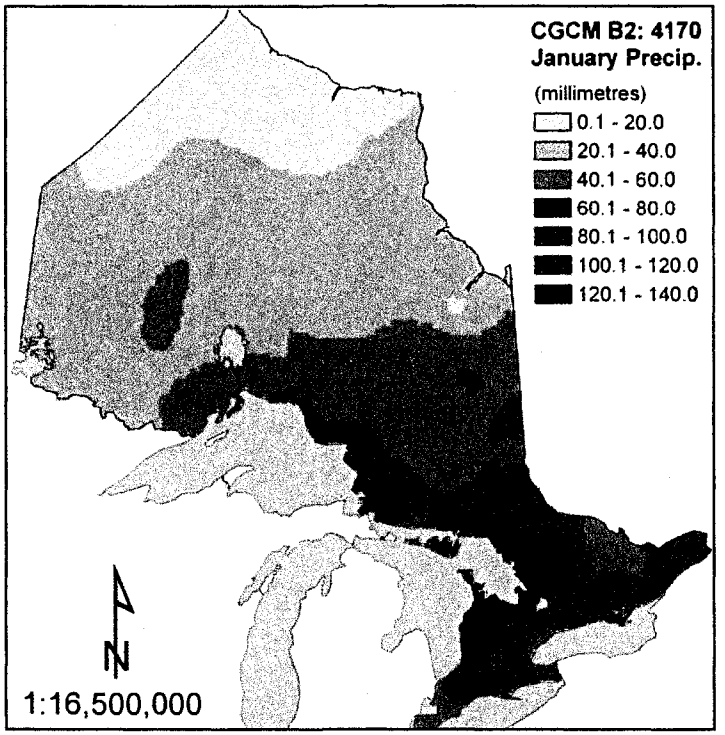

Predicted January precipitation for 2041-2070 based on CGCM2 B2.

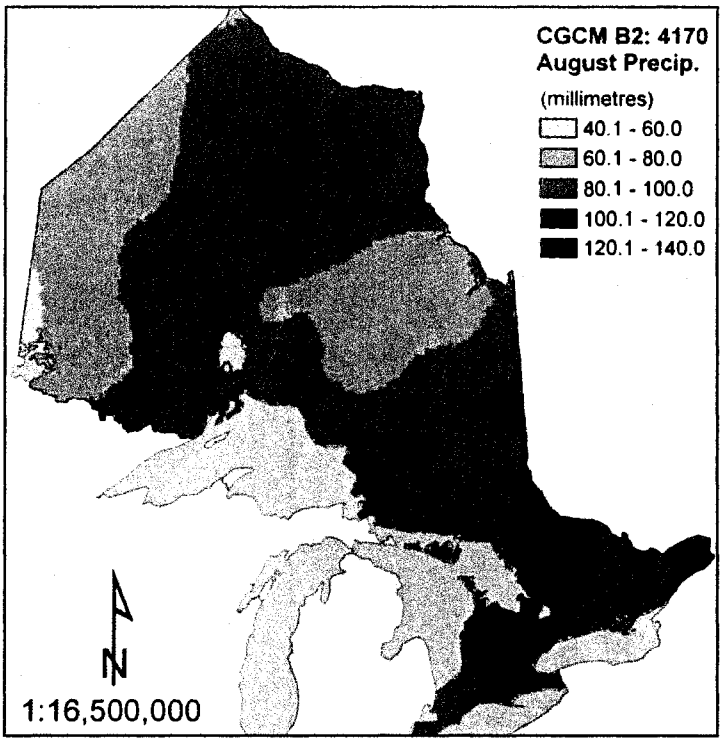

Predicted August precipitation for 2041-2070 based on CGCM2 B2.

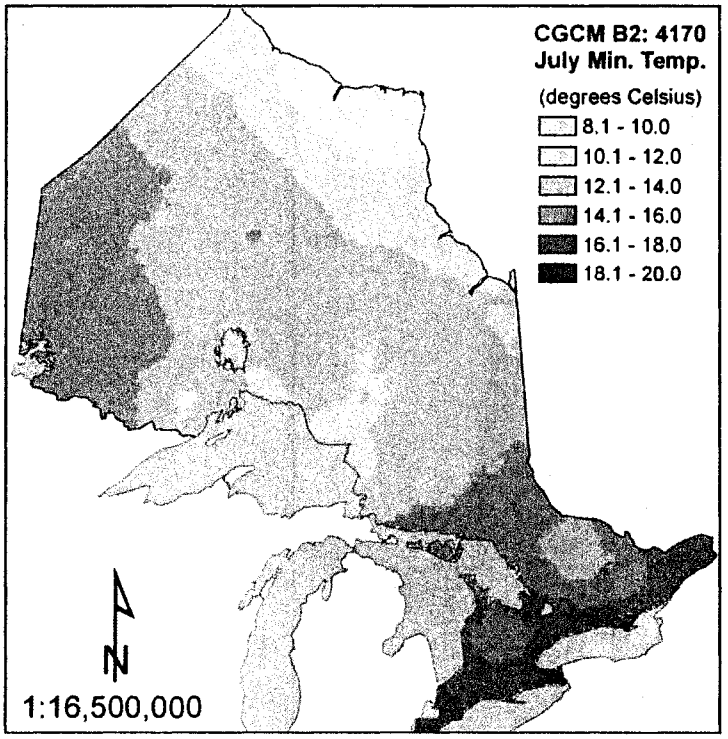

Predicted July minimum temperature for 2041-2070 based on CGCM2 B2.

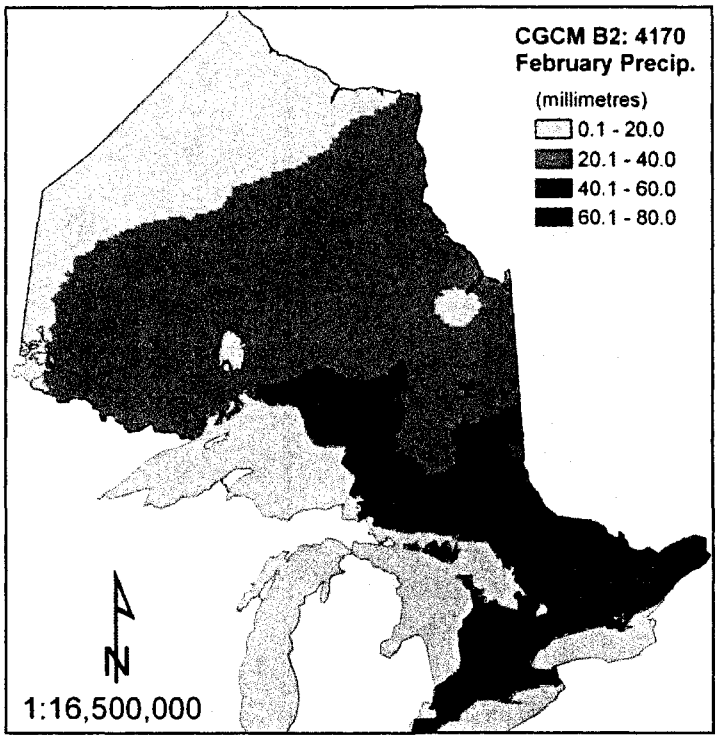

Predicted February precipitation for 2041-2070 based on CGCM2 B2.

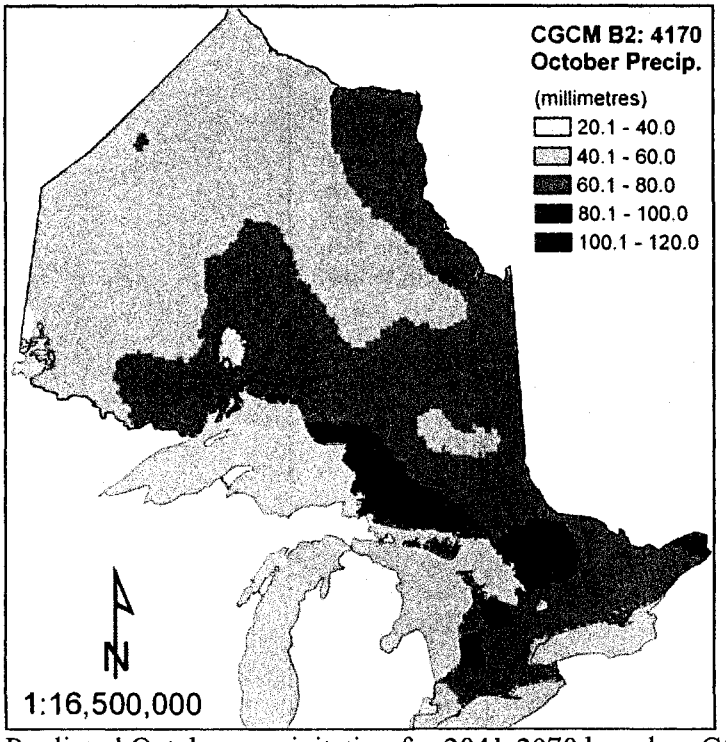

Predicted October precipitation for 2041-2070 based on CGCM2 B2.

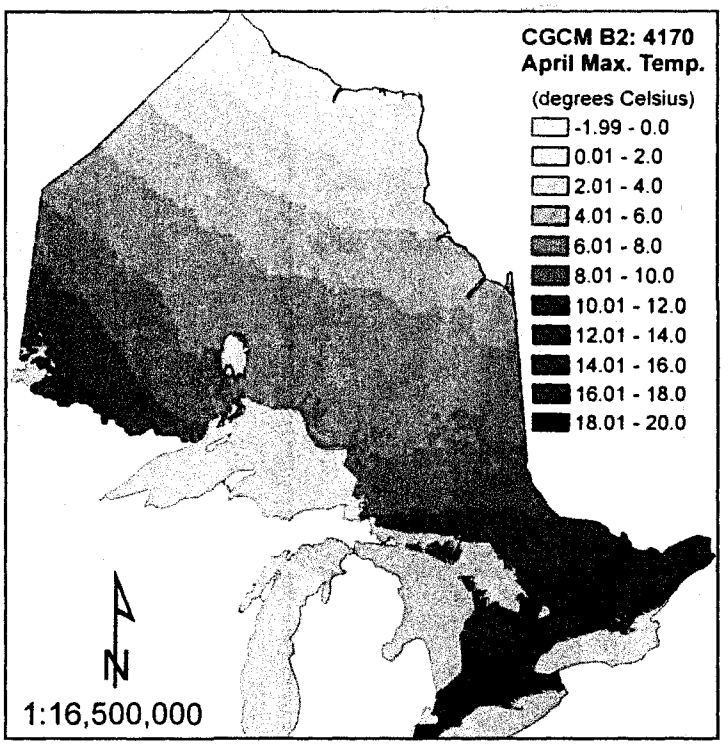

Predicted April maximum temperature for 2041-2070 based on CGCM2 B2.

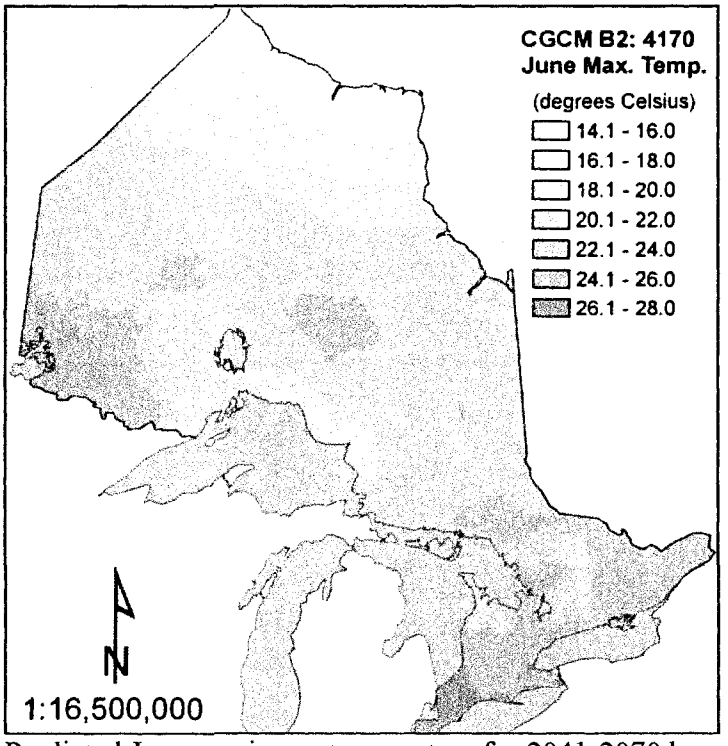

Predicted June maximum temperature for 2041-2070 based on CGCM2 B2.

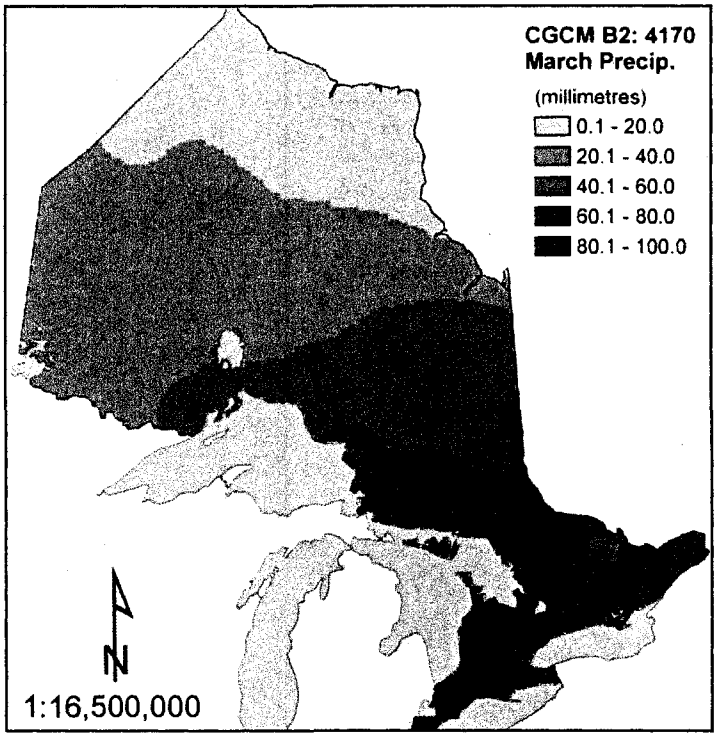

Predicted March precipitation for 2041-2070 based on CGCM2 B2.

HADCM3 A2: 2041-2070

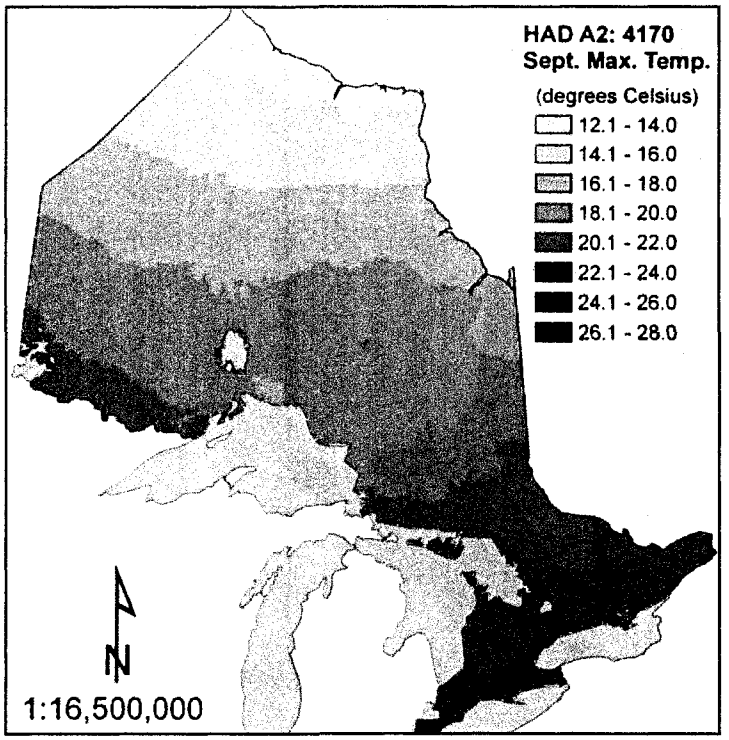

Predicted September maximum temperature for 2041-2070 based on HADCM3 A2.

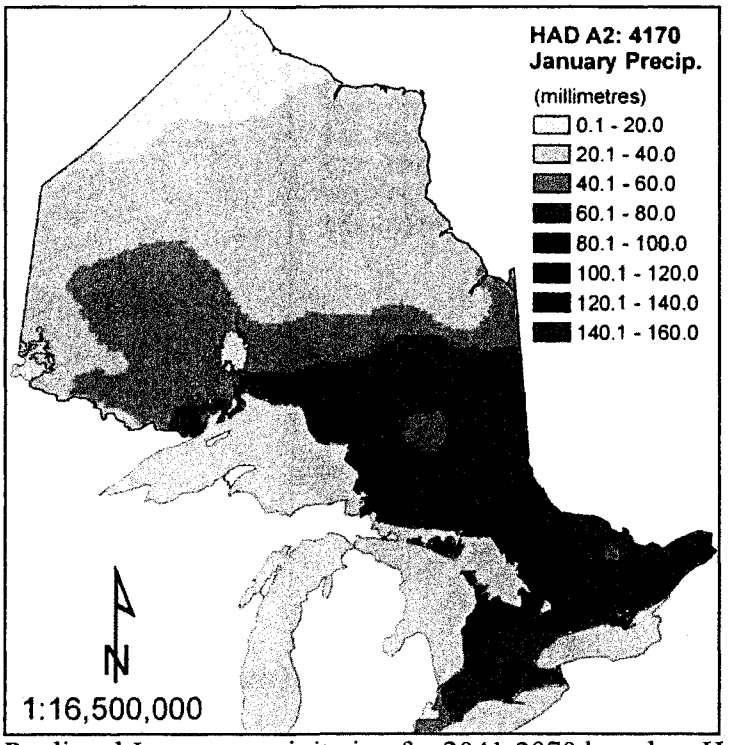

Predicted January precipitation for 2041-2070 based on HADCM3 A2.

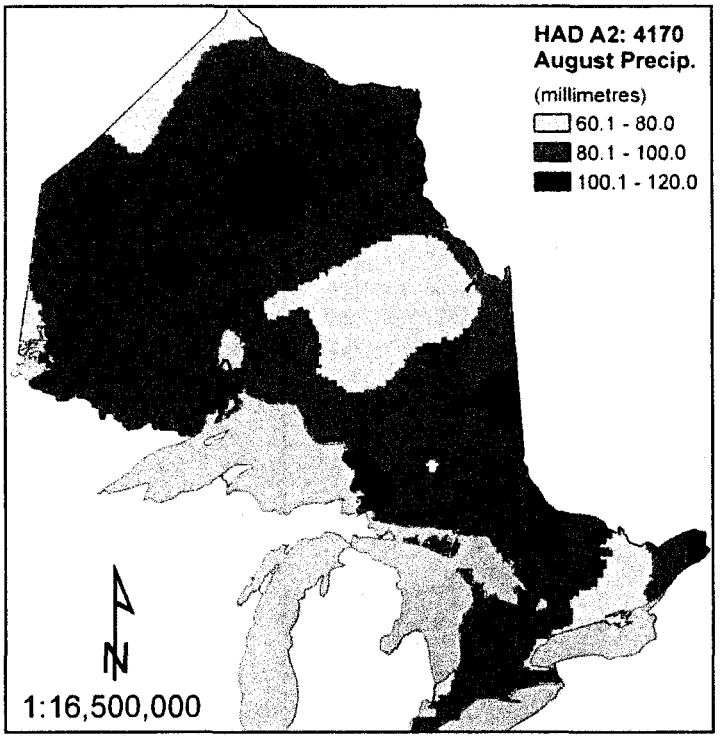

Predicted August precipitation for 2041-2070 based on HADCM3 A2.

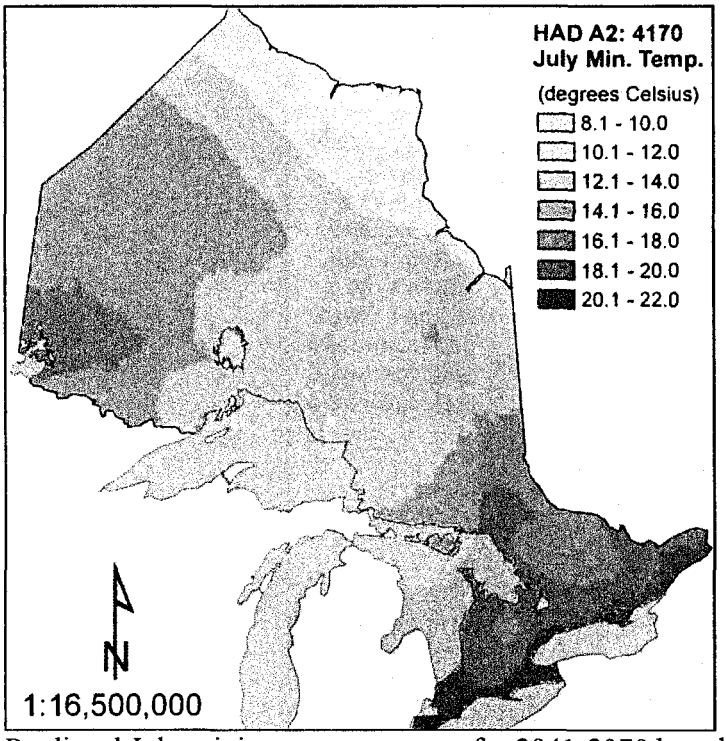

Predicted July minimum temperature for 2041-2070 based on HADCM3 A2.

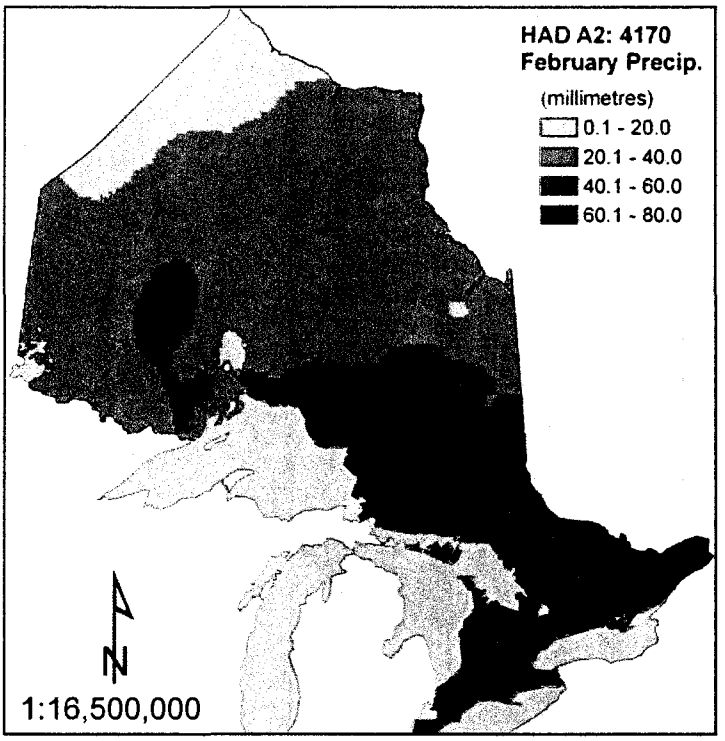

Predicted February precipitation for 2041-2070 based on HADCM3 A2.

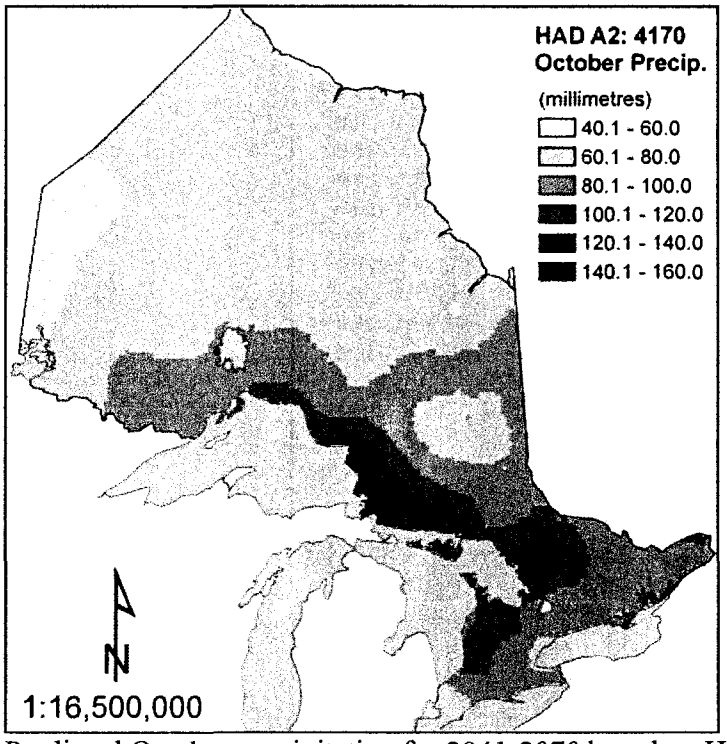

Predicted October precipitation for 2041-2070 based on HADCM3 A2.

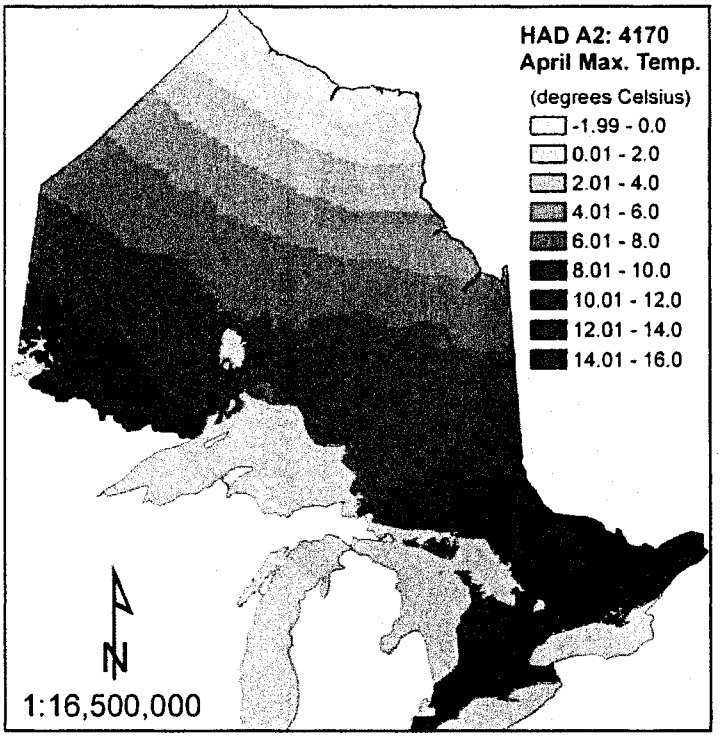

Predicted April maximum temperature for 2041-2070 based on HADCM3 A2.

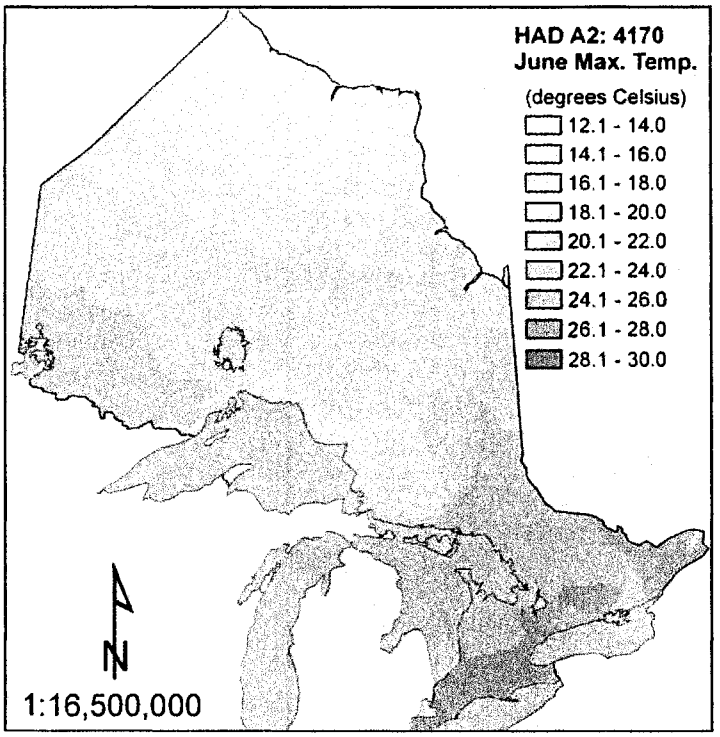

Predicted June maximum temperature for 2041-2070 based on HADCM3 A2.

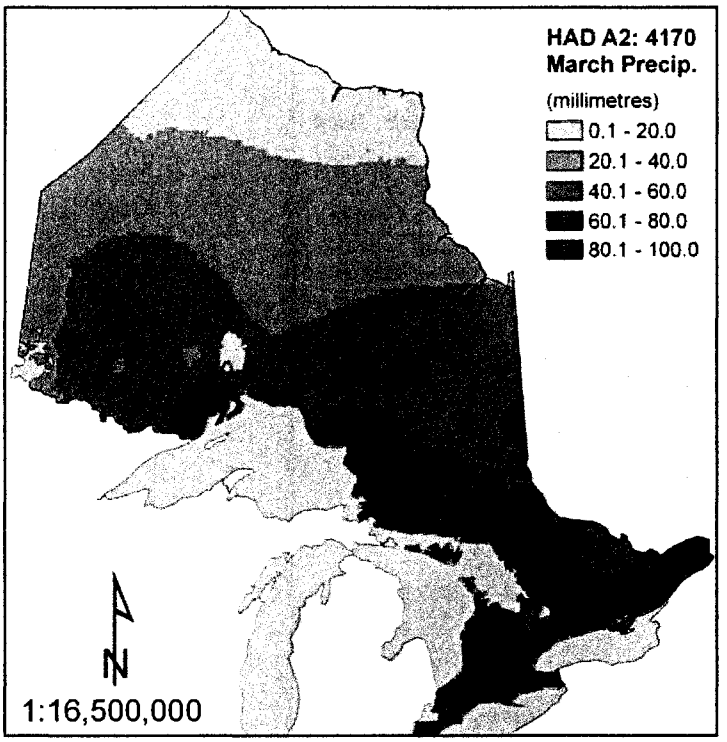

Predicted March precipitation for 2041-2070 based on HADCM3 A2.

HADCM3 B2: 2041-2070

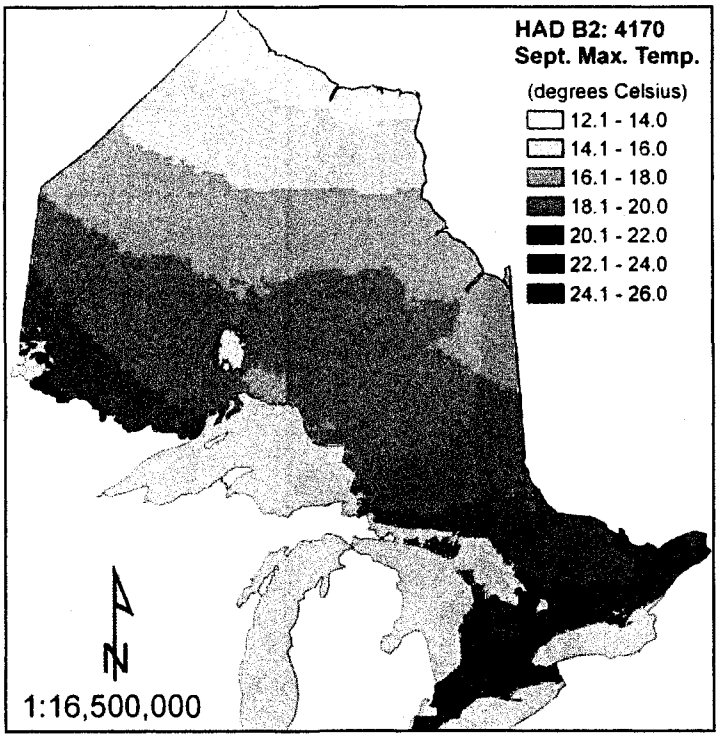

Predicted September maximum temperature for 2041-2070 based on HADCM3 B2.

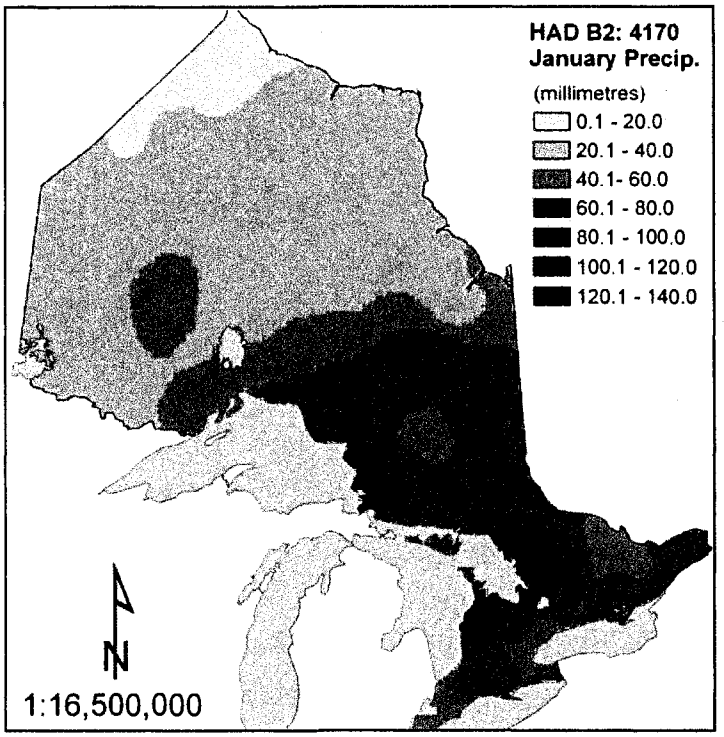

Predicted January precipitation for 2041-2070 based on HADCM3 B2.

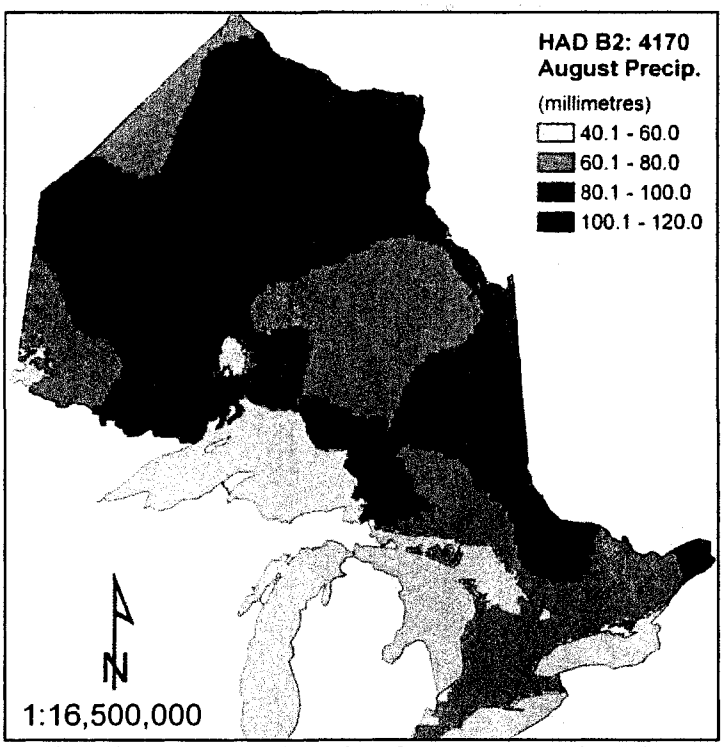

Predicted August precipitation for 2041-2070 based on HADCM3 B2.

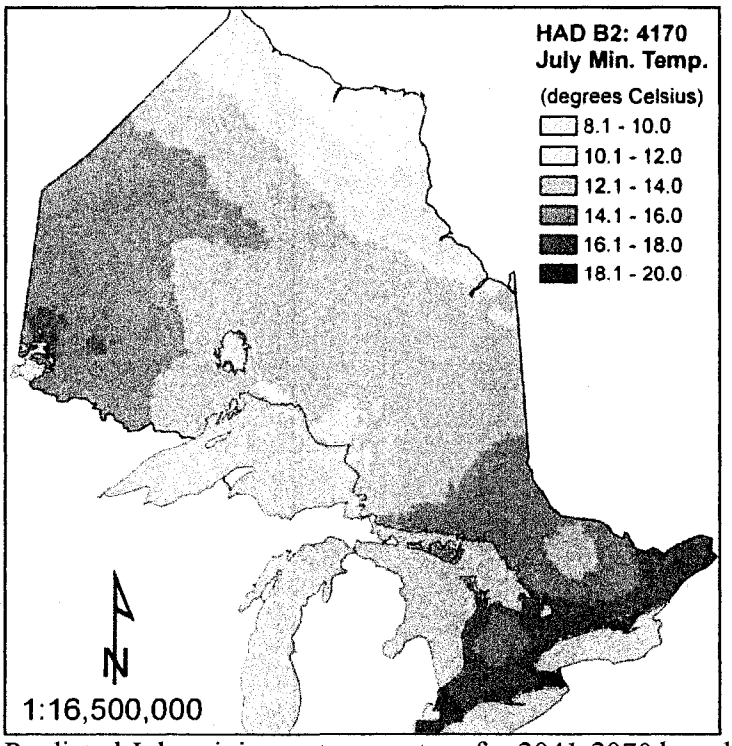

Predicted July minimum temperature for 2041-2070 based on HADCM3 B2.

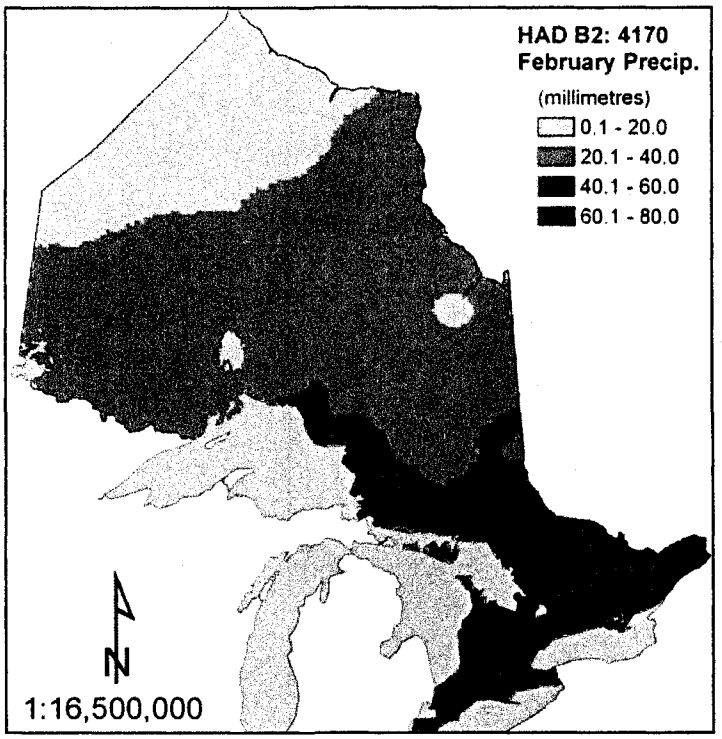

Predicted February precipitation for 2041-2070 based on HADCM3 B2.

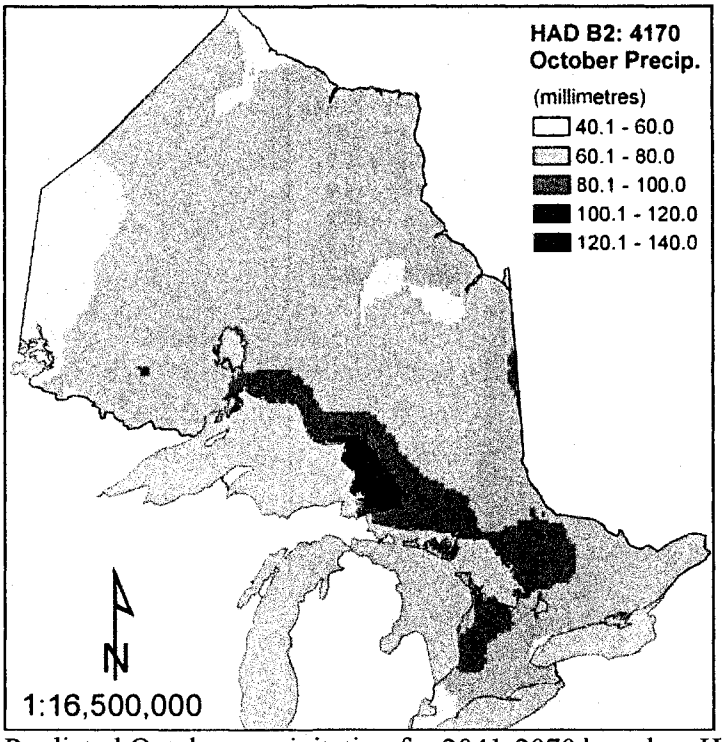

Predicted October precipitation for 2041-2070 based on HADCM3 B2.

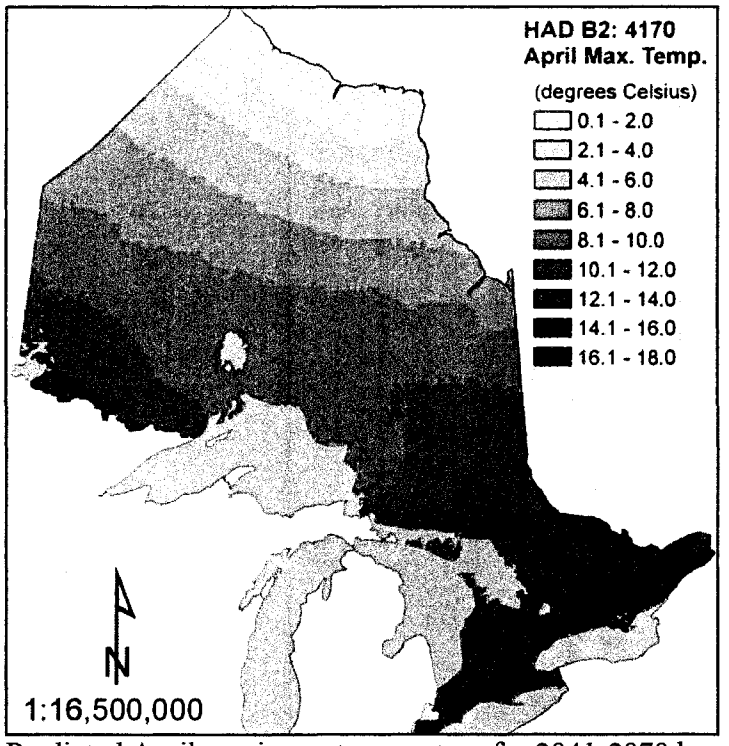

Predicted April maximum temperature for 2041-2070 based on HADCM3 B2.

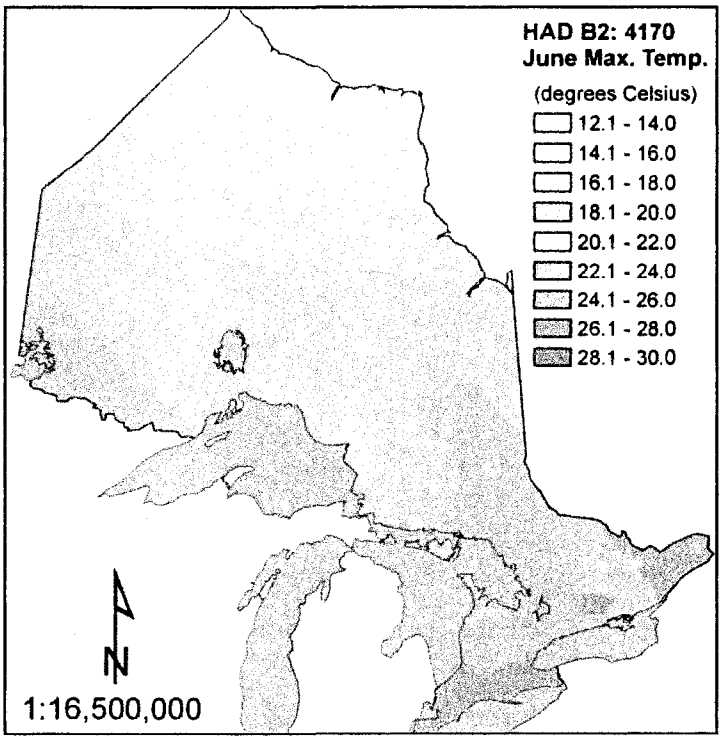

Predicted June maximum temperature for 2041-2070 based on HADCM3 B2.

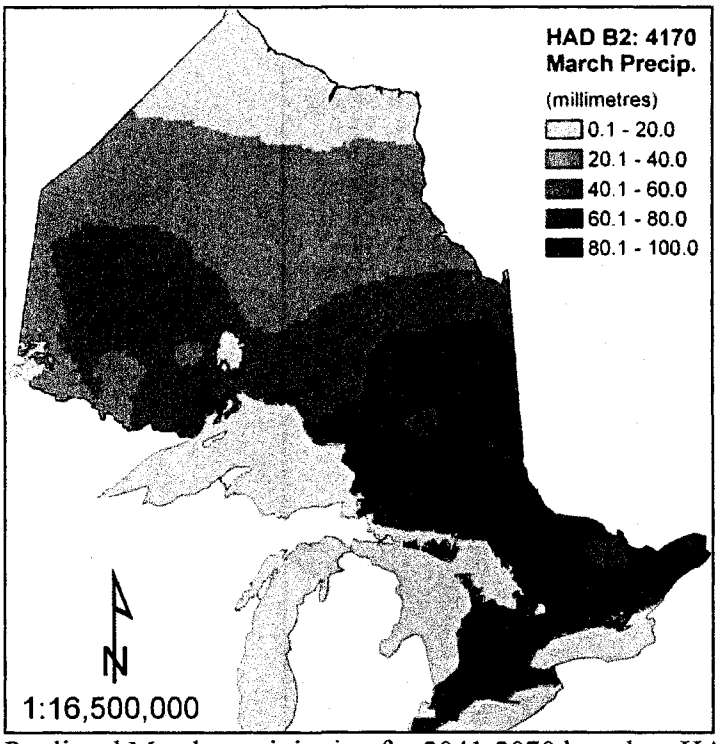

Predicted March precipitation for 2041-2070 based on HADCM3 B2.

CSIRO A2: 2041-2070

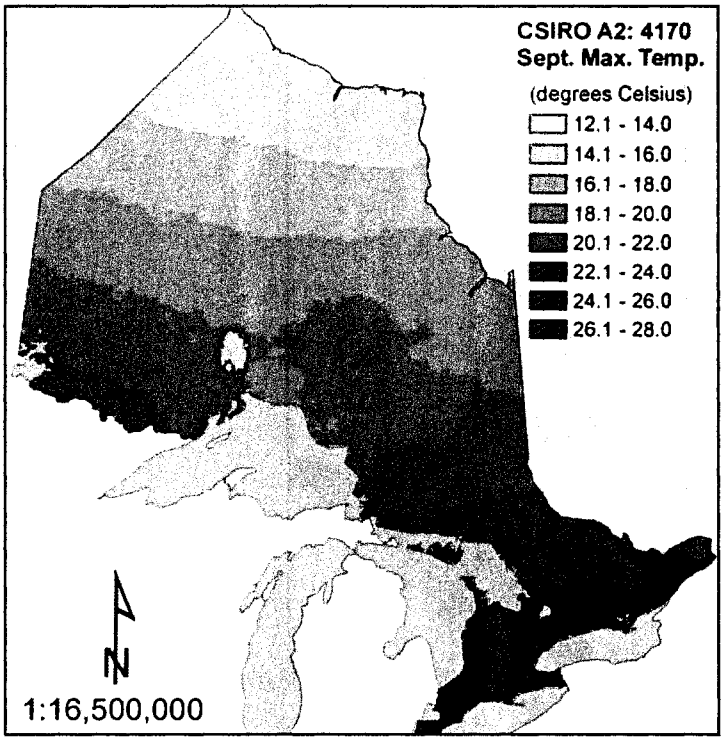

Predicted September maximum temperature for 2041-2070 based on CSIRO A2.

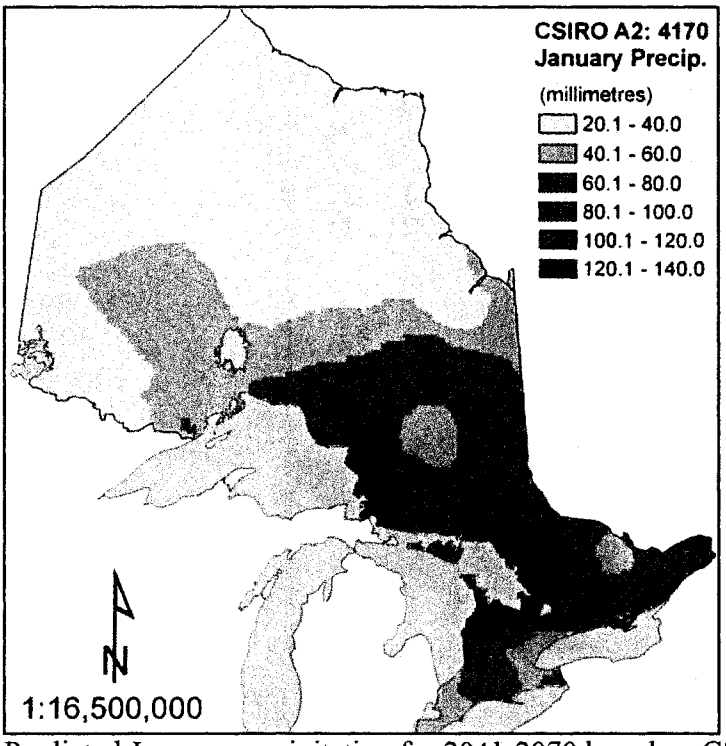

Predicted January precipitation for 2041-2070 based on CSIRO A2.

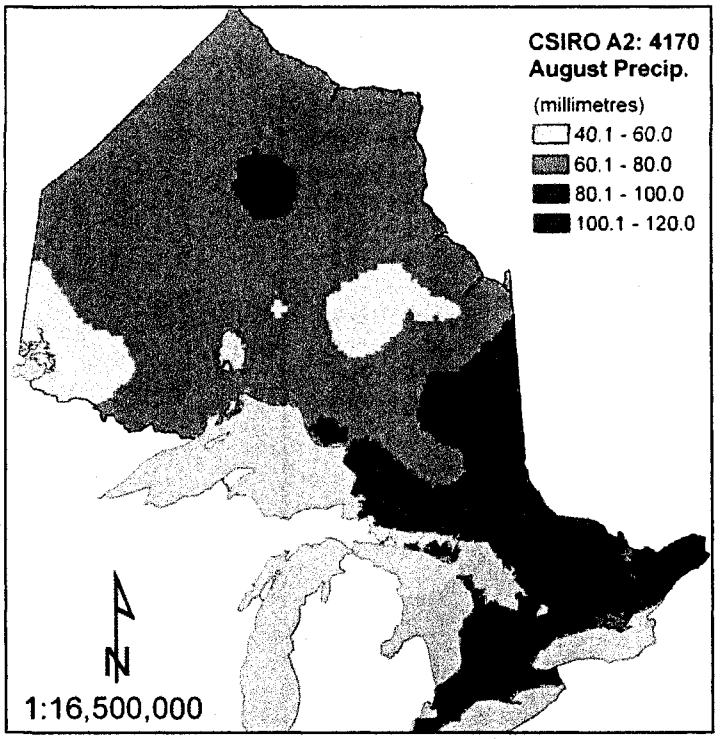

Predicted August precipitation for 2041-2070 based on CSIRO A2.

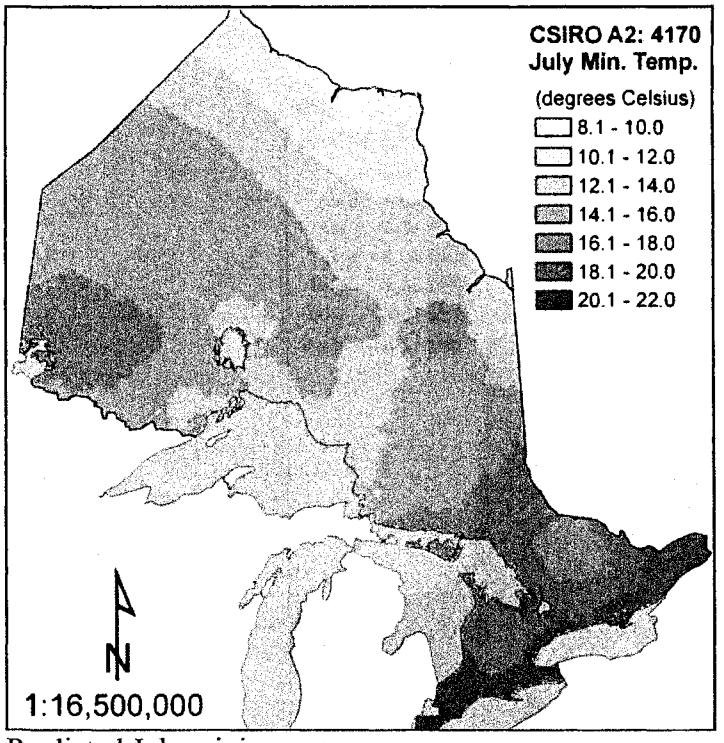

Predicted July minimum tempera

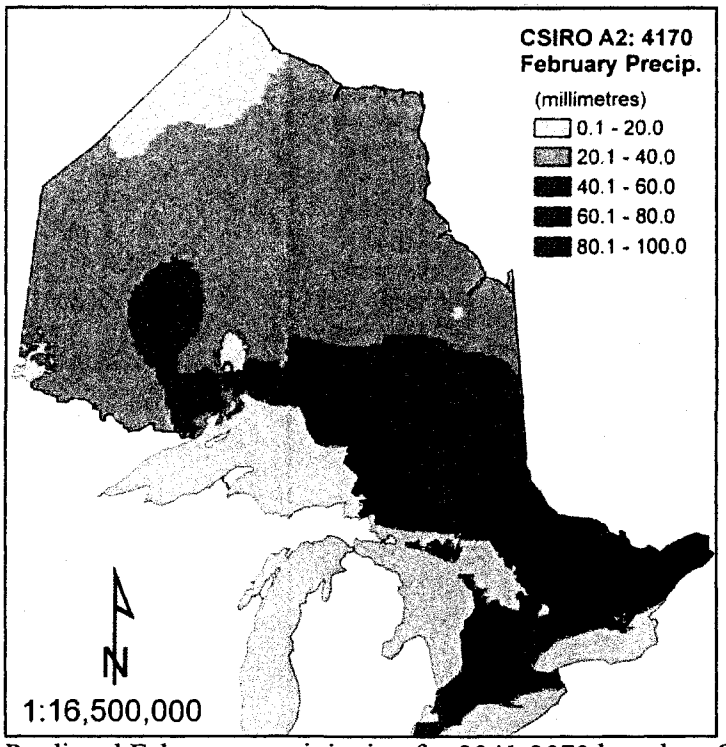

Predicted February precipitation for 2041-2070 based on CSIRO A2.

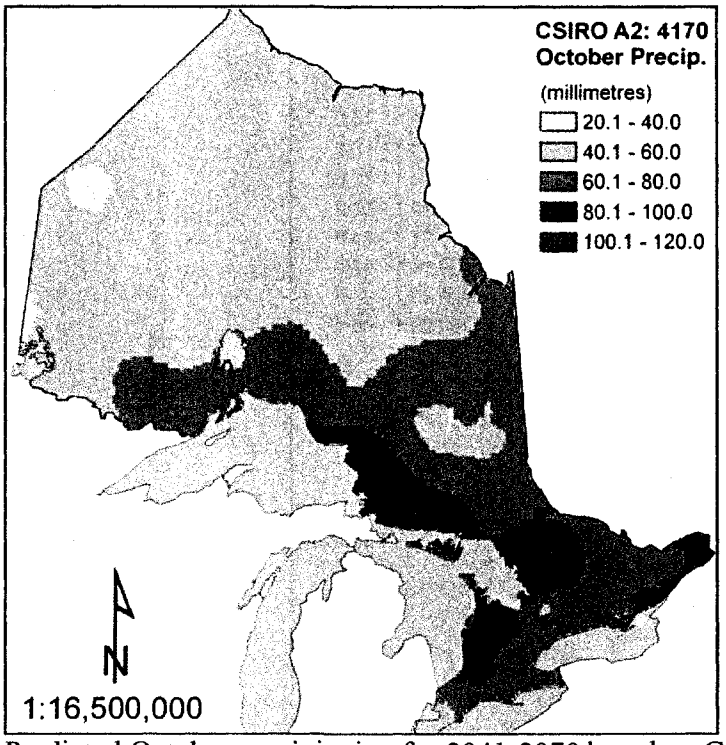

Predicted October precipitation for 2041-2070 based on CSIRO A2.

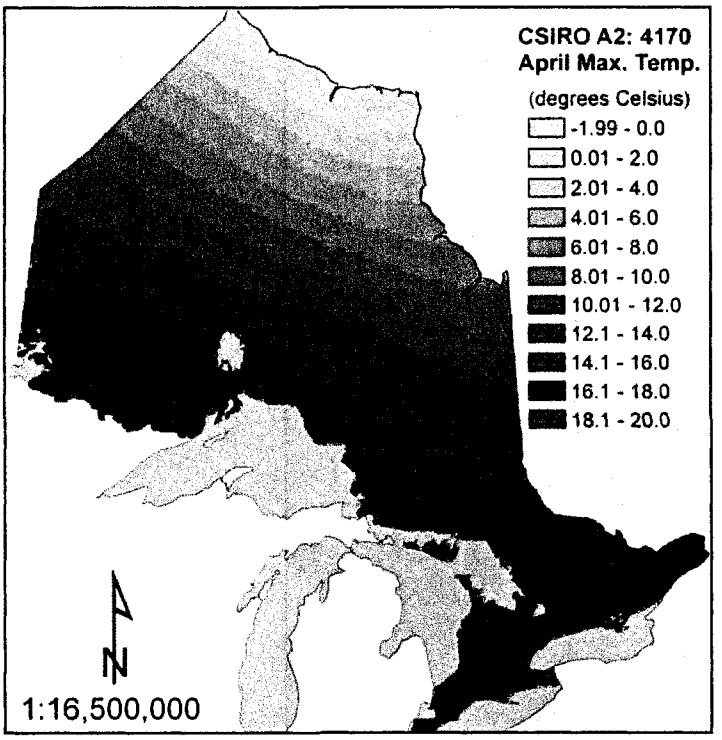

Predicted April maximum temperature for 2041-2070 based on CSIRO A2.

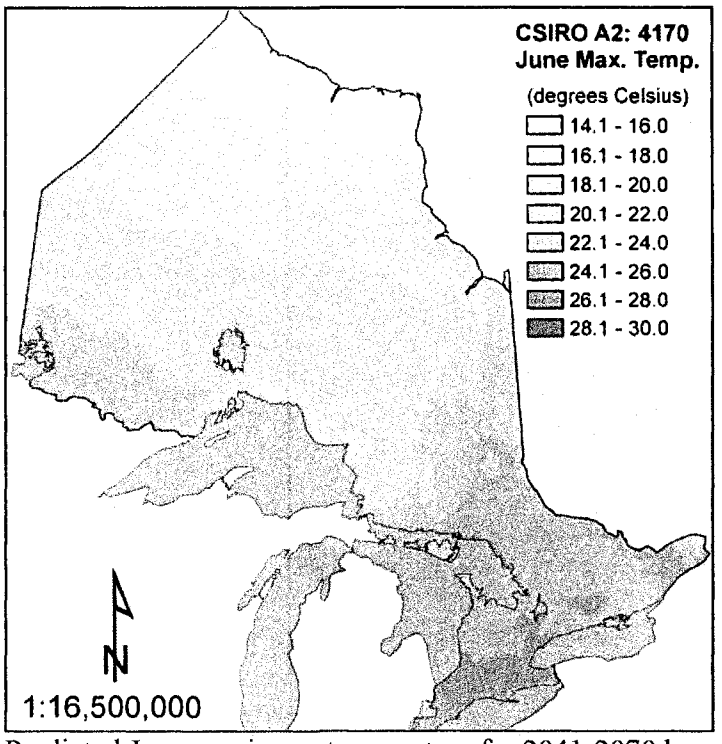

Predicted June maximum temperature for 2041-2070 based on CSIRO A2.

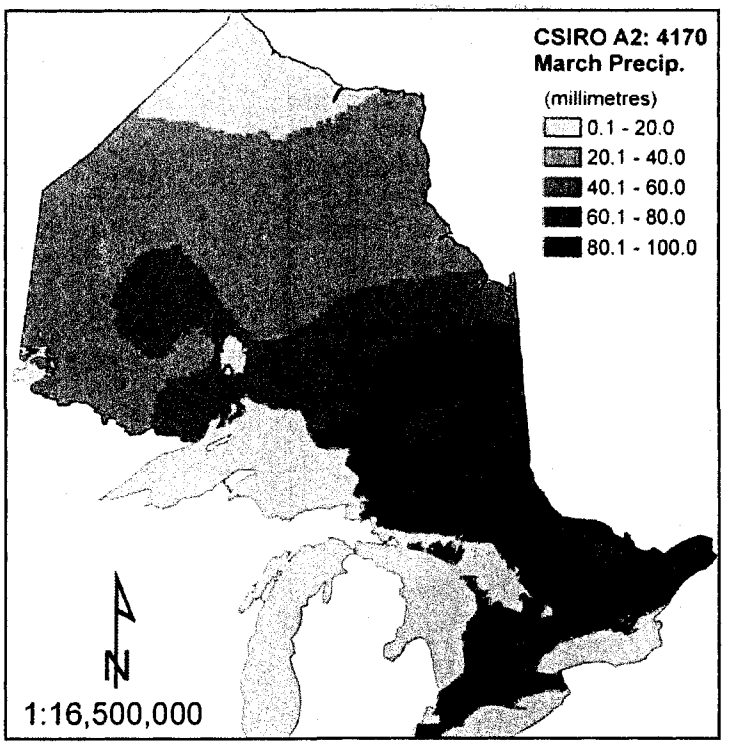

Predicted March precipitation for 2041-2070 based on CSIRO A2.

CSIRO B2: 2041-2070

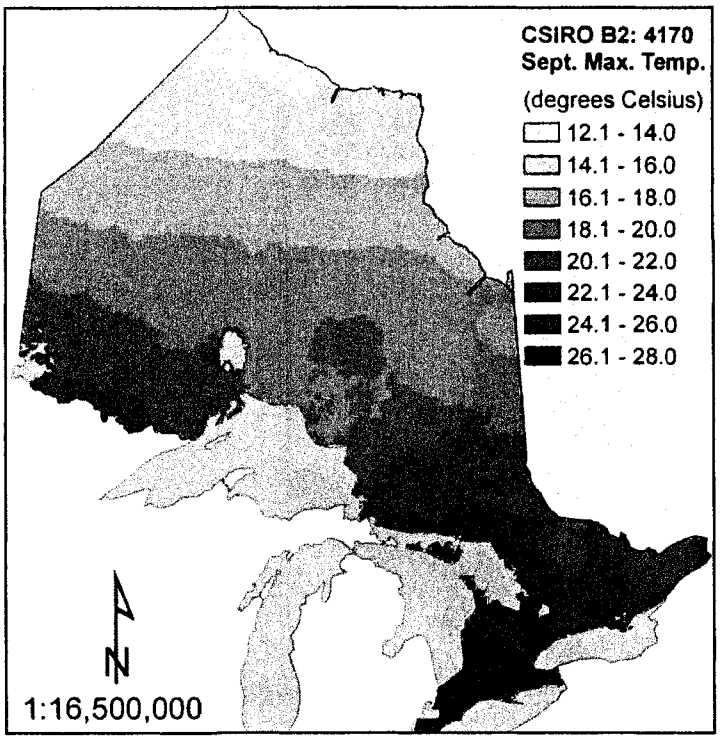

Predicted September maximum temperature for 2041-2070 based on CSIRO B2.

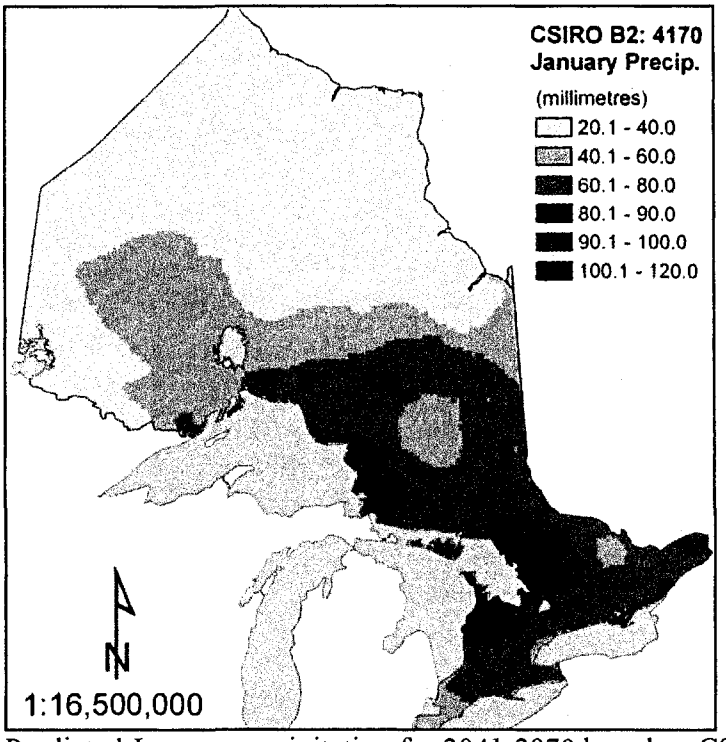

Predicted January precipitation for 2041-2070 based on CSIRO B2.

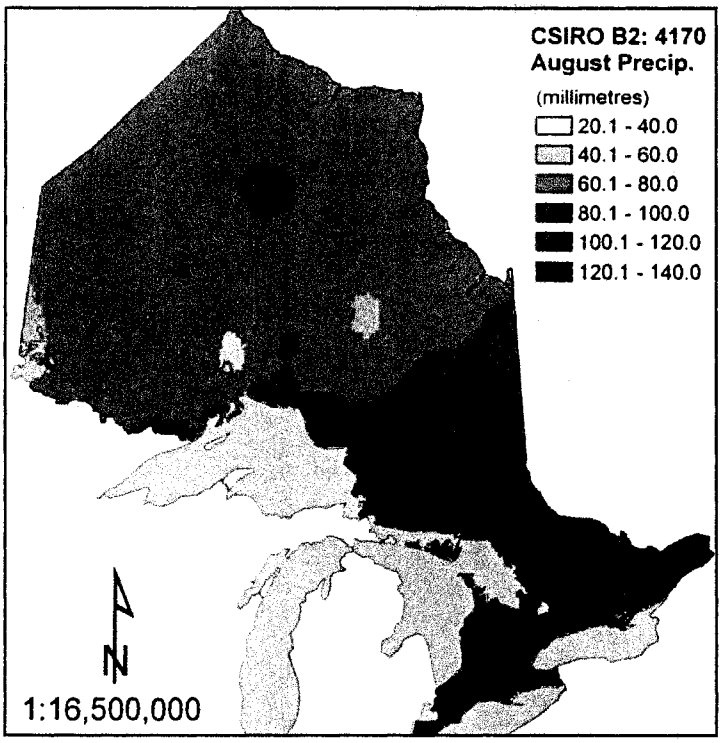

Predicted August precipitation for 2041-2070 based on CSIRO B2.

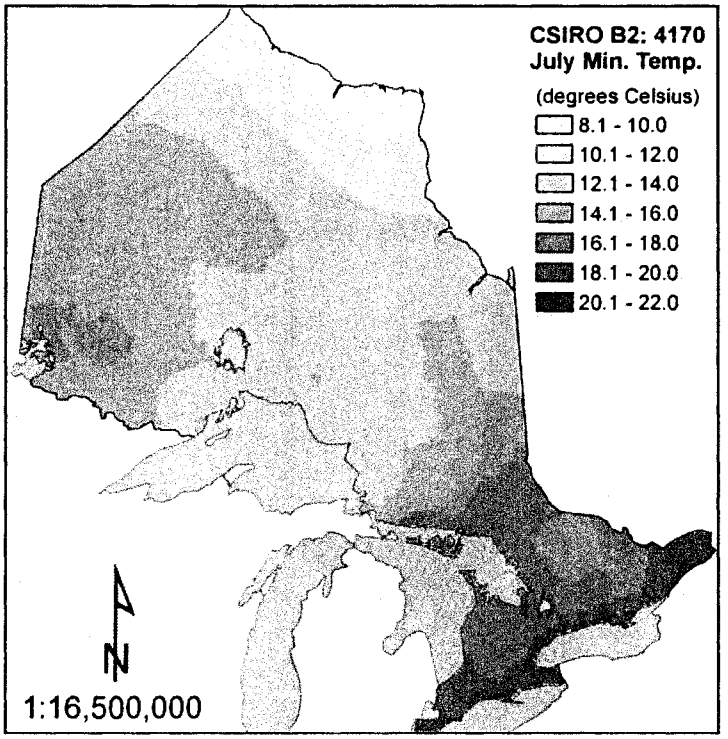

Predicted July minimum temperature for 2041-2070 based on CSIRO B2.

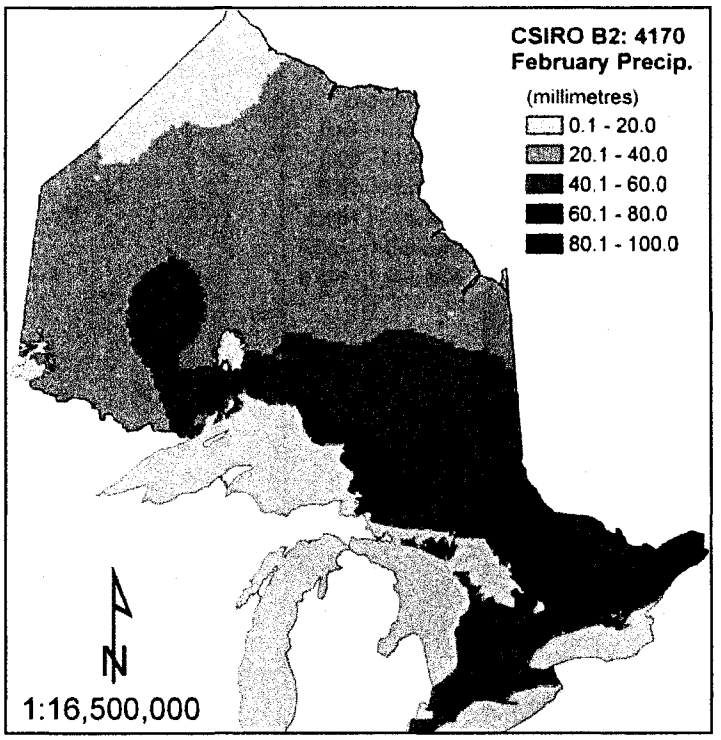

Predicted February precipitation for 2041-2070 based on CSIRO B2.

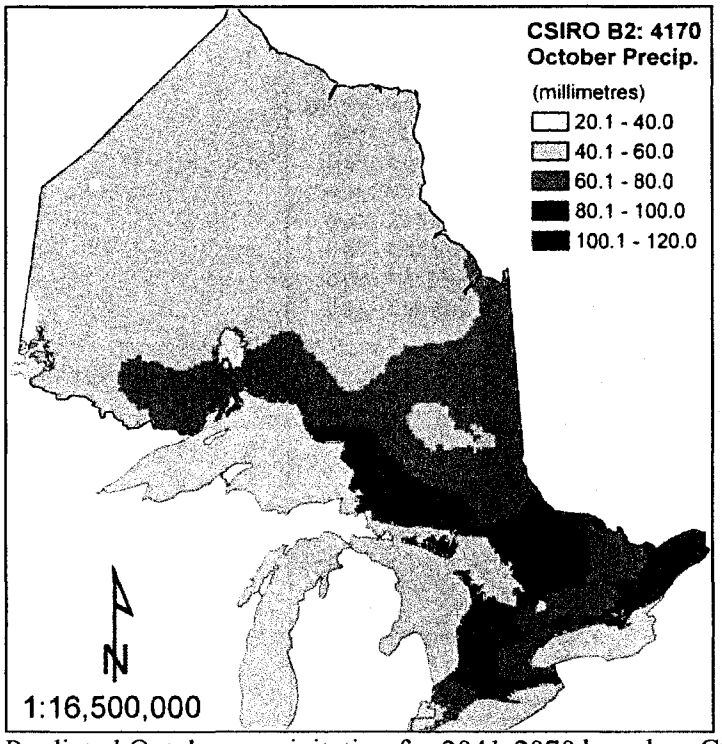

Predicted October precipitation for 2041-2070 based on CSIRO B2.

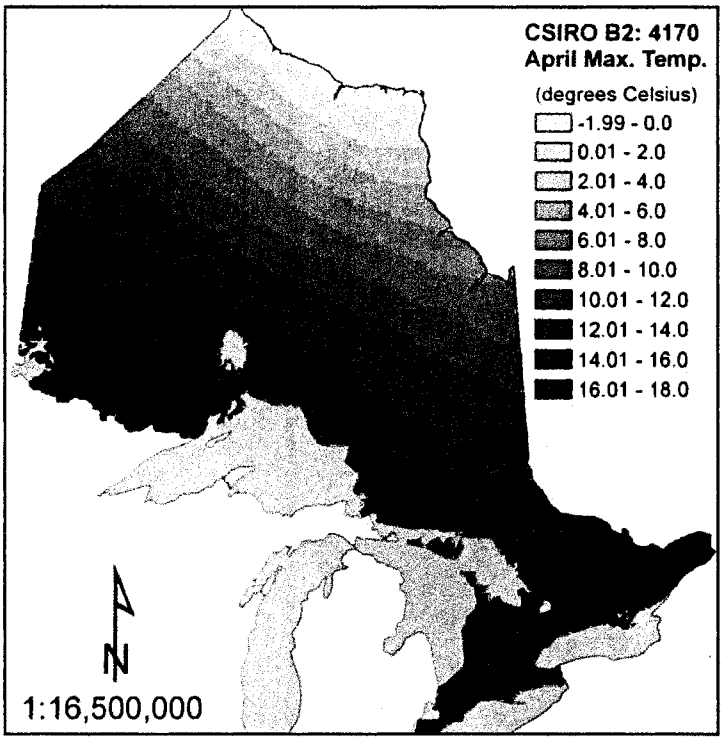

Predicted April maximum temperature for 2041-2070 based on CSIRO B2.

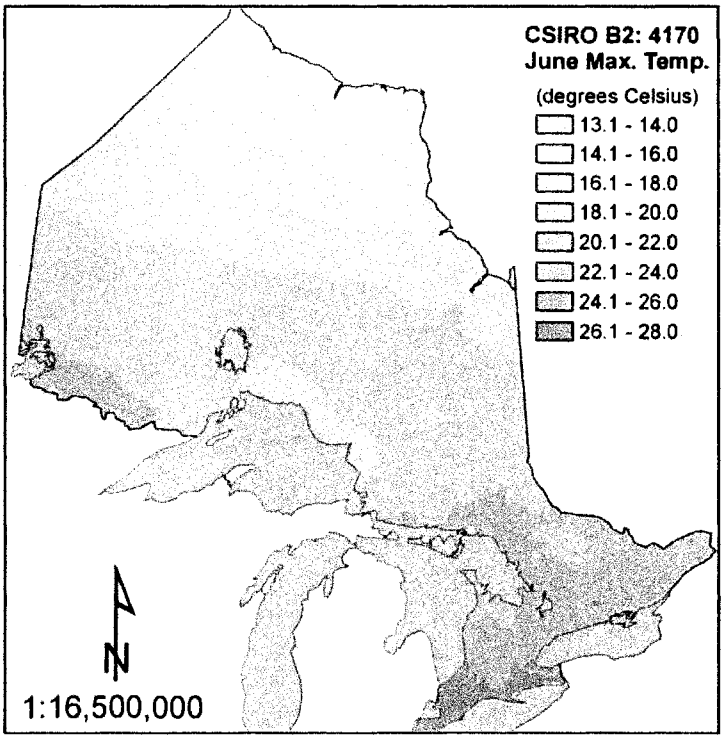

Predicted June maximum temperature for 2041-2070 based on CSIRO B2.

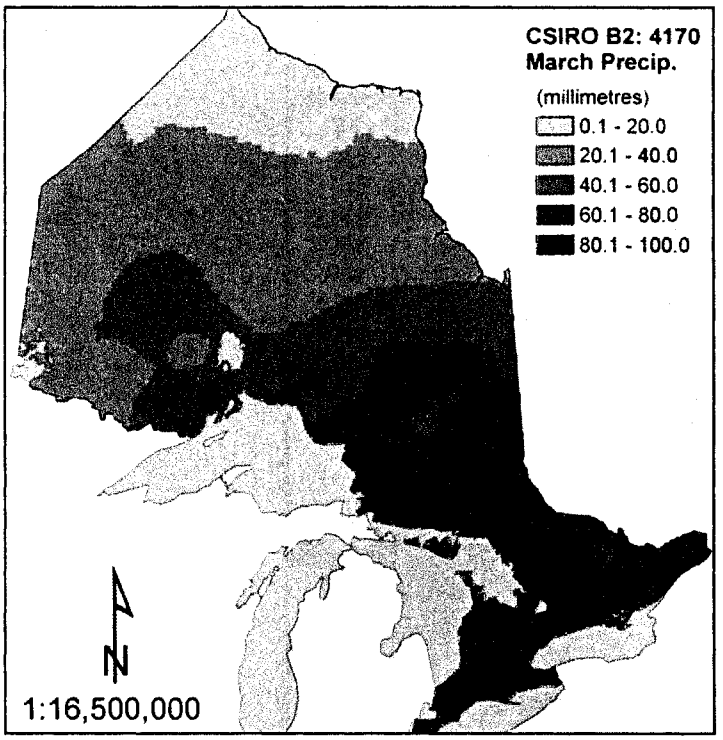

Predicted March precipitation for 2041-2070 based on CSIRO B2.

APPENDIX II: MULTIPLE LINEAR REGRESSIONS OUTPUT FROM SAS SOFTWARE BASED ON THE R^2 SELECTION METHOD

Regression of 3 PCA axes for 127 LLT Sw Sources, 6 tests vs 36 climate variables 1

10:50

Saturday, January 23, 2008

The REG Procedure
Model: MODEL1
Dependent Variable: prin1

R-Square Selection Method

Number in Model	R-Square	Variables in Model
1	0.2066	maymaxt
1	0.2041	junmaxt
1	0.1860	augmaxt
1	0.1825	sepmaxt
1	0.1801	junmint
2	0.2608	sepmaxt junprec
2	0.2541	augmaxt augprec
2	0.2524	augmaxt junprec
2	0.2487	octmaxt junprec
2	0.2486	junmint junprec
3	0.2804	sepmaxt janprec augprec
3	0.2792	marmaxt sepmaxt junprec
3	0.2786	febmaxt octmaxt junprec
3	0.2773	janmint sepmaxt augprec
3	0.2771	marmaxt octmaxt junprec
4	0.3042	sepmaxt janprec augprec decprec
4	0.3036	augmaxt janprec augprec decprec
4	0.2999	junmaxt janprec augprec decprec
4	0.2985	octmaxt janprec augprec decprec
4	0.2974	junmint janprec augprec decprec

Regression of 3 PCA axes for 127 LLT Sw Sources, 6 tests vs 36 climate variables 2

10:50

Saturday, January 23, 2008

The REG Procedure
Model: MODEL1
Dependent Variable: prin2

R-Square Selection Method

Number in Model	R-Square	Variables in Model
1	0.5026	junmint
1	0.4786	julmint
1	0.4778	maymint
1	0.4679	sepmaxt
1	0.4394	aprmint
2	0.5131	junmint junprec
2	0.5090	junmint augprec
2	0.5081	junmint octprec
2	0.5068	junmint augmint
2	0.5060	janmint junmint
3	0.5348	janmint aprmint junmint
3	0.5336	junmint febprec octprec
3	0.5329	julmint febprec octprec
3	0.5327	janmint julmint augmint
3	0.5298	maymint febprec octprec
4	0.5499	janmint marmint junmint sepmint
4	0.5481	janmint marmint junmint augmint
4	0.5479	janmint marmint junmint octmint
4	0.5475	janmint aprmint junmint augmint
4	0.5454	janmint junmint augmint marmaxt

Regression of 3 PCA axes for 127 LLT Sw Sources, 6 tests vs 36 climate variables 3

10:50

Saturday, January 23, 2008

The REG Procedure
Model: MODEL1
Dependent Variable: prin3

R-Square Selection Method

Number in Model	R-Square	Variables in Model
1	0.1124	julprec
1	0.0864	aprmaxt
1	0.0862	febmaxt
1	0.0854	marmaxt
1	0.0810	febmint
2	0.2296	febmaxt marprec
2	0.2182	marmaxt marprec
2	0.2121	marmint marprec
2	0.2056	febmint marprec
2	0.2037	decmaxt marprec
3	0.2696	aprmaxt junmaxt marprec
3	0.2560	aprmaxt maymaxt marprec
3	0.2534	aprmaxt junmaxt febprec
3	0.2520	marmaxt marprec octprec
3	0.2519	janmaxt febmaxt marprec
4	0.2996	decmint janmaxt aprmaxt junmaxt
4	0.2963	aprmint julmint aprmaxt junmaxt
4	0.2917	janmaxt febmaxt aprmaxt maymaxt
4	0.2913	janmaxt aprmaxt maymaxt decmaxt
4	0.2911	janmaxt aprmaxt junmaxt decmaxt

APPENDIX III: REGRESSION STATISTICS

The REG Procedure
Model: MODEL1
Dependent Variable: prin1

Analysis of Variance

Source	DF	Sum of Squares	Mean Square	F Value	Pr > F
Model	3	35.33059	11.77686	15.98	<.0001
Error	123	90.66941	0.73715		
Corrected Total	126	126.00000			

Root MSE	0.85857	R-Square	0.2804
Dependent Mean	-1.5748E-11	Adj R-Sq	0.2629
Coeff Var	-5.45194E12		

Parameter Estimates

Variable	DF	Parameter Estimate	Standard Error	t Value	Pr > |t|	Tolerance
Intercept	1	-8.84174	1.35949	-6.50	<.0001	.
sepmaxt	1	0.34772	0.05388	6.45	<.0001	0.72970
janprec	1	-0.01755	0.00644	-2.72	0.0074	0.65176
augprec	1	0.04245	0.01078	3.94	0.0001	0.79756

The REG Procedure
Model: MODEL1
Dependent Variable: prin2

Analysis of Variance

Source	DF	Sum of Squares	Mean Square	F Value	Pr > F
Model	3	67.14127	22.38042	46.77	<.0001
Error	123	58.85873	0.47853		
Corrected Total	126	126.00000			

Root MSE	0.69176	R-Square	0.5329
Dependent Mean	4.7244E-11	Adj R-Sq	0.5215
Coeff Var	1.464219E12		

Parameter Estimates

Variable	DF	Parameter Estimate	Standard Error	t Value	Pr > |t|	Tolerance
Intercept	1	-2.14362	1.01385	-2.11	0.0365	.
julmint	1	0.27055	0.06232	4.34	<.0001	0.40718
febprec	1	0.03648	0.00987	3.69	0.0003	0.26834

The REG Procedure
Model: MODEL1
Dependent Variable: prin3

Analysis of Variance

Source	DF	Sum of Squares	Mean Square	F Value	Pr > F
Model	3	33.97214	11.32405	15.14	<.0001
Error	123	92.02786	0.74819		
Corrected Total	126	126.00000			

Root MSE	0.86498	R-Square	0.2696
Dependent Mean	1.57481E-11	Adj R-Sq	0.2518
Coeff Var	5.492616E12		

Parameter Estimates

Variable	DF	Parameter Estimate	Standard Error	t Value	Pr > |t|	Tolerance
Intercept	1	4.52079	1.60212	2.82	0.0056	.
aprmaxt	1	0.69129	0.10724	6.45	<.0001	0.21100
junmaxt	1	-0.36767	0.10232	-3.59	0.0005	0.28408
marprec	1	-0.04744	0.01070	-4.43	<.0001	0.48978

APPENDIX IV: FOCAL POINT SEED ZONES AML PROGRAM

```
/* ****************************************************************
/* C:\WorkSpace\swfpsz_feb11\swfpsz_apr21.aml   April 21, 2008
/*
/* aml routine to run a series of 618 focal point seed zones
/*    based on lambert coordinates stored in an ASCII file:
swfptslam.prn
/*    for jack pine in NW Ontario. Overlay pt cov grid: ontptslam (2324
points)
/* Focal Points (618) are stored in coverage: swfptslam
/* ontptslam.pat contains the covering info (2324R, 618C) after program
is run
/* This version is based on grid arithmetic. + or - 1.0 LSD
/*
/*   Two regression grids are intersected in this version.
/*      C:\WorkSpace\swfpsz_feb11\rpc1  C:\WorkSpace\swfpsz_feb11\rpc2
C:\WorkSpace\swfpsz_feb11\rpc3
/*
/* ****************************************************************
&type Running swfpsz
 &messages &off
/* &messages &on
/* Define the file name and open file
/* Set the stop number -- maxn
&setvar maxn 619
/* Set the start number -- n
&setvar n = 1
&setvar cnt = 0
&setvar fil = swfptslam.prn
&label restrt
&setvar filunit = [open %fil% openstatus -read]
/*
/* Check for error in opening file
&if %openstatus% <> 0 &then
   &return &warning Error opening file.
/*
/* Read from file
/*
/* Start the loop
&do &until %cnt% = %n%
     &setvar cnt = %cnt% + 1
    /* Read next line
    &setvar .rec = [read %filunit% readstatus]
&end
/*  line 39
/* Close the file
&if [close %filunit%] <> 0 &then
    &return &warning Unable to close %fil%
     &type Point number %n%
     &type focal point location =  %.rec%
 &messages &off
 /*   &type Running program
    &call gridpl
    &setvar n = %n% + 1
    &setvar cnt = 0
&if %n% lt %maxn% &then  &goto restrt
     &else
&return End of job.
```

```
&routine gridpl
/* Focal Point Seed Zone Program for Ontario white spruce
/* W.H. Parker, Faculty of Forestry and Forest Environment, Lakehead
University
/* Thunder Bay, Ontario
/* April, 2008
/*
/* The first step generates Lambert coords from inputed geo
coordinates.
/*
&severity &error &ignore
/* del sitegeo
/*del sitelam.gen
/* del sitelam.prj
/*kill grd1
/*kill grd2
/*kill grd3
/*kill grd4
/*kill site
/*kill zonelgrp
/*
/* parse x lambert coordinate
/*
&s blank [search %.rec% ' ']
&do &until %blank% ne 1
  &s .rec [after %.rec% ' ']
  &s blank [search %.rec% ' ']
&end
&s .xlam [before %.rec% ' ']
&s .rec [after %.rec% ' ']
/*
/* parse y lambert coordinate
/*
&s blank [search %.rec% ' ']
&do &until %blank% ne 1
  &s .rec [after %.rec% ' ']
  &s blank [search %.rec% ' ']
&end
&s .ylam [before %.rec% ' ']
/*
/* create generate file
/*
&setvar file = sitelam.gen
&setvar funit = [open %file% ostat -write]
&if %ostat% ne 0 &then &return Error %ostat% Unable to open file
%file%.
&s rec '1,'%.xlam%','%.ylam%
/*     &type %rec%
&if [write %funit% %rec%] ne 0 &then &return Error wrting file %file%.
&s rec 'end'
/* &type %rec%
&if [write %funit% %rec%] ne 0 &then &return Error wrting file %file%.
&if [close %funit%] ne 0 &then &return Cannot close file %file%
generate site
input sitelam.gen
points
q
```

```
&setvar file = runnumber
&setvar funit = [open %file% ostat -write]
&if %ostat% ne 0 &then &return Error %ostat% Unable to open file
%file%.
&s rec 'Zone'%n%
/*     &type %rec%
&if [write %funit% %rec%] ne 0 &then &return Error wrting file %file%.
&if [close %funit%] ne 0 &then &return Cannot close file %file%
additem ONTPTSLAM.PAT ONTPTSLAM.PAT z%n% 4 5 b
grid
display 9999
mapextent rpc1
&setvar filgrd1 = rpc1
&setvar filgrd2 = rpc2
&setvar filgrd3 = rpc3
&setvar wchfile = tempwch
&watch %wchfile%
ap cellvalue %filgrd1% %.xlam% %.ylam% none
ap cellvalue %filgrd2% %.xlam% %.ylam% none
ap cellvalue %filgrd3% %.xlam% %.ylam% none
&watch &off
&setvar funit = [open %wchfile% openstatus -read]
      &setvar rec1 = [read %funit% readstatus]
      &s rec1 [after %rec1% 'value ']
      &setvar rec2 = [read %funit% readstatus]
      &s rec2 [after %rec2% 'value ']
&setvar rec3 = [read %funit% readstatus]
      &s rec3 [after %rec3% 'value ']
&if [close %funit%] ne 0 &then
     &return &warning Unable to close %wchfile%
/* &messages &on
/* &type Calculating adjusted rpca1 grid
grd1 = %filgrd1% - %rec1%
/* &type Calculating adjusted rpca2 grid
grd2 = %filgrd2% - %rec2%
/* &type Calculating adjusted rpca3 grid
grd3 = %filgrd3% - %rec3%
/* &type Calculating intersected rpca1, rpca2, and rpca3 grids (+ or -
1.0 lsd)
grd4 = con(grd1 ge -.61 & grd1 le .61 & grd2 ge -.59 & grd2 le .59 &
grd3 ge -.61 & grd3 le .61,1,0)
&messages &on
list GRD4.VAT
&messages &off
setmask ontptslamgrd
zone1grp = regiongroup(grd4, z1table, eight, #, #, #)
q
joinitem ONTPTSLAM.PAT z1table ONTPTSLAM.PAT value
&s VAR = Z%n%
&DATA ARC INFO
  ARC
  SEL ONTPTSLAM.PAT
  CALC %VAR% = LINK
  SEL Z1TABLE
  ERASE Z1TABLE
  Y
  Q STOP
```

```
&END
DROPITEM ONTPTSLAM.PAT ONTPTSLAM.PAT LINK
copy grd4 may1_11sd%n%
/* &type RegPCA1 value =  %rec1%
/* &type RegPCA2 value =  %rec2%
/* &type RegPCA3 value =  %rec3%
arcplot
display 1040 8
fpzn%n%
pagesize 11 8.5
mapext grd4
mappos cen cen
shadeset fpshades3.shd
gridnodatasymbol yellow
gridshades grd4 value identity nowrap
linecolor black
arcs provslam
linecolor blue
arcs lakeslam
markersymbol 70
markercolor black
markersize .3
points site
 markerset mineral.mrk
 markersymbol 102
 markersize .08
 markercolor green
 points swfptslam
 markersize .02
 markercolor black
 points ontptslam
textset font.txt
textsymbol 5
textsize .1
move 10 8
textfile runnumber
&messages &on
 q
 &return
&return end of job
```

APPENDIX V: MAXIMAL COVERING MODEL

```
TITLE   Breeding_zone_selection

INDEX

 c_xj:=(x1,   x2,    x3,    x4,    x5,    x6,    x7,    x8,    x9,
       x10,   x11,   x12,   x13,   x14,   x15,   x16,   x17,   x18,
       x19,   x20,
x21,   x22,   x23,   x24,   x25,   x26,   x27,   x28,   x29,   x30,
       x31,   x32,   x33,   x34,   x35,   x36,   x37,   x38,   x39,
       x40,
x41,   x42,   x43,   x44,   x45,   x46,   x47,   x48,   x49,   x50,
       x51,   x52,   x53,   x54,   x55,   x56,   x57,   x58,   x59,
       x60,
x61,   x62,   x63,   x64,   x65,   x66,   x67,   x68,   x69,   x70,
       x71,   x72,   x73,   x74,   x75,   x76,   x77,   x78,   x79,
       x80,
x81,   x82,   x83,   x84,   x85,   x86,   x87,   x88,   x89,   x90,
       x91,   x92,   x93,   x94,   x95,   x96,   x97,   x98,   x99,
       x100,
x101,  x102,  x103,  x104,  x105,  x106,  x107,  x108,  x109,  x110,
       x111,  x112,  x113,  x114,  x115,  x116,  x117,  x118,  x119,
       x120,
x121,  x122,  x123,  x124);

       c_yi:=(y1,    y2,    y3,    y4,    y5,    y6,    y7,    y8,
       y9,    y10,   y11,   y12,   y13,   y14,   y15,   y16,   y17,
       y18,   y19,   y20,
y21,   y22,   y23,   y24,   y25,   y26,   y27,   y28,   y29,   y30,
       y31,   y32,   y33,   y34,   y35,   y36,   y37,   y38,   y39,
       y40,
y41,   y42,   y43,   y44,   y45,   y46,   y47,   y48,   y49,   y50,
       y51,   y52,   y53,   y54,   y55,   y56,   y57,   y58,   y59,
       y60,
y61,   y62,   y63,   y64,   y65,   y66,   y67,   y68,   y69,   y70,
       y71,   y72,   y73,   y74,   y75,   y76,   y77,   y78,   y79,
       y80,
y81,   y82,   y83,   y84,   y85,   y86,   y87,   y88,   y89,   y90,
       y91,   y92,   y93,   y94,   y95,   y96,   y97,   y98,   y99,
       y100,
y101,  y102,  y103,  y104,  y105,  y106,  y107,  y108,  y109,  y110,
       y111,  y112,  y113,  y114,  y115,  y116,  y117,  y118,  y119,
       y120,
y121,  y122,  y123,  y124,  y125,  y126,  y127,  y128,  y129,  y130,
       y131,  y132,  y133,  y134,  y135,  y136,  y137,  y138,  y139,
       y140,
y141,  y142,  y143,  y144,  y145,  y146,  y147,  y148,  y149,  y150,
       y151,  y152,  y153,  y154,  y155,  y156,  y157,  y158,  y159,
       y160,
y161,  y162,  y163,  y164,  y165,  y166,  y167,  y168,  y169,  y170,
       y171,  y172,  y173,  y174,  y175,  y176,  y177,  y178,  y179,
       y180,
y181,  y182,  y183,  y184,  y185,  y186,  y187,  y188,  y189,  y190,
       y191,  y192,  y193,  y194,  y195,  y196,  y197,  y198,  y199,
       y200,
y201,  y202,  y203,  y204,  y205,  y206,  y207,  y208,  y209,  y210,
       y211,  y212,  y213,  y214,  y215,  y216,  y217,  y218,  y219,
       y220,
```

```
y221,  y222,  y223,  y224,  y225,  y226,  y227,  y228,  y229,  y230,
       y231,  y232,  y233,  y234,  y235,  y236,  y237,  y238,  y239,
       y240,
y241,  y242,  y243,  y244,  y245,  y246,  y247,  y248,  y249,  y250,
       y251,  y252,  y253,  y254,  y255,  y256,  y257,  y258,  y259,
       y260,
y261,  y262,  y263,  y264,  y265,  y266,  y267,  y268,  y269,  y270,
       y271,  y272,  y273,  y274,  y275,  y276,  y277,  y278,  y279,
       y280,
y281,  y282,  y283,  y284,  y285,  y286,  y287,  y288,  y289,  y290,
       y291,  y292,  y293,  y294,  y295,  y296,  y297,  y298,  y299,
       y300,
y301,  y302,  y303,  y304,  y305,  y306,  y307,  y308,  y309,  y310,
       y311,  y312,  y313,  y314,  y315,  y316,  y317,  y318,  y319,
       y320,
y321,  y322,  y323,  y324,  y325,  y326,  y327,  y328,  y329,  y330,
       y331,  y332,  y333,  y334,  y335,  y336,  y337,  y338,  y339,
       y340,
y341,  y342,  y343,  y344,  y345,  y346,  y347,  y348,  y349,  y350,
       y351,  y352,  y353,  y354,  y355,  y356,  y357,  y358,  y359,
       y360,
y361,  y362,  y363,  y364,  y365,  y366,  y367,  y368,  y369,  y370,
       y371,  y372,  y373,  y374,  y375,  y376,  y377,  y378,  y379,
       y380,
y381,  y382,  y383,  y384,  y385,  y386,  y387,  y388,  y389,  y390,
       y391,  y392,  y393,  y394,  y395,  y396,  y397,  y398,  y399,
       y400,
y401,  y402,  y403,  y404,  y405,  y406,  y407,  y408,  y409,  y410,
       y411,  y412,  y413,  y414,  y415,  y416,  y417,  y418,  y419,
       y420,
y421,  y422,  y423,  y424,  y425,  y426,  y427,  y428,  y429,  y430,
       y431,  y432,  y433,  y434,  y435,  y436,  y437,  y438,  y439,
       y440,
y441,  y442,  y443,  y444,  y445,  y446,  y447,  y448,  y449,  y450,
       y451,  y452,  y453,  y454,  y455,  y456,  y457,  y458,  y459,
       y460,
y461,  y462,  y463,  y464,  y465,  y466,  y467,  y468,  y469,  y470,
       y471,  y472,  y473,  y474,  y475,  y476,  y477,  y478,  y479,
       y480,
y481,  y482,  y483,  y484,  y485,  y486,  y487,  y488,  y489,  y490,
       y491,  y492,  y493,  y494,  y495,  y496,  y497,  y498,  y499,
       y500,
y501,  y502,  y503,  y504,  y505,  y506,  y507,  y508,  y509,  y510,
       y511,  y512,  y513,  y514,  y515,  y516,  y517,  y518,  y519,
       y520,
y521,  y522,  y523,  y524,  y525,  y526,  y527,  y528,  y529,  y530,
       y531,  y532,  y533,  y534,  y535,  y536,  y537,  y538,  y539,
       y540,
y541,  y542,  y543,  y544,  y545,  y546,  y547,  y548,  y549,  y550,
       y551,  y552,  y553,  y554,  y555,  y556,  y557,  y558,  y559);

       r_point:=(p1,  p2,    p3,    p4,    p5,    p6,    p7,    p8,
       p9,    p10,   p11,   p12,   p13,   p14,   p15,   p16,   p17,
       p18,   p19,   p20,
p21,   p22,   p23,   p24,   p25,   p26,   p27,   p28,   p29,   p30,
       p31,   p32,   p33,   p34,   p35,   p36,   p37,   p38,   p39,
       p40,
```

p41, p42, p43, p44, p45, p46, p47, p48, p49, p50,
p51, p52, p53, p54, p55, p56, p57, p58, p59,
p60,
p61, p62, p63, p64, p65, p66, p67, p68, p69, p70,
p71, p72, p73, p74, p75, p76, p77, p78, p79,
p80,
p81, p82, p83, p84, p85, p86, p87, p88, p89, p90,
p91, p92, p93, p94, p95, p96, p97, p98, p99,
p100,
p101, p102, p103, p104, p105, p106, p107, p108, p109, p110,
p111, p112, p113, p114, p115, p116, p117, p118, p119,
p120,
p121, p122, p123, p124, p125, p126, p127, p128, p129, p130,
p131, p132, p133, p134, p135, p136, p137, p138, p139,
p140,
p141, p142, p143, p144, p145, p146, p147, p148, p149, p150,
p151, p152, p153, p154, p155, p156, p157, p158, p159,
p160,
p161, p162, p163, p164, p165, p166, p167, p168, p169, p170,
p171, p172, p173, p174, p175, p176, p177, p178, p179,
p180,
p181, p182, p183, p184, p185, p186, p187, p188, p189, p190,
p191, p192, p193, p194, p195, p196, p197, p198, p199,
p200,
p201, p202, p203, p204, p205, p206, p207, p208, p209, p210,
p211, p212, p213, p214, p215, p216, p217, p218, p219,
p220,
p221, p222, p223, p224, p225, p226, p227, p228, p229, p230,
p231, p232, p233, p234, p235, p236, p237, p238, p239,
p240,
p241, p242, p243, p244, p245, p246, p247, p248, p249, p250,
p251, p252, p253, p254, p255, p256, p257, p258, p259,
p260,
p261, p262, p263, p264, p265, p266, p267, p268, p269, p270,
p271, p272, p273, p274, p275, p276, p277, p278, p279,
p280,
p281, p282, p283, p284, p285, p286, p287, p288, p289, p290,
p291, p292, p293, p294, p295, p296, p297, p298, p299,
p300,
p301, p302, p303, p304, p305, p306, p307, p308, p309, p310,
p311, p312, p313, p314, p315, p316, p317, p318, p319,
p320,
p321, p322, p323, p324, p325, p326, p327, p328, p329, p330,
p331, p332, p333, p334, p335, p336, p337, p338, p339,
p340,
p341, p342, p343, p344, p345, p346, p347, p348, p349, p350,
p351, p352, p353, p354, p355, p356, p357, p358, p359,
p360,
p361, p362, p363, p364, p365, p366, p367, p368, p369, p370,
p371, p372, p373, p374, p375, p376, p377, p378, p379,
p380,
p381, p382, p383, p384, p385, p386, p387, p388, p389, p390,
p391, p392, p393, p394, p395, p396, p397, p398, p399,
p400,
p401, p402, p403, p404, p405, p406, p407, p408, p409, p410,
p411, p412, p413, p414, p415, p416, p417, p418, p419,
p420,

```
p421,  p422,  p423,  p424,  p425,  p426,  p427,  p428,  p429,  p430,
       p431,  p432,  p433,  p434,  p435,  p436,  p437,  p438,  p439,
       p440,
p441,  p442,  p443,  p444,  p445,  p446,  p447,  p448,  p449,  p450,
       p451,  p452,  p453,  p454,  p455,  p456,  p457,  p458,  p459,
       p460,
p461,  p462,  p463,  p464,  p465,  p466,  p467,  p468,  p469,  p470,
       p471,  p472,  p473,  p474,  p475,  p476,  p477,  p478,  p479,
       p480,
p481,  p482,  p483,  p484,  p485,  p486,  p487,  p488,  p489,  p490,
       p491,  p492,  p493,  p494,  p495,  p496,  p497,  p498,  p499,
       p500,
p501,  p502,  p503,  p504,  p505,  p506,  p507,  p508,  p509,  p510,
       p511,  p512,  p513,  p514,  p515,  p516,  p517,  p518,  p519,
       p520,
p521,  p522,  p523,  p524,  p525,  p526,  p527,  p528,  p529,  p530,
       p531,  p532,  p533,  p534,  p535,  p536,  p537,  p538,  p539,
       p540,
p541,  p542,  p543,  p544,  p545,  p546,  p547,  p548,  p549,  p550,
       p551,  p552,  p553,  p554,  p555,  p556,  p557,  p558,  p559);

DATA

d_points_per_zone[r_point,c_xj]:=[
p1,    x25,   1,
p1,    x26,   1,
p1,    x41,   1,
p1,    x42,   1,
p1,    x43,   1,
p1,    x58,   1,
.
.
.
];

d_y_trigger[r_point, c_yi]:= [
p1     , y1,  1,
p2     , y2,  1,
p3     , y3,  1,
p4     , y4,  1,
p5     , y5,  1,
p6     , y6,  1,
p7     , y7,  1,
.
.
.
];


BINARY VARIABLES

 v_zone[c_xj];

VARIABLES
v_point[c_yi];

MODEL
```

```
MAX SUM (c_yi: v_point);


SUBJECT TO

c1[r_point]:
SUM(c_xj: v_zone * d_points_per_zone) - SUM(c_yi: v_point *
d_y_trigger) >= 0;

SUM(c_xj:
 v_zone * 1)    <= 4;

c3[c_yi]:
       v_point <=1;

       END
```